INVESTIGATION OF METHODS FOR MEASURING THE EQUIVALENT ELECTRICAL PARAMETERS OF QUARTZ CRYSTALS

By

Samuel N. Witt
and
Vance Keith Woodcox

Progress Report No. 1 - 3

Final Report

2A
12-B

Project No. A-362
Contract No. DA-039 SC-74948
Department of the Army Project: 3-26-05-703

Placed by the U. S. Army Signal
Research and Development Laboratories
Fort Monmouth, New Jersey

Engineering Experiment Station
Georgia Institute of Technology
Atlanta, Georgia
1957-58

PROGRESS REPORT NO. 1

PROJECT NO. A-362

INVESTIGATION OF METHODS FOR MEASURING THE EQUIVALENT ELECTRICAL PARAMETERS OF QUARTZ CRYSTALS

By

SAMUEL N. WITT, JR. AND VANCE KEITH WOODCOX

- o - o - o - o - o -

CONTRACT NO. DA-36-039-SC-74948
DEPARTMENT OF THE ARMY PROJECT: 3-26-05-703

- o - o - o - o - o -

15 OCTOBER 1957 TO 15 JANUARY 1958

PLACED BY THE U. S. ARMY
SIGNAL ENGINEERING LABORATORIES
FORT MONMOUTH, NEW JERSEY

Engineering Experiment Station
Georgia Institute of Technology
Atlanta, Georgia

ENGINEERING EXPERIMENT STATION
of the Georgia Institute of Technology
Atlanta, Georgia

PROGRESS REPORT NO. 1

PROJECT NO. A-362

INVESTIGATION OF METHODS FOR MEASURING THE EQUIVALENT ELECTRICAL PARAMETERS OF QUARTZ CRYSTALS

By

SAMUEL N. WITT, JR. AND VANCE KEITH WOODCOX

- o - o - o - o - o -

CONTRACT NO. DA-36-039-SC-74948
DEPARTMENT OF THE ARMY PROJECT: 3-26-05-703

- o - o - o - o - o -

The object of this project is to develop methods for measuring the equivalent electrical parameters of quartz crystals in the frequency range of 175 to 300 mc/sec.

15 OCTOBER 1957 TO 15 JANUARY 1958

PLACED BY THE U. S. ARMY
SIGNAL ENGINEERING LABORATORIES
FORT MONMOUTH, NEW JERSEY

TABLE OF CONTENTS

LIST OF FIGURES

LIST OF APPENDIX FIGURES

LIST OF TABLES

I. PURPOSE

The purpose of the project is fourfold:

1. To continue the study and investigation of methods and techniques for measuring the equivalent electrical parameters of quartz crystal units in the frequency range of 175 to 300 mc/sec, including:

   (a) determination of measurement errors,

   (b) development of a means for directly measuring the power drive of a crystal unit, and

   (c) development of means for measuring the effective resistance of the crystal unit at the series resonant condition.

2. Utilize the information from Investigation 1., above, in the establishment of a standard crystal measurement system which will:

   (a) measure the effective resistance of the crystal at any frequency within the crystal resonance range with a target accuracy of $\pm$ 1 percent,

   (b) determine the phase angle of the crystal at any frequency within the crystal resonance range with a target accuracy of $\pm$ 1 degree,

   (c) include a means of measuring directly the power drive of a crystal unit within $\pm$ 20 percent, and

   (d) be capable of determining the equivalent electrical parameters of the crystal unit.

3. Utilize the information from Investigations 1. and 2. in investigations of circuitry for ultimate utilization in the development of a practical crystal test instrument for the frequency range 175 to 300 mc/sec which will:

(a) measure the effective resistance of the crystal unit at series resonance within a resistance range of 20 to 200 ohms with an accuracy of $\pm$ 5 percent,

(b) subject the crystal to any power drive within 0.2 and 4 mw and provide a means of determining directly the power drive with an accuracy of $\pm$ 20 percent,

(c) provide a means of operating the crystal within $\pm$ 0.0005 percent of the series resonant frequency, and

(d) have a power drive versus resistance characteristic from 175 to 300 mc/sec which will not vary more than 3 to 1 for the resistance range of 40 to 150 ohms.

4. Investigate any other problems pertinent to crystal measurements in the VHF range which are mutually agreed upon by the contractor and the Contracting Officer's Technical Representative.

II. ABSTRACT

Efforts to improve the calibration accuracy of the Crystal Measurement Standard were continued. Re-evaluation of sources of error substantiated the previous conclusion that the principal source of error is the measurement bridge. Accordingly, a new measurement bridge (General Radio Admittance Meter) has been ordered to include special calibration by the manufacturer.

An Eddystone UHF Communications Receiver Type 770U was ordered and delivered. Initial tests indicated that this receiver has sufficient sensitivity for efficient use as a null detector. Some problems were encountered, however, with r-f leakage. These were corrected by the extensive use of special shielding and filtering. Final evaluation of the receiver is not yet complete.

A crystal power measurement system was designed and built for use with the Crystal Measurements Standard. Accuracies better than $\pm$ 20 percent were obtained for a VSWR of less than 5 and for power levels between 0.05 and 3 mw. The system has not yet undergone complete testing and calibration.

Other crystal measurement methods investigated included a method proposed by Dr. Issac Koga of the University of Tokyo, Tokyo, Japan. Modifications of the Koga method permitted laboratory measurements at frequencies well beyond the lower megacycle region for which the method was developed. Another measurement method which is basically similar to the Koga method is described in detail in this report. This latter method is suitable, at least in theory, for use with VHF and UHF crystals. Conclusive laboratory evaluation has not yet been made.

III. PUBLICATIONS, LECTURES, REPORTS AND CONFERENCES

No publications, lectures or reports have resulted from work under this contract.

Dr. G. K. Guttwein of USASEL visited Georgia Tech on 26 November 1957. Future courses of technical action were discussed. It was mutually agreed that the major technical emphasis of the current project should be placed upon the development of the Crystal Measurements Standard. It was also agreed that various novel methods of measuring the parameters of quartz crystals should be investigated. These included, in particular, methods relating to those proposed by Dr. Issac Koga of the University of Tokyo, Tokyo, Japan. (At the time of the conference, Dr. Koga was serving temporarily on the Georgia Tech staff and thus entered into the discussions concerning his methods of measuring crystal parameters.) Representing Georgia Tech at the conference were Mr. W. B. Wrigley, Head of the Communications Branch; Mr. S. N. Witt, Jr., Project Director; and Mr. V. K. Woodcox, Research Assistant.

IV. FACTUAL DATA

A. Introduction

This project is sponsored by the Frequency Control Branch of the United States Army Signal Engineering Laboratories, Fort Monmouth, New Jersey under Contract No. DA-36-039-SC-74948. The number A-362 was assigned by the Georgia Institute of Technology and the project was started on 15 October 1957.

This project is essentially a continuation of the work which was begun under Contracts DA-36-039-SC-56730 and DA-36-039-SC-71191 with emphasis as outlined in Chapter I of this report.

Under Contract DA-36-039-SC-71191, much effort was directed toward the development of a Crystal Measurements Standard as well as toward the development of CI Meter types of instruments. A Crystal Measurements Standard System making use of commercial equipment was proposed. A block diagram of this system is shown in Figure 1. The various components indicated were selected on the basis of their availability and their suitability for integration into the complete system. The state of development of the system at the inception of the current project is summarized as follows:

1. Crystal measurements were accomplished using bridge techniques with accuracies, under near ideal conditions, of the order of $\pm$ 5 percent error. Generally, errors were much greater than 5 percent, principally because of poor instrument calibrations and lack of sufficient null detection sensitivity. Other sources of error were coaxial line mismatches and r-f leakage. Errors inherent in mathematical computations were essentially eliminated by the use of electronic digital computers.

2. Crystal drive level was roughly determined by voltage measurements at the crystal. The accuracy obtained by this means was very poor, thus making the method unsatisfactory for continued use.

3. Proper interpretation of measurement data permitted the calculation of all crystal parameters; however, the calculations generally required the use of electronic computers and, in some cases, other complicated mathematical procedures. It was not possible to develop a single equivalent circuit which explained the behavior of all crystal samples.

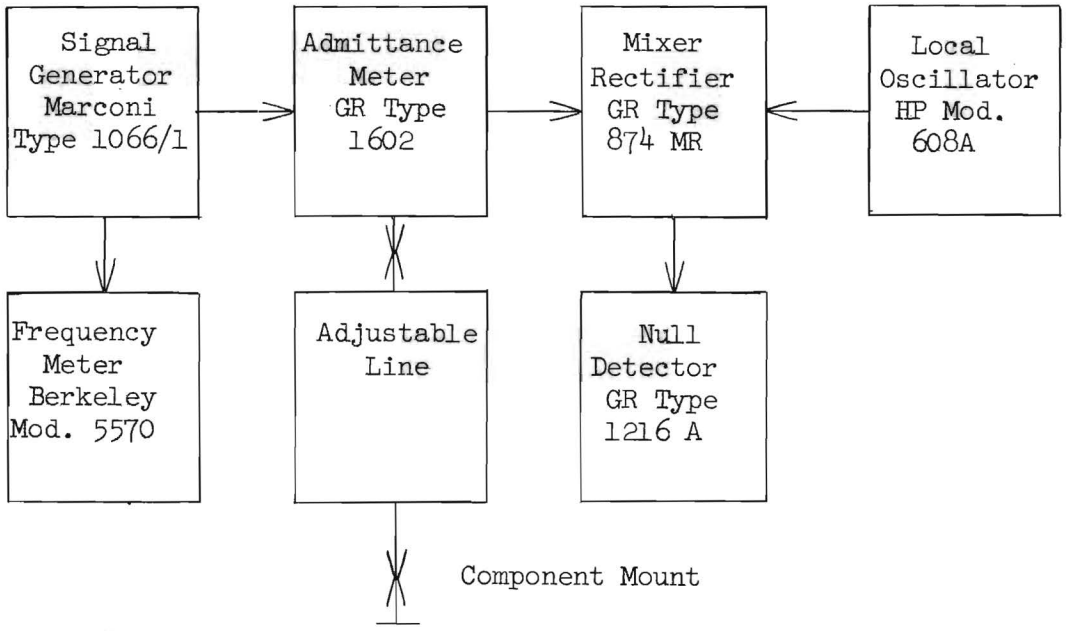

Figure 1. Block Diagram of the Prototype Crystal Measurements Standard.

The state of development of the CI Meter type of instrument is summarized as follows:

1. No substitution methods of measurement have been developed which permit the measurement of crystal parameters above 200 mc/sec. Experimental evidence indicates that the substitution method is not satisfactory above 200 mc/sec.

2. A Coaxial Crystal Parameter Bridge was developed which permitted the measurement of the crystal resistance. It was desirable that the bridge be excited by an oscillator whose frequency is controlled by the crystal under test; however this was not possible over any extended frequency range.

3. Several crystal controlled oscillators were developed for possible eventual application in CI Meter types of instruments. However, none of these oscillators worked satisfactorily with the Crystal Parameter Bridge.

Developments in power measurements included a Prototype Power Meter for use with the Crystal Parameter Bridge. This instrument was not suitable for use with the Crystal Measurements Standard.

From the above data it was decided that the initial efforts on the current project should be directed toward:

1. obtaining instruments having improved calibration and determining their accuracy in the Crystal Measurements Standard,

2. obtaining a receiver or other instrument having sufficient null detection sensitivity,

3. developing a means for measuring crystal drive level in the Crystal Measurements Standard, and

4. investigating other promising crystal measurement systems.

The study under Item 1. resulted in the purchase of a new General Radio Type 1602B Admittance Meter and accessory equipment. This purchase included special calibration of the instrument to better than normal accuracy. The instrument has not yet been delivered.

The study under Item 2. resulted in the purchase of an Eddystone Model 770U UHF Communications Receiver. This item was partially evaluated for use

as a sensitive null detector. The receiver performed satisfactorily in all respects except for r-f leakage. Extensive efforts were directed toward reducing this leakage.

The study under Item 3. resulted in the development of a power measuring system which promises to provide sufficient accuracy for use with the Crystal Measurements Standard. The long- and short-term stability of the system appears to be more than adequate; however, the system does not yet include facilities for self calibration. Such facilities may not be necessary except for an occasional check, once the system has been initially calibrated.

The studies under Item 4. have thus far included various systems based upon, or related to, the methods which were proposed by Dr. Issac Koga for use at lower frequencies. One such system resulted in the moderately accurate determination of the Q of a quartz crystal at 175 mc/sec. Mathematical analysis of this system became so complicated, however, that it was felt that tests should be discontinued temporarily in favor of simpler systems. Another related measurement system was theoretically designed. A prototype of this system was constructed and put through initial tests. Evaluation data for this system is not yet available due to the lack of suitable test instruments and the lack of satisfactory calibration procedures.

B. Crystal Measurements Standard

1. Calibration of Instruments

Data from the previous project indicated that the principal source of error in the Crystal Measurements System was the lack of precise calibration of the various instruments which were used. Justification for this conclusion was based upon the assumption that terminations used as impedance standards were precisely calibrated. The terminations used were the General Radio Type 874-W100

and 874-W200 which are claimed to have an impedance magnitude accuracy of one percent with a very small phase angle at frequencies below 300 mc/sec. No provisions were available locally for checking the calibration of these terminations. However, one sample of the GR-874-W100 termination was submitted to the National Bureau of Standards by USASEL for calibration purposes. The resulting data are given in Table I.

TABLE I

ELECTRONIC COMPUTER CORRECTIONS OF NATIONAL BUREAU OF STANDARDS DATA ON GENERAL RADIO TERMINATION TYPE 874-W100, SERIAL NO. 111

	NBS DATA		CORRECTED DATA	
Frequency (mc/sec)	Impedance Magnitude (ohms)	Impedance Angle (degrees)	Impedance Magnitude (ohms)	Impedance Angle (degrees)
50	99.9	-0.8	99.91	-0.096
60	99.8	-0.9	99.82	-0.057
70	99.8	-1.1	99.83	-0.116
80	99.8	-1.2	99.83	-0.076
90	99.7	-1.4	99.74	-0.137
100	99.7	-1.5	99.75	-0.097
110	99.7	-1.7	99.77	-0.156
120	99.6	-1.8	99.68	-0.118
130	99.6	-2.0	99.70	-0.178
140	99.6	-2.1	99.71	-0.138
150	99.5	-2.3	99.63	-0.201
160	99.5	-2.4	99.64	-0.160
170	99.4	-2.6	99.57	-0.224
180	99.4	-2.7	99.58	-0.184
190	99.3	-2.9	99.51	-0.248
200	99.3	-3.0	99.52	-0.208
210	99.3	-3.2	99.55	-0.268
220	99.2	-3.3	99.47	-0.233
230	99.2	-3.5	99.50	-0.293
240	99.1	-3.6	99.42	-0.258
250	99.0	-3.8	99.36	-0.324
260	99.0	-3.9	99.38	-0.284
270	98.9	-4.1	99.32	-0.350
280	98.9	-4.2	99.34	-0.311
290	98.8	-4.4	99.28	-0.377
300	98.8	-4.5	99.31	-0.337

Note: The nominal impedance of this termination is 100 ohms. The data are corrected for an effective difference in length of 0.783 cm between the termination and the reference short.

In the calibration of the W100 termination, a General Radio Type 874-WN3 Short-Circuit Termination was used to establish the reference plane. A difference in length of approximately 0.8 cm between the W100 termination and the short-circuit termination was not taken into account by the National Bureau of Standards. These data were subsequently corrected by means of a digital computer at Georgia Tech. Both the original data and the corrected data are included in Table I. If it is assumed that this sample of the W100 type termination is typical, then the validity of previous work based upon this type of termination is verified.

Many other possible sources of system errors were considered with the conclusion that the principal source of error was due to the bridge or basic impedance measuring instrument. The conclusion was the same whether the General Radio Type 1602B Admittance Meter or the Hewlett-Packard Model 803A VHF Bridge was used. It was thus necessary that a more accurate bridge be obtained before other sources of error could be accurately evaluated. Various inquiries were made concerning current commercial instruments, including the availability of special calibration. Upon this basis, a new General Radio Type 1602B Admittance Meter was ordered. The General Radio Company agreed to calibrate the instrument in their laboratory to within approximately one percent over the frequency range from 175 to 300 mc/sec. This accuracy applies at an admittance level of 20 millimhos and will be somewhat poorer at greatly different admittances. Auxiliary equipment such as terminations and a component mount were ordered at the same time to also be calibrated. This equipment has not yet been received.

It is anticipated that when the new equipment is received a calibration check will be made using the various terminations with various lengths of transmission line. From these data other sources of error can be evaluated and the overall system accuracy can be determined.

2. Detector Systems

Another source of error in the Crystal Measurements Standard System was the lack of sufficient null detection sensitivity to permit accurate adjustment of the bridge. This difficulty arises from one of the requirements of the system to maintain the crystal drive at very low levels (between 0.2 and 4 mw). Previous data indicated that none of the several null detection systems tested had sufficient sensitivity. The possibility of using commercial high-frequency communication receivers was considered. However, it was found that a very limited number of such receivers were manufactured. Of those available, only one, the Eddystone Model 770U, was found which was both reasonably priced and covered all of the desired frequency range. The distributor of this receiver provided data which indicated that it would offer appreciable improvement over previous detection systems. The receiver was ordered and was delivered in December 1957.

The null-detection sensitivity curve for the Eddystone receiver is presented in Figure 2.

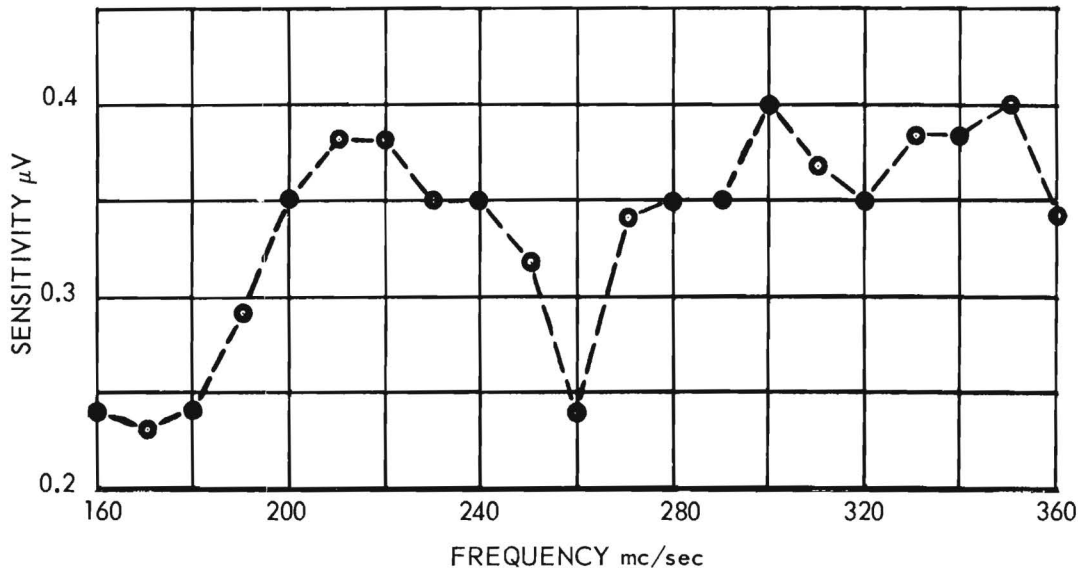

Figure 2. Null Detection Sensitivity of Eddystone Receiver Type 770U.

One difficulty encountered with the Eddystone receiver was that of r-f leakage from external sources. This was objectionable only at frequencies where television stations or other strong signals were present. However, it was felt that the source of leakage should be eliminated because of the possibility of direct coupling between the signal generator or other instruments and the receiver.

When the receiver was enclosed in a screened box it was found that a principal source of leakage was the power cable. Thus a filter consisting of two feed-thru capacitors and an r-f choke was installed in each power connection at the receiver.

To use the receiver as a null detector it was desirable to replace the internal signal level meter with an external meter of greater sensitivity. The connection of these additional leads to the receiver became another source of r-f leakage. Thus, choke-capacitor filters were installed in these leads also.

Even with the filter installations indicated above, the r-f leakage was still appreciable. This was due to the relatively large openings in the case of the receiver. Because of the difficulty of installing copper screening in the receiver case, a small double shielded screen box was constructed to house the entire receiver. Additional filters were added at each of the external connections as indicated in Figure 3. The resulting total signal leakage was reduced by more than 40 db. The maximum received signal strength from external sources occurred between 198 and 204 mc/sec (Television Channel 11) and represented an equivalent input of less than 0.2 microvolt into a 75-ohm load, after the shielding was completed.

3. Power Measurements

In the Crystal Measurements Standard System, it is desirable that some means be provided for continuously monitoring the crystal drive level. The power measurement system must satisfy three conditions:

1. it must be able to measure r-f power down to 0.2 mw with accuracies on the order of $\pm$ 20 percent,
2. it must not affect the crystal impedance measurements to any noticeable degree, and
3. it must be simple to operate, preferably direct reading.

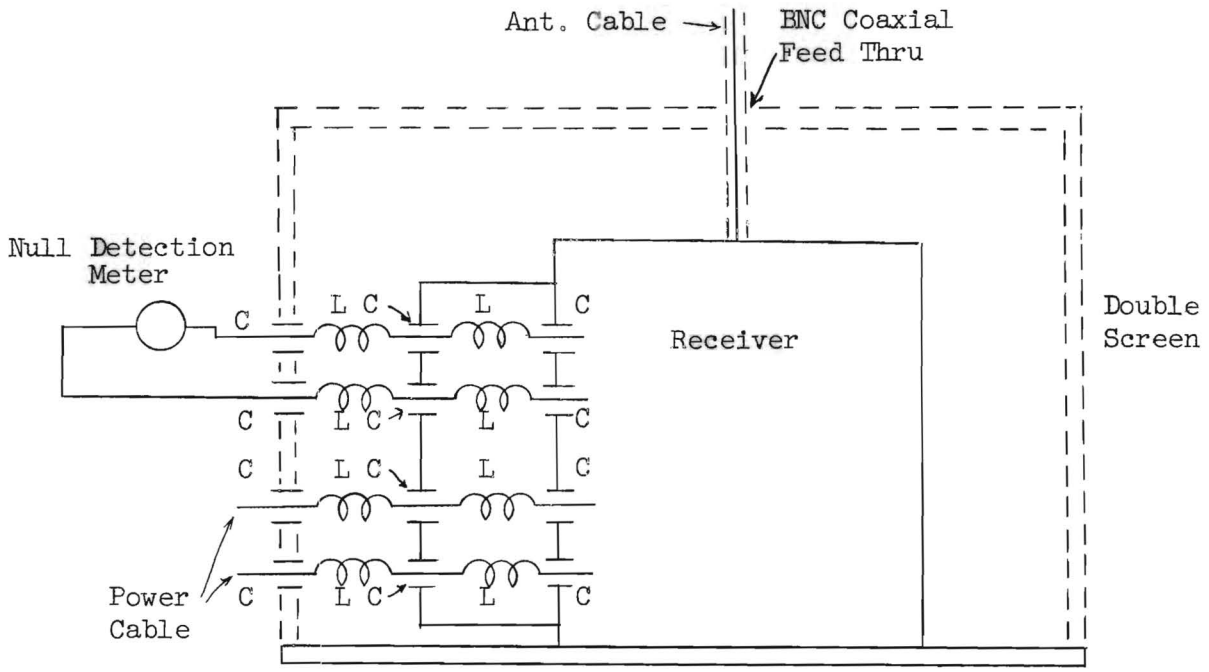

C = Centralab FT-2300
Feed Thru Capacitor
L = Ohmite Z-235 Choke

Figure 3. Stray Signal Shielding of Eddystone Receiver.

From transmission line theory, the net forward power in any coaxial system is equal to the incident power less the reflected power according to the relation:

$$P = \frac{(E^+)^2}{R_o} - \frac{(E^-)^2}{R_o} \qquad (1)$$

where R_o is the characteristic resistance of the line. Therefore, by

independently monitoring the incident and reflected voltages, E^+ and E^-, on the coaxial line, it is possible to determine the net forward power. The Hewlett Packard 764D dual directional coupler provides a means for monitoring the incident and reflected voltage waves since the voltages at its two outputs are proportional to E^+ and E^-. Furthermore, previous data indicated that the insertion of the coupler into the coaxial line had negligible effects on the accuracy of the crystal impedance measurements.

To measure the r-f voltage out of the directional coupler, a square-law detector was used. This detector provided a d-c voltage proportional to $(E^+)^2$ or $(E^-)^2$ and thus proportional to incident or reflected power. The d-c voltages were measured by the bridge setup shown in Figure 4.

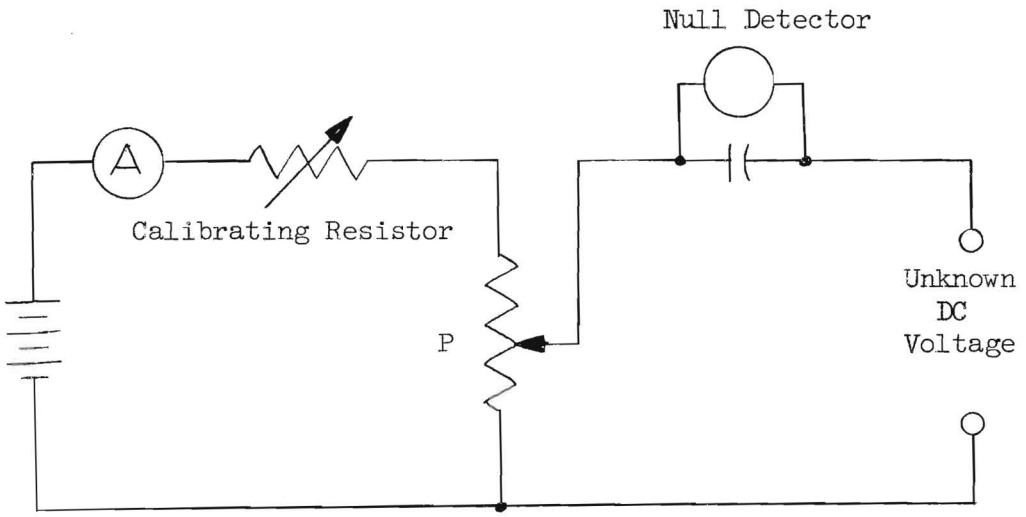

Figure 4. D-C Bridge for Power Measurement System.

A 5000 ohm Helipot potentiometer (P) was used as the balancing device for the bridge. The potentiometer linearity of $\pm$ 0.5 percent permitted the bridge to be calibrated by a known d-c voltage to establish a reference reading on the microammeter (A). The unknown voltage then could be read directly from the

Helipot dial. A Minneapolis Honeywell Electronik Null Indicator was used to provide adequate sensitivity for balancing the bridge.

Since power is proportional to the difference of the squared incident voltage and the squared reflected voltage, it is therefore proportional to the difference of the d-c voltages from the two detectors, one on each of the outputs of the directional coupler. This assumes that both detectors are precisely square-law and have matched gain factors. The output voltage, E, of a diode detector for an r-f input voltage, e, is approximated by

$$E = Ae^{k} \qquad (2)$$

where A and k are constants. The constant k must have a magnitude of 2 to provide square-law detection. Also, if two diodes are to provide the same output when supplied with the same input voltage the constants A must be equal.

From a limited supply of diodes, two were selected that were fairly well matched and were placed in a system shown in Figure 5. Resistances of 50 ohms

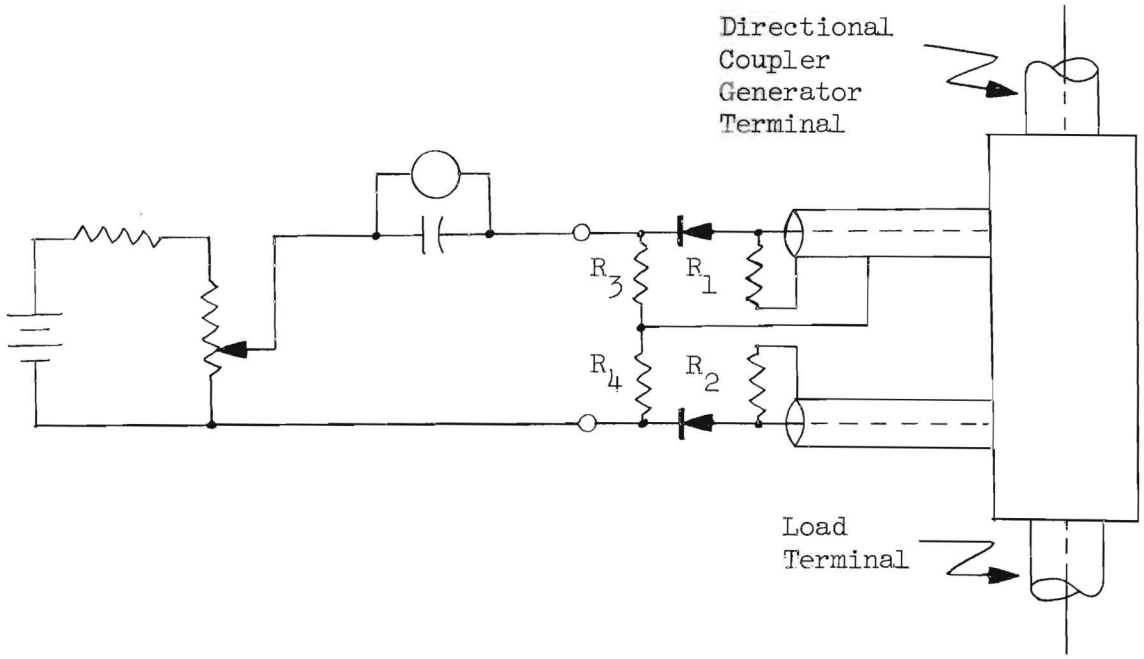

Figure 5. Crystal Power Measurement System.

were chosen for R_1 and R_2 to terminate the coaxial line from the directional coupler and thus provide the proper r-f voltage across the detectors. The values of the diode load resistors, R_3 and R_4, were made sufficiently small so that the sensitivity of the null indication would not be greatly reduced. As a first choice, 22 K for each was selected.

By using the Marconi Signal Generator and the variable attenuator at its output, r-f voltage versus d-c voltage curves were run on each of the diodes. After plotting on log-log paper, it was found that the output of both diodes had the form of Equation 2 but the exponent, k, was of the order of 1.8 instead of 2, which would introduce power measurement errors. After some study it was determined that the exponents, k, varied with the value of the load resistors R_3 and R_4. After considerable experimentation it was found possible to correct the value of k from 1.8 to 2 for the two particular diodes by making R_3 equal to 8 K, and R_4 equal to 12 K. The factors, A, were not exactly equal but were assumed to be sufficiently well matched for initial investigations.

To determine the accuracy of the power measurement system, it was necessary to know the true power delivered to a standard load. To measure this power a Hewlett-Packard Model 403C power meter with an input impedance of 50 ohms was used as the load. This meter has a claimed accuracy of $\pm$ 5 percent. The measurement setup is shown in Figure 6.

Since the Marconi Signal Generator has a maximum power output on the order of 3 mw and since at the present time no auxiliary amplifier was available, the tests were performed over the power range from 0.05 mw to 3 mw at a frequency of 200 mc/sec. The Helipot dial of Figure 5 was adjusted to 3.00 (out of a full-scale reading of 10.00) for a power input of 3 mw as indicated by the HP power meter. The power measurement system agreed with the HP power meter to an

accuracy of + 0 percent and - 1.4 percent of the indicated reading over the entire range. The results are tabulated in Table II. It must be assumed that the relative accuracy of the HP power meter is much better than $\pm$ 5 percent or that cancellation of errors occurred. The possibility of the latter was dismissed after a consideration of previous data based on the attenuator dial of the Marconi Signal Generator (an identical nonlinearity of the attenuator would have been required to account for the results obtained). Of course, it is possible that the absolute power level calibration could have been off more than 1.4 percent.

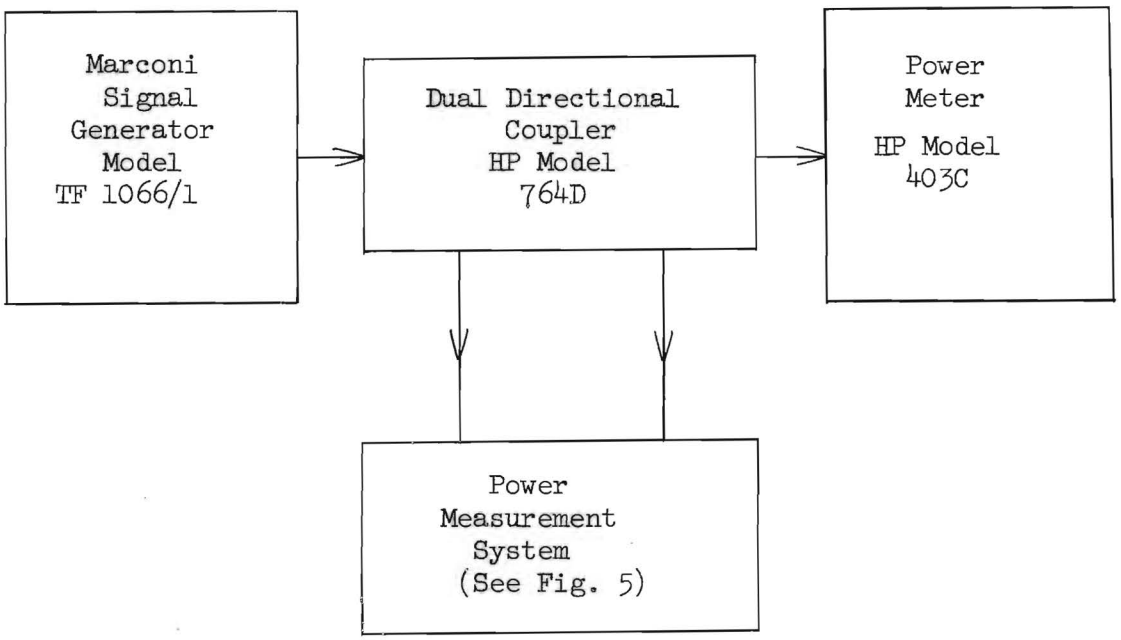

Figure 6. Calibration of Power Measurement System.

The main sources of error in the system are caused by the variation in the voltage standing wave ratio and frequency. For Table II the VSWR was unity, and therefore ($\bar{E}$) was equal to zero at all times. As the VSWR is

increased, ($\bar{E}$) increases and the resultant d-c voltage out of the two diodes becomes the difference of two relatively large numbers. Since the diodes are not perfectly matched, a small error in either d-c voltage with respect to the relatively small difference of the two d-c voltages represents a relatively large system error. To determine the effects of large standing wave ratios on the accuracy of the system, an adjustable line and shorted stub were used in conjunction with the HP power meter as shown in Figure 7. It was found that

TABLE II

POWER MEASUREMENT CALIBRATION DATA AT UNITY VSWR

Power Input* (mw)	Power Reading** (mw)	Power Input* (mw)	Power Reading** (mw)
3.00	3.00	1.25	1.25
2.75	2.74	1.00	0.99
2.50	2.48	0.75	0.75
2.25	2.25	0.50	0.49
2.00	1.99	0.10	0.10
1.75	1.74	0.08	0.08
1.50	1.48	0.05	0.05

* As measured by HP-403C power meter.

** Dial reading of Helipot was adjusted to read 3.00 for 3-mw input and unity VSWR.

the error was less than + 13 percent and - 2 percent for a VSWR ranging from 1 to 5 at a frequency of 200 mc/sec. The results are tabulated in Table III. Similar effects were observed at 400 mc/sec.

Better matching of the diode characteristics will reduce the errors resulting from large variations in the VSWR.

The second source of system errors, which is variations in frequency, has not been thoroughly investigated. However, it is believed that most of this

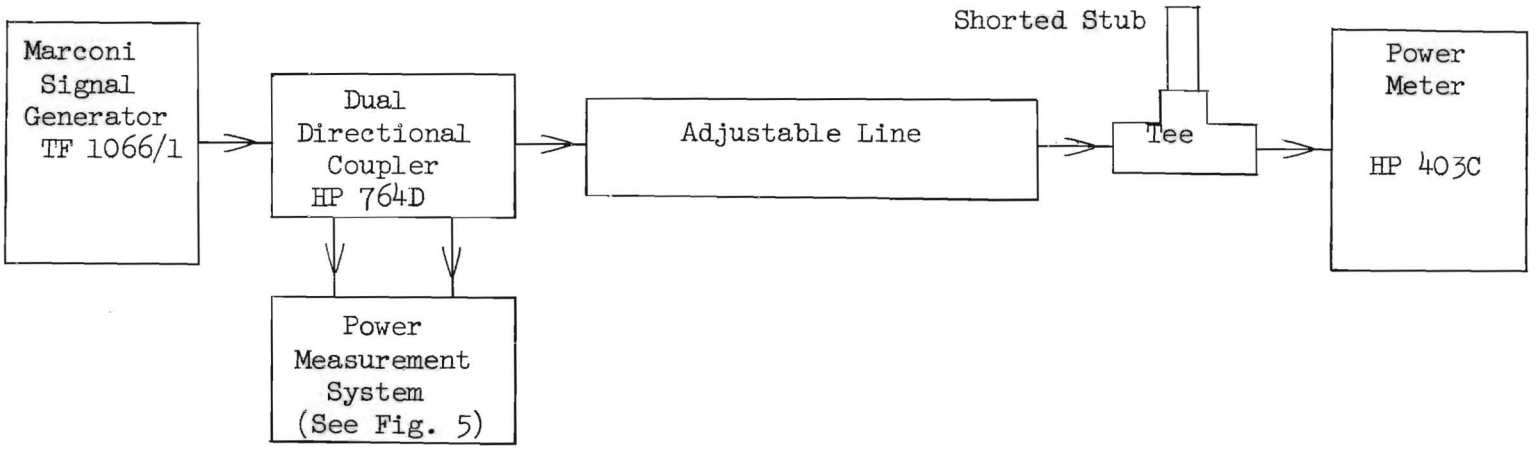

Figure 7. Determination of Effects of VSWR on Accuracy of Power Measurement System.

error can be attributed directly to the frequency characteristics of the directional coupler. The coupling coefficients of the directional coupler are claimed to be constant within $\pm$ 1 db between 216 and 450 mc/sec. Laboratory data show the coupler to be down in response by 3 db at 150 mc/sec. However, if it is found that the frequency effects are independent of other sources of error, a simple calibration curve can be devised to correct for the frequency error.

TABLE III

EFFECTS OF VSWR ON POWER MEASUREMENT CALIBRATION

Power Input* (mw)	Power Reading** (mw)	VSWR	Power Input* (mw)	Power Reading** (mw)	VSWR
3.00	3.00	1	0.30	0.30	1
3.00	3.00	2	0.30	0.30	2
3.00	3.38	5	0.30	0.33	5
1.00	1.00	1	0.05	0.50/	1
1.00	0.99	2	0.05	0.51/	1.4
1.00	1.13	5	0.05	0.52/	3.8

* As measured by HP-403C power meter

** Dial reading of Helipot was adjusted to read 3.00 for 3-mw input and unity VSWR.

/ Reading of the Helipot dial was readjusted to read 0.5 for 0.05-mw input and unity VSWR to obtain better scale resolution.

It may be observed that the substitution of a d-c millivoltmeter in the place of the d-c bridge of Figure 5 would provide a direct-reading power measurement system at some sacrifice in accuracy.

C. Other Measurement Systems

1. State of the Art

It is desirable that a practical crystal test instrument be developed such that the use of external auxiliary equipment is minimized. Such instruments

as the various Crystal Impedance Meters satisfy this requirement at frequencies below about 175 mc/sec. It is evident that the Crystal Measurements Standard does not satisfy this requirement.

Other desirable properties of a practical crystal test instrument are that it (1) be easy to operate, (2) provide data in a form readily interpreted, (3) be readily portable, and (4) be self calibrating or require only infrequent external calibration.

The substitution method satisfies all of these requirements in theory. However, when attempts are made to apply substitution principles at frequencies above 200 mc/sec many difficulties are encountered. In particular, practical circuit elements can no longer be represented as lumped elements. This effect produces additional sources of phase shift in oscillator circuits such that the phase stability of crystal controlled oscillators becomes very poor. Also, at higher frequencies most crystals do not display a zero-phase-shift resonance so that resistive substitution is meaningless.

The Crystal Parameter Bridge, which was developed on the previous contract, is capable of providing reasonably accurate measurements at the higher frequencies provided it can be suitably excited. Two methods of excitation are possible: (1) excitation by a simple oscillator whose frequency is controlled by the bridge and crystal under test and (2) excitation by a highly stable self-controlled oscillator. Several attempts have been made to design oscillators to be controlled by the crystal under test but none have been successful because of the large crystal-Q degradation by the bridge. The use of a highly stable self-controlled oscillator violates the requirement of keeping the instrument simple. In addition, the adjustment procedure for the Crystal Parameter Bridge is not as convenient as might be desired.

For the above reasons, it appeared that a new and different approach to the crystal measurement problem was desirable. Such an approach was provided by Dr. Issac Koga in a series of lectures presented at the School of Electrical Engineering of the Georgia Institute of Technology during October and November 1957.*

2. The Koga Method

The method of quartz crystal measurements proposed by Dr. Koga is summarized as follows. In Figure 8, the series combination of C_A and C_S is made

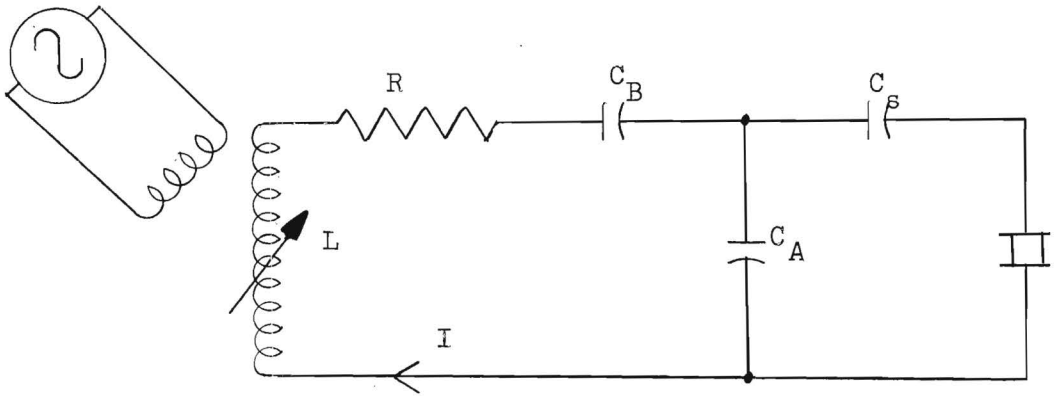

Figure 8. The Koga Method of Crystal Measurements.

equal to the desired load capacitance of the crystal. The capacitor C_B is made small compared to C_A. The circuit is excited by loosely coupling a variable frequency oscillator to the inductance as shown. The inductance, L, is tuned so that the electric circuit resonance occurs at the crystal resonant frequency. As the oscillator frequency is varied in the vicinity of crystal resonance, the

* A limited number of copies of a paper entitled "Some Notes on Quartz Crystal Units" by Dr. Issac Koga are available by contacting Samuel N. Witt, Jr., Engineering Experiment Station, Georgia Institute of Technology, Atlanta, Ga.

current variation will be as indicated in Figure 9. Figure 10 shows an expanded scale portion of Figure 9. In Figure 10, the currents I_A and I_B are recorded.

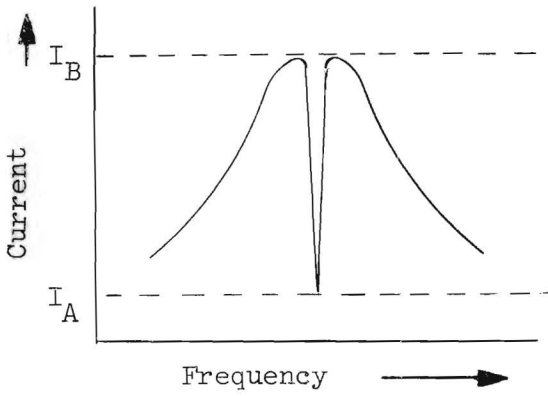

Figure 9. Current-vs-Frequency Response of Figure 8.

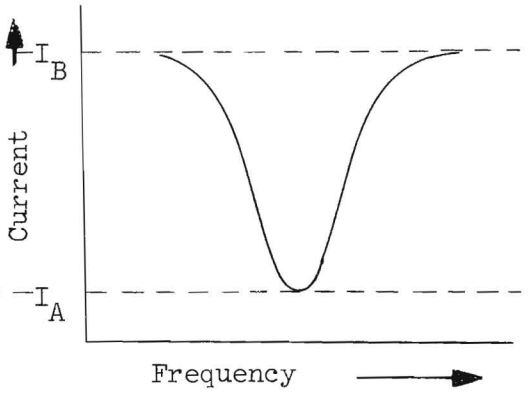

Figure 10. Scale Expansion of Figure 9.

The equivalent resistance, R_Q, of the crystal is then given approximately by

$$R_Q = K \frac{1}{I_B/I_A - 1} \tag{3}$$

where

$$K = \frac{1}{R} \left(\frac{1}{\omega C_A}\right)^2 \quad . \tag{4}$$

It may be observed that only the ratio of I_B to I_A is required; however, the absolute values of R and C_A are required. The frequency may, of course, be readily measured.

The necessity of measuring R and C_A may also be dispensed with by removing the crystal and C_S and substituting a resistor, W, which must be large enough so that $1/W^2$ can be neglected compared with $(\omega C_A)^2$. The phase angle of the resistor at the frequency of concern must be very nearly zero. If I_C is the

maximum value of current with W connected and I_D is the maximum current with W removed, then K of Equation (4) becomes

$$K = W\left(\frac{I_D}{I_C} - 1\right). \qquad (5)$$

Again, it is not necessary that the absolute values of current be measured since only the ratio appears in the equation.

The above procedure is applicable for practical crystal measurements only when the crystal can be accurately represented by the equivalent circuit of Figure 11.

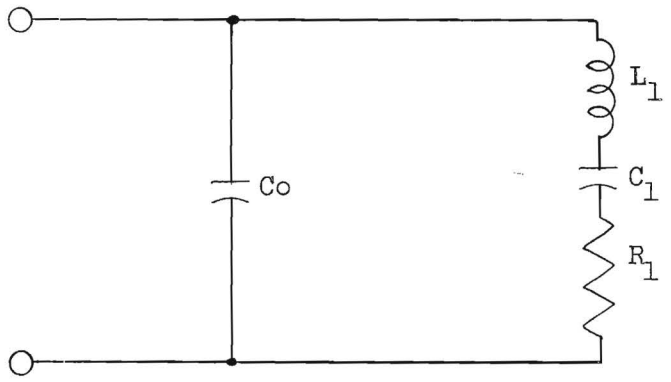

Figure 11

Figure 11. Low-Frequency Equivalent Circuit of a Quartz Crystal.

At high frequencies where holder inductance and resistance become appreciable, Equations (3), (4), and (5) must be appropriately modified. This, however, requires an exceedingly complicated mathematical procedure which has not yet been fully developed. It was concluded that sufficient personnel time was not available on the project to develop the necessary mathematics. However, the method was tested in the laboratory at a frequency of 175 mc/sec. The equivalent resistance of the crystal was not calculated because a suitable resistor, W, was not available. Alternate calculations of the Q of the crystal

were made using mathematics provided by Dr. Koga. Values of Q ranging from 20,000 to 40,000 were obtained compared to a value of 53,000 obtained from bridge measurements. The curve from which the Q was calculated is reproduced in Figure 12.

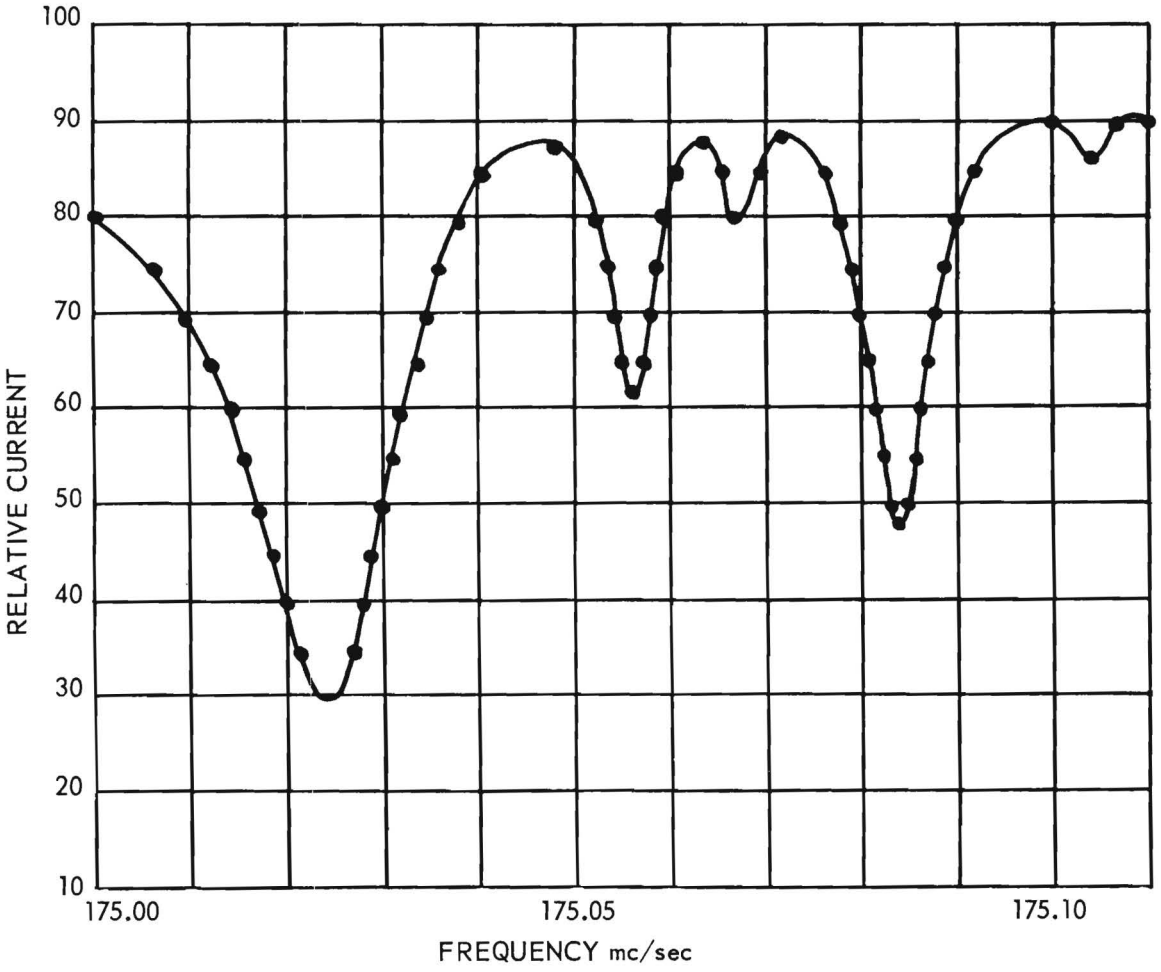

Figure 12. Current Variations for Crystal No. FA-116 in Circuit Similar to Figure 8.

Figure 12 reveals some interesting information concerning the crystal, for purposes other than parameter determination. For example, the frequency and relative magnitude of spurious responses are readily determined. It is also obvious that the spurious responses distort the main response in such a

way that the Q is not constant. In particular, the value of Q changes rather suddenly at the point of minimum current. It is, of course, necessary to take this into account when comparing the Q determination by this method with the determination from bridge measurements.

A mechanical-electric sweeping system was also constructed to vary the frequency of the source oscillator and provide a synchronized oscilloscope sweep voltage. A photograph taken using this system is shown in Figure 13. It should be noted that the ordinate in this figure is proportional to the square of the current which accounts for differences in appearance between Figures 12 and 13. Additional differences occur due to excessive sweep speed (several cycles per second) used with the latter. This difficulty can be readily eliminated.

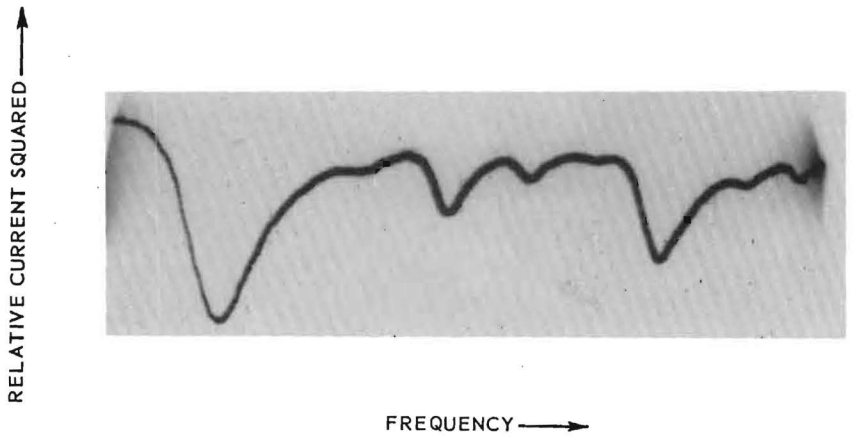

Figure 13. Photographic Record Corresponding to Figure 12.

3. A Developmental System

A crystal measurement system similar to the Koga method has been devised for use at higher frequencies. The mathematical derivation for this system is included in the appendix section of this report. A practical circuit arrangement for the application of this method is shown in Figure 14. The only instruments required are a reasonably stable signal generator and an instrument

for measuring the r-f current. In the figure, the inductor, L_2, is used to resonate the circuit consisting of L_2, L_L, R_L, C_o and R_2 to the crystal frequency. The resistor, R_2, is included in the circuit to facilitate the measurement of current by means of an r-f voltmeter. The resistor, R_g, is the unavoidable internal resistance of the signal generator; however, it serves the useful purpose of reducing the Q of the electric circuit resonance. The summarizing paragraphs of the appendix describe the method used to calculate the more important parameters of the crystal.

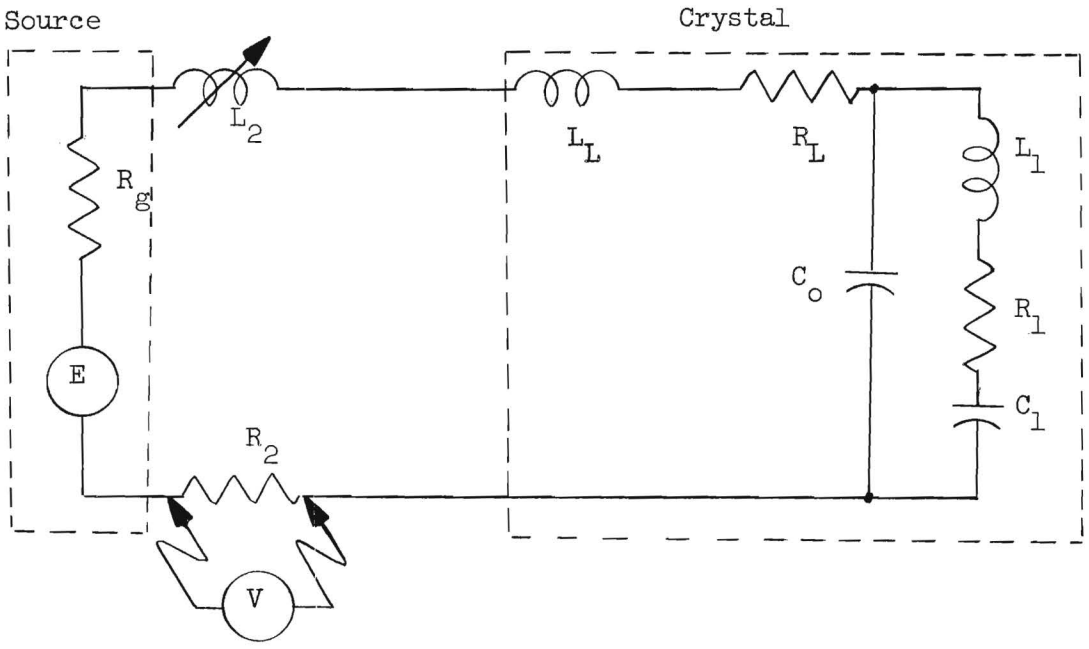

Figure 14. A Developmental UHF Crystal Measurement System.

From laboratory considerations, a number of deficiencies of this method become apparent. These may be understood by considering the physical arrangement of the components of Figure 14 as shown in the sketch of Figure 15.

The sketch shows three crystal sockets and a type N coaxial connector mounted in a small metal box with interconnections as indicated. The inductor,

L_2, and resistor, R_2, are mounted on crystal bases which may be plugged into the sockets provided. A diode is connected between the common resistor-crystal terminal and a terminal mounted on the face of the box. The use of a diode for voltage (and, therefore, current) measurement was selected to obtain sufficiently sensitive current measurements while at the same time not loading the circuit capacitively. This procedure, however, requires that the input-output characteristics of the diode be carefully determined. The required calibration has not yet been accomplished because of the very low voltages and currents involved. Sample crystal curves have, however, been run, but satisfactory parameter calculations have not yet been possible because of the lack of current calibration. This deficiency of the system may be overcome by finding a calibrated means for measuring the current (or voltage) which does not upset the lumped parameter configuration of the circuit.

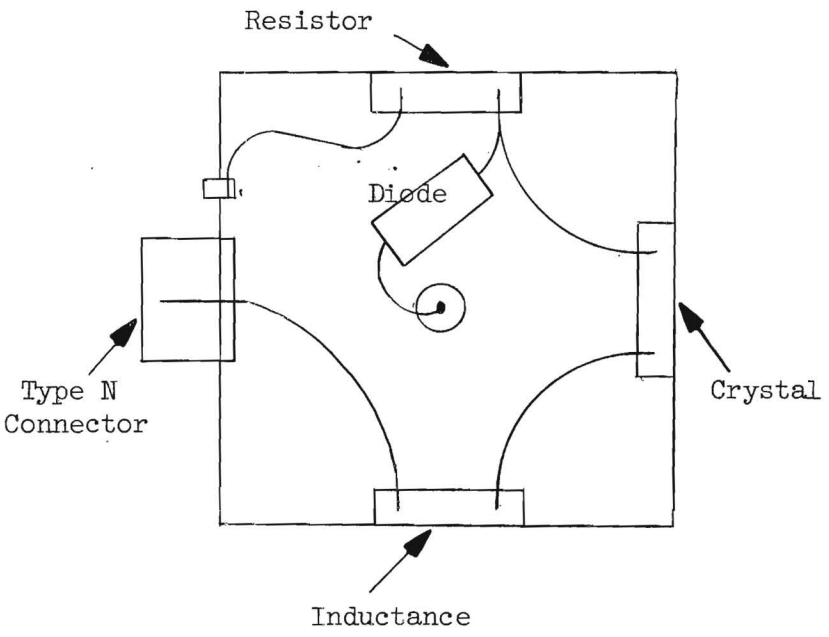

Figure 15. Physical Arrangement for Components of Figure 14.

The requirement that all of the circuit elements in the system must be of a lumped rather than distributed character is in itself a serious disadvantage. The relatively long leads required to interconnect the various components, for example, introduced errors not considered by the mathematics. It is believed, however, that smaller physical spacing might provide satisfactory performance at frequencies as high as 300 mc/sec.

Sufficient laboratory data using this method of measurement have not yet been obtained. Thus, the suitability of the method for practical crystal measurements cannot yet be evaluated. In addition, simplifications in the method of reducing the data must be developed.

V. CONCLUSIONS

National Bureau of Standards' calibration data supplied to USASEL on a General Radio Type 874-W100 Termination have strengthened the belief that the principal source of calibration error in the Crystal Measurements Standard is the measurement bridge. This, of course, is based on the assumption that the termination calibrated by NBS is typical. To improve the overall system calibration, a new General Radio Admittance Meter has been ordered. The instrument is to be specially calibrated by the manufacturer to within about $\pm$ 1 percent for measurements within the restricted range of interest.

With the purchase of an Eddystone Model 770U UHF Communications Receiver sufficient null-detection sensitivity is now available for efficient use with most UHF measurement bridges. The major deficiency of the Eddystone receiver was excessive r-f leakage into the receiver from external sources. Ample shielding and filtering produced a reduction in leakage to a satisfactorily low level. It is anticipated, however, that additional leakage problems will be encountered with conventional flexible coaxial cable.

A power measurement system for use with the Crystal Measurements Standard was developed. Present errors are less than $\pm$ 20 percent for all combinations of VSWR from 1 to 5 and all power levels from 0.05 to 3 mw. Under condtions of low VSWR the accuracy is even better. The major source of error in the system is the unbalance in the diodes used with the directional couplers. Indications are that the present balance between diodes can be appreciably improved by further laboratory experimentation. Errors due to frequency variations are still appreciable; however, these errors appear to be caused by the directional coupler rather than other components. If this proves to be the case, then a simple frequency correction curve independent of VSWR and actual power level can

be provided. Thus the complete system will remain direct-reading with only simple corrections being required for frequency effects.

Several other types of crystal measurement systems were considered. Further investigations of the various substitution methods were temporarily discontinued because of the difficulty in controlling phase characteristics at higher frequencies. Work on the Crystal Parameter Bridge was also discontinued because of the lack of suitable excitation sources. A new approach to the measurement problem was advanced by Dr. Issac Koga. However, this method was directly applicable only in the lower megacycle frequency range. Modifications of the method permitted some valid information to be obtained on certain crystals but adequate mathematical substantiation of the modifications proved to be prohibitively difficult.

Another measurement method, basically similar to that of Dr. Koga, was developed mathematically. This method is directly applicable at higher frequencies where crystal holder parameters have appreciable influence on measurements. The method, however, has not yet undergone thorough laboratory investigation and evaluation. A number of problems, including the accurate relative measurement of low-level r-f currents, must be investigated before the practicability of the method can be predicted. Simplified mathematical procedures for reducing measurement data are also desirable. On the other hand the method, even in its present state of development, was found useful for obtaining normally difficult-to-obtain information on the spurious responses of high-frequency crystals.

VI. PROGRAM FOR NEXT INTERVAL

The program for the next quarter will be a continuation of the work reported in the preceding pages with special emphasis on the following items:

1. thorough testing of the new General Radio Admittance Meter when it arrives, including an evaluation of its accuracy,

2. completion of the power measurement system for the Crystal Measurements Standard, including complete calibration,

3. investigations and evaluations of the sources of error in the Crystal Measurements Standard,

4. measurement of crystal parameters using the Crystal Measurements Standard,

5. further study of data reduction methods for the Crystal Measurements Standard,

6. further evaluation of the Eddystone receiver,

7. further investigations into methods of crystal measurement relating to the Koga method, and

8. development of instrumentation for other types of crystal measurement systems.

VII. IDENTIFICATION OF KEY TECHNICAL PERSONNEL

The personnel who have contributed to this project are as follows:

James E. Lane	Technical Assistant	40 Hours
Samuel N. Witt, Jr.	Project Director Research Engineer	240 Hours
Vance Keith Woodcox	Research Assistant	480 Hours

The background and qualifications of these men are presented in the following paragraphs.

Mr. James E. Lane, Technical Assistant, was employed by this project for part-time work on 1 January 1958. Mr. Lane has previously been connected with the Station as a technician on various other projects including the forerunner of this project. He has had 4 years' experience in military electronic maintenance and was recently in the employment of Radiation, Inc., Melbourne, Florida for a period of 9 months. Mr. Lane received his Bachelor's Degree in Industrial Management at Georgia Tech and is currently pursuing studies toward the Bachelor's Degree in Physics at Georgia Tech.

Mr. Samuel N. Witt, Jr., Project Director and Research Engineer, was employed half-time by the project at its initiation. Mr. Witt, who holds the degree of Master of Science in Electrical Engineering from Georgia Tech, is currently pursuing studies toward a Doctor of Philosophy degree in that field. Mr. Witt has been with the station more than 6 years on various electronic research and developmental projects which have included work in the fields of transistors, oscillators, radar circuitry and communication circuitry. He was employed half-time on the forerunner of this project. He has also served one year as electronics instructor in the U. S. Navy and one year as electrical

engineering instructor at Tennessee Polytechnic Institute and is currently serving half-time as Lecturer in the School of Electrical Engineering at Georgia Tech.

Mr. Vance Keith Woodcox, Research Assistant, was employed full-time by this project at its initiation. Mr. Woodcox completed work toward his Bachelor's Degree in Electrical Communications with highest honors at Georgia Tech and is currently pursuing studies toward a Master's Degree in the same field. He has had various experience in electronic parts and servicing. He is a member of Phi Eta Sigma, Eta Kappa Nu, Tau Beta Pi, Phi Kappa Phi, and IRE.

Respectfully submitted:

Samuel N. Witt, Jr.
Project Director

Approved:

W. B. Wrigley, Head
Communications Branch
of the
Physical Sciences Division

VIII. APPENDIX

The equivalent electrical parameters of a UHF quartz crystal can be represented to a fair approximation by the circuit of Figure 1. The elements L_1, C_1 and R_1 represent the motional arm. The holder is represented by L_L, R_L and C_o. Typical element values for a crystal at an overtone response of 250 mc/sec are:

$L_1 = 2.23 \cdot 10^{-3}$ hy $\qquad L_L = 3.0 \cdot 10^{-8}$ hy

$C_1 = 1.82 \cdot 10^{-16}$ fd $\qquad C_o = 5.0 \cdot 10^{-12}$ fd

$R_1 = 100$ ohms $\qquad R_L = 15$ ohms

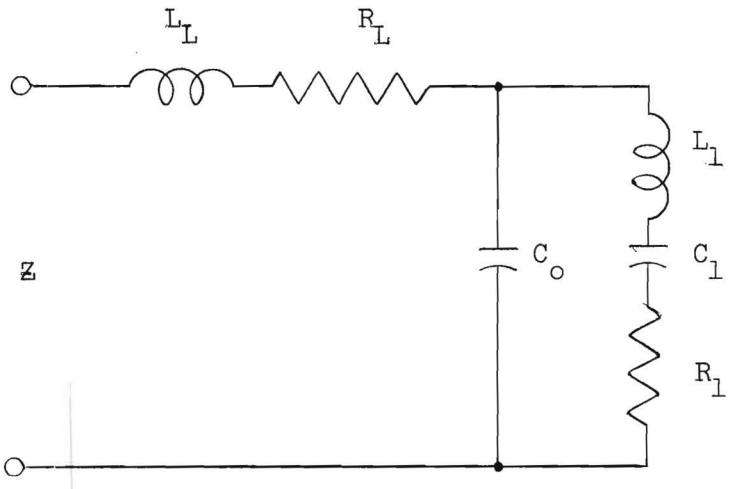

Figure 1. The Equivalent Circuit of a UHF Quartz Crystal.

The impedance, Z, of the crystal as a function of frequency, ω, can be written as

$$Z = j\omega L_L + R_L + \frac{1}{j\omega C_o} + \left(\frac{1}{\omega C_o}\right)^2 \left(\frac{1}{R_1 + j\omega L_1 + \frac{1}{j\omega C_1} + \frac{1}{j\omega C_o}}\right) . \qquad (1)$$

Let ω_o be defined as a frequency for which

$$j\omega_o L_L + \frac{1}{j\omega_o C_o} = j\omega_o L_1 + \frac{1}{j\omega_o C_1} + \frac{1}{j\omega_o C_o} = 0 \quad . \qquad (2)$$

To satisfy this condition it is generally necessary that the value of L_L be increased by the addition of an external inductance.

For $\omega = \omega_o$, the impedance of the crystal becomes

$$Z = R_L + \left(\frac{1}{\omega_o C_o}\right)^2 \frac{1}{R_1} \tag{3}$$

and for ω near ω_o the impedance may be approximated as

$$Z \approx R_L + \left(\frac{1}{\omega_o C_o}\right)^2 \frac{1}{R_1 + j\omega L_1 + \frac{1}{j\omega C_1} + \frac{1}{j\omega C_o}} \tag{4}$$

where it is assumed that

$$\frac{\omega L_L}{R_L} >> \frac{\omega L_1}{R_1} \quad .$$

Let $X = \omega L_1 - \frac{1}{\omega C_1}$ and $K_1 = \frac{1}{\omega_o C_o} \approx \frac{1}{\omega C_o}$ for $\omega \approx \omega_o$. Equation (4) becomes

$$Z \approx R_L + \left(\frac{1}{\omega_o C_o}\right)^2 \frac{R_1 - j(X - K_1)}{R_1^2 + (X - K_1)^2} \quad . \tag{5}$$

If K_2 is defined as $R_1 K_1^2 + R_L R_1^2$, Equation (5) becomes

$$Z \approx \frac{K_2 + R_L(X - K_1)^2 - jK_1^2(X - K_1)}{R_1^2 + (X - K_1)^2}$$

or

$$|Z|^2 \approx \frac{[K_2 + R_L(X - K_1)^2]^2 + K_1^4(X - K_1)^2}{[R_1^2 + (X - K_1)^2]^2} \quad . \tag{6}$$

Current maximums and minimums occur when

$$\frac{d|Z|^2}{d\omega} = \left\{[K_2 + L_L(X - K_1)^2]^2 + K_1^4(X - K_1)^2\right\} (-2)[R_1^2 + (X - K_1)^2]^{-3}(2) \quad .$$

$$(X - K_1) + [R_1^2 + (X - K_1)^2]^{-2} \cdot \left\{2[K_2 + R_L(X - K_1)^2]\, R_L(2)(X - K_1)\right.$$

$$\left. + K_1^4(2)(X - K_1)\right\} = 0 \ . \qquad (7)$$

One factor of this expression is $(X - K_1) = 0$ giving a solution $X = K_1$ as a maximum value of $|Z|^2$ and therefore of $|Z|$. However, this defines the frequency ω_o. Therefore, the impedance at this maximum becomes

$$Z = R_L + \left(\frac{1}{\omega_o C_o}\right)^2 \frac{1}{R_1} = R_L(\omega_o L_L)^2/R_1 \qquad (8)$$

without any approximations. Since $Z = |Z|$ at $\omega = \omega_o$, R_1 may be determined by determining a ratio of voltage to current magnitudes providing R_L, ω_o and L_L can be determined.

Figure 2 shows a sketch of the variations of $|I| = |E|/|Z|$ as a function of frequency. The frequency, ω_o, may be readily identified and determined as the point of minimum current.

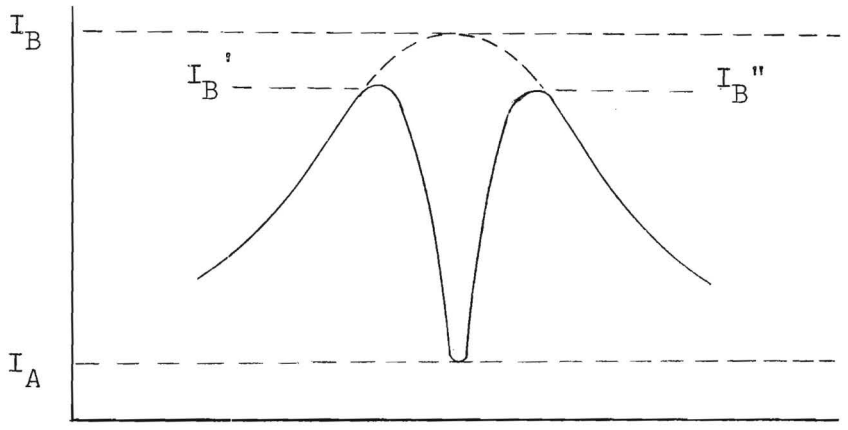

Figure 2. High-Frequency Crystal Current Variations.

If the motional arm, (R_1, L_1 and C_1), of the crystal could be removed, the impedance of the holder would be

$$Z_H = R_L + j\omega L_L + \frac{1}{j\omega C_o} \quad . \tag{9}$$

At $\omega = \omega_o$, the impedance would become

$$Z_H = |Z_H| = R_L = |E| / |I_B| \quad . \tag{10}$$

If $Z = |Z|$ of Equation (8) is replaced by E/I_A where I_A is the minimum current as shown in Figure 2 and if the result is divided by Equation (10), then

$$\frac{I_B}{I_A} = 1 + \frac{1}{R_L} \left(\frac{1}{\omega_o C_o}\right)^2 \frac{1}{R_1} \quad . \tag{11}$$

If the motional arm can be de-energized as supposed in arriving at Equation (9) and if R_L and C_o can be determined by some other means, it is then not even necessary to provide absolute voltage and current calibrations. For example, the voltage may be held constant for all measurements and only the relative current measured. Referring again to Figure 2, it may be seen that if I_B can be shown to be approximately equal to I_B' or I_B'' it is then not even necessary to remove the motional arm. (The difference between I_B, I_B' and I_B'' is exaggerated in the figure for convenience in defining the terms.)

The two current maximums may be found by obtaining the magnitude of Z in Equation (1), differentiating this with respect fo ω, and setting the result equal to zero. The approximation of Equation (3) can no longer be used since ω is not now sufficiently close to ω_o. The mathematics involved in the proposed differentiation process become very difficult, thus other approximations will be required.

Consider the admittance plot of Figure 3 where $Y = \frac{1}{Z}$ of Equation (1) and the parameters are such that Equation (2) is satisfied. The insert is exaggerated so that the various points may be readily identified. It may be seen that $|Y_B'|$ and $|Y_B''|$ are always less than $|Y_B|$. Also, $|Y_D'|$ and $|Y_D''|$ are always less than $|Y_B'|$ and $|Y_B''|$. Thus if $|Y_D'|$ and $|Y_D''|$ can be shown to be sufficiently close to $|Y_B|$ then most certainly $|Y_B'|$ and $|Y_B''|$ will be sufficiently close for use as an approximation to $|Y_B|$. But $|Y_D'|$ and $|Y_D''|$ occur when the susceptance of the circuit is zero, which is the same as saying that the reactance of the circuit is zero. Thus, it is sufficient to set the imaginary part of Z equal to zero. Therefore,

$$\omega L_L - \frac{1}{\omega C_o} - \left(\frac{1}{\omega C_o}\right)^2 \frac{\omega L_1 - \frac{1}{\omega C_1} - \frac{1}{\omega C_o}}{R_1^2 + \left(\omega L_1 - \frac{1}{\omega C_1} - \frac{1}{\omega C_o}\right)^2} = 0. \qquad (12)$$

Rearranging,

$$\omega^2 = \frac{1}{L_L C_o}\left(\frac{\omega L_1 - \frac{1}{\omega C_1}}{\omega L_1 - \frac{1}{\omega C_1} - \frac{1}{\omega C_o}}\right)$$

$$= \frac{1}{L_L C_o}\left[\frac{\omega^2 - (\omega_o')^2}{\omega^2 - \omega_o^2}\right] \qquad (13)$$

where

$$(\omega_o')^2 = \frac{1}{L_1 C_1} \qquad \text{and} \qquad \omega_o^2 = \frac{1}{L_1}\left(\frac{1}{C_1} + \frac{1}{C_o}\right) = \frac{1}{L_L C_o}$$

and under the assumption that

$$R_1^2 \ll \left(\omega L_1 - \frac{1}{\omega C_1} - \frac{1}{\omega C_o}\right)^2 . \qquad (14)$$

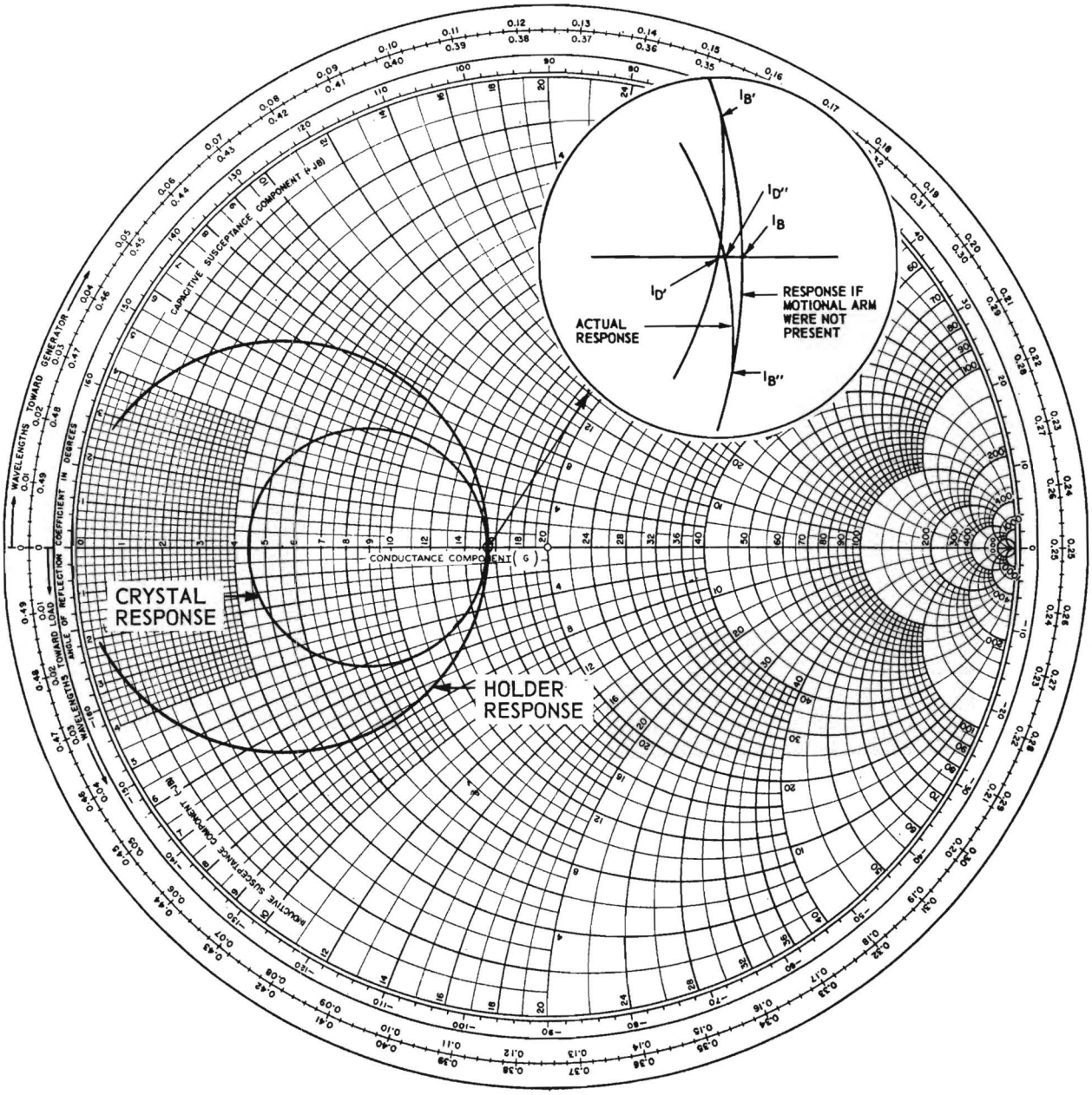

Figure 3. Admittance Diagram of a High Frequency Crystal.

Factoring,

$$\omega^2 = \omega_o^2 \frac{(\omega - \omega_o')(\omega + \omega_o')}{(\omega - \omega_o)(\omega + \omega_o)} \quad . \tag{15}$$

Since

$$\left.\begin{aligned} &\frac{\omega + \omega_o'}{\omega + \omega_o} \approx 1 \quad , \\ &\omega^2 = \omega_o^2 \frac{\omega - \omega_o'}{\omega - \omega_o} \end{aligned}\right\} \tag{16}$$

or

$$\omega = \omega_o \sqrt{\frac{\omega - \omega_o'}{\omega - \omega_o}} = \omega_o \sqrt{1 + \frac{\omega_o - \omega_o'}{\omega - \omega_o}} \quad .$$

Since $\omega_o - \omega_o' \ll \omega - \omega_o$, Equation (16) may be approximated as

$$\omega \approx \omega_o + 2\omega_o \left(\frac{\omega_o - \omega_o'}{\omega - \omega_o}\right) \quad . \tag{17}$$

Let $\omega = \omega_o + \Delta\omega$. Then Equation (17) becomes

$$\omega_o + \Delta\omega = \omega_o + 2\omega_o \left(\frac{\omega_o - \omega_o'}{\omega_o + \Delta\omega - \omega_o}\right) \tag{18}$$

or

$$\Delta\omega = 2\omega_o \left(\frac{\omega_o - \omega_o'}{\Delta\omega}\right) \tag{19}$$

giving

$$\Delta\omega^2 = 2\omega_o (\omega_o - \omega_o') \quad . \tag{20}$$

Therefore,

$$\Delta\omega = \pm\sqrt{2\omega_o(\omega_o - \omega_o')} \tag{21}$$

and

$$\omega \approx \omega_o \pm \sqrt{2\omega_o(\omega_o - \omega_o')} \quad . \tag{22}$$

It must now be shown that $Z \approx R_L$ at the frequency specified by Equation (22). This may be accomplished by considering separately the real and imaginary parts of Z.

The real part of Z becomes

$$\mathrm{Re}(Z) = R_L + \left(\frac{1}{\omega C_o}\right)^2 \frac{1}{R_1}\left[\frac{1}{1 + \frac{\left(\omega L_1 - \frac{1}{\omega C_1} - \frac{1}{\omega C_o}\right)^2}{R_1^2}}\right] \quad . \tag{23}$$

It is only necessary to show that the second term is negligible. In the bracketed term, let

$$\omega L_1 - \frac{1}{\omega C_1} - \frac{1}{\omega C_o} = X_o = \frac{L_1}{\omega}(\omega^2 - \omega_o^2) \tag{24}$$

and substitute

$$\omega^2 = (\omega_o + \Delta\omega)^2 \approx \omega_o^2 + 2\Delta\omega\omega_o$$

$$= \omega_o^2 \pm 2\omega_o \sqrt{2\omega_o(\omega_o - \omega_o')} \quad ,$$

which is obtained from Equations (18) and (22), into Equation (24), giving

$$X_o = \frac{2L_1\omega_o}{\omega} \sqrt{2\omega_o(\omega_o - \omega_o')} \quad . \tag{25}$$

Therefore,

$$\frac{X_o^2}{R_1^2} = \left(\frac{\omega_o L_1}{R_1}\right)^2 \frac{8}{\omega^2}\left[\omega_o(\omega_o - \omega_o')\right] \tag{26}$$

and Equation (23) may be written as

$$\mathrm{Re}(Z) = R_L + \left(\frac{1}{\omega C_o}\right)^2 \frac{1}{R_1}\left[\frac{1}{1 + X_o^2/R_1^2}\right] . \tag{27}$$

For the purpose of showing that $X_o^2/R_1^2 >> 1$, ω in Equation (26) may be replaced by ω_o giving

$$\frac{X_o^2}{R_1^2} = \frac{8Q_o^2}{\omega_o}(\omega_o - \omega_o') \tag{28}$$

where

$$Q_o = \frac{\omega_o L_1}{R_1} .$$

Equation (28) may be further simplified since

$$\begin{aligned}\omega_o - \omega_o' &= \sqrt{\frac{1}{L_1}\left(\frac{1}{C_1} + \frac{1}{C_o}\right)} - \sqrt{\frac{1}{L_1}\left(\frac{1}{C_1}\right)} \\ &\approx \left[\sqrt{\frac{1}{L_1 C_1}} + \frac{1}{2}\,\frac{1/L_1 C_o}{\sqrt{\frac{1}{L_1 C_1}}}\right] - \sqrt{\frac{1}{L_1 C_1}} \\ &= \frac{1}{2}\,\omega_o'\,\frac{C_1}{C_o} \approx \frac{1}{2}\,\omega_o\,\frac{C_1}{C_o}\end{aligned} \tag{29}$$

where the first approximation is obtained by using only the first two terms of a binomial expansion.

Therefore,

$$\begin{aligned}\frac{X_o^2}{R_1^2} &\approx \frac{8Q_o^2}{\omega_o}\left(\frac{1}{2}\right)\omega_o\,\frac{C_1}{C_o} = \frac{4Q_o^2 C_1}{C_o} \\ &= \frac{4\omega_o L_1 C_1 Q_o}{R_1 C_o} = \frac{4Q_o}{\omega_o R_1 C_o} .\end{aligned} \tag{30}$$

For a crystal having the parameters

$$Q_o = 10^4,$$

$$\omega_o = 300 \cdot 2\pi \cdot 10^6 \text{ rad/sec}, \qquad (31)$$

$$R_1 = 200 \text{ ohms},$$

and $$C_o = 7 \cdot 10^{-12} \text{fd}.$$

Equation (30) becomes

$$\frac{X_o^2}{R_1^2} \approx 1.6 \cdot 10^4 .$$

(It may be noted that this result validates the assumption of Equation (14) since the right side of Equation (14) is X_o^2.)

Equation (27) becomes

$$\text{Re}(Z) = R_L + 18 \cdot 10^{-4} \approx R_L$$

where R_L will generally be greater than 50 ohms in a practical measurement system.

The imaginary part of Z is zero within the accuracy of the approximations by the condition imposed by Equation (12). For the parameter values of Equations (31), Im(Z) is less than one percent of R_L for practical values of R_L. The error in calculating the magnitude of Z due to Im(Z) is therefore, less than 0.01 percent.

It will be observed that the parameter values of Equations (31) were chosen for the most adverse conditions likely to be encountered.

The results of Equations (12) through (31) may now be applied to rewrite Equations (11) as

$$\frac{I_B}{I_A} \approx \frac{I_B'}{I_A} \approx \frac{I_B''}{I_A} \approx 1 + \frac{1}{R_L}\left(\frac{1}{\omega_o C_o}\right)^2 \frac{1}{R_1} \quad . \tag{32}$$

Before R_1 can be calculated it is still necessary, of course, to determine the values of R_L and C_o. C_o of the crystal can be measured at a low frequency. R_L can be calculated from Equation (10) provided absolute voltage and current calibrations can be made since I_B may be replaced by I_B' or I_B''. R_L may also be determined by combining with Equation (32) a second similar equation obtained by increasing R_L by some amount ΔR and again determining the current ratio. The two equations may then be solved simultaneously for R_L. R_1 may then be calculated from Equation (32).

Q_o may be determined from the following consideration. Let

$$\left.\begin{aligned} \Delta &= \frac{\omega}{\omega_o} - \frac{\omega_o}{\omega} \quad , & Q &= \frac{\omega_o L_L}{R_L} \\ \text{and} \qquad Q_o &= \frac{\omega_o L_1}{R_1} = \frac{1}{R_1 \omega_o C_1} \quad . \end{aligned}\right\} \tag{33}$$

The normalized current, U, is

$$U = \frac{I}{E} R_L \quad . \tag{34}$$

From Equations (1), (33) and (34)

$$\frac{1}{U} = 1 + jQ\Delta + K \frac{1}{1 + jQ_o\Delta} \tag{35}$$

where

$$K = \frac{1}{R_L R_1}\left(\frac{1}{\omega C_o}\right)^2 \quad . \tag{36}$$

The quantity K is essentially constant over the frequency range near ω_o. Therefore,

$$K \approx \frac{1}{R_L R_1} \left(\frac{1}{\omega_o C_o}\right)^2 . \tag{37}$$

For $Q\Delta \ll 1$, which is true for ω very near to ω_o, Equation (35) becomes

$$(Q_o\Delta)^2 = \frac{(1 + K)^2 U^2 - 1}{1 - U^2} . \tag{38}$$

If the current variations are as indicated in Figure 4 and since K is considered constant, K may be evaluated at $\Delta = 0$ from Equation (35) as

$$K + 1 = \frac{1}{U} = \frac{b}{a} . \tag{39}$$

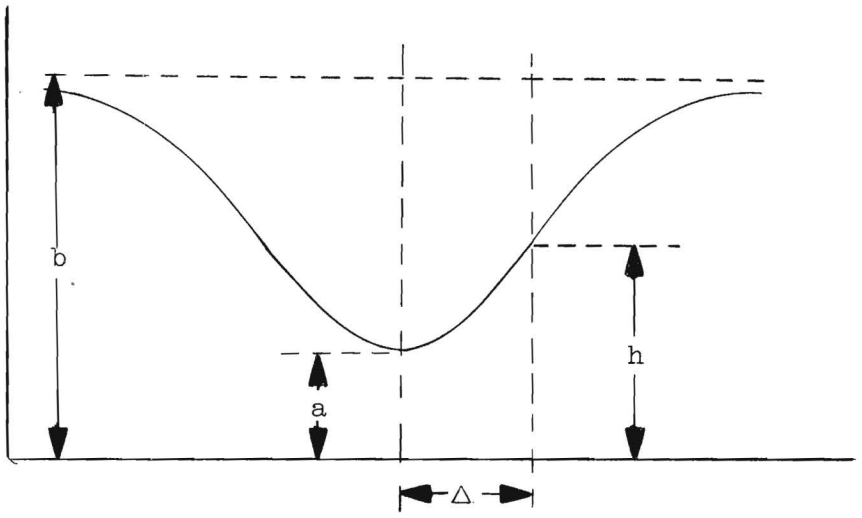

Figure 4. Crystal Current Variations.

With this result, Equation (38) becomes

$$(Q_o\Delta)^2 = \frac{\left(\frac{h}{a}\right)^2 - 1}{1 - \left(\frac{h}{b}\right)^2} = \frac{b^2}{a^2} \frac{h^2 - a^2}{b^2 - h^2} . \tag{40}$$

Since Δ is readily measured, Q_o may be readily calculated from Equation (40).

To summarize, the crystal parameters may be obtained as follows:

1. Plot points on the current response curve as indicated by Figure 4, recording relative current amplitude and frequency at points a and b and some arbitrary point h.

2. Increase R_L by adding an external resistor and record the new currents a and b.

3. Substitute the two values of a and b into Equation (32) and solve for R_L (note that I_A and I_B are respectively equal to a and b).

4. Measure C_o at some low frequency and substitute C_o, R_L and ω_o together with a and b into Equation (32) and solve for R_1.

5. Substitute a, b and h into Equation (40) and solve for Q_o (Δ is the difference of two known frequencies).

6. Since Q_o, ω_o and R_1 are now known, L_1 and C_1 may be found from the last of Equations (33).

This procedure has been applied to a theoretical crystal by use of an electronic computer. Typical element values for the equivalent circuit of a crystal were selected and the corresponding current plotted for unity voltage. From this curve alone, the above steps were used to calculate the various crystal parameters. The calculated data agreed with the original data to an accuracy limited only by the resolution in reading the curve. This indicated that none of the approximations in arriving at the above steps contributed any appreciable errors.

PROGRESS REPORT NO. 2

PROJECT NO. A-362

INVESTIGATION OF METHODS FOR MEASURING THE EQUIVALENT ELECTRICAL PARAMETERS OF QUARTZ CRYSTALS

By

SAMUEL N. WITT, JR. AND VANCE KEITH WOODCOX

- o - o - o - o - o -

CONTRACT NO. DA-36-039 SC-74948
DEPARTMENT OF THE ARMY PROJECT: 3-26-05-703

- o - o - o - o - o -

15 JANUARY 1958 TO 15 APRIL 1958

PLACED BY THE U. S. ARMY
SIGNAL ENGINEERING LABORATORIES
FORT MONMOUTH, NEW JERSEY

Engineering Experiment Station
Georgia Institute of Technology
Atlanta, Georgia

ENGINEERING EXPERIMENT STATION
of the Georgia Institute of Technology
Atlanta, Georgia

PROGRESS REPORT NO. 2

PROJECT NO. A-362

INVESTIGATION OF METHODS FOR MEASURING THE EQUIVALENT ELECTRICAL PARAMETERS OF QUARTZ CRYSTALS

By

SAMUEL N. WITT, JR. AND VANCE KEITH WOODCOX

- o - o - o - o - o -

CONTRACT NO. DA-36-039 SC-74948
DEPARTMENT OF THE ARMY PROJECT: 3-26-05-703

- o - o - o - o - o -

The object of this project is to develop methods for measuring the equivalent electrical parameters of quartz crystals in the frequency range of 175 to 300 mc/sec.

15 JANUARY 1958 TO 15 APRIL 1958

PLACED BY THE U. S. ARMY
SIGNAL ENGINEERING LABORATORIES
FORT MONMOUTH, NEW JERSEY

TABLE OF CONTENTS

This report contains 47 pages.

LIST OF FIGURES

I. PURPOSE

The purpose of the project is fourfold:

1. To continue the study and investigation of methods and techniques for measuring the equivalent electrical parameters of quartz crystal units in the frequency range of 175 to 300 mc/sec, including:

   (a) determination of measurement errors,

   (b) development of a means for directly measuring the power drive of a crystal unit, and

   (c) development of means for measuring the effective resistance of the crystal unit at the series resonant condition.

2. Utilize the information from Investigation 1., above, in the establishment of a standard crystal measurement system which will:

   (a) measure the effective resistance of the crystal at any frequency within the crystal resonance range with a target accuracy of $\pm$ 1 percent,

   (b) determine the phase angle of the crystal at any frequency within the crystal resonance range with a target accuracy of $\pm$ 1 degree,

   (c) include a means of measuring directly the power drive of a crystal unit within $\pm$ 20 percent, and

   (d) be capable of determining the equivalent electrical parameters of the crystal unit.

3. Utilize the information from Investigations 1. and 2. in investigations of circuitry for ultimate utilization in the development of a practical crystal test instrument for the frequency range 175 to 300 mc/sec which will:

(a) measure the effective resistance of the crystal unit at series resonance within a resistance range of 20 to 200 ohms with an accuracy of $\pm$ 5 percent,

(b) subject the crystal to any power drive within 0.2 and 4 mw and provide a means of determining directly the power drive with an accuracy of $\pm$ 20 percent,

(c) provide a means of operating the crystal within $\pm$ 0.0005 percent of the series resonant frequency, and

(d) have a power drive versus resistance characteristic from 175 to 300 mc/sec which will not vary more than 3 to 1 for the resistance range of 40 to 150 ohms.

4. Investigate any other problems pertinent to crystal measurements in the VHF range which are mutually agreed upon by the contractor and the Contracting Officer's Technical Representative.

II. ABSTRACT

The major developments during this report period centered around elements of the Crystal Measurements Standard. Some crystal measurement data were obtained principally to evaluate various sources of error in the system. As a result of these data it was found necessary to construct various radio-frequency amplifiers to provide isolation between the Marconi Signal Generator and the Admittance Meter.

A new General Radio Admittance Meter with special calibration curves was received together with various standard terminations. This equipment was not completely evaluated.

Shielding of the Eddystone UHF Receiver for use as a null detector was further improved to a point where leakage was negligible. Commercial filters and laboratory constructed copper-covered cables were incorporated to obtain the improvements. The equivalent noise input to the receiver was found to be less than 0.3 microvolts over the frequency range of interest.

The accuracy of the crystal power measurement system was further improved by the addition of a potentiometer across the output of one of the directional coupler diodes. By using the specially prepared frequency calibration curve, accuracies to within $\pm$ 10 percent were obtained over the frequency range from 175 to 300 mc/sec and for voltage standing wave ratios from 1 to 6.5 and powers between 0.2 and 10 mw.

The crystal measurement system described in the APPENDIX of Progress Report No. 1 was investigated further. Close agreement in measurements was obtained for one crystal at 245 mc/sec. Poor agreement resulted for the same crystal at 175 mc/sec.

III. PUBLICATIONS, LECTURES, REPORTS AND CONFERENCES

No publications, lectures or reports have resulted from work under this contract.

A visit to USASEL was made on February 18, 1958 by Samuel N. Witt, Jr. of Georgia Tech to discuss technical activities and progress on this project. Because of weather conditions, the Signal Engineering Laboratories were closed on this day and the planned conference could not be held. However, Mr. D. Pochmersky was contacted and a conference at another location resulted. The first Progress Report was discussed in detail. Other discussions concerning the future technical activities of the project ensued. It was agreed that future efforts should be directed as proposed in the PURPOSE and PROGRAM FOR NEXT INTERVAL sections of the report. No changes in objectives or methods of approach resulted from this conference.

On February 18, 1958, Mr. Pochmersky and Mr. Witt visited Mr. R. A. Soderman at General Radio Company, West Concord, Massachusetts. A conference was held concerning the calibration of a General Radio Admittance Meter Type 1602B and associated equipment which has been ordered by the project for use with the Crystal Measurements Standard. Mr. Soderman stated that he believed that overall calibration could be accomplished to within about one percent maximum error over the frequency range from 100 to 400 mc/sec and for admittance magnitudes of the order of 20 millimhos. Admittance Meter readings requiring the use of high multiplying factors would be less accurate.

IV. FACTUAL DATA

A. Introduction

This project is essentially a continuation of the work which was begun under Contract DA-36-039 SC-71191. Major emphasis on this project, however, has been on the development of the Crystal Measurements Standard.

During the first quarter of this project several improvements were made in the Crystal Measurements Standard. These included primarily the addition of an Eddystone UHF Receiver for use as a null detector with the General Radio Admittance Meter, the addition of a crystal drive level measurement system, and the selection and purchase of a new GR Admittance Meter to be specially calibrated for use in the system.

The UHF receiver was delivered near the end of the first quarter and was only partially evaluated in Progress Report No. 1. The evaluation is concluded in this report together with further descriptions of the necessary shielding and filtering to prevent external r-f leakage and interference.

The crystal drive level measurement system was essentially completed during the first quarter; however, some further refinements and extensive calibrations were made during the current period. Overall accuracy of the system now exceeds the initial requirements specified in the PURPOSE section of this report.

The new GR Admittance Meter and other auxiliary equipment were ordered during the first quarter but were only recently received. This equipment was specially calibrated by the manufacturer for use with the Crystal Measurements Standard. This equipment has not yet been completely evaluated due to its recent arrival.

Some crystal measurements were made during the first quarter and continued during this quarter to further evaluate possible sources of error in the Crystal

Measurements Standard. These measurements resulted in the construction of several high-frequency r-f amplifiers to provide isolation between the Marconi Signal Generator and the Admittance Meter. The need for such amplifiers was recognized previously because of the maximum drive level requirements. It was previously reported that commercial amplifiers were not available for this purpose. Recent developments have, however, made available at least one commercial amplifier which is believed to be capable of providing the necessary gain and isolation. Such an amplifier has been ordered.

A new method of measuring the parameters of quartz crystals was reported in Progress Report No. 1. This method was based on a modification of a low-frequency measurement procedure proposed by Dr. Issac Koga of Tokyo, Japan. The method was only partially evaluated during the first quarter and investigations have continued through the current quarter. No conclusions concerning the eventual possible accuracy of this method have yet been reached; however, as previously stated, the present system does provide some useful information concerning quartz crystals at high frequencies. In particular, useful information about spurious responses is readily obtained.

B. Crystal Measurements Standard

1. Experimental Crystal Data

The Crystal Measurements Standard, as shown in Figures 1 and 2, was used to measure the parameters of several quartz crystals in the frequency range from 175 to 300 mc/sec. Crystals and responses which have been previously described in reports under Contract No. DA-36-039 SC-71191 were used so that direct comparisons could be made. Most of the circle diagrams were identical within the resolution of the instruments. However, it was observed that with some crystals, frequency discrepancies were present at points along the circle diagrams. To

better analyze this phenomenon, the conductive and susceptive components of the crystal responses were plotted as functions of frequency. A typical result is

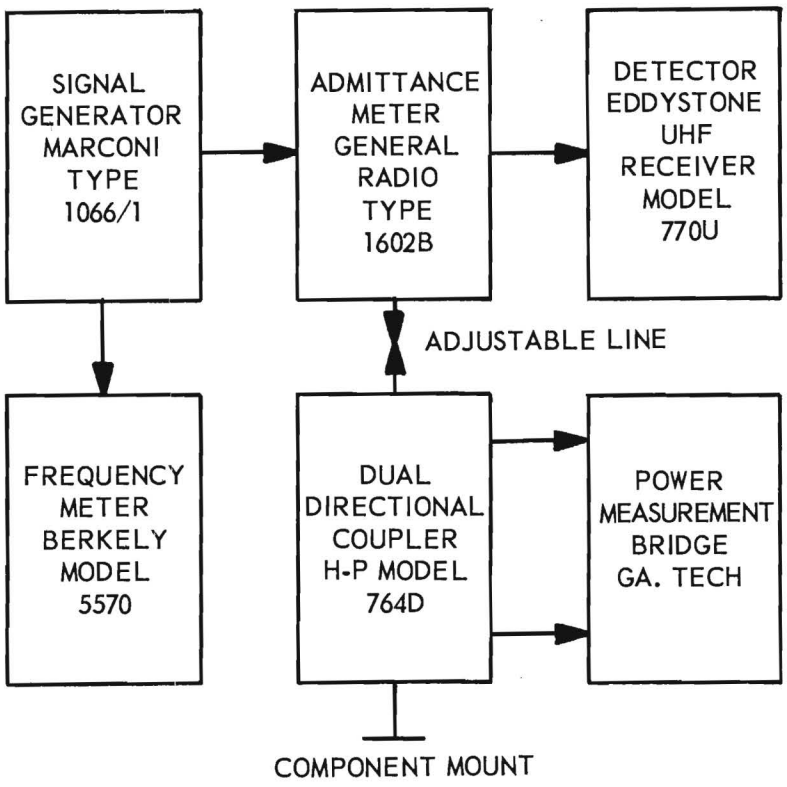

Figure 1. Block Diagram of the Prototype Crystal Measurements Standard.

shown in Figure 3. Shown also in the figure are the curves for the same crystal plotted from data obtained more than a year ago. Several experiments were performed in an attempt to determine the cause of the discontinuity in the recent measurements.

It was determined that discontinuities as shown in Figure 3 generally occurred when no isolation was used between the Marconi Signal Generator and the Admittance Meter. It appeared that the reactive loading of the crystal on the

Figure 2. A Typical Setup of the Crystal Measurements Standard.

generator produces some type of frequency modulation that results in erroneous readings on the Berkeley Frequency Meter. The exact nature of the phenomena have not been determined; however, satisfactory preventative measures have been found. It is only necessary to provide approximately 20 db of isolation between the signal generator and the Admittance Meter. Since the output of the signal generator was already too low to obtain the maximum required crystal drive level, the isolation was obtained by the addition of a r-f amplifier between the signal generator and the Admittance Meter. An attenuator pad was also included

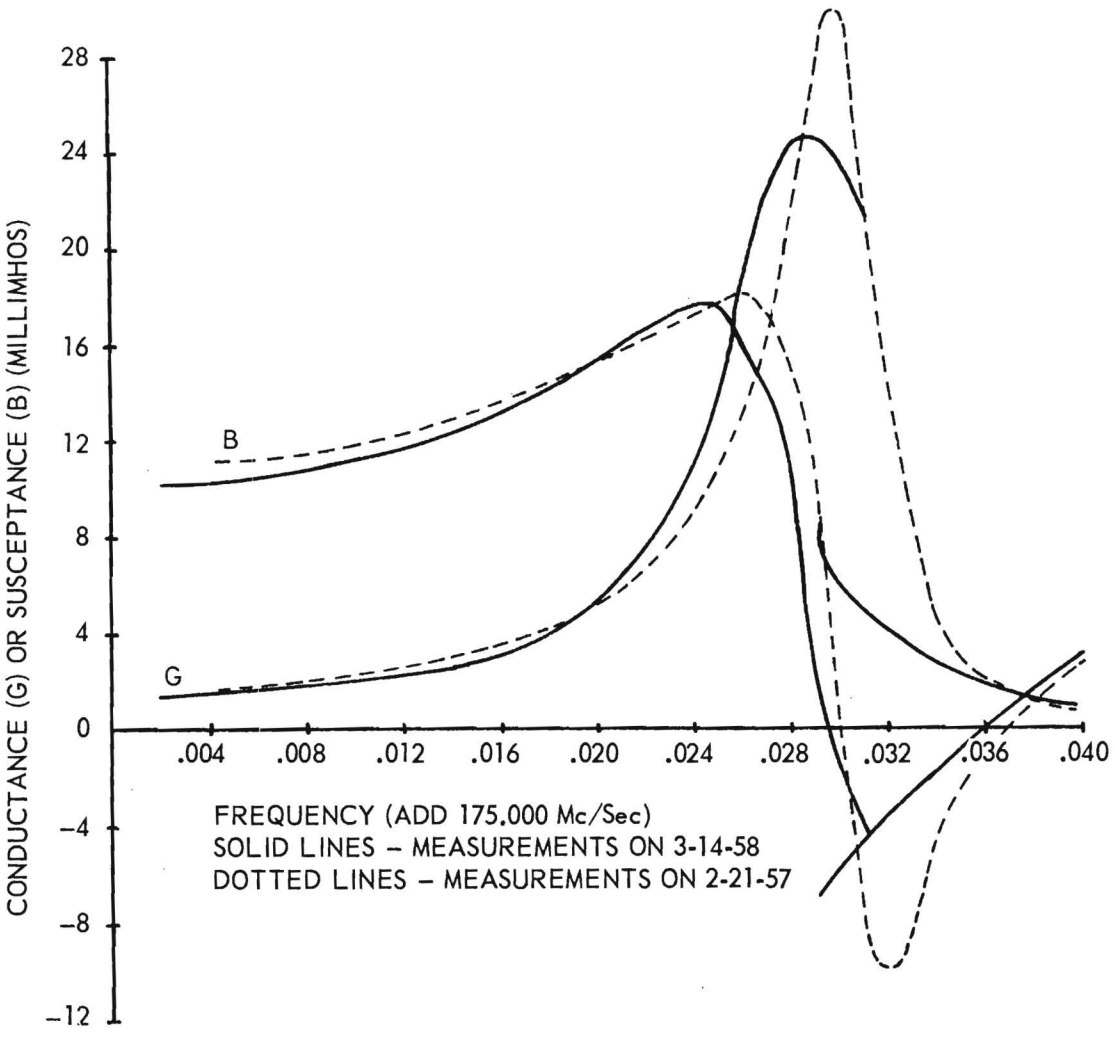

Figure 3. Crystal Measurement Discontinuities Caused by Close Coupling.

for some measurements, depending upon the frequency involved and the amount of amplifier gain available. Amplifiers used for this purpose are discussed in a later section of this report.

When the amplifier isolation was used in repeating the run of Figure 2, curves were obtained which still did not compare favorably with the results of a year ago. All discontinuities were, however, eliminated. The equipment used for the current run and for the run a year ago was identical with the exception of the null detector, the power measuring system, and some additional shielding of cables. Several factors can, however, account for differences observed: (1) the crystal characteristics may have changed during the elapsed time, (2) the Admittance Meter calibration may have changed slightly, (3) r-f leakage in the earlier setup may have caused some error, (4) the introduction of the directional coupler may cause some error which has not yet been detected because of other larger errors, and (5) temperature and crystal drive level were probably different. Shortly after an investigation was begun to evaluate these possible errors, a new Admittance Meter was received from General Radio Company. It was therefore, decided that further investigations with the older Admittance Meter would serve no useful purpose since all future measurements would be made with the new instrument. Thus, this investigation was temporarily discontinued.

At the same time that the above investigation was being conducted, efforts were being made to further evaluate the effects of the directional coupler on the accuracy of the measurements. Data indicated that the coupler introduced negligible error into the system. However, the data will not be presented here since they were obtained with the original Admittance Meter, whose accuracy was insufficient to detect small errors. All of these investigations will be continued at a later date with the new Admittance Meter.

The new Admittance Meter was not received from General Radio Company in time to obtain general crystal measurement data for this report.

2. Radio-Frequency Amplifiers

It is desirable to include an r-f amplifier between the Marconi Signal Generator and the Admittance Meter for two reasons: (1) to eliminate the discontinuity phenomenon as described previously and (2) to increase the output of the signal generator so that crystal drive levels of at least 4 mw may be obtained even in high resistance crystals. An amplifier to accomplish these purposes, when used with the Marconi Signal Generator, should have the following specifications: (1) 20 db of gain from 175 to 300 mc/sec, (2) input and output impedances of 50 ohms, (3) maximum power output of at least 30 mw into a 50-ohm load, (4) at least 20 db of isolation between the input and output, and (5) either broadband characteristics or provisions for easy tuning over the desired frequency range. No commercially available amplifiers having these specifications have been found.

Efforts have been directed toward constructing an amplifier to meet the above specifications. A literature investigation of chain-amplifiers indicated that an amplifier to provide the necessary gain at the required impedance level would require an excessive number of tubes. Other possibilities included such amplifier types as cavity amplifiers and transmission line amplifiers. However, the maximum obtainable gain using only one tuned circuit would be limited to about 10 db for a single tube. Several prototype amplifiers were constructed and tested. Three workable amplifiers resulted, each having a maximum gain of less than 10 db and each covering most of the required frequency range. A picture of these amplifiers is shown in Figure 4. In addition to insufficient gain, each of the amplifiers had other disadvantages.

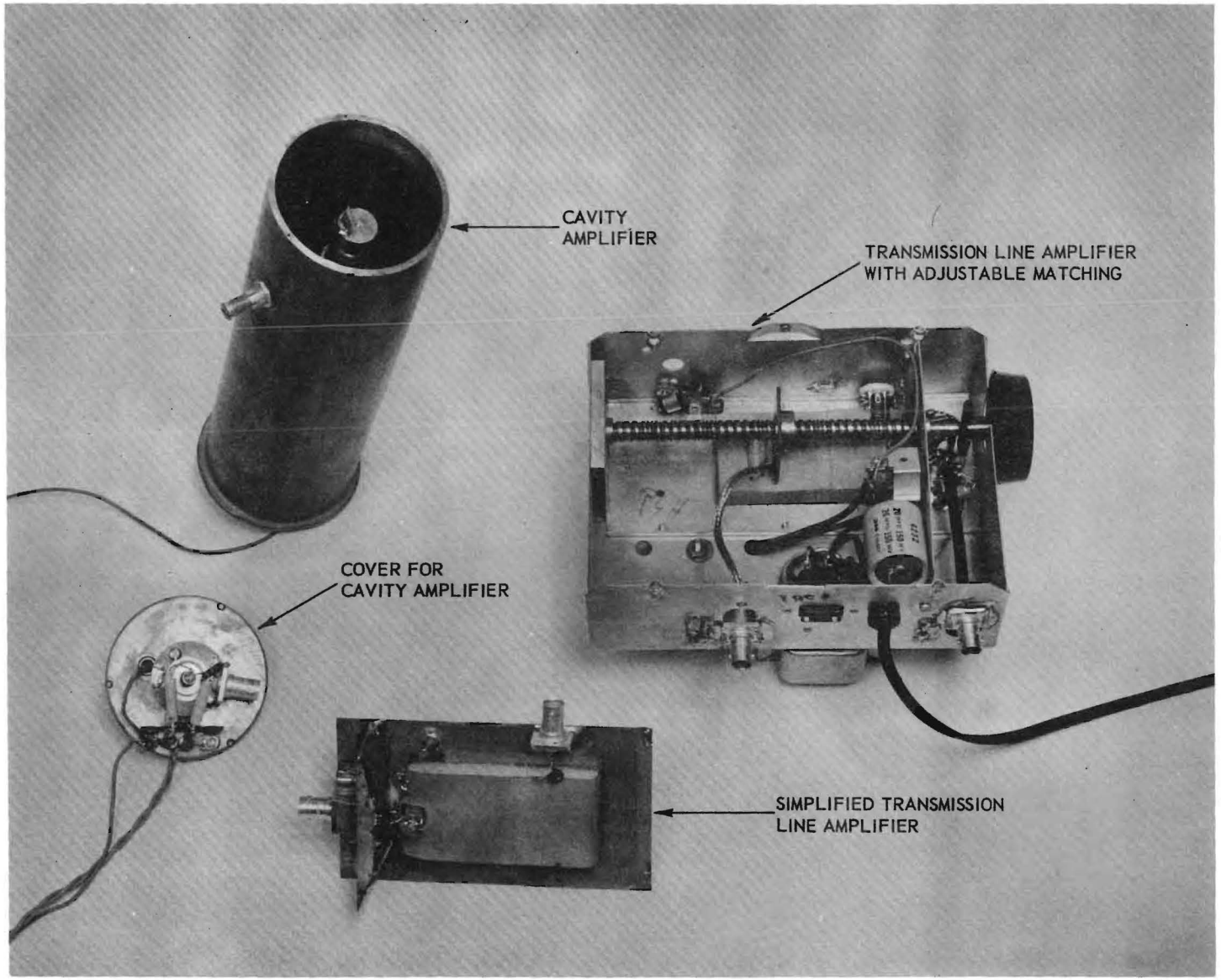

Figure 4. Typical R-F Amplifiers.

The tuning of the cavity amplifier was critical because of the high-Q of the tuned circuit. Its frequency coverage extended from 150 to 280 mc/sec and its input and output impedances could be readily adjusted to 50 ohms at any one frequency. For a mean impedance level adjustment, the gain varied from 10 db to as low as 7 db as the frequency was varied. Because of its grounded grid configuration using a 5876 pencil triode, the amplifier provided adequate input-output isolation.

The simplified transmission line amplifier made use of a Western Electric 417A high-transconductance triode in a grounded grid configuration. Because of the very high transconductance, difficulties were encountered with oscillations. The difficulties were also partially caused by the fact that the filament pins of this tube are located adjacent to the plate pin, thus providing a feedback path from plate to cathode. This amplifier, at times, provided gains as high as 20 db, but would oscillate when tuned to other frequencies. When the amplifier was modified to make it completely stable, only 3 or 4 db of gain could be obtained. The amplifier was unsuitable for routine use for this reason.

The transmission line amplifier with adjustable matching consisted of a modification of an Electro-Voice UHF Television Booster. The input and output circuits were reconnected for parallel rather than push-pull operation. The plate transmission line was modified for single-ended operation with a variable position output tap. The amplifier used two of 6AN4 type tubes whose combined output capacitance necessitated the use of a short transmission line to tune to the highest frequency. With the two tubes in use, a gain of 6 db was obtained from 200 to 300 mc/sec. When one tube was removed, the amplifier tuned from 210 to 330 mc/sec with gains from 5.5 db to 10.5 db respectively. Some instability was encountered both with a single tube and with two tubes in use.

Regeneration accounts for the higher gain at some frequencies with the single tube than with two tubes.

Of the three amplifiers, the cavity amplifier provided the most consistently stable operation. However, it was necessary to retune the amplifier during some crystal measurement runs.

Examining the characteristics of the various tubes used with the different amplifiers shows that some of the gains obtained are greater than theoretically possible for grounded grid operation with direct input at the cathodes at a 50-ohm impedance level. Higher gains resulted from either wanted or unwanted regeneration. Still higher gains could have been obtained in some cases by using a tuned transformer in the cathode circuits, which would, however, have necessitated the use of ganged tuning and would also have aggravated the regeneration problems.

It was concluded that none of the amplifiers were completely satisfactory for the intended purpose. Investigations were again made concerning the availability of commercial amplifiers. A chain amplifier has been ordered which, it is believed, will prove satisfactory although it will not provide the full 20 db of gain which is desired.

3. Calibration of Instruments

During this report period a new Admittance Meter Type 1602B and other coaxial components were received from General Radio Company together with specially prepared calibration data. A calibration chart was supplied with the Admittance Meter to provide admittance corrections for improved accuracy in the frequency range from 175 to 300 mc/sec and particularly for admittance magnitudes of the order of 20 millimhos. These calibration charts are included here as Figures 5 and 6 to illustrate the types of corrections required and the order

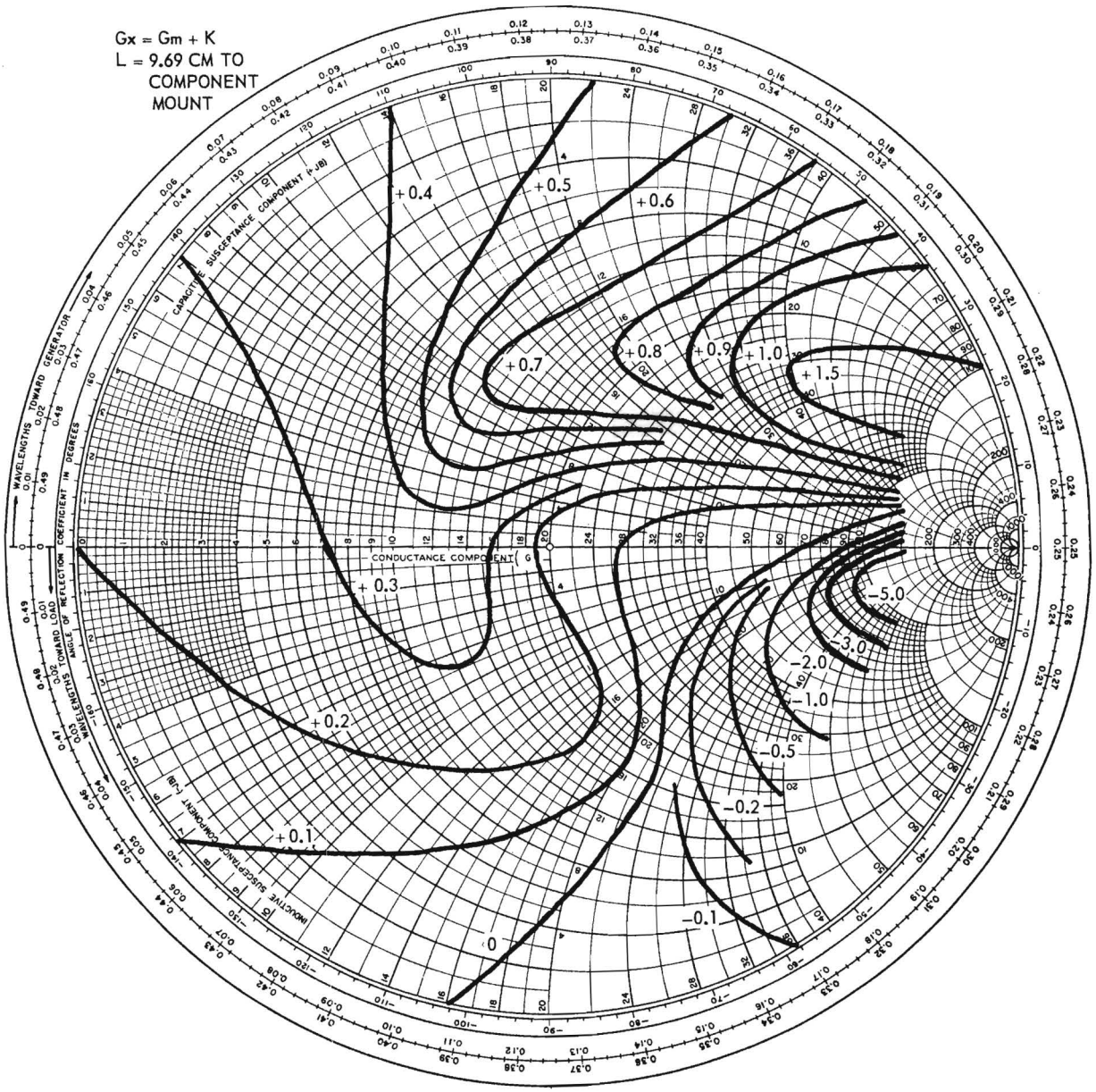

Figure 5. Conductance Corrections for GR Admittance Meter Serial No. 1401.

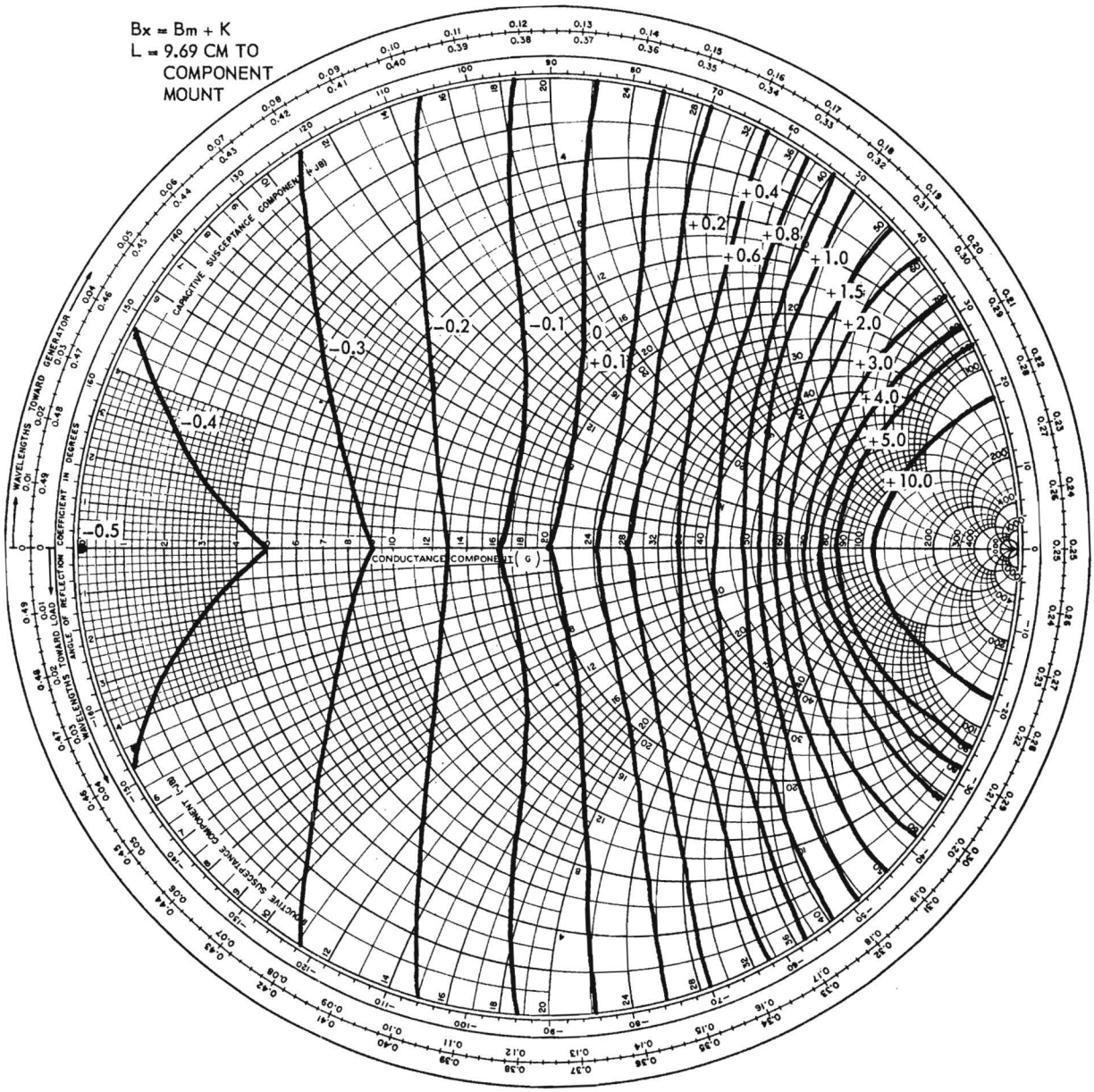

Figure 6. Susceptance Corrections for GR Admittance Meter Serial No. 1401.

of the accuracy to be expected both with and without the application of corrections. It should be noted that these charts are valid only for the particular Admittance Meter whose serial number is indicated. It should also be noted that this instrument is a standard production run instrument and was not modified in any way to obtain this accuracy.

Also ordered and received with the Admittance Meter were three resistive terminations and one component mount. The component mount together with its open and short terminations were specially adjusted in length by General Radio Company to equal the length of the standard resistive terminations. Calibration data on the resistive terminations are shown in Figure 7. These terminations were purchased as an aid in calibrating the complete Crystal Measurements Standard.

The Admittance Meter and other equipment were not received in time to perform any cross-calibration measurements during this report period.

Data obtained during this report period concerning the calibration of other instruments are discussed in a later section under Power Measurements.

4. Detector Systems

Further evaluation data have been compiled on the Eddystone Model 770U Receiver which was received during the last report period. It was determined that the Centralab Feed Thru Capacitors and the Ohmite Chokes installed between the outer shield box and the receiver as shown in Figure 3 of Progress Report No. 1 did not provide sufficient isolation. To further improve the filtering, these components were replaced by four Tobe Filterettes as shown in Figure 8. The manufacturer's specifications state that this filter has a 45-db attenuation at 150 kc/sec and greater than 45-db attenuation from 150 kc/sec to 1000 mc/sec. It was also determined that the standard RG-58 BNC cable used between the

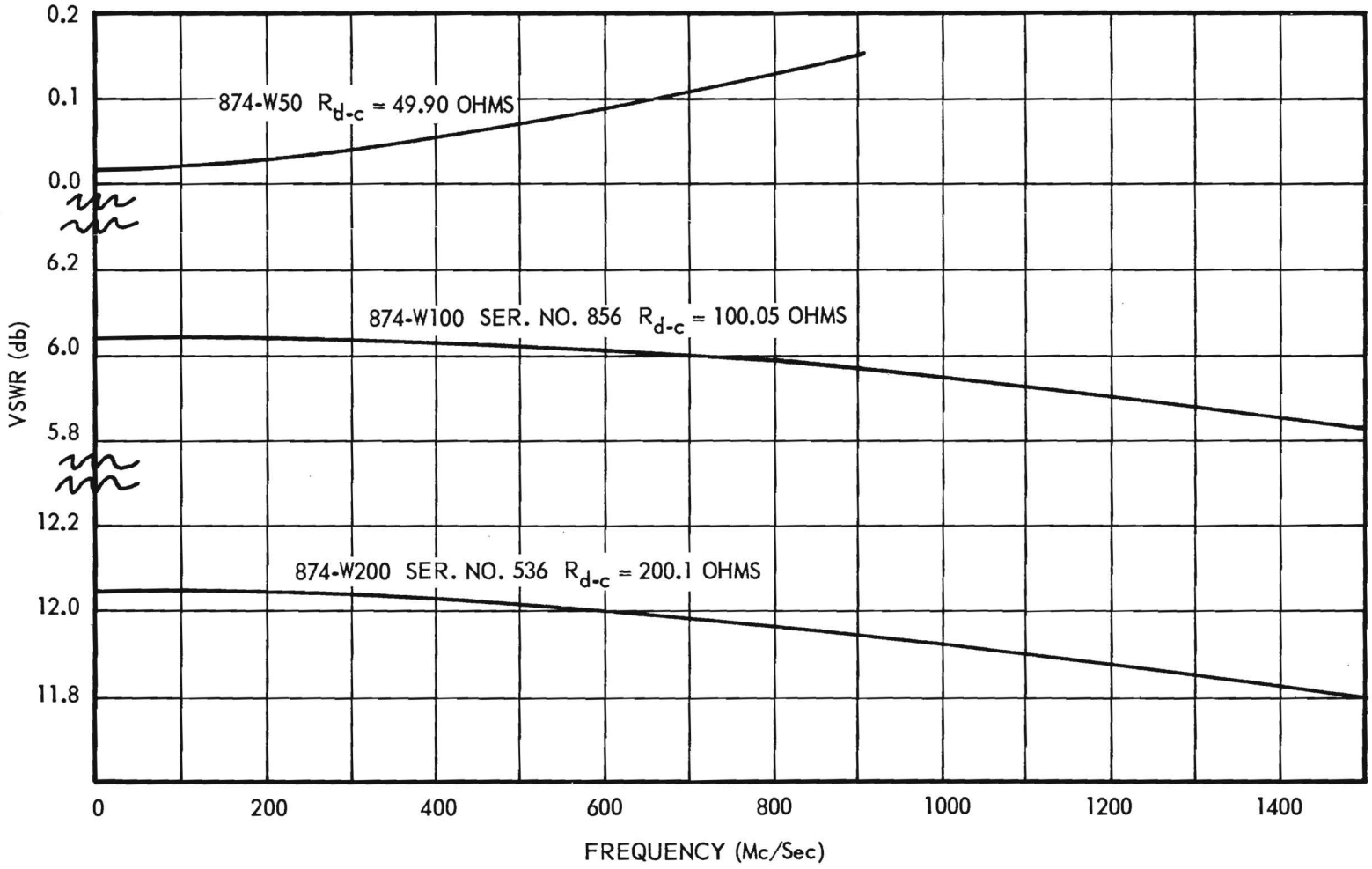

Figure 7. Calibration of GR Resistive Terminations with Serial Numbers as Shown.

receiver antenna terminal and the Admittance Meter was not sufficiently shielded to eliminate it as a source of stray signal pickup. Tests were made with other types of commercial cable with the same results. A special cable was finally made up by inserting a RG-58 cable into a copper tube and soldering both ends to BNC connectors. This modified cable provided adequate shielding.

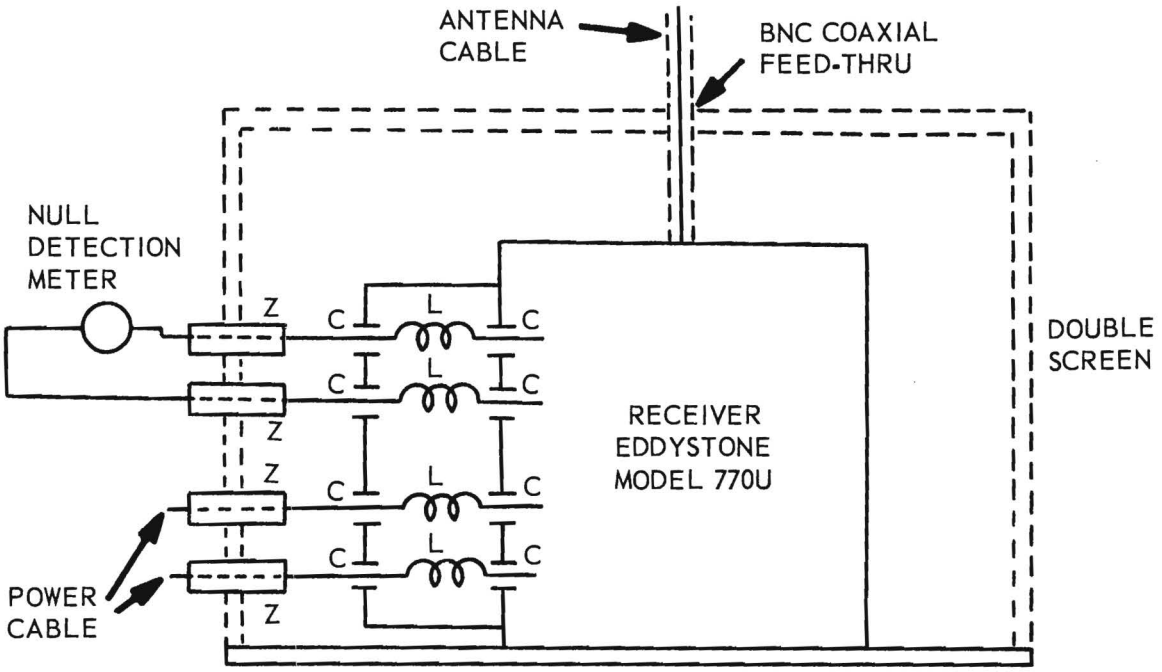

Figure 8. Stray Signal Shielding of the Eddystone UHF Receiver.

To determine the effectiveness of the various shieldings, several data runs were made. The first run was performed with all shieldings in use and with no external signal source. The receiver remained in the shield box with the cover closed. One end of the special copper-covered cable was placed on the antenna terminal and the other end was terminated with a short-circuit. A plot of the output current versus frequency is given in Figure 9(a). Except for two isolated responses, one at 225 mc/sec, and the other at 270 mc/sec, the

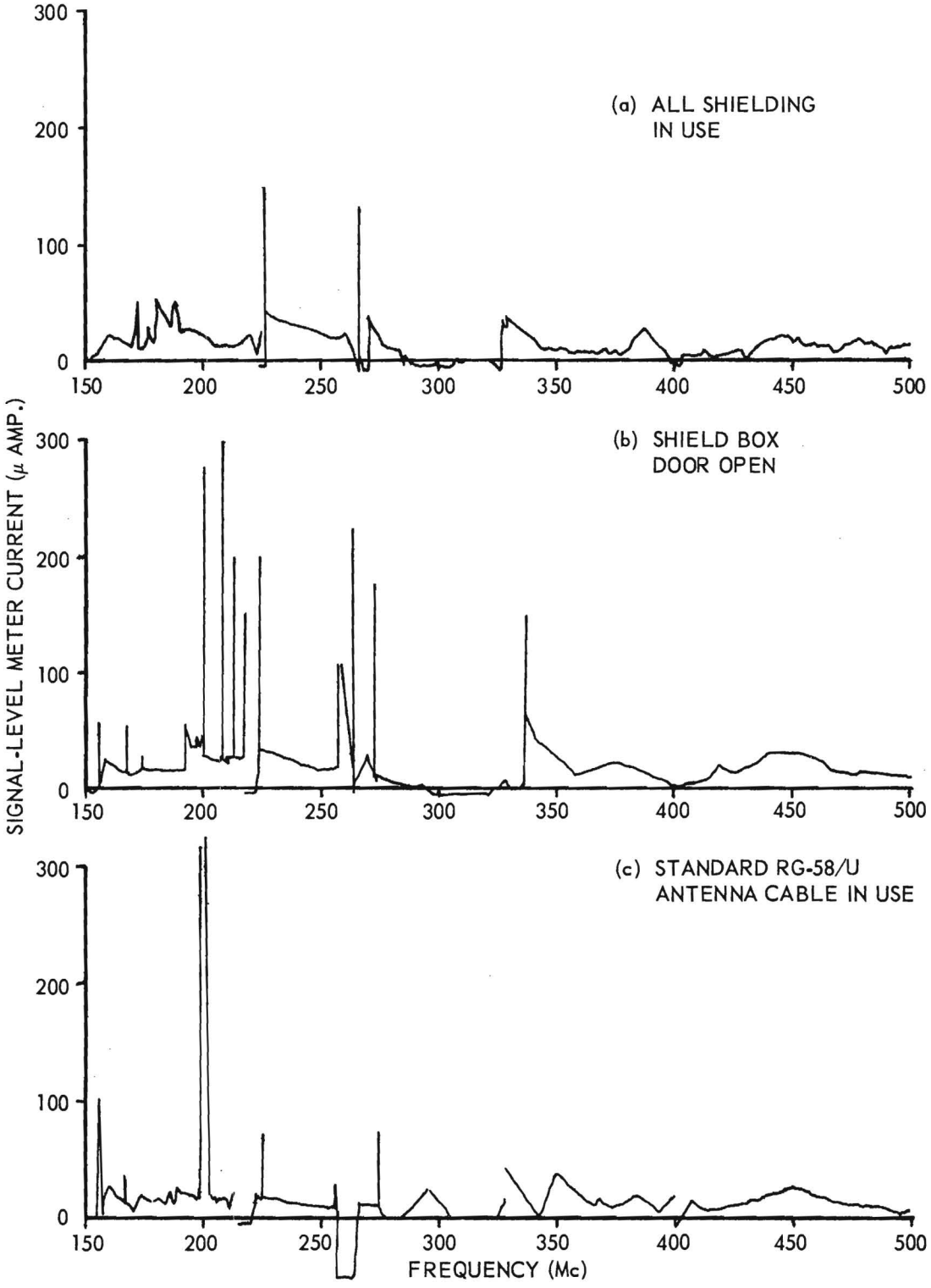

Figure 9. Results of Shielding the Eddystone UHF Receiver.

Signal-Level-Meter output current was less than 40 ua. These two isolated responses did not change in magnitude upon opening the door of the shield box, and it was therefore assumed that they were internal spurious responses of the receiver.

It was originally proposed to remove all the shieldings to show the increase in the various responses of the receiver. However, by merely opening the door of the shield box the responses increased so greatly that it was not necessary to completely remove the shieldings to demonstrate this effect. A graph of these results is given in Figure 9(b).

In a third run the receiver remained in the shield box with the door closed, but the copper-covered cable was replaced by the standard RG-58/U cable. The increased responses, as shown in Figure 9(c), at 155, 198, and 204 mc/sec may be noted, with the latter two due to television Channel 11. Two interesting phenomena occurred during this run. The first was the reduction of the magnitude of the spurious responses at 225 and 270 mc/sec. It was first believed that the length of cable used on the antenna input caused the occurrence of these spurious responses. To eliminate such occurrences, a matching network consisting of a 22-ohm series resistor and a 220-ohm shunt resistor was put in series with the antenna cable at the input of the receiver. The spurious responses still remained, however, with the same magnitude as before and were still a function of the type and length of cable used. Due to the decreased sensitivity of the system, the matching network was removed.

The second phenomena was the extreme negative reading of the d-c ammeter in the frequency range from 262 to 267 mc/sec. This was caused by the r-f section of the receiver going into oscillation. This oscillation was directly attributed to the BNC cable used in the third run. At the frequency of

oscillation, the length of the cable was such as to reflect an impedance into the antenna terminals which caused the receiver to oscillate. The oscillation and negative reading of the ammeter was eliminated by simply changing the length of cable used for the antenna. A length was found which did not cause oscillation at any frequency within the range of the receiver.

Two sensitivity runs, one with the AVC on and the other with the AVC off, as shown in Figure 10, were made at 250 mc/sec to determine the relation between the signal level meter reading and the r-f signal input voltage. It may be noted

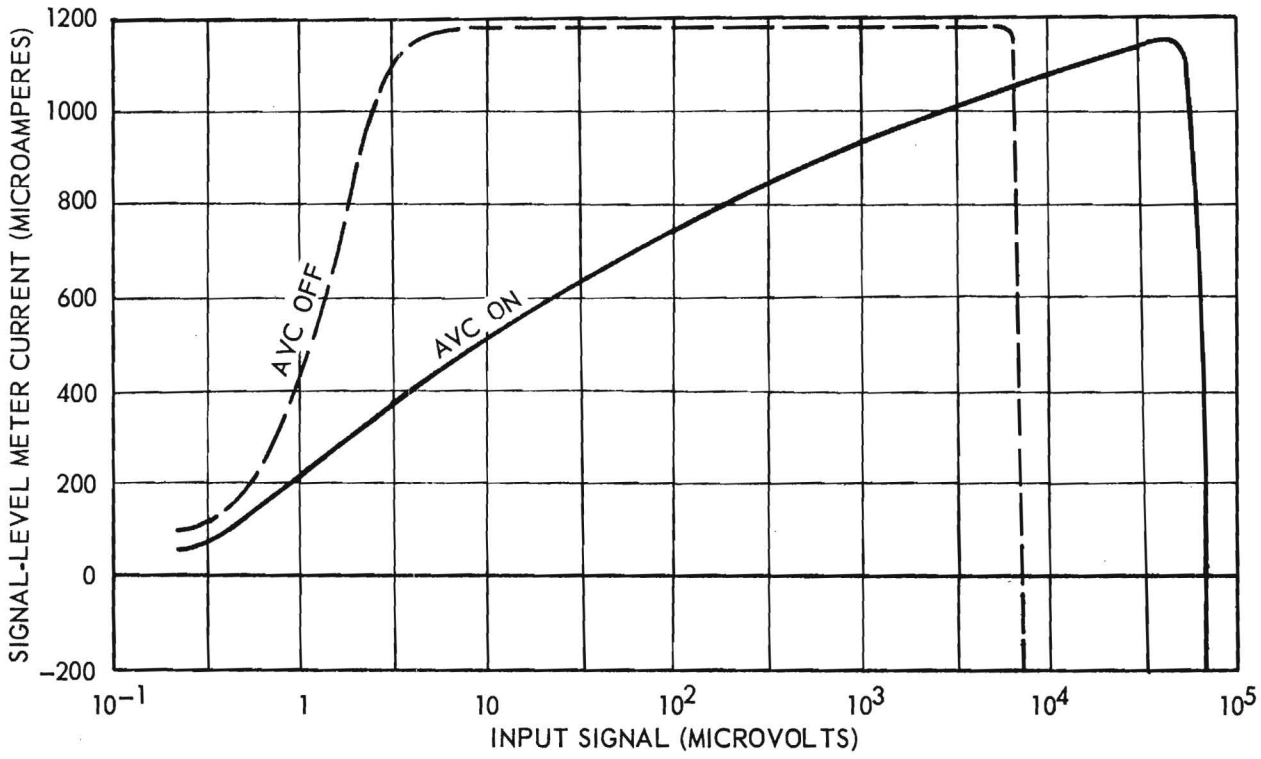

Figure 10. Eddystone Signal-Level Meter Sensitivity at 250 Mc/Sec.

from the graph that the curve is much steeper with the AVC turned off than it is when the AVC is on; however, the dynamic range of the curve is much less. For initial measurements in locating a null, the AVC control should be left on,

but as the exact null is reached better resolution may be obtained with the control turned off. The occurrence of the negative reading of the ammeter due to excessive input signal may also be noted from this graph.

Figure 10 will aid in estimating the amplitudes of the responses shown in Figure 9. No efforts were made to determine the amplitudes of the various responses in microvolts since day-to-day changes produce variations by factors as great as five. Also, the sensitivity curve of Figure 10 is subject to some variation with ambient conditions and is valid only at the frequency specified.

Other tests indicated that the equivalent noise at the input of the receiver is less than 0.3 μv at all frequencies.

The two occurrences of negative signal-level-meter reading referenced above are due to excessively large signals in the i-f channel of the receiver. When very large signals are applied to the receiver, the AVC diode is overloaded and draws excessive current from the delay bias source. The delay bias is obtained from a voltage divider between the receiver's plate supply line and ground. The same divider is used in the signal level meter bridge circuit. Thus, when the AVC diode is overloaded the negative reading of the signal level meter results.

5. Power Measurement System

Further evaluation of the crystal power measurement system as shown in Figure 11 was conducted during this report period. A typical setup of the system is shown in conjunction with the Admittance Meter in Figure 12.

To improve the accuracy of the system, work was directed toward better matching of the outputs of the two diodes used. Previously, the value of the diode load resistor was selected so that the constant k in the equation

$$E_{out} = Ae_{in}^{k} , \qquad (1)$$

for each diode, was equal to 2. However, for a matched output, the constant A must be exactly the same for both diodes. It was necessary to correct the value

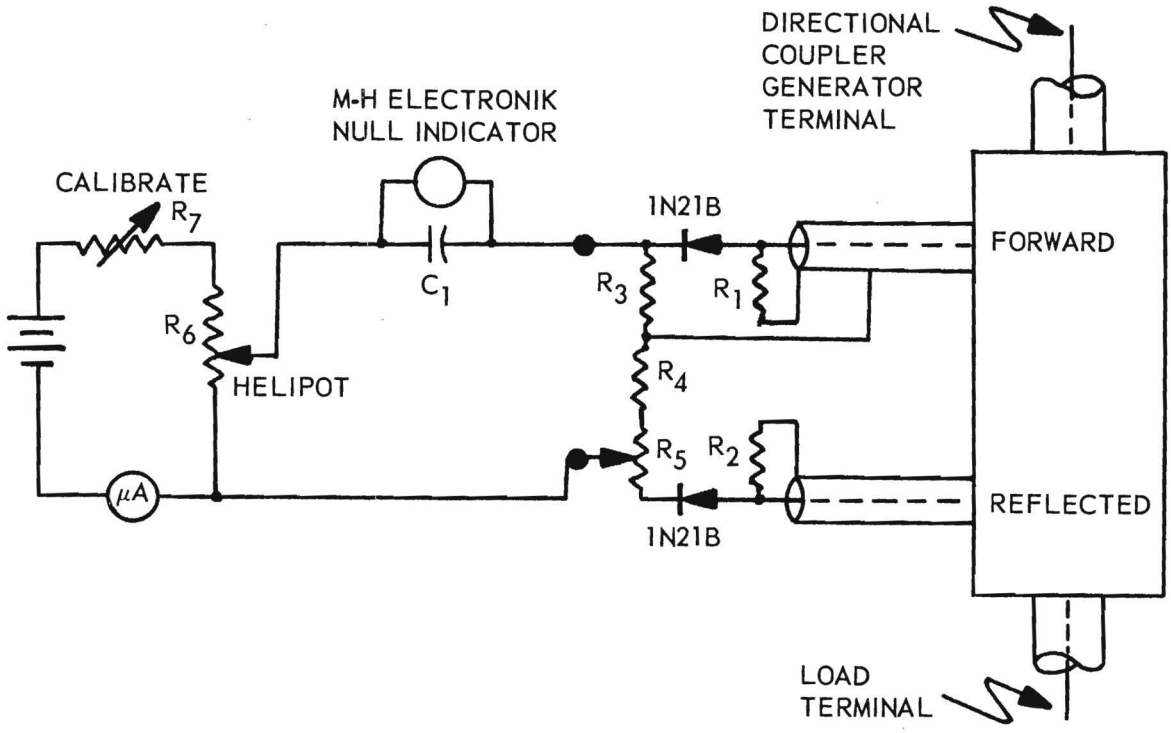

Figure 11. The Crystal Power Measurement System.

of A for one of the diodes used in the power measuring system in order to improve the overall accuracy. First attempts to match the diodes consisted of tapping down on the output of the diode with the larger value of A by use of fixed resistors, keeping the total load resistance on the diode the same. This varied the value of A without affecting k. Because of the thermal sensitivity of the diode when soldering test resistors into position or even touching the diode mount by hand, exact matching was difficult to obtain. To adjust the output of one of the diodes without handling the mount, a potentiometer, R_5, was connected, as shown in Figure 11. The potentiometer knob provided thermal isolation from the diode mount.

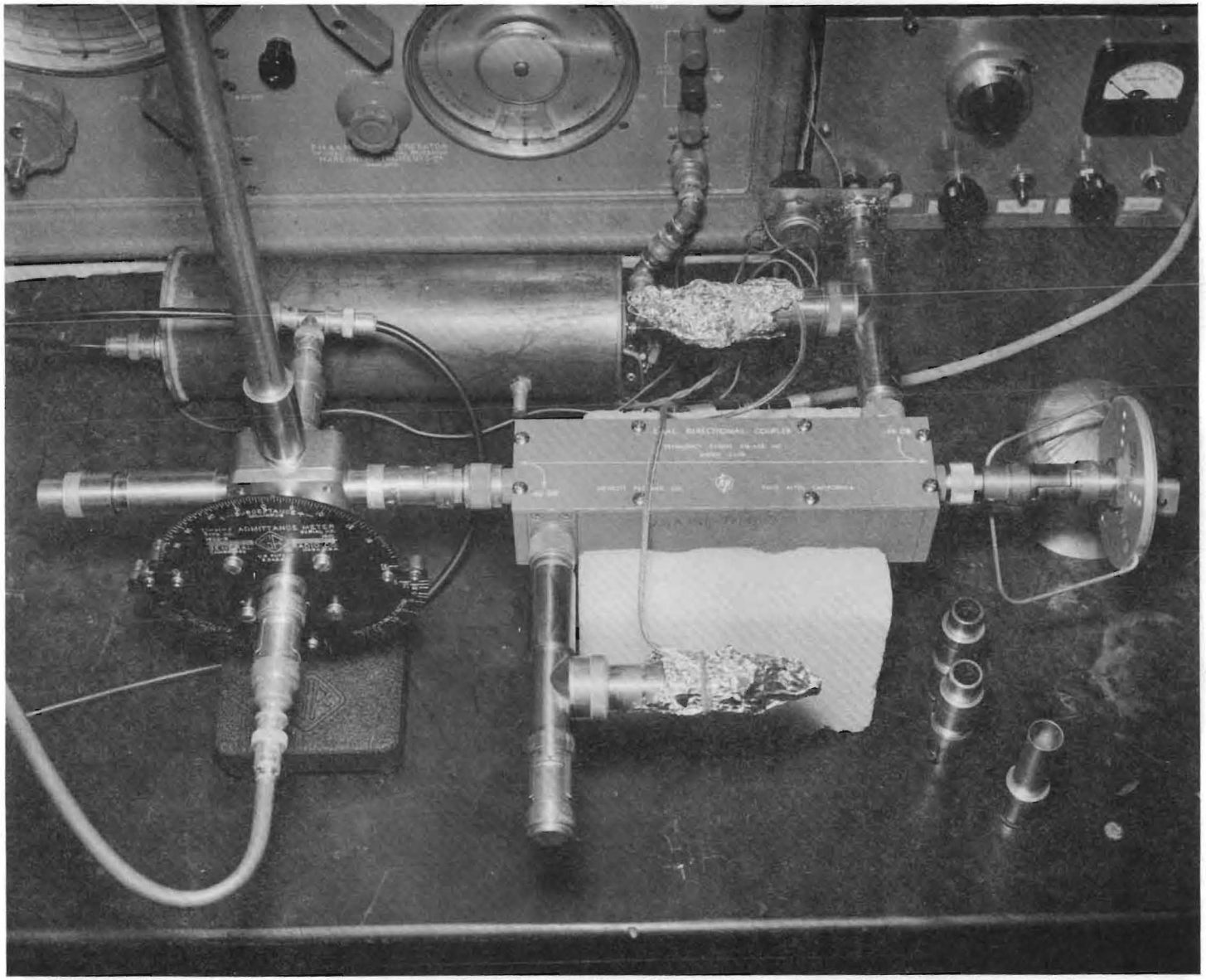

Figure 12. Typical Setup of the Power Measurement Equipment.

To adjust the potentiometer, the transmission line was terminated in an open circuit. This meant that E^+ and E^- were of equal magnitude, neglecting losses in the line. The potentiometer was then adjusted so that the resultant d-c voltage of the two diodes was zero.

To measure the accuracy of the system, the setup shown in Figure 13 was used. The setup was basically the same as Figure 7 in Progress Report No. 1, except for the addition of the cavity amplifier, Millivac Voltmeter, and the additional directional coupler. Since the output voltage amplitude of the Marconi Signal Generator was not sufficient, the cavity amplifier described previously was used so that tests could be made up to a drive level of 9 mw. Originally the VSWR was determined by removing one of the rectifiers and reading forward and reverse power independently. However, this necessitated handling of the rectifier mounts which thereby introduced thermal errors. To eliminate these errors, an additional directional coupler and Millivac voltmeter were used. The Millivac does not read the exact r-f voltage at each output of the directional coupler due to inaccuracies in the meter itself, and due to mismatch and line length between the coupler probe and meter probe. The mismatch and line length errors cancel, however, since the mismatch and line lengths are identical at each directional coupler output and since only the voltage ratio is required to determine the VSWR. Inaccuracies in the meter only lead to small errors in the calculation of the VSWR.

The system was first evaluated at 200 mc/sec, which is the frequency at which the diodes were originally matched and tested. The resulting data are given in Table I.

For a VSWR of unity and drive levels from 0.1 mw to 9 mw, the measurement system agreed with the Hewlett-Packard power meter to within +2.5 percent and

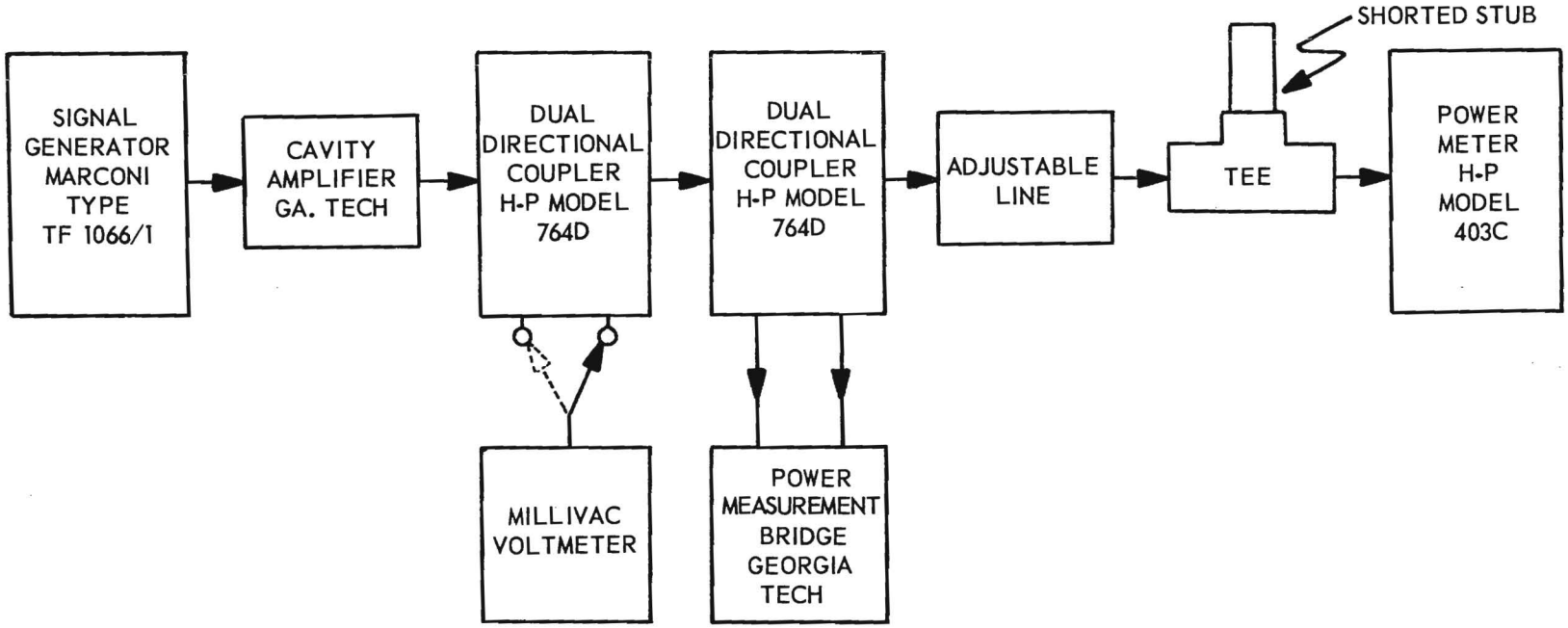

Figure 13. Setup for Determining the Accuracy of the Power Measurement System.

TABLE I

POWER MEASUREMENT SYSTEM ERRORS AT 200 MC/SEC

Power Measured By H-P 403C (Mw)	Power Measured By Power Measurement System: Short Line (Mw)	Long Line (Mw)	VSWR	Maximum Error (%)
.05	.06		1	20
.05	.06	.05	1.2	20
.05	.06		1.4	20
.05	.06	.05	2.3	20
.05	.06		3.0	20
.05	.06	.05	5.0	20
.05	.06		6.5	20
.10	.10		1.0	0
.10	.11	.10	1.2	10
.10	.11		1.4	10
.10	.11	.10	2.3	10
.10	.11		3.0	10
.10	.11		5.0	10
.10	.10	.09	6.5	10
.20	.20		1.0	0
.20	.20	.20	1.2	0
.20	.20		1.4	0
.20	.20	.20	2.3	0
.20	.20		3.0	0
.20	.20		5.0	0
.20	.19	.19	6.5	5
.40	.41		1.0	2.5
.40	.40	.41	1.2	2.5
.40	.40		1.4	0
.40	.40	.40	2.3	0
.40	.39		3.0	2.5
.40	.31		5.0	2.5
.40	.37	.37	6.5	7.5
.60	.61		1.0	1.7
.60	.61	.61	1.2	1.7
.60	.61		1.4	1.7
.60	.61	.60	2.3	1.7
.60	.60		3.0	0
.60	.58		5.0	3.4
.60	.57	.61	6.5	5.1
.80	.80		1.0	0
.80	.82	.82	1.2	2.5
.80	.82		1.4	2.5
.80	.82	.81	2.3	2.5

TABLE I (Continued)

POWER MEASUREMENT SYSTEM ERRORS AT 200 MC/SEC

Power Measured By H-P 403C (Mw)	Power Measured By Power Measurement System: Short Line (Mw)	Power Measured By Power Measurement System: Long Line (Mw)	VSWR	Maximum Error (%)
.80	.81		3.0	1.3
.80	.79		5.0	1.3
.80	.77	.77	6.5	3.8
1.0	1.02		1.0	2
1.0	1.01	1.00	1.2	1
1.0	1.02		1.4	2
1.0	1.02	1.00	2.3	2
1.0	1.02		3.0	2
1.0	1.00		5.0	0
1.0	1.03	0.96	6.5	3
2.0	2.01		1.0	0.5
2.0	2.00	2.04	1.2	2.0
2.0	2.00		1.4	1.5
2.0	2.03		2.3	1.5
2.0	2.03	2.02	3.0	1.5
2.0	2.01		5.0	0.5
2.0	2.00	2.00	6.5	0
3.0	3.04		1.0	1.3
3.0	3.04	3.10	1.2	1.3
3.0	3.06		1.4	2.0
3.0	3.06	3.08	2.3	2.7
3.0	3.06		3.0	2.0
3.0	3.06		5.0	2.0
3.0	3.06	3.12	6.5	2.0
4.0	4.02		1.0	0.5
4.0	4.06	4.14	1.2	1.5
4.0	4.13		1.4	3.3
4.0	4.11	4.11	2.3	2.9
4.0	4.10		3.0	2.5
4.0	4.10		5.0	2.5
4.0	4.13	4.10	6.5	3.3
5.0	5.06		1.0	1.2
5.0	5.09	5.16	1.2	3.2
5.0	5.12		1.4	2.4
5.0	5.14	5.14	2.3	2.8
5.0	5.14		3.0	2.8
5.0	5.18	5.14	5.0	3.6
5.0	5.23		6.5	4.6

TABLE I (Concluded)

POWER MEASUREMENT SYSTEM ERRORS AT 200 MC/SEC

Power Measured By H-P 403C (Mw)	Power Measured By Power Measurement System: Short Line (Mw)	Power Measured By Power Measurement System: Long Line (Mw)	VSWR	Maximum Error (%)
6.0	6.08		1.0	1.3
6.0	6.13	6.23	1.2	2.2
6.0	6.18		1.4	3.0
6.0	6.21	6.20	2.3	3.5
6.0	6.21		3.0	3.5
6.0	6.23	6.20	5.0	3.8
6.0	6.26		6.5	4.3
7.0	7.14		1.0	2.0
7.0	7.18	7.27	1.2	3.9
7.0	7.20		1.4	2.9
7.0	7.26	7.26	2.3	3.7
7.0	7.26		3.0	3.7
7.0	7.31	7.28	5.0	4.4
7.0	7.35		6.5	5.0
8.0	8.15		1.0	1.9
8.0	8.17	8.31	1.2	3.9
8.0	8.27		1.4	3.4
8.0	8.26	8.34	2.3	4.5
8.0	8.36		3.0	4.5
8.0	8.38	8.32	5.0	4.8
8.0	8.35		6.5	4.4
9.0	9.12		1.0	1.3
9.0	9.25	9.35	1.2	3.9
9.0	9.29		1.4	3.2
9.0	9.38	9.39	2.3	4.3
9.0	9.38		3.0	4.2
9.0	9.48	9.38	5.0	5.3
9.0	9.41		6.5	4.6

-0 percent. As the VSWR was increased, the errors increased. Two sources can contribute to these increased errors: (1) errors internal to the measurement system, and (2) actual power losses in the reactive stub and adjustable line producing the high VSWR.

To confirm the second item as a source of error, it may be noted that the power measurement system always reads high with standing wave ratios greater than unity. Any loss in the reactive stub would be read by the power measurement system only and not by the HP power meter. Differences between two readings with the same VSWR but different line lengths can be attributed to a failure in obtaining exactly the same VSWR, or a change in the position of E_{max} and E_{min} and therefore the magnitude of losses which might occur at certain discontinuities in the line. For the system at 200 mc/sec, the maximum error for VSWR of from 1 to 6.5 is approximately 5 percent for power levels greater than 0.2 mw.

The output of the directional coupler varies with frequency; however, both outputs vary in the same manner. If, at frequency f_1,

$$E_{01} = KE^{+} \quad , \tag{2}$$

then

$$E_{02} = KE^{-} \tag{3}$$

where E_{01} and E_{02} represent the outputs from the forward and reverse couplers respectively. The d-c voltage to the bridge will be

$$V_{d\text{-}c} = A(E_{01})^2 - A(E_{02})^2 = AK^2[(E^{+})^2 - (E^{-})^2] = CP, \tag{4}$$

where

$$P = \frac{1}{R_o}\,[(E^{+})^2 - (E^{-})^2] \tag{5}$$

and

$$C = AK^2R_o \quad . \tag{6}$$

If, at frequency f_2,

$$E_{01} = K'KE^{+} \tag{7}$$

then

$$E_{02} = K'KE^{-} \tag{8}$$

and

$$V_{d\text{-}c} = A(E_{01})^2 - A(E_{02})^2 = AK^2(K')^2\,[(E^+)^2 - (E^-)^2]$$

$$= (K')^2\,(CP) \qquad (9)$$

where P and C are given by Equations 5 and 6.

Thus the effect of the directional coupler is to change the magnitude of the d-c voltage applied to the bridge by a multiplier, $(K')^2$, which is a function only of frequency and can therefore be compensated for by changing the value of the standard current in the bridge.

A plot of the required standard current versus frequency to make the power measurement system direct reading is given in Figure 14. By setting up the power measuring system from this graph it is possible to read power directly from the Helipot dial on the bridge at any given frequency.

If the transmission line is terminated in an open circuit, equal voltages are applied to both diodes. If any given value of voltage is applied to the line, and the potentiometer (R_5) is adjusted so that the resultant d-c output is zero, then if the diodes are perfectly matched, the resultant d-c output should remain zero as the input voltage is reduced to zero. For the power measuring system it has been determined that for any input voltage that produces a power, X, into a 50-ohm load, by setting the system up by the above procedure the output remains zero to within 0.01X. This is true regardless of the frequency; however, it has been found that the actual value of $\underline{k}$ for both diodes does vary somewhat with frequency and this will tend to increase the maximum system error slightly.

To determine the overall accuracy of the system, the setup shown in Figure 13 was again used. To initially calibrate the instrument the graph of Figure 14 was used to set up the standard current through the bridge at each frequency.

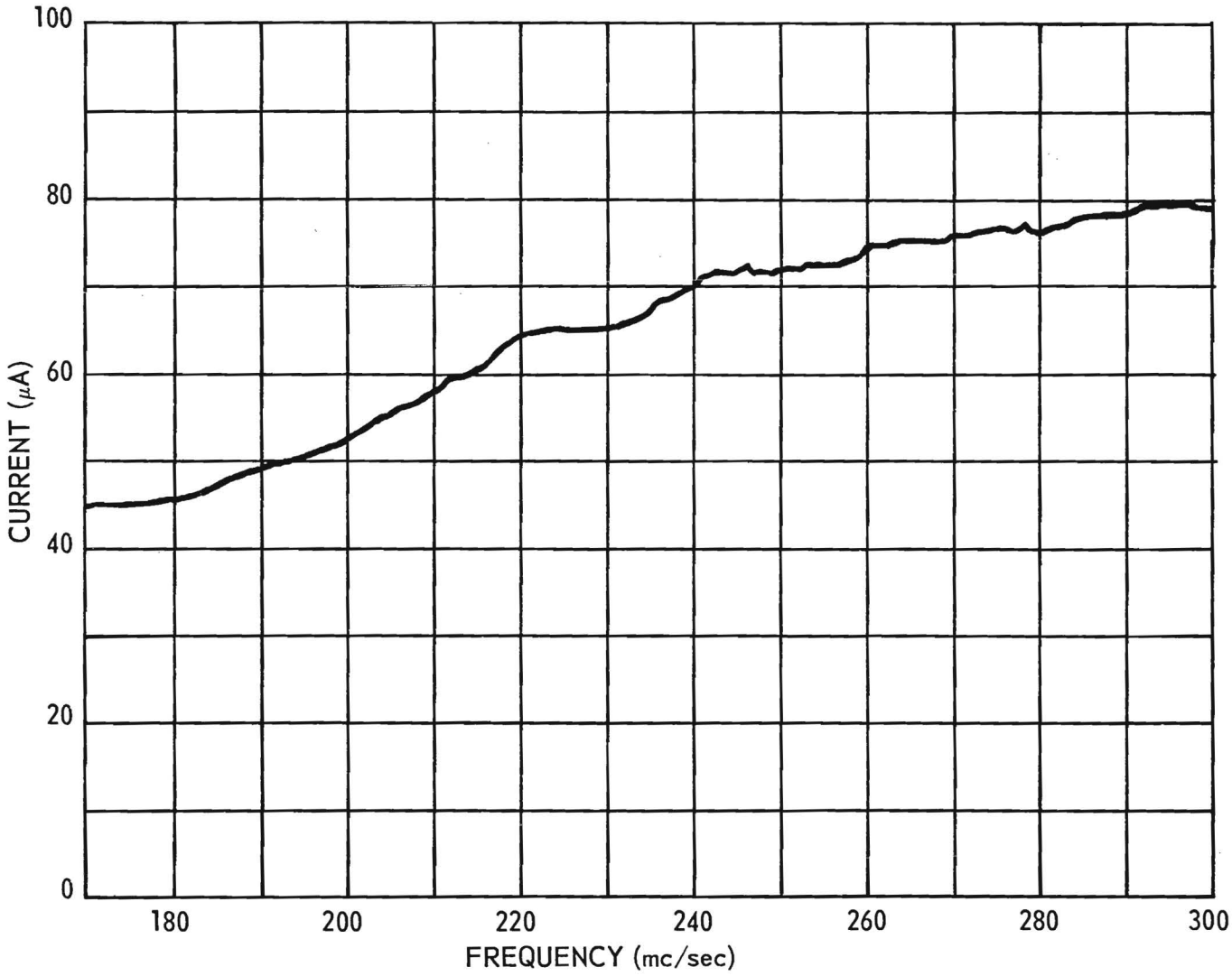

Figure 14. Calibration Currents for the Power Measurement System.

To set the potentiometer (R_5), an open circuit was placed on the end of the transmission line and the potentiometer adjusted for zero output with maximum voltage input. After placement of the reactive stub in parallel with the open circuit, the power measuring system indicated a certain amount of power depending on the drive level and the position of the stub. By readjusting the potentiometer (R_5), it was possible to compensate for these losses with any given stub length at all drive levels with the same accuracy as defined above (i.e. - 0.01X). However, this compensated for losses at a VSWR of infinity and, therefore, did not entirely compensate for losses at a VSWR other than infinity. Also, as the stub length was changed, the magnitude of the losses changed and, therefore, the compensation was not effective at all stub lengths. A setting for (R_5) was chosen to give a minimum error over the range of stub lengths to be used. This compensating adjustment of R_5 therefore establishes a least upper bound on the error of the entire system.

Other measurement accuracy data were obtained over the frequency range from 175 to 300 mc/sec for a VSWR from 1 to 6.5. The VSWR at 300 mc/sec was limited to 5.3 due to the minimum length of the shorting stub used in the test. Graphs of the results are given in Figures 15 through 18. Since complete data had already been obtained for the system at 200 mc/sec, typical points were selected for the graph at 200 mc/sec from the data presented in Table I. The solid line on each graph represents the desired zero error reading of the power measurement system. The dotted lines enclose an area representing regions of error less than 10 percent. It can be seen that the power measurement system has an overall error of less than $\pm$ 10 percent for a VSWR from 1.0 to 6.5, power levels from 0.1 to 10.0 mw, and frequencies from 175 to 300 mc/sec.

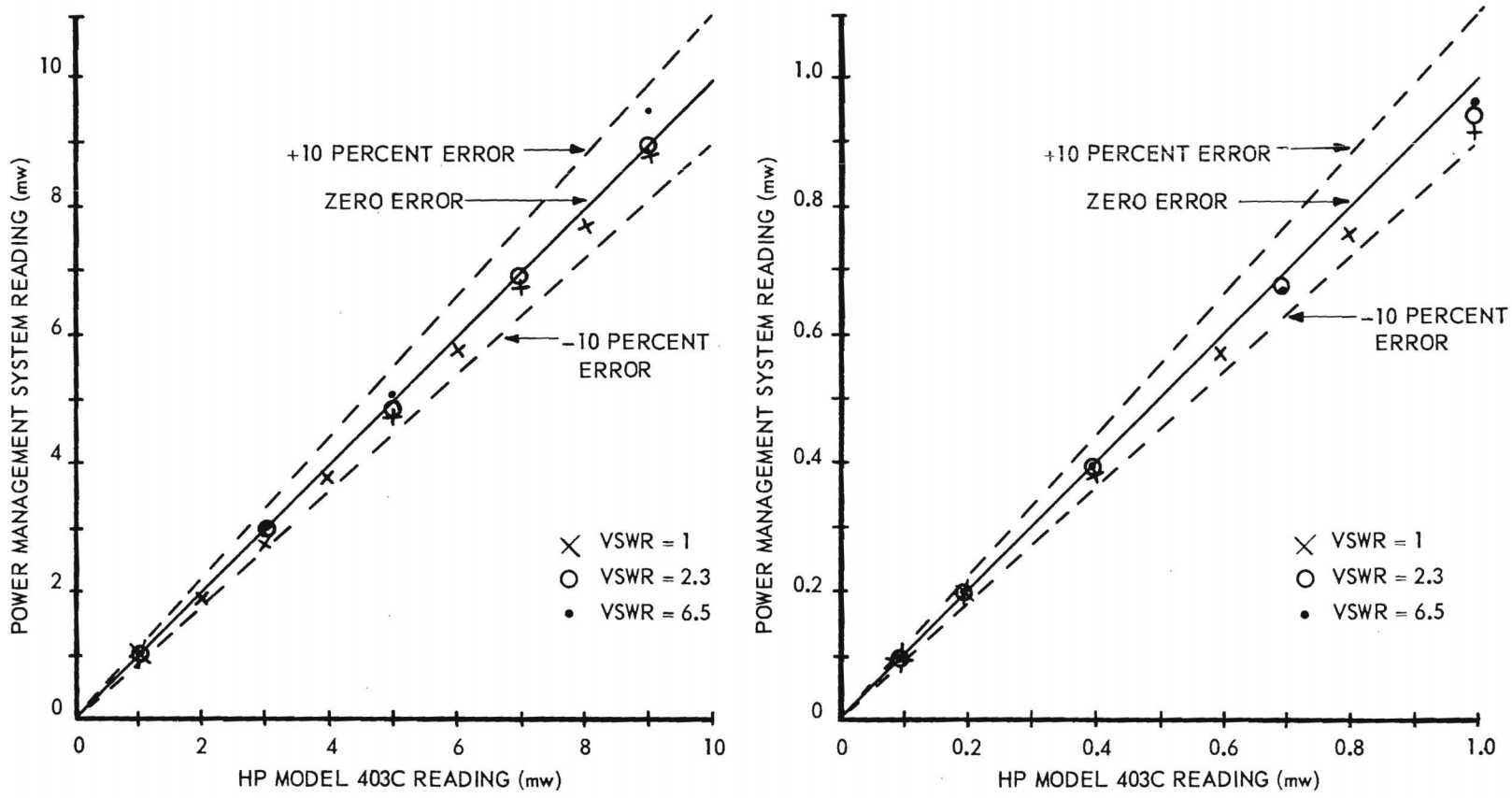

Figure 15. Power Measurement System Errors at 170 Mc/Sec.

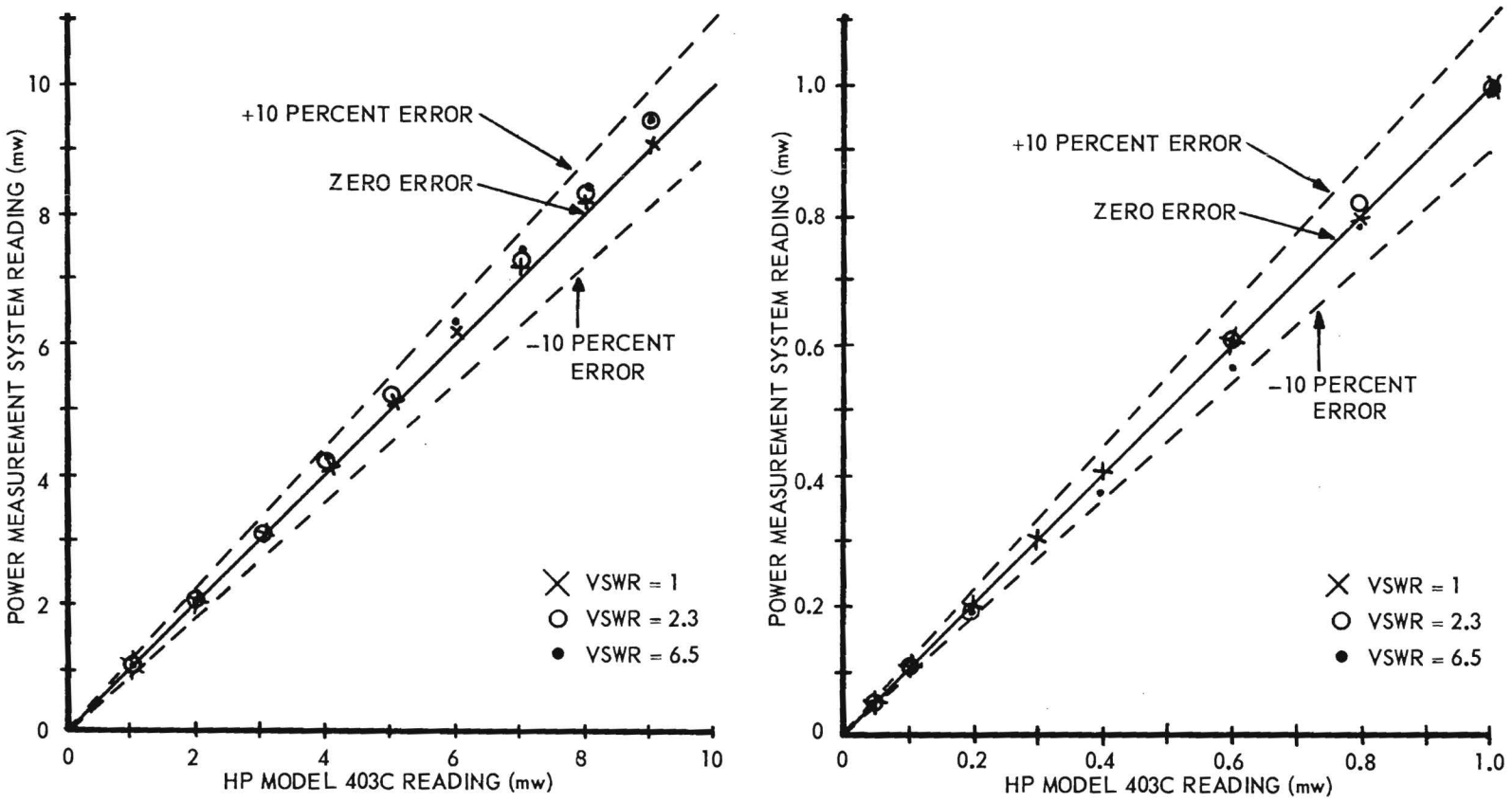

Figure 16. Power Measurement System Errors at 200 Mc/Sec.

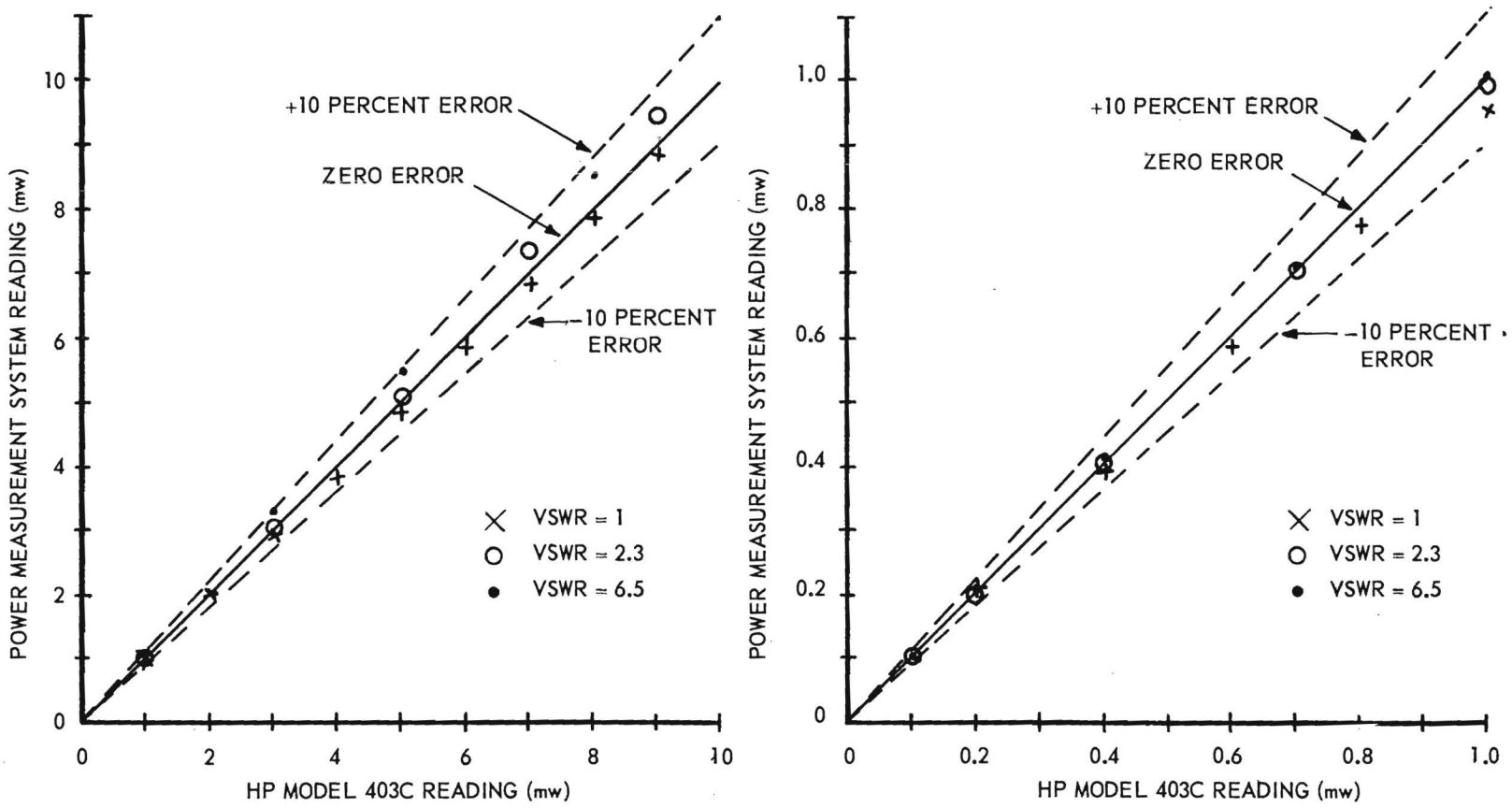

Figure 17. Power Measurement System Errors at 250 Mc/Sec.

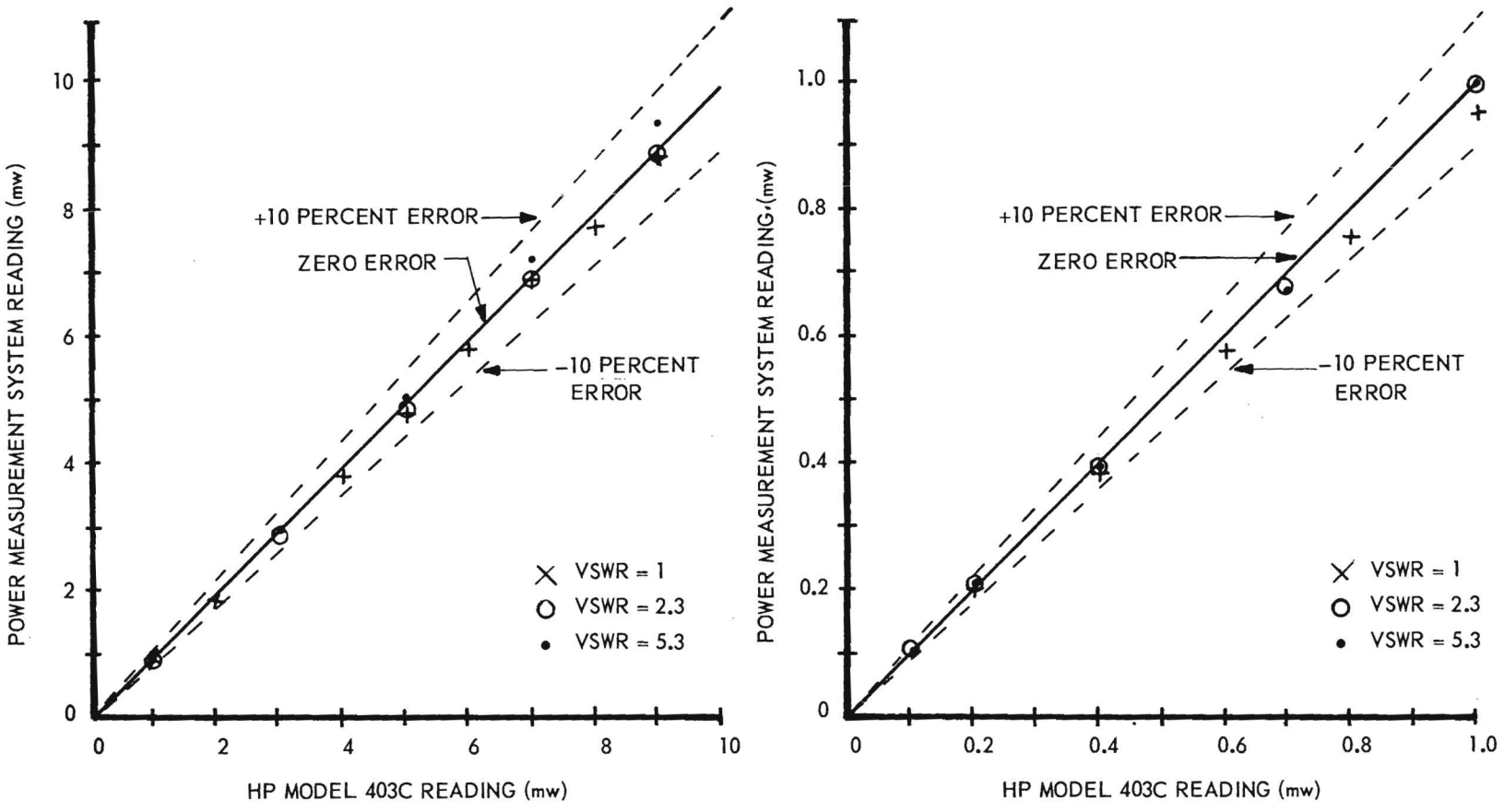

Figure 18. Power Measurement System Errors at 300 Mc/Sec.

It must be noted that the error of ± 10 percent is referred to the HP-403C which has a specified error of less than ± 5 percent. It was brought out in Progress Report No. 1, that the linearity of the HP-403C was somewhat better than ± 5 percent. The small nonlinearity would tend to increase or decrease the power measurement system error only slightly, and the larger error of ± 5 percent represents a reference calibration error, and can be eliminated by the procurement of a more accurate power standard.

The actual sources of error in the system come from three areas:

(1) the inaccuracy in setting up the initial standard current from Figure 14,

(2) variations in the value of the constant k of the diodes with frequency, and

(3) overcompensation of the line losses with the potentiometer (R_5).

The errors due to (1) are usually small and may be considered negligible. The errors due to (2) are the largest errors in the system and could be reduced appreciably by varying the d-c load on the diodes as the frequency is changed. Such a complication of the system is considered unjustified, however, since overall accuracy is already within the required limits. The error due to (3) is not actually an error in the power measuring system but rather a power loss caused by the method used in testing the system. That this is true is apparent since the total coaxial line length beyond the directional coupler should be considered a part of the load; however, the HP 403C Power Meter reads only the power in its resistive termination, thus losses occurring in the line and stubs used to produce the high VSWR are read by one system but not by the other. It has not yet been possible to prove this hypothesis since no method has been found to eliminate the unwanted losses. A possibility for making more precise calibrations would be to obtain tunable bolometers having various resistance values

other than 50 ohms and calibrated for use with the HP 403C Power Meter which could be used for producing VSWR values other than unity. If this were done it is believed that the accuracy of the system would be found to be much better than the ± 10 percent stated above. In other words, it is believed that the greater portion of the 10 percent error is due to actual power losses in the lines used to produce the high VSWR values.

C. Other Measurement Systems

1. Test Results

A further investigation was conducted during this report period of the crystal measurement system described in the APPENDIX of Progress Report No. 1. This system will herein be referred to as the equivalent circuit method. A component mount was constructed as shown in Figure 19. The pins of the adjacent

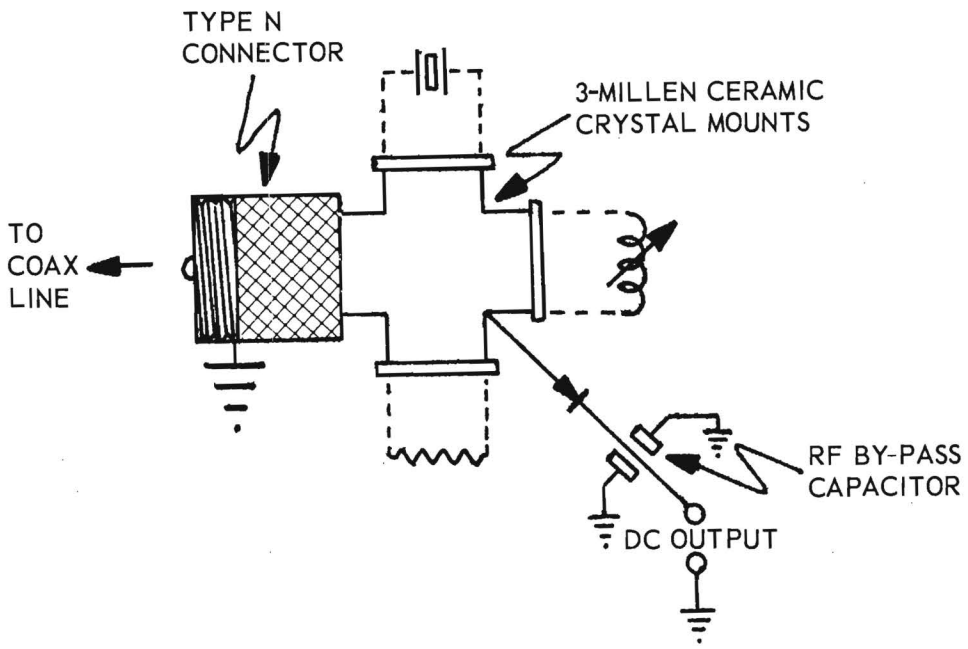

Figure 19. Component Mount for the Equivalent Circuit Crystal Measurement Method.

crystal sockets were directly soldered together in order to eliminate as much lead length as possible. Three crystal mounts were used in the system, one for the actual crystal under test, one for the addition of a variable inductor or a variable capacitor, and one for the addition of a standard resistor. The electrical circuit was made to resonate at approximately the resonant frequency of the crystal by the adjustment of an added inductance or capacitance. The current flowing in the circuit was measured by placing a diode across the standard resistor and reading the d-c voltage output. The current was then a constant multiplier of the square root of the measured d-c voltage.

Crystal No. FA-116 was chosen as the crystal to be tested since large amounts of previous data on this crystal were available for comparison of results. The first test was performed at 245 mc/sec. From the equations given in the APPENDIX of Progress Report No. 1, Q_o (Q_o is here defined as the Q of the crystal's motional arm) was calculated to be 36,000, R_1 to be 144 ohms, and f_o' to be 245.0443 mc/sec. From Progress Report No. 4 of Contract DA-36-039 SC-71191, pp 22-25, Q_o was given as 36,000, R_1 as 103 ohms, and f_o' as 245.0460 mc/sec for the same crystal. Similar tests were performed on this crystal at 175 mc/sec yielding Q_o = 34,000 and R_1 = 66 ohms. Calculations from Admittance Meter data at 175 mc/sec gave Q_o = 53,000 and R_1 = 33 ohms.

It can be seen from the above data that very close agreement was achieved at 245 mc/sec while very poor agreement was obtained at 175 mc/sec.

Errors in the equivalent circuit measurement method can arise from many sources. Three main sources of errors are:

(1) use of resistive elements having reactive components,

(2) presence of distributed parameters in the circuit, and

(3) failure to keep the source voltage constant.

The results at 245 mc/sec indicate that the equivalent circuit method can provide fairly close agreement with Admittance Meter measurements if the errors can be sufficiently reduced.

2. Variations in Crystal Q

It has been found that the Q_o of a crystal is not unique. That is, various values of Q_o may be obtained by applying different methods of calculation. Because of spurious responses, crystal motional arm circle diagrams as plotted on a Smith chart are usually distorted. A distorted circle generally yields a higher value of Q_o than would a perfect circle when the Q_o is calculated from the half-power points and when the distortion is due to spurious responses. Furthermore, the Q_o will vary depending on whether the half-power points, quarter-power points, three-quarter-power points, etc. are used in the calculation, which is contrary to the results which would be obtained for a simple series resonant circuit.

Another method of calculating Q is based on the susceptance and conductance curves for the motional arm. If a plot of the susceptance and conductance of a series resonant circuit is drawn, it can be shown that the Q_o of the circuit is given by the equation,

$$Q_o = \frac{\omega_o}{2G} \left[\frac{d(-B)}{d\omega}\right] \Bigg|_{\omega = \omega_o} \qquad (10)$$

where G is the conductance at ω_o and B represents the susceptance. However, for an imperfect series resonant circuit (i.e., one with distributed parameters or spurious resonances) the value of Q_o given by Equation 10 does not necessarily agree with the value calculated from the half-power points.

The Q_o of Crystal No. FA-116 was rechecked at 245 mc/sec using Equation 10. The holder parameters of the crystal were first subtracted and Equation 10 was then applied to the points on the circle. The resulting value for Q_o was 33,000.

The results of various Q_o measurements for the motional arm of Crystal No. FA-116 at 245 mc/sec are summarized as follows:

(1) Q_o obtained from half-power measurements using Admittance Meter data = 36,000,

(2) Q_o obtained from Equation 10 using Admittance Meter data = 33,000, and

(3) Q_o obtained from the equivalent circuit measurement method = 36,000.

Equation 10 has not yet been used to calculate the Q_o for this crystal at 175 mc/sec.

Equation 10 may also be used for calculating the Q of a complete crystal and holder. Figure 20 shows a typical crystal conductance and susceptance diagram.

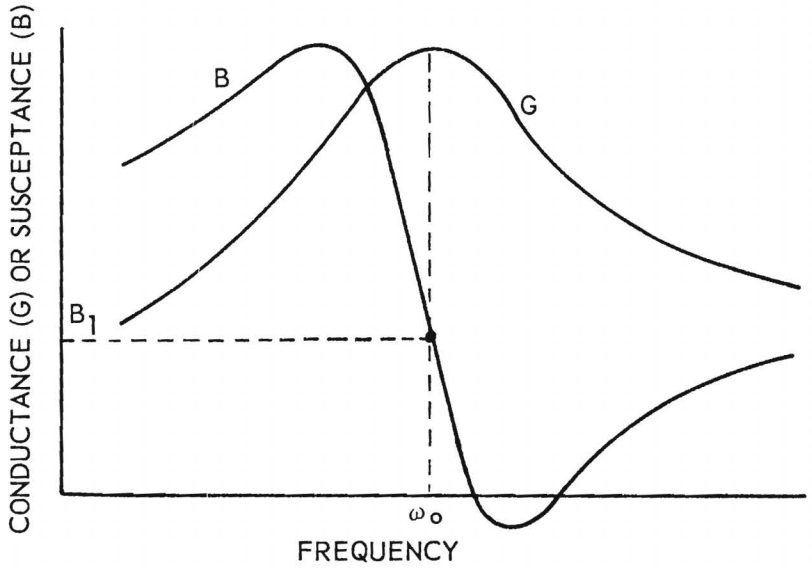

Figure 20. Typical Crystal Conductance and Susceptance Diagram.

If the frequency, ω_o, at maximum conductance is assumed to be the resonant frequency of an equivalent series resonant circuit, the susceptance, B_1, at the same frequency will correspond to a point of zero susceptance in the equivalent

circuit. Equation 10 may then be applied at this point. For crystal No. FA-116, the Q at 245 mc/sec was found to be 23,000 and at 175 mc/sec was found to be 33,000.

It may be noted that the above results dispute a statement on page 25 of Progress Report No. 4, Contract DA-36-039 SC-71191, which implies the Q of this crystal is decreased very little by the presence of holder parameters. A re-calculation of the previous data indicates that an error was made in reporting the Q of the complete crystal as 34,000. The value should have been 24,000.

V. CONCLUSIONS

The Crystal Measurements Standard designed around a factory calibrated Admittance Meter must include an isolation amplifier to eliminate loading variations on the Marconi Signal Generator. A gain of 20 db over the frequency range of 175 to 300 mc/sec is desired to cover the specified dynamic range of drive level. Some compromise on these amplifier requirements may be necessary. Shielding of the Eddystone Receiver detector and interconnecting cables is quite critical but has been satisfactorily accomplished. Tests of this receiver indicate that initial null location should be done without AVC since this circuit introduces considerable dynamic range compression. Other tests indicate that the equivalent noise at the input of the receiver is less than 0.3 μv at all frequencies. Data indicates that the power measuring directional coupler introduces negligible error in the system.

Since the factory calibrated Admittance Meter has been received it is felt that further studies with the Georgia Tech owned instrument should be discontinued in view of cross calibration problems.

The directional coupler power measurement device has demonstrated an overall error of less than $\pm$ 10 percent for a VSWR from 1.0 to 6.5, power levels from 0.1 to 10.0 mw, and frequencies from 175 to 300 mc/sec. Since this is within the specified limits, further work on this component of the overall crystal measurement system is not contemplated at this time.

Further studies of the equivalent circuit method of measuring crystal parameters indicate fairly close agreement with Admittance Meter measurements provided that the inherent errors in the former system can be recognized and controlled or minimized.

VI. PROGRAM FOR NEXT INTERVAL

The program for the next quarter will be a continuation of the work reported in the preceding pages with the exception of the following items:

1. further work on the crystal drive level measurement system will be discontinued since the system now satisfies the specified requirements, and

2. further work on and evaluation of the Eddystone Receiver will be discontinued since it now satisfies the null detection requirements.

Special emphasis will be given the following items:

1. thorough testing of the new General Radio Admittance Meter and terminations,

2. investigation and evaluation of other sources of error in the Crystal Measurements Standard,

3. evaluation of the high-frequency r-f amplifier when it arrives,

4. measurement of crystal parameters using the Crystal Measurement Standard,

5. further study of data reduction methods for the Crystal Measurements Standard,

6. further study of the equivalent circuit crystal measurement method, and

7. development of instrumentation for other types of crystal measurement systems.

VII. IDENTIFICATION OF KEY TECHNICAL PERSONNEL

Biographical sketches of the key technical personnel were included in Progress Report No. 1. The time contributed by each during the present report period is:

James E. Lane	Technical Assistant	200 Hours
Samuel N. Witt, Jr.	Project Director Research Engineer	240 Hours
Vance Keith Woodcox	Research Assistant	480 Hours

Respectfully submitted:

Samuel N. Witt, Jr.
Project Director

Approved:

W. B. Wrigley, Head
Communications Branch
of the
Physical Sciences Division

PROGRESS REPORT NO. 3

PROJECT NO. A-362

INVESTIGATION OF METHODS FOR MEASURING THE EQUIVALENT ELECTRICAL PARAMETERS OF QUARTZ CRYSTALS

By

SAMUEL N. WITT, JR. AND VANCE KEITH WOODCOX

- o - o - o - o - o -

CONTRACT NO. DA-36-039 SC-74948
DEPARTMENT OF THE ARMY PROJECT: 3-26-05-703

- o - o - o - o - o -

15 APRIL 1958 TO 15 JULY 1958

PLACED BY THE U. S. ARMY
SIGNAL ENGINEERING LABORATORIES
FORT MONMOUTH, NEW JERSEY

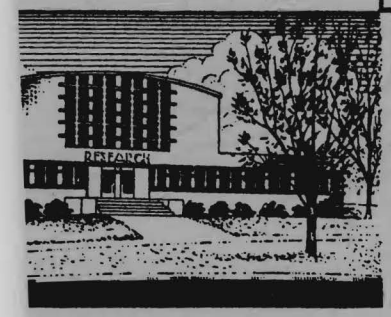

Engineering Experiment Station
Georgia Institute of Technology
Atlanta, Georgia

ENGINEERING EXPERIMENT STATION
of the Georgia Institute of Technology
Atlanta, Georgia

PROGRESS REPORT NO. 3

PROJECT NO. A-362

INVESTIGATION OF METHODS FOR MEASURING THE EQUIVALENT ELECTRICAL PARAMETERS OF QUARTZ CRYSTALS

By

SAMUEL N. WITT, JR. AND VANCE KEITH WOODCOX

- o - o - o - o - o -

CONTRACT NO. DA-36-039 SC-74948
DEPARTMENT OF THE ARMY PROJECT: 3-26-05-703

- o - o - o - o - o -

The object of this project is to develop methods for measuring the equivalent electrical parameters of quartz crystals in the frequency range of 175 to 300 mc/sec.

15 APRIL 1958 TO 15 JULY 1958

PLACED BY THE U. S. ARMY
SIGNAL ENGINEERING LABORATORIES
FORT MONMOUTH, NEW JERSEY

TABLE OF CONTENTS

This report contains 43 pages.

LIST OF FIGURES

I. PURPOSE

The purpose of the project is fourfold:

1. To continue the study and investigation of methods and techniques for measuring the equivalent electrical parameters of quartz crystal units in the frequency range of 175 to 300 mc/sec, including:

   (a) determination of measurement errors,

   (b) development of a means for directly measuring the power drive of a crystal unit, and

   (c) development of means for measuring the effective resistance of the crystal unit at the series resonant condition.

2. Utilize the information from Investigation 1., above, in the establishment of a standard crystal measurement system which will:

   (a) measure the effective resistance of the crystal at any frequency within the crystal resonance range with a target accuracy of $\pm$ 1 percent,

   (b) determine the phase angle of the crystal at any frequency within the crystal resonance range with a target accuracy of $\pm$ 1 degree,

   (c) include a means of measuring directly the power drive of a crystal unit within $\pm$ 20 percent, and

   (d) be capable of determining the equivalent electrical parameters of the crystal unit.

3. Utilize the information from Investigations 1. and 2. in investigations of circuitry for ultimate utilization in the development of a practical crystal test instrument for the frequency range 175 to 300 mc/sec which will:

(a) measure the effective resistance of the crystal unit at series resonance within a resistance range of 20 to 200 ohms with an accuracy of $\pm$ 5 percent,

(b) subject the crystal to any power drive within 0.2 and 4 mw and provide a means of determining directly the power drive with an accuracy of $\pm$ 20 percent,

(c) provide a means of operating the crystal within $\pm$ 0.0005 percent of the series resonant frequency, and

(d) have a power drive versus resistance characteristic from 175 to 300 mc/sec which will not vary more than 3 to 1 for the resistance range of 40 to 150 ohms.

4. Investigate any other problems pertinent to crystal measurements in the VHF range which are mutually agreed upon by the contractor and the Contracting Officer's Technical Representative.

II. ABSTRACT

Experimental data on several VHF quartz crystals were obtained using the Crystal Measurements Standard System. One method of analyzing the data to determine the various crystal parameters is briefly described. Some study was made of another analysis method involving a modified equivalent circuit. A complete evaluation of these analysis methods has not yet been completed.

Two commercial wide-band radio-frequency amplifiers were received during this report period. The two amplifiers in cascade provide greater than 25 db gain into a 50-ohm load over the frequency range from 175 to 300 mc/sec. The amplifiers provide adequate isolation of the signal generator in the measurements system. Low-pass filters were also obtained for use with the amplifiers for harmonic rejection.

Efforts to evaluate the General Radio Admittance Meter calibration were continued. Impedance measurement errors of less than one percent and one degree for magnitude and phase angle respectively were obtained under some conditions. When the directional coupler of the power measurement system was included in the transmission line, errors increased considerably. Efforts to evaluate and reduce these errors are described.

The power measurement system was essentially completed during the previous report period; however, a sensitive micro-voltmeter to be used to make the system direct reading was evaluated and ordered during this period.

Modifications were made in the Equivalent Circuit Crystal Measurement System so that the actual circuit would more closely approach the theoretical behavior as described by the mathematics. As compared to previous results, closer agreement was obtained between this method and other methods for calculating the Q of a test crystal.

III. PUBLICATIONS, LECTURES, REPORTS AND CONFERENCES

No publications or reports have resulted from work under the contract during this report period.

A paper entitled "VHF Crystal Parameter Measurements" was presented by Mr. Samuel N. Witt, Jr. at the 12th Annual Frequency Control Symposium in Asbury Park, New Jersey on 7 May 1958.

While in attendance at the Frequency Control Symposium, brief conferences were held between Mr. W. B. Wrigley, Mr. Samuel N. Witt, Jr., and Mr. V. K. Woodcox of the Georgia Institute of Technology and Mr. D. Pochmersky and Dr. G. K. Guttwein of USASRDL. No changes in project objectives or methods of approach resulted from these conferences.

IV. FACTUAL DATA

A. Introduction

Various experimental crystal measurements were made during the first two quarters of this project to determine the suitability of different units included in the Crystal Measurements Standard System. Further VHF and UHF crystal measurements were made during this period to obtain data from which crystal analysis methods could be studied. Various digital computer programs have been written to perform the necessary data reductions.

The need for signal isolation between the signal generator and the Admittance Meter of the Crystal Measurements Standard was previously reported. Attempts were made to construct isolation amplifiers with only limited success as described in Progress Report No. 2. Commercial radio-frequency amplifiers have since been purchased. Test results are included in this report.

During the first two quarters of this project, several improvements were made in the Crystal Measurements Standard. An Eddystone UHF Receiver was added as a null detector, a crystal drive level measurement system was developed, and a new specially calibrated General Radio Admittance Meter was purchased. During this report period, the calibration of the new Admittance Meter has been extensively analyzed. It has been found that the calibration of the basic Admittance Meter is generally satisfactory but that the addition of other equipment, such as the directional coupler required for use with the power measurement system, decreases the overall accuracy. Thus the primary efforts have been to determine means for correcting the overall system calibration to obtain the required accuracy of one percent for impedance magnitude and one degree for phase angle.

The power measurement system was completed and calibrated during the second quarter; however, an additional instrument, a sensitive micro-voltmeter, was

recently ordered to convert the bridge balance and null detection system to a direct-reading system. This instrument has not yet been received.

A new method of measuring the parameters of quartz crystals was reported in Progress Report No. 1. This method has since been named the Equivalent Circuit Crystal Measurement System. Data obtained during the second quarter yielded good accuracy in calculating the Q of a crystal in some instances while in other instances the accuracy was very poor. Modifications made during the current quarter have tended to improve the overall accuracy.

B. Crystal Measurements Standard

1. Experimental Crystal Data

The characteristics of several quartz crystals have been measured using the setup shown in Figure 1. This setup is the same as described in previous

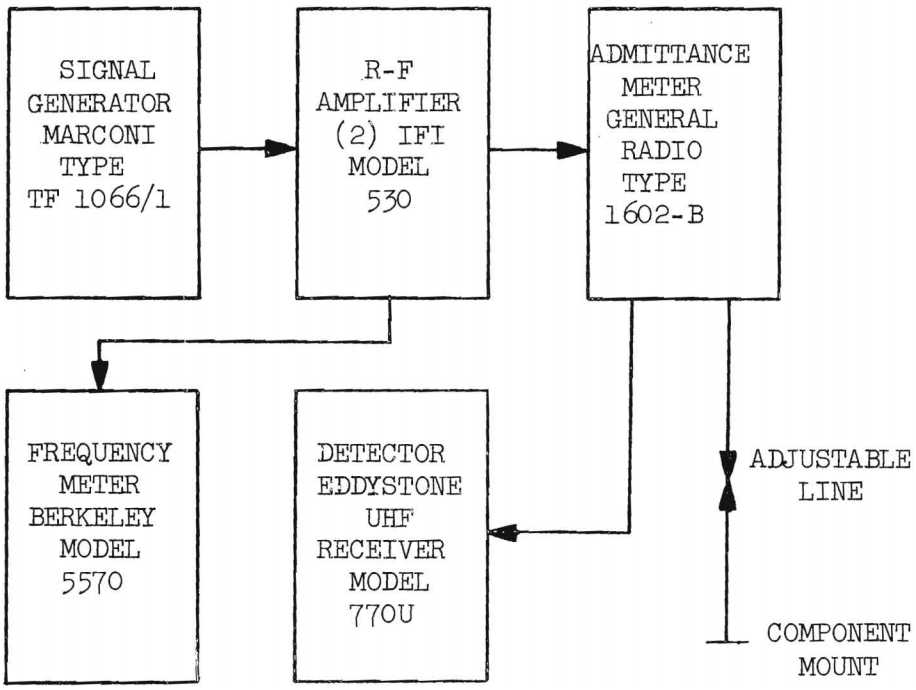

Figure 1. Crystal Measurements Standard System.

reports except that r-f isolation amplifiers have been added and the recently purchased General Radio Admittance Meter has been substituted for the older instrument which was used previously. The r-f amplifier was found necessary for the elimination of discontinuities as described in Progress Report No. 2. Details concerning the amplifier are discussed in a later section of this report. The accuracy and calibration of the new Admittance Meter are also discussed elsewhere. The power measurement system was omitted from the setup since its effect upon admittance measurement accuracy has not yet been fully determined.

The results of a typical crystal measurement run are shown in Figure 2. This particular run is for crystal No. FA-116 plugged into a GR component mount which is attached directly to the Admittance Meter. The fixed line length between the crystal and measurement points in the Admittance Meter was 9.69 cm. Thus all of the points are rotated by this fixed line length. A digital computer program was used to subtract the line length from each of the approximately 240 data points. The total computer time required for this operation was less than 20 minutes including program loading on an IBM-650 computer. The data, after the 9.69 cm of line have been subtracted, are shown in Figure 3.

The curves of Figure 3 could have been obtained directly by using a half-wavelength line between the crystal and Admittance Meter at each frequency. This would, however, have required precision line length adjustments at each of many frequencies and would, therefore, have been considerably more time consuming. Accuracy of the measurements was also an important consideration as will be discussed later.

For any given set of crystal measurement data, such as presented in Figure 3, all of the crystal parameters can be precisely calculated at each overtone frequency, the only additional data required being the frequency at several of

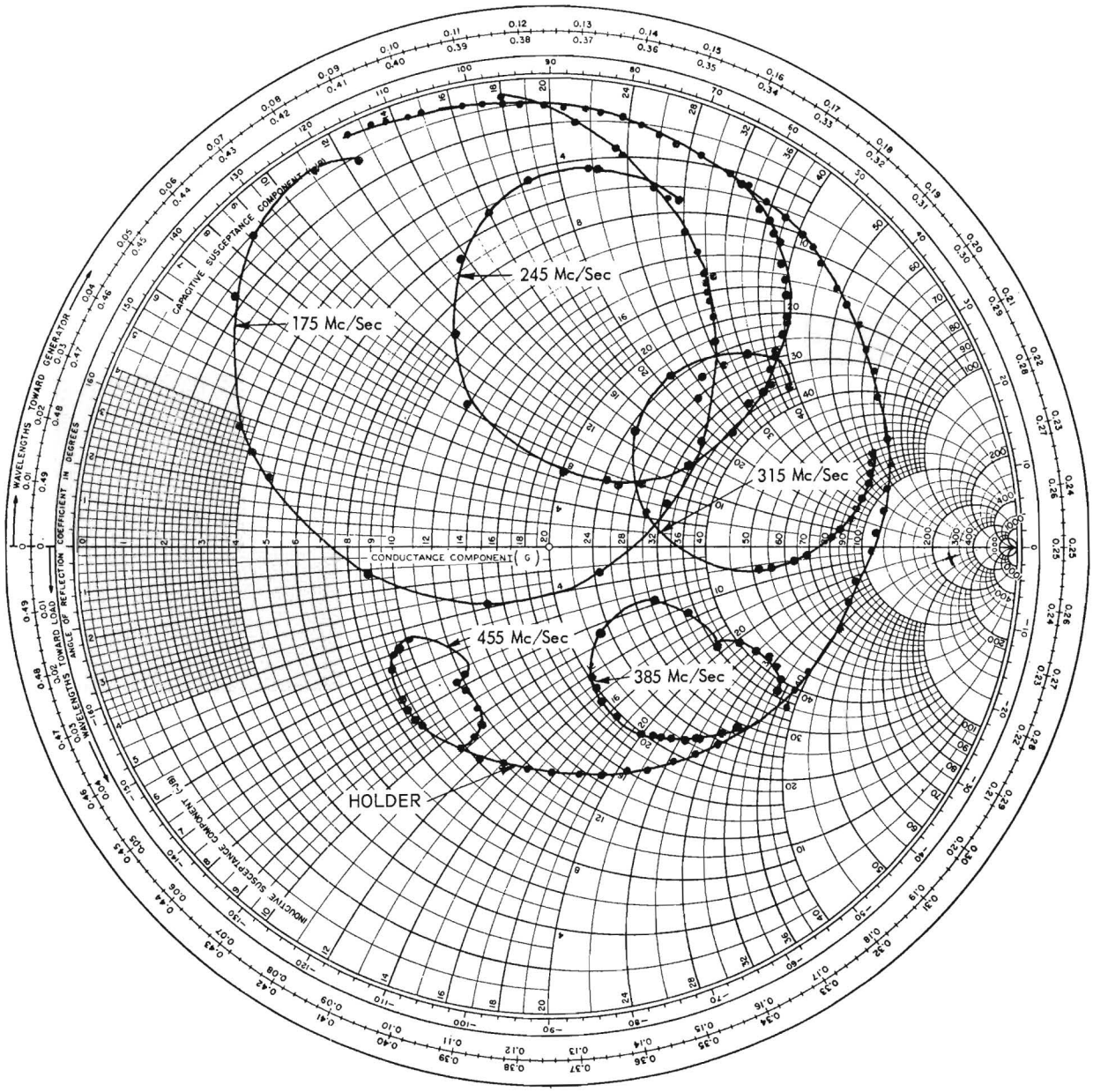

Figure 2. Test Crystal with 9.69 Cm of Transmission Line.

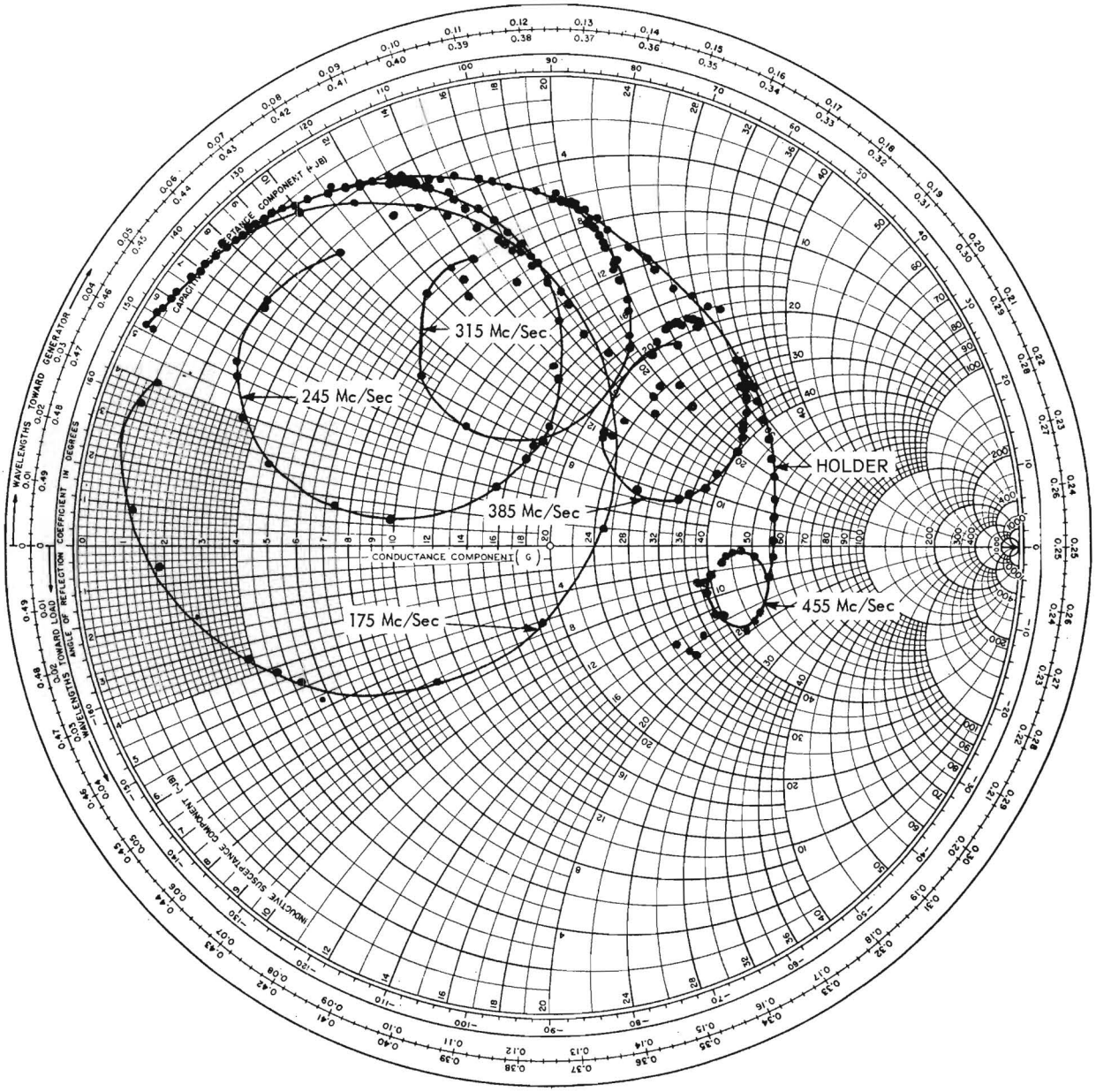

Figure 3. Admittance Characteristics of Test Crystal with Transmission Line Subtracted.

the points. However, certain simplifications in the original data are desirable. For example, the spurious responses have already been omitted from Figure 2 and 3 for simplicity. Also, it is known that if the spurious responses were not present, the principal response at each overtone would be essentially a perfect circle. Thus it is desirable to further simplify the data as shown in Figure 4 where perfect circles are used to represent the holder and all crystal overtone responses.

The data of Figure 3 were compared with corresponding data obtained for the same crystal more than a year ago. Appreciable differences were observed. Similar comparisons were made for other crystals, some of which showed appreciable differences and others which did not. A microscopic examination of the crystals showing the greatest differences revealed minute cracks in the bases. It was assumed that leaks were responsible for the differences in readings. The probability of base leaks can therefore eliminate the feasibility of long term measurement comparison unless great care in handling of the crystals is exercised.

2. Crystal Data Analysis

Several methods exist for reducing the data of Figure 4 together with frequency information to crystal equivalent circuits. The methods differ both in theory and results; however, each of the common methods is based on its particular assumed equivalent circuit. The most commonly used equivalent circuit for VHF-UHF crystals is shown in Figure 5. The element C_o' may or may not be required depending upon the method of mounting the crystal holder while making the measurements.

The value of R_L of Figure 5 may be found to be 17.5 ohms by taking the reciprocal of the maximum conductance of the holder circle of Figure 4 regardless of whether or not C_o' is present.

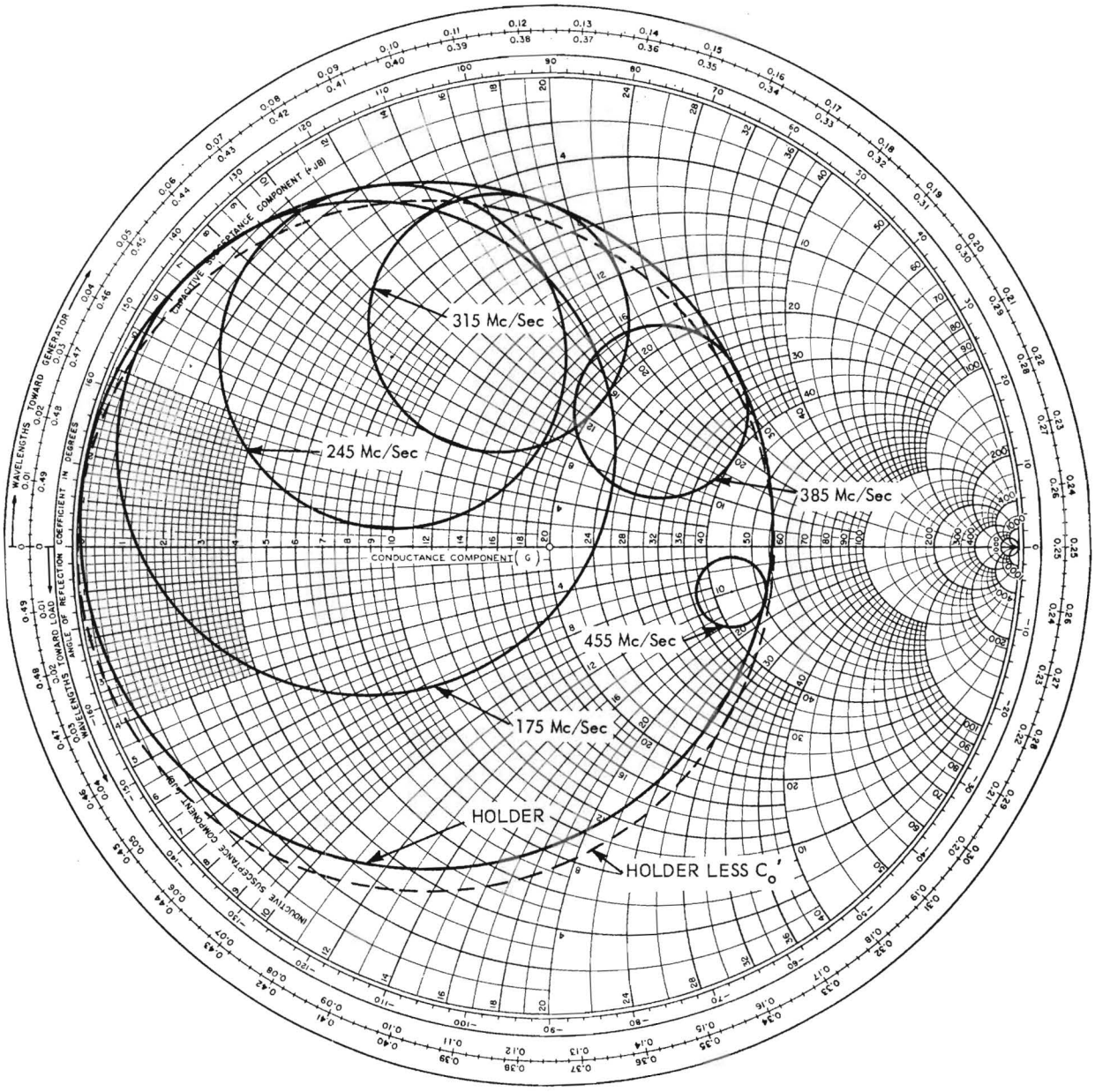

Figure 4. Perfect Circle Approximations of Test Crystal Characteristics.

It will be noted in Figures 3 and 4 that the center of the holder circle does not fall on the zero susceptance axis. This can be caused either by subtracting

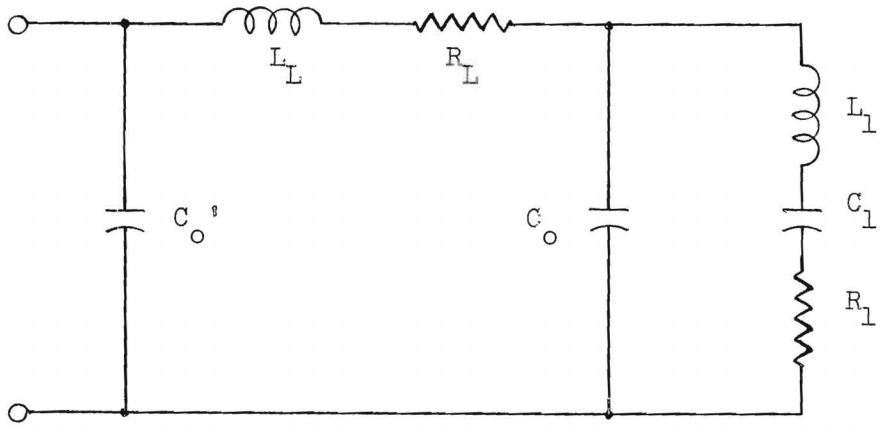

Figure 5. Common Equivalent Circuit for a VHF Quartz Crystal.

an incorrect line length when transforming the data from Figure 2, or it can be caused by the presence of a C_o' across the terminals of the holder. The assumption that the component mount is the length specified by the manufacturer eliminates the possibility of an incorrect line subtraction. A theoretical examination of the equivalent circuit with a C_o' present would reveal that the response is no longer a true circle; however, when C_o' is very small the response is very close to a true circle.

Other factors, such as nonlinear elements, can also account for the displacement of the center of the holder circle. For example, it has been stated by some researchers that C_o is a function of frequency. It is also very likely that the holder resistance varies with frequency. This could, be due to skin effect in the internal leads connecting the quartz plate to the holder pins. Enough evidence has not yet been collected to permit a complete evaluation of this displacement. However, the assumption that it is due to a C_o' introduces only small errors at overtone frequencies below 300 mc/sec.

The dotted circle of Figure 4 shows the approximate holder response with the C_o' removed. The correction is based on a value of C_o' of 0.69 mmfd as calculated at a frequency of 300 mc/sec.

The other holder parameters, L_L and C_o, can be readily calculated from the dotted circle of Figure 4, since this circle now represents a true series resonant response. It is only necessary to know the admittances and frequencies at any two points. The necessary equations can be readily derived from the equations for a simple series resonant circuit. Such calculations yield L_L = 29.9 mμh and C_o = 3.97 mmfd for the test crystal of Figure 4.

To complete the calculations, the holder parameters are removed from the crystal overtone responses and the remaining circles again treated as simple series resonant circuits to calculate L_1, C_1, and R_1. The Q and other parameters of the crystal may then be calculated by conventional methods.

Another method of calculating the crystal parameters has been proposed by Dr. Erich Hafner in USASEL (USASRDL) Engineering Report No. E-1216. His method divides the holder resistance as shown in Figure 6. This analysis has been applied to the test crystal of Figure 4 at 245 mc/sec. Calculated values for R_L

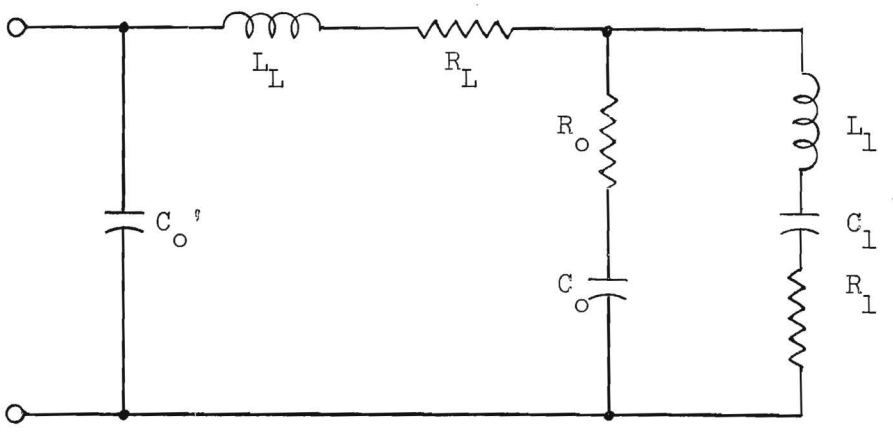

Figure 6. Hafner Equivalent Circuit for a VHF Quartz Crystal.

and R_o were 0.7 and 16.8 ohms respectively. Computer programs have been prepared to check the validity of these calculations, however, the analysis is not yet complete.

3. Radio-Frequency Amplifiers

During this report period, two Instruments for Industry Model 530 wideband chain amplifiers were received. Originally only one amplifier was ordered, but the gain of one amplifier alone was not sufficient for some crystal measurement applications, particularly under mismatched conditions.

The manufacturer specifies that the bandpass of the amplifier is 10 kc to 300 mc/sec, having 18 db voltage gain into a matched load. The input and output impedances of the amplifier are 135 and 150 ohms respectively.

Since the Crystal Measurements Standard System uses 50-ohm coaxial components, the inputs and outputs of the amplifiers will be mismatched and the gain of each amplifier will be reduced. A matching network could be placed on each of the inputs and outputs to match the amplifiers; however, the loss due to the insertion of the networks is often greater than the loss due to mismatched conditions.

In initial tests of the amplifiers it was observed that the output was not constant for constant input conditions. It was assumed that the output variations were due to variation in grid bias. Thus the internal bias source was disconnected and replaced by a 6-volt dry cell. The output fluctuations continued, but were not as severe. The internal B^+ supply was then replaced by an external regulated supply. This reduced the fluctuations to a negligible amount.

A plot of the power gain for various load conditions is given for one of the amplifiers in Figure 7. Also included is a plot of the power gain for the other amplifier working into a 50-ohm load, and a plot of the two amplifiers in cascade working into the same load. The cable impedance in all cases was 50 ohms.

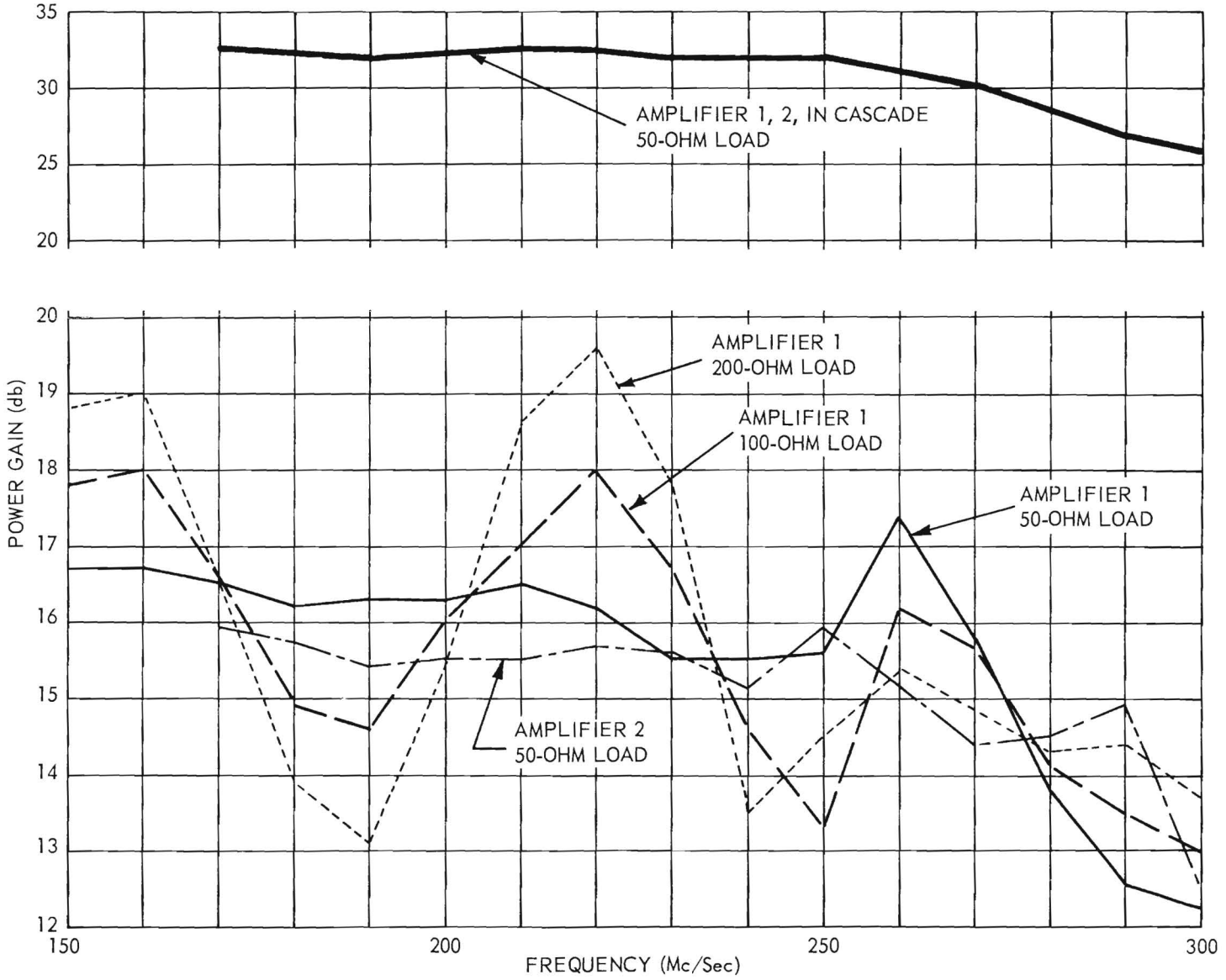

Figure 7. Power Gain Characteristics of IFI Wide-Band Amplifiers.

The apparent cycling of the gain as frequency was varied was due to the mismatch of the coaxial line at both input and output of the amplifier. Since the minimum gain of the two amplifiers in cascade, as shown in Figure 7, is greater than the original requirement of 20 db, and since the power must be adjusted to predetermined values at each frequency and load as indicated by the power measurement system, it was not considered necessary that the gain of the amplifiers be constant over their frequency range.

A test run was made on one of the amplifiers to determine the magnitude of harmonic distortion that would be introduced into the system. The Marconi Signal Generator was adjusted to a frequency of 90 mc/sec and the data obtained as shown in Table I. The data are only approximate and depend on the dial calibration of an AN/APR-4 radar receiver which was used as an output indicator.

TABLE I

THE HARMONIC GENERATION OF A RADIO-FREQUENCY AMPLIFIER

Fundamental Frequency (Mc/Sec)	Amplifier Input Level (Mv)	Harmonic Frequency (Mc/sec)	Harmonic Output (Db Below Fundamental)	
			Signal Gen. (Db)	Amplifier (Db)
90	2	180	44	44
90	2	270	36	36
90	100	180	48	27
90	100	270	40	40

With an input of 2 mv, the amplifier does not introduce appreciable harmonic distortion. However, it can be seen that more distortion is introduced with an input of 100 mv. To eliminate possible errors in crystal measurements due to harmonic excitation, two Microlab Corporation low-pass filters were purchased. The cutoff frequencies specified by the manufacturer are 300 mc/sec for

the Model FL-301, and 400 mc/sec for the Model FL-401. Microlab specifies that the stop band limit of their filters is greater than six times the cutoff frequency. A 200 mc/sec low-pass filter (Model LP-200, Microphase Corporation) was already in possession of the project. The characteristics of the three filters are shown in Figure 8. It can be noted that for any frequency in the range 175 to 300 mc/sec, use of the various filters will provide harmonic rejection of at least 40 db up to the sixth harmonic of the fundamental assuming a stop band limit as specified.

4. Calibration of Instruments

Extensive efforts have been made to determine the accuracy of the new General Radio Admittance Meter Type 1602B during this report period. No definite conclusions can yet be made concerning the expected overall accuracy of the Crystal Measurements Standard using this instrument; however, some of the more important calibration data will be presented here.

The instrument correction charts supplied by the manufacturer were presented in Progress Report No. 2. At that time it was believed that accuracies of the order of one percent for impedance magnitude and one degree for phase angle could be obtained when measuring impedances near 50 ohms resistance. This has since been substantiated by the data shown in Figure 9 for three different terminations mounted directly on the Admittance Meter. It will be noted that the accuracy with the 50-ohm termination is well within one percent for magnitude and one degree for phase angle. The accuracy with the 100-ohm termination is slightly poorer than was obtained with the 50-ohm termination. For the 200-ohm termination the error exceeds one percent for magnitude but is almost within one degree for phase angle. This data run was repeated on two other occasions with approximately the same results.

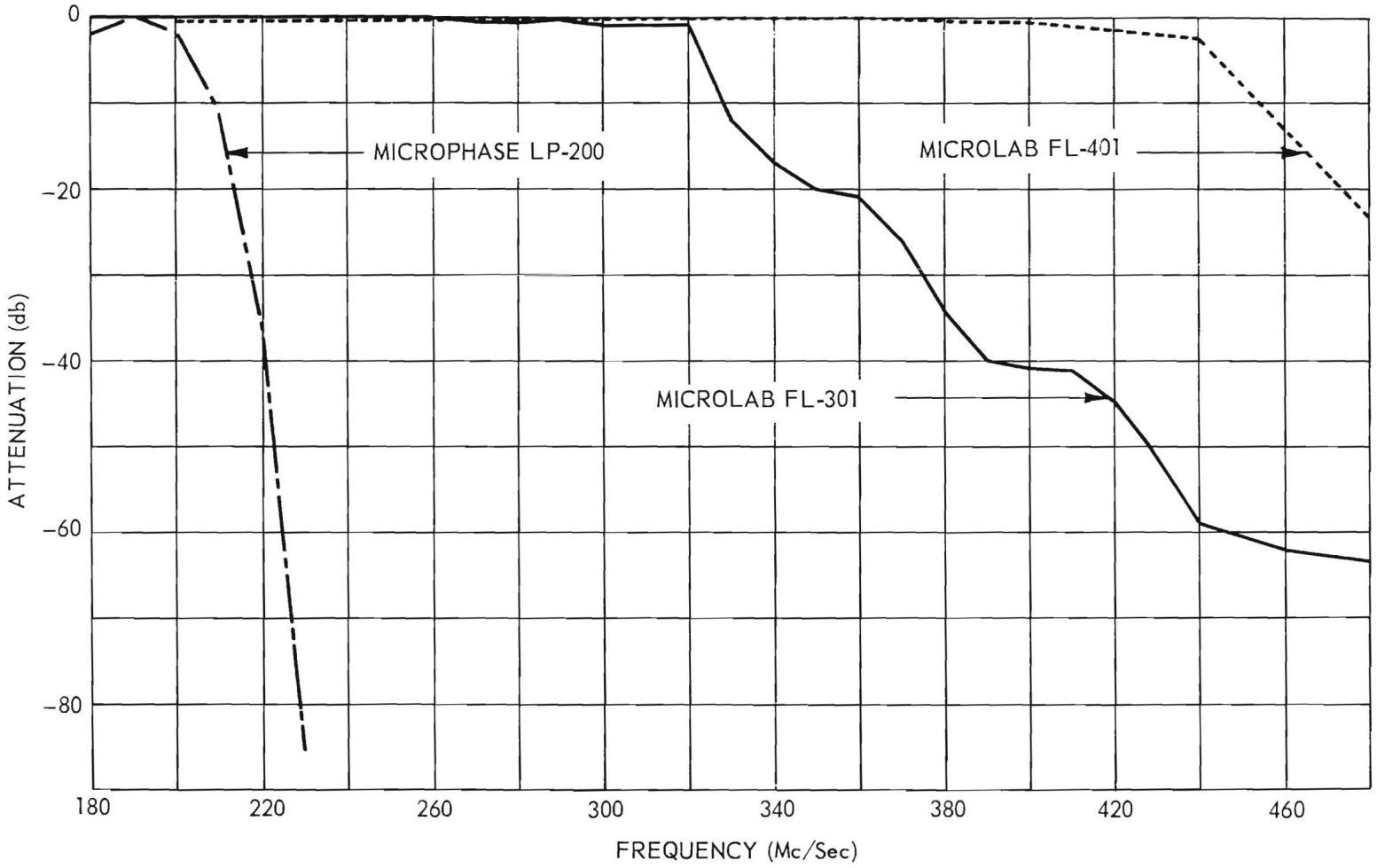

Figure 8. Frequency Characteristics of Low-Pass Radio-Frequency Filters.

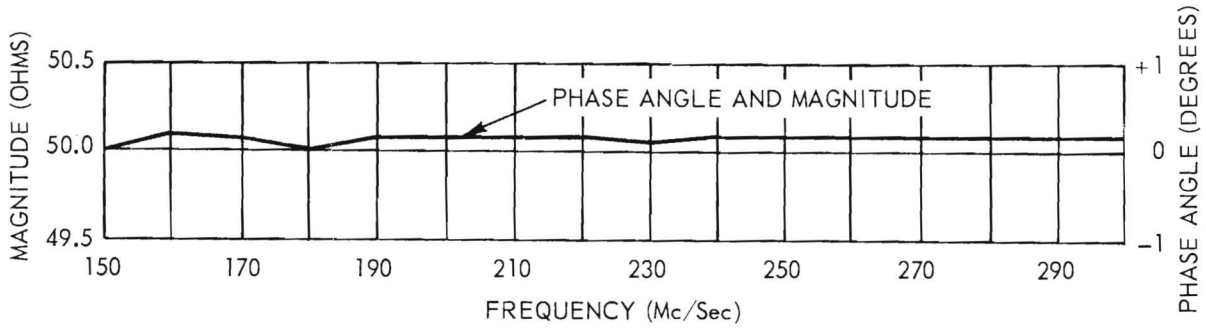

(a) 50-OHM TERMINATION

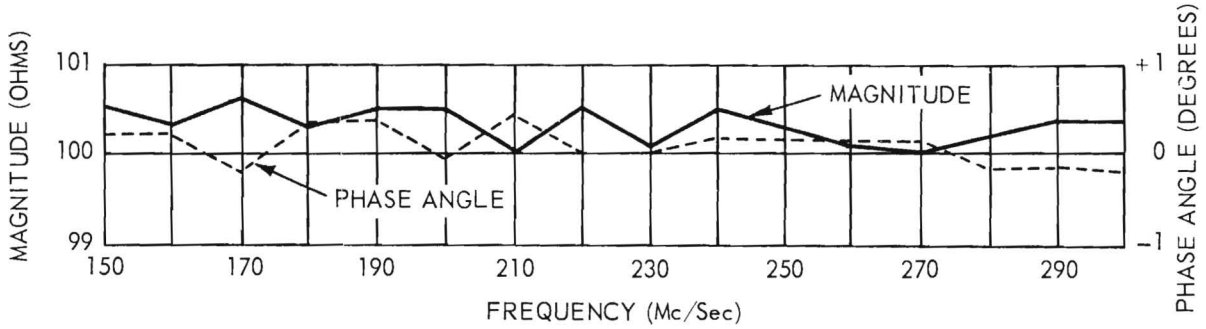

(b) 100-OHM TERMINATION

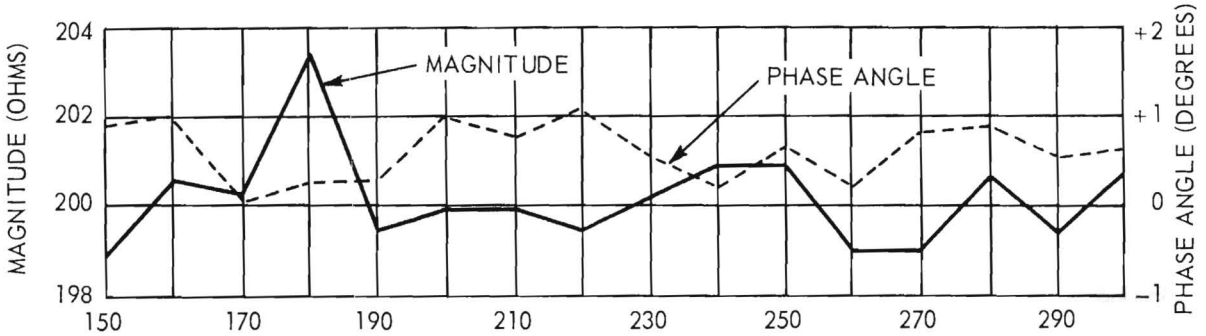

(c) 200-OHM TERMINATION

Figure 9. Admittance Meter Measurements on Resistive Terminations with Minimum Line Length.

A study of the Admittance Meter dials partially explains the errors shown in Figure 9. For example, the resolution at 5 millimhos on the dials (200 ohms) is only one percent if it is assumed that readings can be made to one-tenth of the smallest division. This precision in reading is generally not possible without optical aids.

The data shown in Figure 9 were obtained with the terminations mounted directly on the Admittance Meter. The calculated electrical separation between the termination terminals and the internal bridge terminals was 9.69 cm. The Admittance Meter readings were first corrected by using the charts presented as Figures 5 and 6 of Progress Report No. 2. The 9.69 cm of 50-ohm transmission line were then subtracted by a digital computer using a specially prepared program. No line losses were considered since the correction charts included such effects.

The particular terminations, line lengths, and frequencies used in the above run are capable of checking the calibration of the Admittance Meter only over a very limited range of the Smith chart. As a result, the data presented cannot lead to any general conclusions concerning the overall accuracy of the instrument.

Since the procedure for measuring the drive level of a crystal involves the insertion of a Hewlett-Packard Dual Directional Coupler Model 764D between the component mount and the Admittance Meter, additional data runs were made with the coupler in position but using the standard terminations to replace the component mount. The results are shown in Figure 10. The data for these curves were again obtained by applying the instrument corrections and then subtracting the electrical length of the complete transmission line. It was necessary to determine this electrical length by a series of open- and short-circuit measurements over the frequency range. As the calculated length showed wide variations under various conditions an average value was calculated. The accuracy of the choice can be evaluated from the phase angle curves of Figure 10.

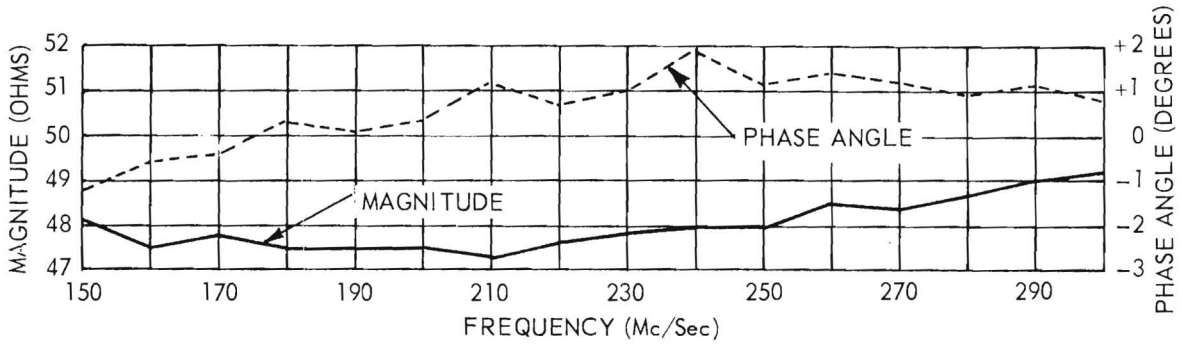

(a) 50-OHM TERMINATION

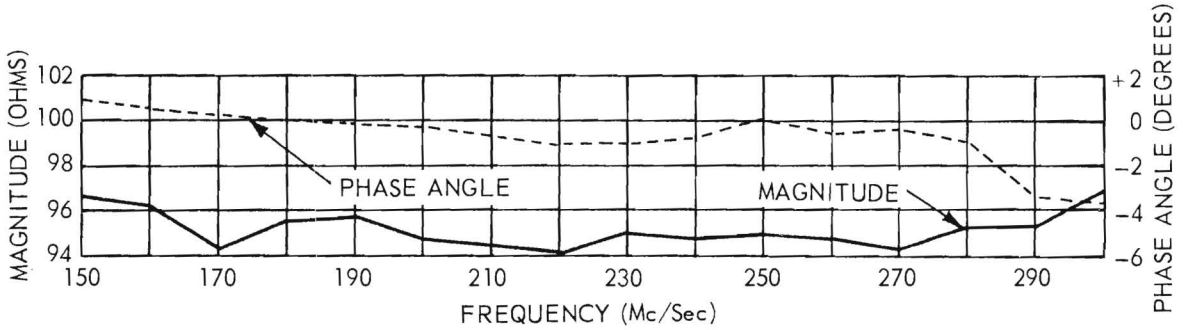

(b) 100-OHM TERMINATION

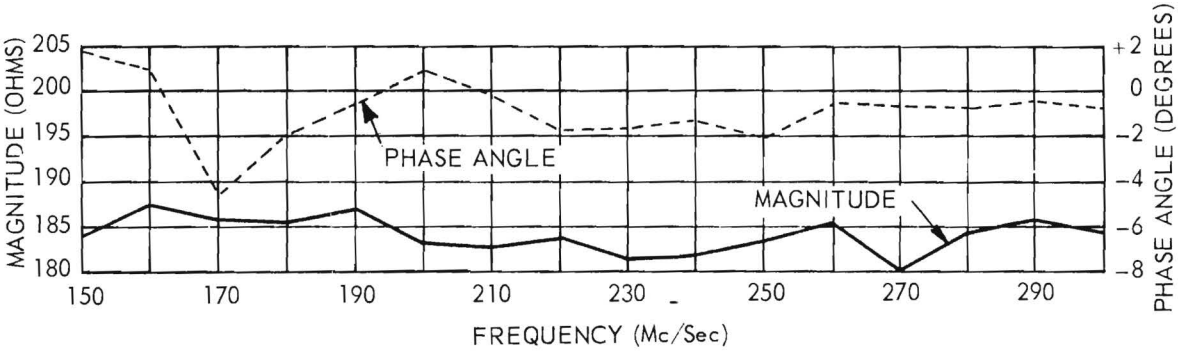

(c) 200-OHM TERMINATION

Figure 10. Admittance Meter Measurements on Resistive Terminations with a Dual Directional Coupler Inserted in the Coaxial Line.

It was first assumed that the large errors indicated by Figure 10 were due to excessive losses in the directional coupler. The coupler was therefore replaced by an approximately equal (40-cm) length of air-dielectric transmission line. A repeat of the data run yielded the results shown in Figure 11. It will be observed that the errors are of approximately the same magnitude.

A series of evaluation tests were initiated to determine the sources of error when the directional coupler or additional transmission line was in use. The first consideration was the effects of the multiplying dial of the Admittance Meter. It is desirable, due to the construction of the instrument, that all measurements be made such that conductance and susceptance readings both remain less than 20-millimhos or such that the multiplying factor is unity. This was possible with the choice of terminations and frequencies used with the minimum line length (9.69-cm). However, when the longer line lengths were used, multiplying factors as high as 5 were required. To determine the magnitude of errors introduced by the multiplier dial, a series of measurements were made by setting the multiplier to discrete values between one and two and recording the conductance and susceptance readings. It was found that the multiplier could account for errors greater than one percent. A recheck of the data of Figures 10 and 11, however, showed no general correlation between the multiplying factor and the observed errors. Although this source of error is important, it is not considered to be the major factor in this case.

Probably the most logical sources of error are transmission line deficiencies of various types. The following method was considered for correcting for some of these deficiencies.

At any single frequency, a transmission line of arbitrary length may be represented as a two-terminal pair network as shown in Figure 12. Since the line

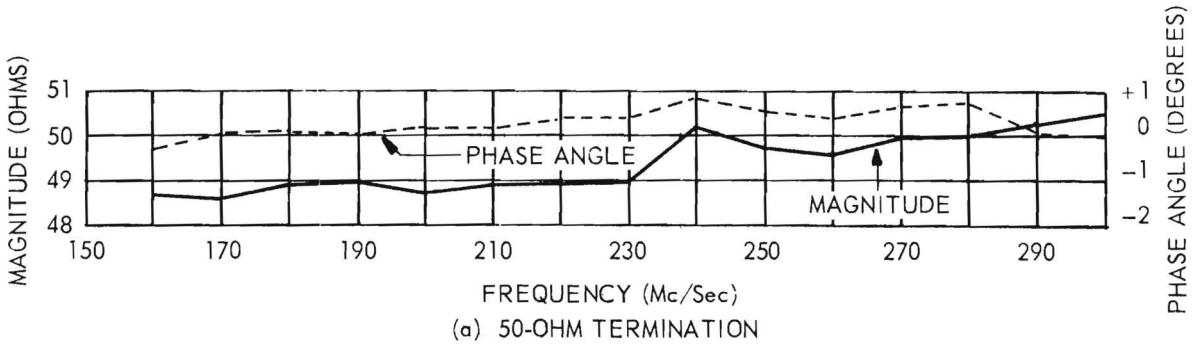

(a) 50-OHM TERMINATION

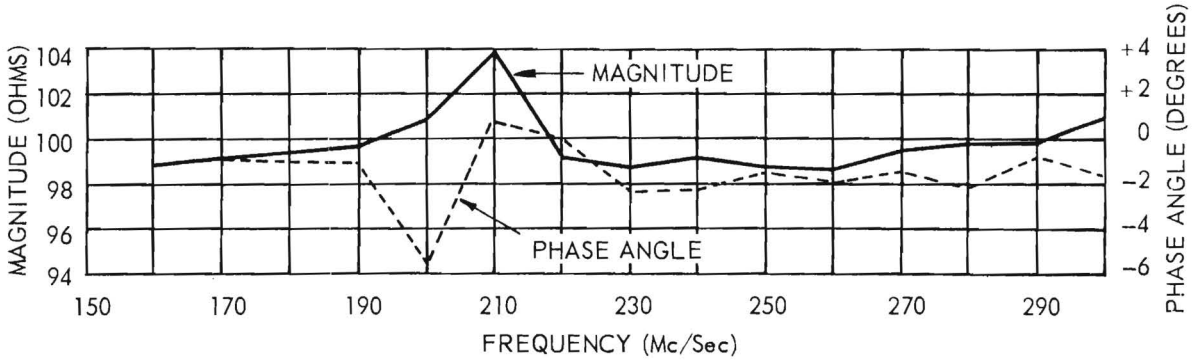

(b) 100-OHM TERMINATION

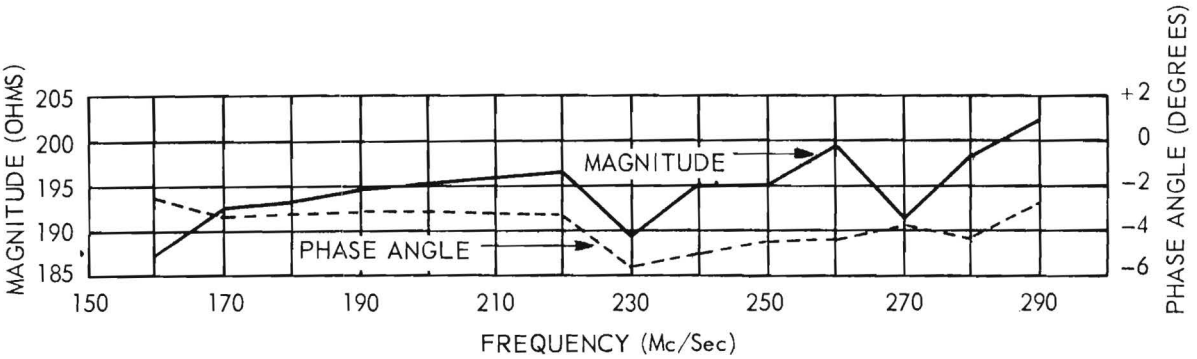

(c) 200-OHM TERMINATION

Figure 11. Admittance Meter Measurements on Resistive Terminations with a 40-Cm Line Length.

is symmetrical, both shunt admittances may be labeled Y_a. Y_b is the series admittance of the equivalent pi-circuit. Y_L represents an arbitrary load. If $Y_{(s)}$ and $Y_{(o)}$ are used to represent the sending-end admittance with the load terminals

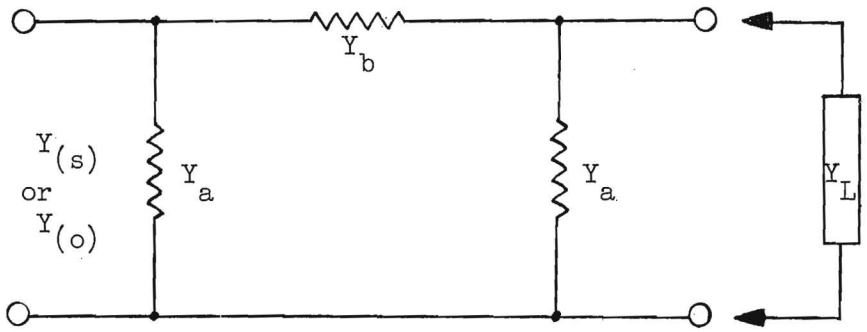

Figure 12. Network Approximation of a Transmission Line.

respectively shorted and opened, the conventional transmission line equation,

$$Z = Z_o \frac{Z_R + Z_o \tanh \gamma \ell}{Z_o + Z_R \tanh \gamma \ell} \quad , \tag{1}$$

becomes

$$Y_{(s)} = \frac{1}{Z_o} \coth \gamma \ell \tag{2}$$

for the short-circuit condition and

$$Y_{(o)} = \frac{1}{Z_o} \tanh \gamma \ell \tag{3}$$

for the open-circuit condition, where Z_R represents the receiving end condition, γ is the propagation constant, ℓ is the line length, and Z_o is the characteristic impedance of the line.

But, from Figure 12,

$$Y_{(s)} = Y_a + Y_b \tag{4}$$

and

$$Y_{(o)} = Y_a + \frac{Y_a Y_b}{Y_a + Y_b} \quad . \tag{5}$$

Substituting Y_a from Equation 4 into Equation 5 yields

$$Y_{(o)} = Y_{(s)} - Y_b + \frac{(Y_{(s)} - Y_b)Y_b}{Y_{(s)}} \tag{6}$$

or

$$Y_{(o)}Y_{(s)} = (Y_{(s)} - Y_b)(Y_{(s)} + Y_b) = Y_{(s)}^2 - Y_b^2 \ , \tag{7}$$

from which

$$Y_b^2 = Y_{(s)}^2 - Y_{(o)}Y_{(s)} \quad . \tag{8}$$

Letting $Y_o = 1/Z_o$ in Equation 8 and substituting $Y_{(s)}$ and $Y_{(o)}$ from Equations 2 and 3 gives

$$\begin{aligned} Y_b^2 &= Y_o^2 \coth^2 \gamma\ell - Y_o^2 \tanh \gamma\ell \coth \gamma\ell \\ &= Y_o^2 (\coth^2 \gamma\ell - 1) = Y_o^2 \operatorname{csch}^2 \gamma\ell \end{aligned} \tag{9}$$

or

$$Y_b = \frac{Y_o}{\sinh \gamma\ell} \quad . \tag{10}$$

From Equation 4

$$\begin{aligned} Y_a &= Y_{(s)} - Y_b = Y_o \coth \gamma\ell - \frac{Y_o}{\sinh \gamma\ell} \\ &= Y_o \left(\frac{\cosh \gamma\ell - 1}{\sinh \gamma\ell}\right) \ . \end{aligned} \tag{11}$$

But,

$$\cosh X - 1 = 2 \sinh^2 \frac{X}{2} \tag{12}$$

and

$$\sinh X = 2 \sinh \frac{X}{2} \cosh \frac{X}{2} \tag{13}$$

or

$$\frac{\cosh X - 1}{\sinh X} = \frac{\sinh X/2}{\cosh X/2} = \tanh \frac{X}{2} \quad . \tag{14}$$

Therefore,

$$Y_a = Y_o \tanh \frac{\gamma \ell}{2} \quad . \tag{15}$$

When the load, Y_L, of Figure 12 is connected, the input admittance, Y, becomes

$$Y = Y_a + \frac{(Y_a + Y_L)\, Y_b}{Y_a + Y_b + Y_L}$$

$$= \frac{Y_a(Y_a + Y_b) + Y_L(Y_a + Y_b) + Y_a Y_b}{(Y_a + Y_b) + Y_L} \quad . \tag{16}$$

Equation 16 may be simplified by replacing $(Y_a + Y_b)$ by $Y_{(s)}$ as in Equation 4 to yield

$$Y = \frac{Y_{(s)}(Y_a + Y_L) + Y_a Y_b}{Y_{(s)} + Y_L}$$

$$= Y_{(s)} \frac{(\frac{Y_a Y_b}{Y_{(s)}} + Y_a) + Y_L}{Y_{(s)} + Y_L} \quad . \tag{17}$$

Further simplification results from substituting Equation 5 into Equation 17 to obtain

$$Y = Y_{(s)} \frac{Y_{(o)} + Y_L}{Y_{(s)} + Y_L} \tag{18}$$

or

$$Y_L = Y_{(s)} \frac{Y_{(o)} - Y}{Y - Y_{(s)}} \quad . \tag{19}$$

For a half-wavelength line, since $Y_{(s)}$ is very large

$$Y_{\lambda/2} = Y_{(s)} \frac{Y_{(o)} + Y_L}{Y_{(s)} + Y_L} \Bigg|_{Y_{(s)} \to \infty} = Y_{(o)} + Y_L \tag{20}$$

or

$$Y_L = Y_{\lambda/2} - Y_{(o)} \quad . \tag{21}$$

Equation 19 was programmed on a digital computer and used to correct the original data of Figures 10 and 11. The results were approximately the same as obtained from line subtractions. Even greater errors were obtained in some cases near quarter- and half-wavelength points where either $Y_{(o)}$ or $Y_{(s)}$ became very large. This method of line length correction was cross-checked with the 9.69-cm data of Figure 9 and showed very good agreement. It is interesting to note that this method of line length subtraction does not require a knowledge of the actual line length or of the frequency. In addition, it should compensate for some if not all of the line deficiencies. On a practical basis, it did not, however, accomplish this later purpose.

In an attempt to reduce some of the errors encountered when using the directional coupler or a coaxial line section between the Admittance Meter and the termination, several sources of error were considered.

The first consideration concerned the admittance calculation procedure just described. As mentioned above, when the frequency is such that the line length is near a quarter- or half-wavelength, the admittance of either the short- or

open-circuit termination is very large and, therefore, requires a large multiplying factor on the Admittance Meter dial. At such lengths, if the conductance with the open- or short-circuit termination were actually zero, as it would be for a perfect termination and perfect coaxial line, but were recorded as 0.1 millimho (one-fifth of the smallest division on the conductance scale), a multiplying factor of ten would make the conductance appear to be 1 millimho instead of zero. This becomes an appreciable conductance when compared with the readings with the resistive terminations, and would introduce large errors in the calculations of the impedance of the terminations. In an attempt to eliminate this occurrence, the line was assumed to be lossless and the conductive readings of either the open-circuit termination, the short-circuit termination, or both were assumed to be zero. The directional coupler and 40-cm line data were rerun on the computer with each of these three assumptions and the results replotted. The accuracies were improved near 150 and 300 mc/sec, but the overall accuracy was as poor or poorer than that of the line subtraction methods. This result would seem plausible since under the above assumptions, the admittance calculation method reduces to a line subtraction method and thus defeats its originally intended purpose.

One possible source of error in the measurement system is incorrect coaxial line impedances. Accordingly, the diameters of the center conductor of several samples of coaxial line were measured. It was found that the variations in diameters could produce variations in the impedance of the lines greater than one percent.

Assuming that the lines were lossless, but of the wrong impedance, three samples of the 40-cm line data, one for each of the resistive terminations, were selected for further study. By trial and error, a resistive impedance (Z_o = 51.39 ohms) was found which, when used in conjunction with the transmission line

equation, resulted in impedance magnitudes of 50, 100, and 200 ohms respectively for the three terminations. The remaining 40-cm line data were then run in the computer using 51.39 ohms for Z_o instead of 50 ohms. The results are shown in Figure 13. It can be seen from the graph that this type of compensation is not adequate since the magnitude of the impedance of the terminations is increased too much at the lower frequencies while it is not increased enough at the higher frequencies. The data indicated that the errors in the 40-cm line run and the directional coupler run were caused by line losses in addition to a possible impedance error.

The general transmission line equation which applies to any uniformly distributed parameter line is

$$Z = Z_o \frac{Z_r + Z_o \tanh \gamma \ell}{Z_o + Z_r \tanh \gamma \ell} \tag{22}$$

where

$$\gamma = \sqrt{(G + j\omega B)(R + j\omega L)} \tag{23}$$

and

$$Z_o = \sqrt{\frac{R + j\omega L}{G + j\omega B}} \quad . \tag{24}$$

It can be seen that both Z_o and γ are functions of frequency and that five unknowns (G, B, R, L, and ℓ) exist for any given line. Solving for these five unknowns is a difficult task due to the complexity of the equations involved even if the input data is precise. The difficulty is further compounded by the limited resolution of the Admittance Meter and limited accuracy of the correction charts. Also, the above equation is valid only if the line is uniform, which, due to connectors and the physical qualities of the line, is not entirely true.

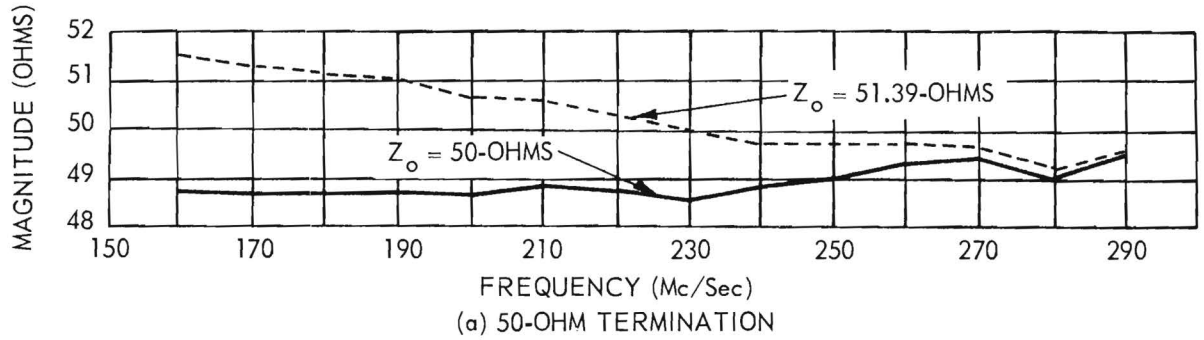

(a) 50-OHM TERMINATION

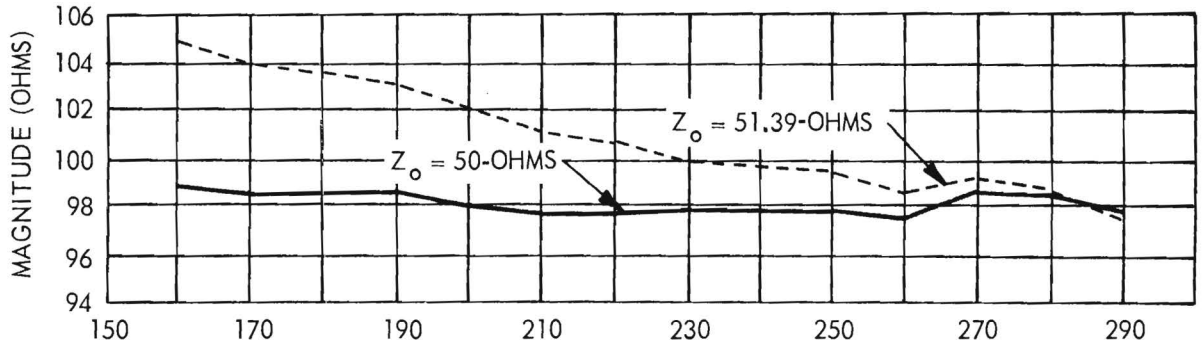

(b) 100-OHM TERMINATION

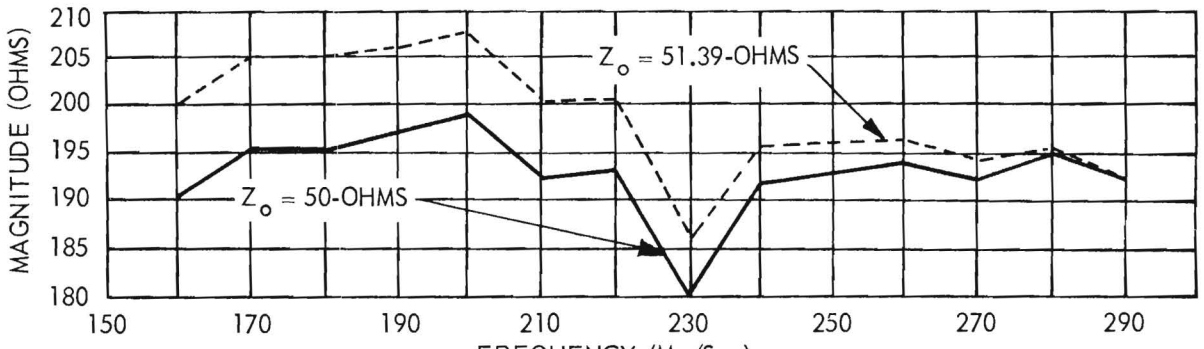

(c) 200-OHM TERMINATION

Figure 13. Impedance Level Compensation of 40-Cm Transmission Line Data.

Because of the lack of personnel time, further efforts to correlate these factors were temporarily discontinued.

An alternate method of improving the measurement accuracy with the directional coupler is to place the coupler in a half-wavelength transmission line. This method has the advantage that the Admittance Meter directly reads the actual admittance of the crystal or termination after dial corrections have been made, thus eliminating the necessity of using the computer for line subtractions. Also, if the total line is lossless, the actual physical length and impedance of the line need not be known. The disadvantages of the half-wavelength method are threefold: (1) line loss compensations are inconvenient to make, (2) the method requires more personnel time for obtaining the same amount of data than does fixed line methods due to the time required to set up the half-wavelength line for each frequency, and (3) Admittance Meter calibrations cannot be readily checked since only one point is represented on a Smith chart for each termination as frequency is varied.

The normal procedure used in setting up a half-wavelength line is to place an open-circuit termination on the end of the coaxial line and vary the length of the line until the Admittance Meter and detector system null at zero susceptance. When this setup procedure was used, phase angles of the order of 3 or 4 degrees were obtained for the terminations. However, an inspection of the correction charts showed the susceptive correction for a reading of $0 + j0$ to be $-j0.5$. The line was therefore not set at an exact half-wavelength. In a second run, the Admittance Meter was set to a reading of $0 + j0.5$ and the line adjusted so that the detector indicated a null. After corrections then, the susceptance of the open-circuit termination was zero, indicating a half-wavelength line. The results for such a run with the three terminations using a coaxial air line are shown in Figure 14. The directional coupler was not used in the line for the run since it was desirable to determine the best possible accuracy.

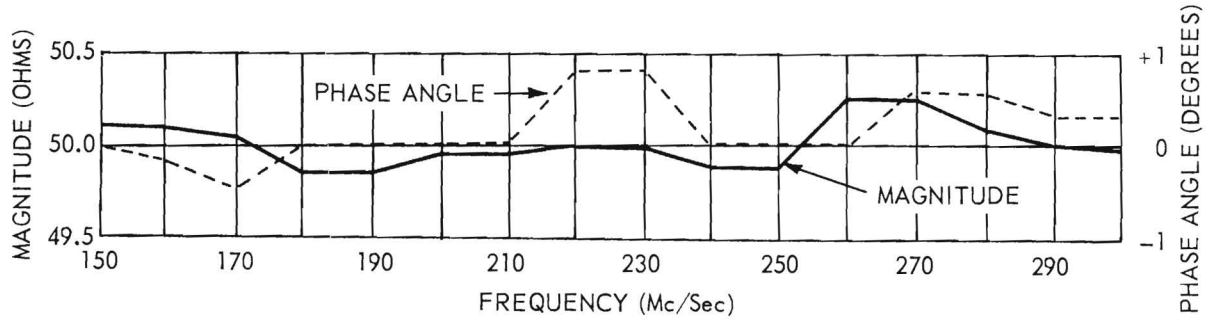

(a) 50-OHM TERMINATION

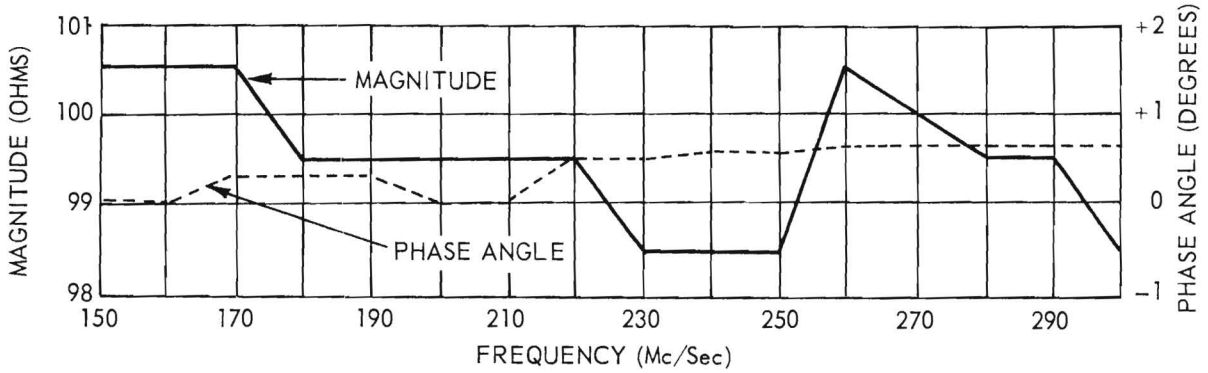

(b) 100-OHM TERMINATION

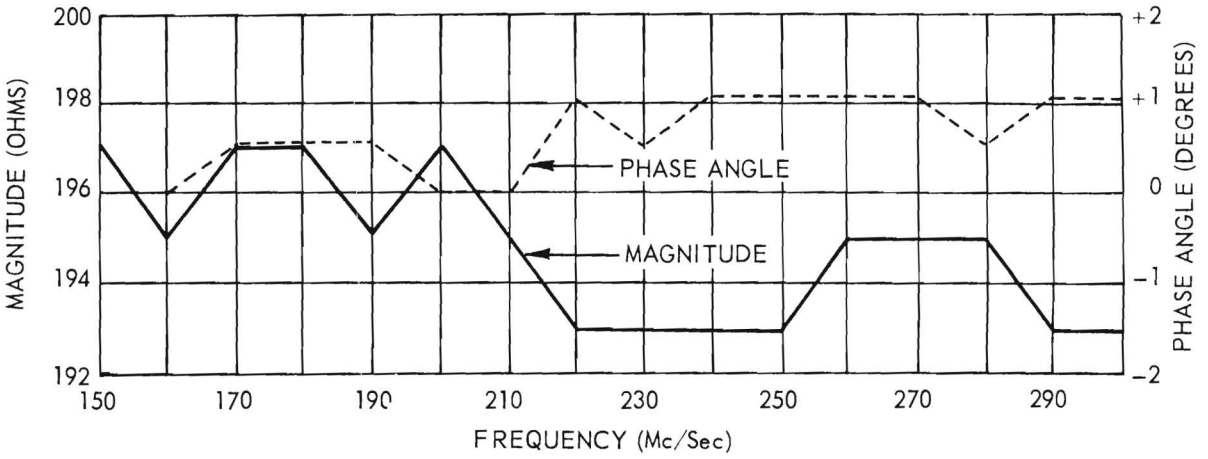

(c) 200-OHM TERMINATION

Figure 14. Admittance Meter Measurements on Resistive Terminations with Half-Wavelength Line.

The accuracy for the 100- and 50-ohm termination is comparable to the 9.69-cm run, while the accuracy for the 200-ohm termination, although better than other coaxial line runs, was not as good as the 9.69-cm run.

Measurements have not yet been made using the directional coupler as a part of the half-wavelength line. This is the next logical step in attempting to find a method whereby the directional coupler may be used in the Admittance Meter measurements without introducing appreciable additional errors.

The following conclusions may be drawn from the preceding data: (1) measurement errors of less than one percent and one degree respectively for impedance magnitude and phase angle are possible when the terminations are placed directly on the Admittance Meter terminals and when the impedance magnitude is of the order of 50 ohms, (2) both the directional coupler and arbitrary lengths of coaxial line introduce appreciable errors in measurements, (3) suitable methods to correct for the errors introduced by the directional coupler and coaxial lines have not yet been found.

5. Power Measurement System

Evaluation and testing of the power measurement system were essentially completed during the period covered by Progress Report No. 2. During the current period two additional factors concerning the system were considered: (1) the effects of the directional coupler on the accuracy of the admittance measurements and (2) the possibility of simplifying the method of reading the crystal power dissipation.

The effects of the directional coupler on the accuracy of the admittance measurements are considered elsewhere in this report. Although the evaluation is not yet complete or conclusive, the possibility that the coupler may completely upset the accuracy of the admittance measurements must be given some consideration. In this event, there is a possibility that the directional coupler

may be placed between the Admittance Meter and the Signal Generator. In this position the power measurement system would read the total power delivered to the crystal plus the power dissipated in the resistive standard of the Admittance Meter. Additional line and stub losses would also be present. It may be possible that these various dissipated powers can be independently evaluated; however, the power measurement system would not be direct reading. Further consideration will not be given to these factors unless it is found that the directional coupler definitely cannot be used between the Admittance Meter and the crystal under test.

Various methods have been considered for simplifying the power measurement procedure. The greatest improvement would be to eliminate the balancing procedure which requires the use of a Helipot and null detector. This can be accomplished by attaching a sufficiently sensitive d-c voltmeter directly to the series-connected diodes at the outputs of the directional coupler. Until recently, sufficiently sensitive and accurate instruments of this type were not available. During this period, four of the currently available sensitive voltmeters were tested in the laboratory. Only two of the instruments had the necessary floating input and one of these instruments had too low an input impedance. The remaining instrument, the Hewlett-Packard Model 425A, was placed on order. The instrument has not yet been received.

C. Other Measurement Systems

1. Test Results

Initial tests of the Equivalent Circuit Crystal Measurement System as described in Progress Report No. 2 showed close agreement in the calculation of crystal Q with other methods for one crystal at 245 mc/sec. For the same crystal at 175 mc/sec, the agreement was poor. To further evaluate the source of the large errors, the electrical resonance data have since been plotted over the frequency range from 120 to 240 mc/sec as shown in Figure 15 (original circuit). It

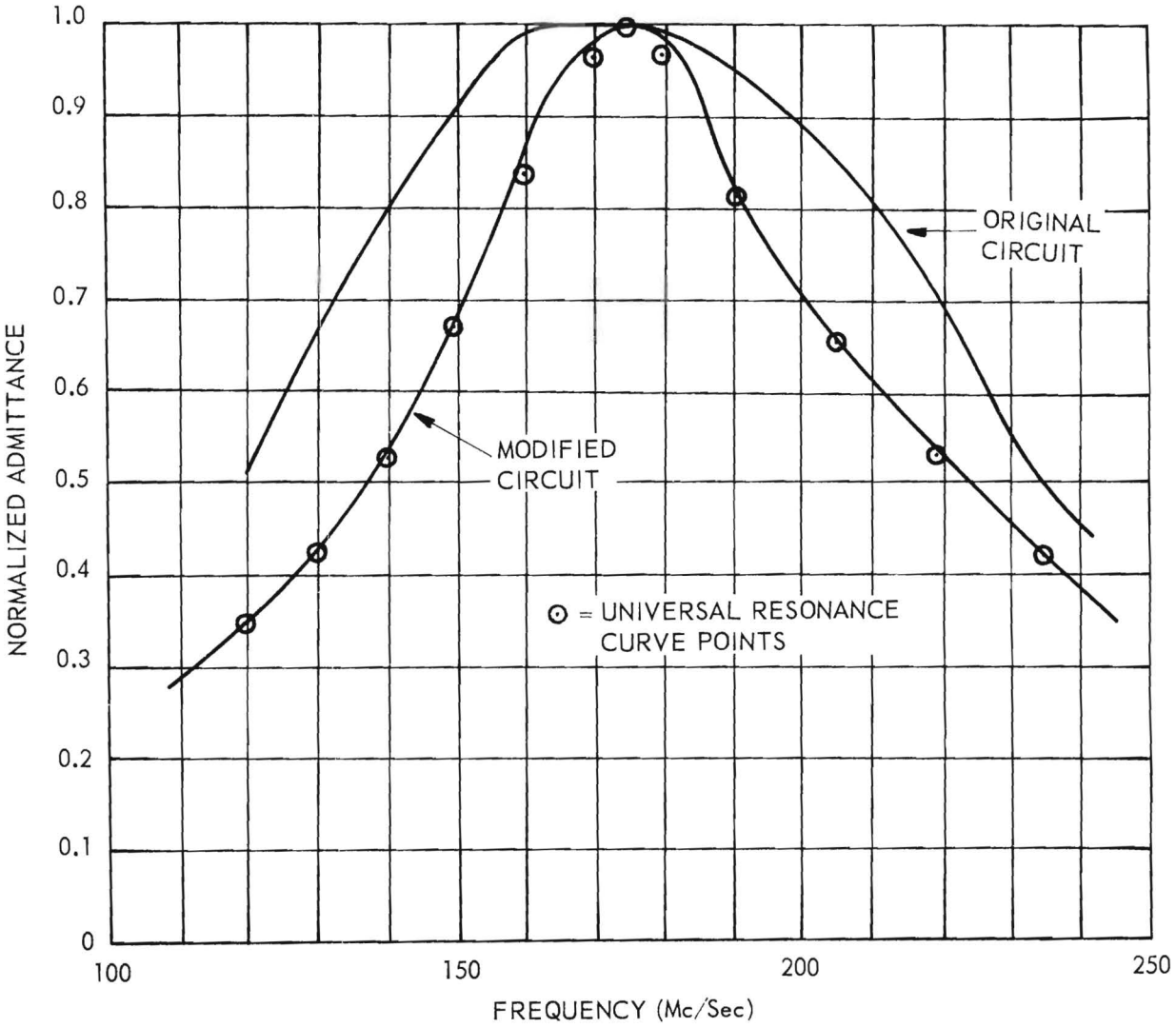

Figure 15. Electrical Resonance Characteristics of the Equivalent Circuit Crystal Measurement System.

can be seen that the graph given does not resemble a series resonant circuit response. The data indicated that a more nearly constant voltage source was needed, thus the circuit was modified as shown in Figure 16. The 47-ohm series resistor and the 5-ohm shunt resistor were used to terminate the coaxial line from the

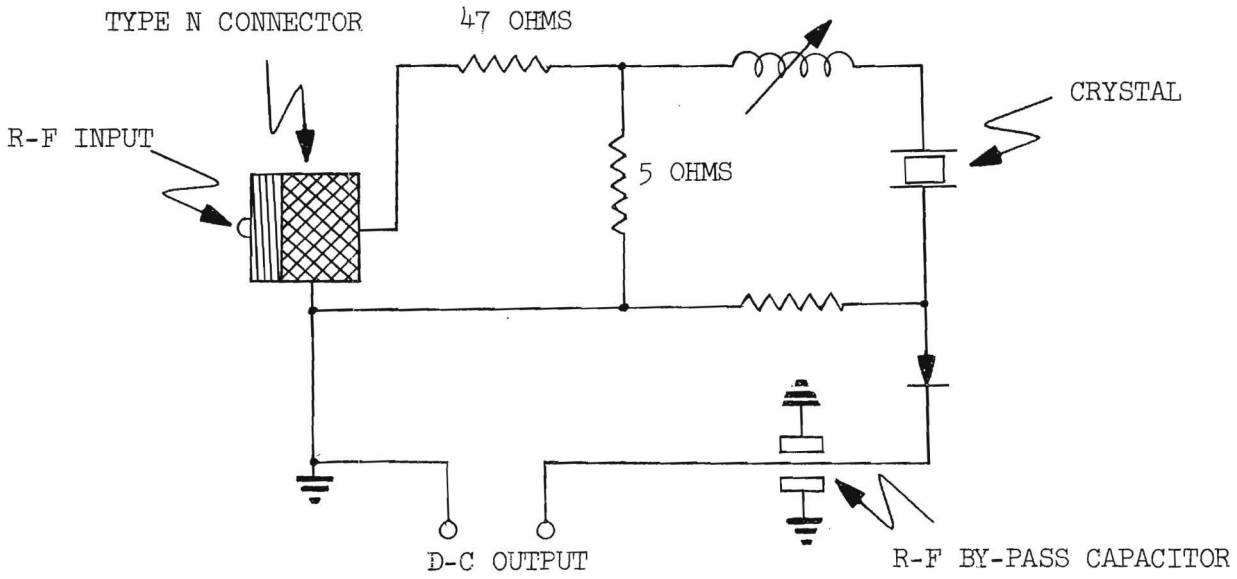

Figure 16. Modified Circuit of the Equivalent Circuit Crystal Measurement System.

Marconi Signal Generator in approximately 50 ohms over a wide range of frequencies. Then by adjusting the carrier signal input to the coaxial line by use of the signal level meter on the signal generator, the signal applied to the actual crystal circuit was held constant. The crystal was again tested at 175 mc/sec and the electrical resonance data shown in Figure 15 (modified circuit) were obtained. The Q of the electrical circuit was calculated from the half-power points. The universal resonance curve for a series resonant circuit with the same Q is also plotted on Figure 15 (circles). The similarity in shape of the

two curves indicated that the circuit was functioning as predicted by mathematics. The calculated Q of the crystal now agreed more closely with that calculated by other methods.

2. Spurious Mode Detection

A block diagram of a proposed spurious mode detection system is shown in Figure 17. The crystal is excited by an oscillator whose frequency is being swept by a saw tooth voltage generator. The current in the measurement circuit (and therefore the relative admittance of the circuit) is measured by placing a diode across a series resistor in the circuit. The output of the diode is connected to a differentiator whose output will be a d-c voltage proportional to the r-f current in the measurement circuit. This d-c voltage is then amplified by a d-c amplifier and displayed on an oscilloscope. The horizontal sweep of the oscilloscope is synchronized by the saw tooth generator. With this system, the magnitude and displacement of spurious responses of the crystal could be directly evaluated by comparison with the main response.

It is interesting to note that at least one instrument (Transitron Model SG-132) is available commercially which may be capable of performing all of the required functions after some internal modifications. This instrument includes:

(1) an r-f oscillator assembly,

(2) a power-stabilizing and power-monitoring circuit,

(3) a sweep generator and modulator circuit,

(4) an oscilloscope,

(5) a marker-generating circuit, and

(6) a power supply circuit.

The internal sweep generator operates at 25 cps. This frequency would probably be too high for crystal operation and therefore would have to be modified

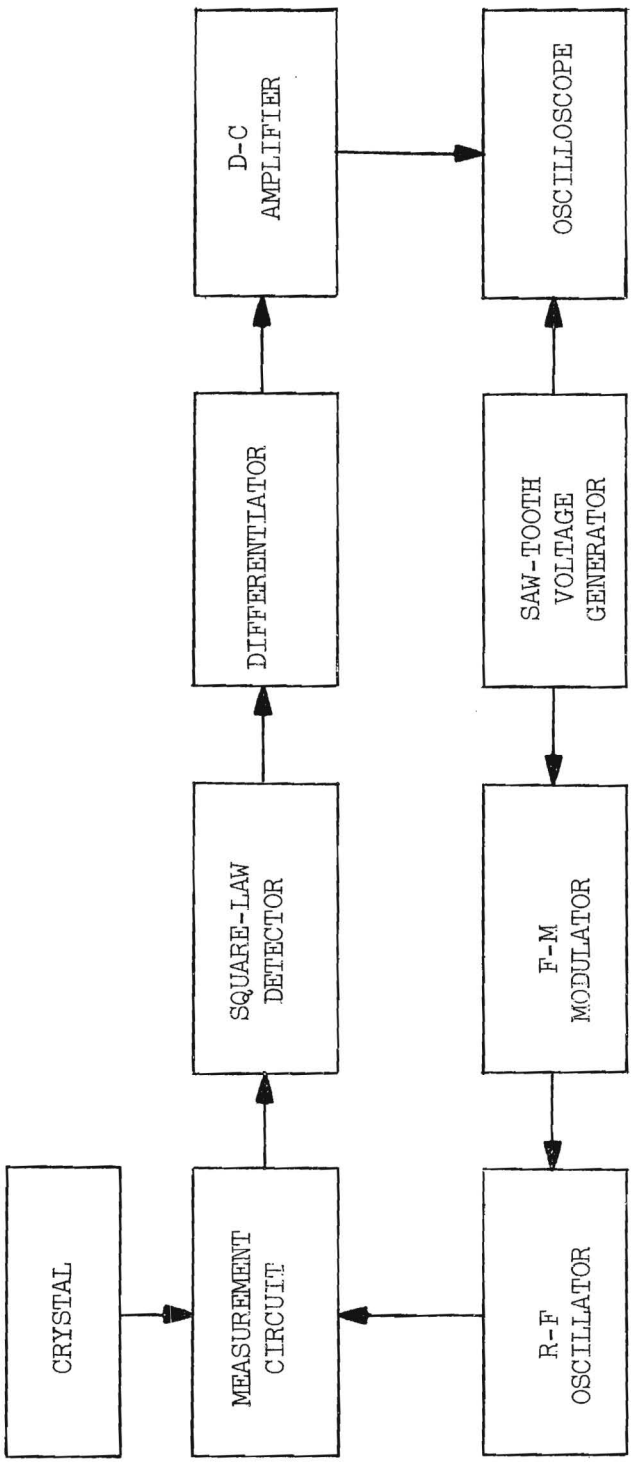

Figure 17. Proposed Spurious Mode Detection and Evaluation System.

to a lower value. If the oscilloscope and frequency modulator circuits are not direct coupled, modifications would have to be made in these circuits for using lower sweep frequencies. Also, minor modifications concerning the frequency deviation would have to be made.

3. Crystal Equivalent Circuits

The original derivation of the Equivalent Circuit Crystal Measurement Method assumed that the capacitance C_o' was zero and that all of the holder resistance appeared directly in series with L_L and not partly in series with C_o. Since some evidence now points to the necessity of modifying the equivalent circuit as was shown in Figure 6, it will be necessary to re-examine the original mathematical derivation. This will not, however, be attempted until more evidence is obtained to justify the equivalent circuit modifications.

V. CONCLUSIONS

Several VHF crystal measurement runs have been made using the Crystal Measurements Standard System. The power measurement system could not be used since calibration of the equipment when using the directional coupler is still questionable. One method of analyzing the crystal data based on the conventional high-frequency crystal equivalent circuit was formalized for use with a digital computer. This method is particularly desirable because of its simplicity; however, some evidence from other activities has indicated the need for modification in the equivalent circuit. Final conclusions concerning analysis must await the collection of additional data.

Two commercial wide-band radio-frequency amplifiers were received and operated successfully for providing isolation and additional gain between the signal generator and the Admittance Meter. However, some modification in the power supplies of the amplifiers were required. Low-pass filters were also obtained for harmonic rejection in the signals driving the test crystals. Their use was desirable because of some harmonic signals generated within the amplifiers under high-level conditions.

The evaluation of the General Radio Admittance Meter has indicated that errors of less than one percent and one degree respectively for impedance magnitude and phase angle are obtainable between the frequencies of 150 and 300 mc/sec when using minimum line length and for impedance magnitudes of the order of 50 ohms. At higher impedance magnitudes, the accuracy is limited by the dial resolution. When the directional coupler or additional transmission line is used between the load and the Admittance Meter, the accuracy is somewhat less. Methods have not yet been found for correcting for the effects of the transmission line or coupler.

A sensitive micro-voltmeter has been ordered for use with the power measurement system. This instrument will eliminate the necessity of using the previous bridge balancing and null detection measurement method at a slight sacrifice in accuracy.

A modification of the Equivalent Circuit Crystal Measurement system resulted in Q calculations which agreed more closely with values calculated from Admittance Meter readings. This was accomplished by modifying the drive arrangement to provide a constant voltage source. Further efforts at evaluating this measurement system have, however, been temporarily discontinued until more information is obtained concerning the equivalent circuits of typical VHF crystals.

VI. PROGRAM FOR NEXT INTERVAL

The program for the next quarter will be a continuation of the work reported in the preceding pages with special emphasis on:

1. completing the calibration checks on the new General Radio Admittance Meter,

2. further evaluating the effects of the directional coupler on measurement accuracies, and

3. measuring and evaluating crystal parameters using the Crystal Measurements Standard.

Further work with the Equivalent Circuit Crystal Measurement Method is not believed to be justified until a more accurate description of typical crystal equivalent circuits can be formulated.

VII. IDENTIFICATION OF KEY TECHNICAL PERSONNEL

Biographical sketches of the key technical personnel were included in Progress Report No. 1. The time contributed by each during the present report period is:

James E. Lane	Technical Assistant	240 Hours
Samuel N. Witt, Jr.	Project Director Research Engineer	240 Hours
Vance Keith Woodcox	Research Assistant	480 Hours

Respectfully submitted:

Samuel N. Witt, Jr.
Project Director

Approved:

W. B. Wrigley, Head
Communications Branch
of the
Physical Sciences Division

FINAL REPORT

PROJECT NO. A-362

INVESTIGATION OF METHODS FOR MEASURING THE EQUIVALENT ELECTRICAL PARAMETERS OF QUARTZ CRYSTALS

By

SAMUEL N. WITT, JR. AND VANCE KEITH WOODCOX

- o - o - o - o - o -

CONTRACT NO. DA-36-039 SC-74948
DEPARTMENT OF THE ARMY PROJECT: 3-26-05-703

- o - o - o - o - o -

15 OCTOBER 1957 TO 14 OCTOBER 1958

PLACED BY THE U. S. ARMY SIGNAL
RESEARCH AND DEVELOPMENT LABORATORIES
FORT MONMOUTH, NEW JERSEY

Engineering Experiment Station
Georgia Institute of Technology
Atlanta, Georgia

ENGINEERING EXPERIMENT STATION
of the Georgia Institute of Technology
Atlanta, Georgia

FINAL REPORT

PROJECT NO. A-362

INVESTIGATION OF METHODS FOR MEASURING THE EQUIVALENT ELECTRICAL PARAMETERS OF QUARTZ CRYSTALS

By

SAMUEL N. WITT, JR. AND VANCE KEITH WOODCOX

- o - o - o - o - o -

CONTRACT NO. DA-36-039 SC-74948
DEPARTMENT OF THE ARMY PROJECT: 3-26-05-703

- o - o - o - o - o -

The object of this project is to develop methods for measuring the equivalent electrical parameters of quartz crystals in the frequency range of 175 to 300 mc/sec.

15 OCTOBER 1957 TO 14 OCTOBER 1958

PLACED BY THE U. S. ARMY SIGNAL
RESEARCH AND DEVELOPMENT LABORATORIES
FORT MONMOUTH, NEW JERSEY

TABLE OF CONTENTS

This report contains 117 pages.

LIST OF FIGURES

LIST OF TABLES

I. PURPOSE

The purpose of the project is fourfold:

1. To continue the study and investigation of methods and techniques for measuring the equivalent electrical parameters of quartz crystal units in the frequency range of 175 to 300 mc/sec, including:

   (a) determination of measurement errors,

   (b) development of a means for directly measuring the power drive of a crystal unit, and

   (c) development of means for measuring the effective resistance of the crystal unit at the series resonant condition.

2. Utilize the information from Investigation 1., above, in the establishment of a standard crystal measurement system which will:

   (a) measure the effective resistance of the crystal at any frequency within the crystal resonance range with a target accuracy of $\pm$ 1 percent,

   (b) determine the phase angle of the crystal at any frequency within the crystal resonance range with a target accuracy of $\pm$ 1 degree,

   (c) include a means of measuring directly the power drive of a crystal unit within $\pm$ 20 percent, and

   (d) be capable of determining the equivalent electrical parameters of the crystal unit.

3. Utilize the information from Investigations 1. and 2. in investigations of circuitry for ultimate utilization in the development of a practical crystal test instrument for the frequency range 175 to 300 mc/sec which will:

(a) measure the effective resistance of the crystal unit at series resonance within a resistance range of 20 to 200 ohms with an accuracy of ± 5 percent,

(b) subject the crystal to any power drive within 0.2 and 4 mw and provide a means of determining directly the power drive with an accuracy of ± 20 percent,

(c) provide a means of operating the crystal within ± 0.0005 percent of the series resonant frequency, and

(d) have a power drive versus resistance characteristic from 175 to 300 mc/sec which will not vary more than 3 to 1 for the resistance range of 40 to 150 ohms.

4. Investigate any other problems pertinent to crystal measurements in the VHF range which are mutually agreed upon by the contractor and the Contracting Officer's Technical Representative.

II. ABSTRACT

The major developments during this contract were concerned with improving the Crystal Measurements Standard System. A new General Radio Admittance Meter was obtained for use with the Standard. The instrument was specially calibrated by the manufacturer. Cross calibration checks by the project indicated that admittance measurements could be made with errors of less than one percent, under certain conditions.

Two commercial chain amplifiers were added to the Crystal Measurements Standard to provide isolation and signal gain between the signal generator and Admittance Meter, and between the frequency measuring equipment and the Admittance Meter. These amplifiers provided adequate isolation and gain at frequencies up to 300 mc/sec. Low-pass filters were also obtained for use with the amplifiers where harmonic rejection was desirable.

The original mixer, i-f amplifier, and local oscillator null detection system was replaced by an Eddystone UHF Receiver to improve the null detection sensitivity. Special shielding precautions were necessary to eliminate spurious signal pick-up from local television stations. The receiver was enclosed in a double screened box which had been provided with low-pass filters for power and signal level meter connections. A solid copper covered cable was constructed to connect the receiver to the Admittance Meter.

A Power Measurement System was developed for use with the Crystal Measurements Standard. By use of a specially prepared frequency calibration curve, accuracies to within $\pm$ 10 percent were obtained for crystal drive level measurements over the frequency range from 175 to 300 mc/sec, for voltage standing wave ratios from 1 to 6.5, and for powers between 0.2 and 10 mw. The Power Measurement System required the use of a dual directional coupler between the Admittance Meter and the crystal component mount. The insertion of the coupler

greatly increased the errors in admittance measurements. Methods for compensating for these additional errors have not yet been developed.

A simplified crystal measurement method, known as the Equivalent Circuit Crystal Measurement Method, was developed mathematically. The method was based upon an assumed crystal equivalent circuit which included the equivalent holder parameters. Close laboratory agreement with other measurement methods was obtained in some cases while poor agreement resulted in other cases. Further work with this method was delayed when evidence indicated that the assumed equivalent circuit might not be sufficiently accurate for the purpose.

The Crystal Measurements Standard System was used to measure the holder and overtone responses of approximately 25 VHF quartz crystals. Various analysis methods were applied to these measurement data. Some of the analyses indicated that the conventional equivalent circuit of a VHF crystal is not a sufficiently good representation for many purposes. An equivalent circuit, proposed by Dr. E. Hafner of USASRDL, was investigated with similar results. These analyses, however, are not yet complete nor conclusive.

III. PUBLICATIONS, LECTURES, REPORTS AND CONFERENCES

No publications (with the exception of the paper described below which was published in the Proceedings of the 12th Annual Frequency Control Symposium) or reports (with the exceptions of Progress Reports 1, 2, and 3, as required by the contract) have resulted from work under this contract.

A paper entitled "VHF Crystal Parameter Measurements" was presented by Mr. Samuel N. Witt, Jr. at the 12th Annual Frequency Control Symposium in Asbury Park, New Jersey on 7 May 1958.

Dr. G. K. Guttwein of USASRDL visited Georgia Tech on 26 November 1957. Future courses of technical action were discussed. It was mutually agreed that the major technical emphasis of the current project should be placed upon the development of the Crystal Measurements Standard. It was also agreed that various novel methods of measuring the parameters of quartz crystals should be investigated. These included, in particular, methods relating to those proposed by Dr. Issac Koga of the University of Tokyo, Tokyo, Japan. (At the time of the conference, Dr. Koga was serving temporarily on the Georgia Tech staff and thus entered into the discussions concerning his methods of measuring crystal parameters.) Representing Georgia Tech at the conference were Mr. W. B. Wrigley, Head of the Communications Branch; Mr. S. N. Witt, Jr., Project Director; and Mr. V. K. Woodcox, Research Assistant.

A visit to USASRDL was made on February 18, 1958 by Samuel N. Witt, Jr., of Georgia Tech, to discuss technical activities and progress on this project. Because of weather conditions, the U. S. Army Signal Laboratories were closed on this day and the planned conference could not be held. However, Mr. D. Pochmersky was contacted and a conference at another location resulted. The first Progress Report was discussed in detail. Other discussions concerning

technical activities of the project ensued. No significant changes in objectives or methods of approach resulted from this conference.

On February 19, 1958, Mr. Pochmersky and Mr. Witt visited Mr. R. A. Soderman at General Radio Company, West Concord, Massachusetts. A conference was held concerning the calibration of a General Radio Admittance Meter Type 1602B and associated equipment which was ordered by the project for use with the Crystal Measurements Standard. Mr. Soderman stated that he believed that overall calibration could be accomplished to within about one percent maximum error over the frequency range from 100 to 400 mc/sec and for admittance magnitudes of the order of 20 millimhos. Admittance Meter readings requiring the use of high multiplying factors would be less accurate.

The 12th Annual Frequency Control Symposium held in Asbury Park, New Jersey on 6, 7 and 8 May 1958 was attended by Mr. Samuel N. Witt, Jr. and Mr. V. K. Woodcox of this project, as well as others representing Georgia Tech. While in attendance at the Symposium, brief conferences were held between the above named personnel, including Mr. W. B. Wrigley, Head of the Communications Branch and Dr. G. K. Guttwein and Mr. D. Pochmersky of USASRDL. No changes in project objectives or methods of approach resulted from these conferences.

Mr. D. Pochmersky of USASRDL visited Georgia Tech on 15 October 1958. The forthcoming Final Report was the principal subject of discussion. It was agreed that the material concerning spurious mode detection and the material concerning r-f amplifier construction as presented in previous quarterly reports should be omitted from the Final Report. Plans for future work were also discussed. It was agreed that future efforts should be directed primarily toward (1) studying the equivalent circuits of HC-6 VHF crystals, (2) developing a production measurement Crystal Impedance Meter type of instrument, and (3) studying the parameters of quartz crystals which are important from the standpoint of oscillator

design. Less emphasis was placed on future developments of the Crystal Measurements Standard. Representing Georgia Tech at the conference were Mr. W. B. Wrigley, Head of the Communications Branch; Mr. S. N. Witt, Jr., Project Director and Mr. V. K. Woodcox, Research Assistant.

IV. FACTUAL DATA

A. Introduction

This project was sponsored by the Frequency Control Branch of the U. S. Army Research and Development Laboratories, Fort Monmouth, New Jersey under Contract No. DA-36-039 SC-74948. The number A-362 was assigned by the Georgia Institute of Technology. The project was started on 15 October 1957 and concluded on 15 October 1958.

This project is essentially a continuation of the work which was begun under Contracts DA-36-039 SC-56730 and DA-36-039 SC-71191 with emphasis as outlined in Chapter I of this report.

Under Contract DA-36-039 SC-71191, much effort was directed toward the development of a Crystal Measurements Standard as well as toward the development of CI Meter types of instruments. A Crystal Measurements Standard System making use of commercial equipment was proposed. A block diagram of this system is shown in Figure 1. The various components indicated were selected on the basis of their availability and their suitability for integration into the complete system. The state of development of the system at the inception of the current project is summarized as follows:

1. Crystal measurements were accomplished using bridge techniques with accuracies, under nearly ideal conditions, of the order of $\pm$ 5 percent error. Generally, errors were much greater than 5 percent, principally because of poor instrument calibrations and lack of sufficient null detection sensitivity. Other sources of error were coaxial line mismatches and r-f leakage. Errors inherent in mathematical computations were essentially eliminated by the use of an electronic digital computer.

2. Crystal drive level was roughly determined by voltage measurements at the crystal. The accuracy obtained by this means was very

poor, thus making the method unsatisfactory for continued use.

3. Proper interpretation of measurement data permitted the calculation of all crystal parameters; however, the calculations generally required the use of electronic computers and, in some cases, other complicated mathematical procedures. It was not possible to develop a single equivalent circuit which explained the behavior of all crystal samples.

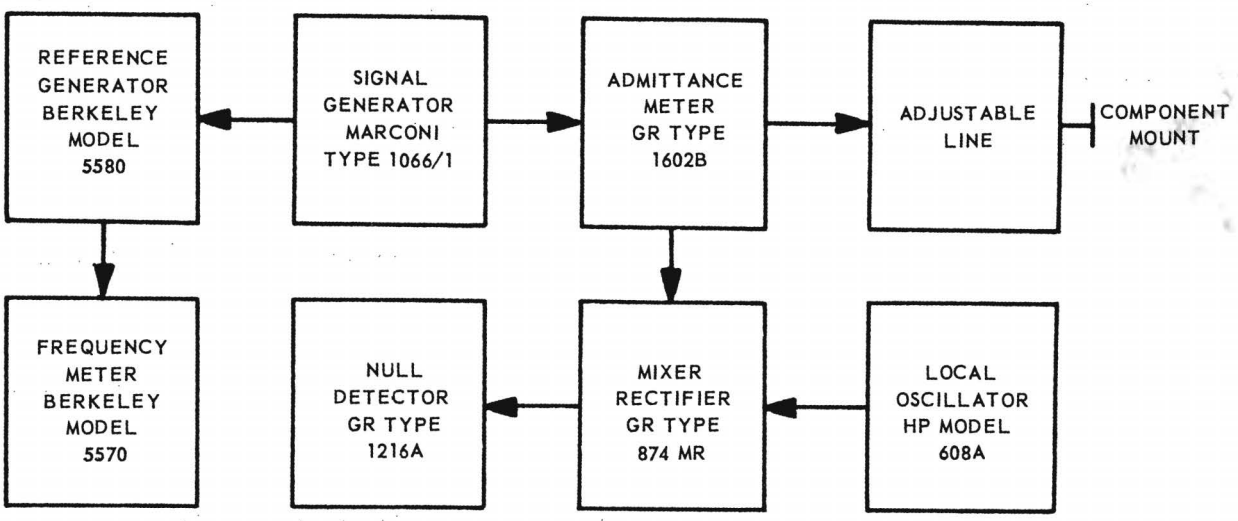

Figure 1. Block Diagram of the Prototype Crystal Measurements Standard.

The state of development of the CI Meter type of instrument is summarized as follows:

1. No substitution methods of measurement have been developed which permit the measurement of crystal parameters above 200 mc/sec. Experimental evidence indicates that the substitution method is not satisfactory above 200 mc/sec.

2. A Coaxial Crystal Parameter Bridge was developed which permitted the measurement of the crystal resistance. It was desirable that the bridge be excited by an oscillator whose frequency is controlled

by the crystal under test; however this was not possible over any extended frequency range.

3. Several crystal controlled oscillators were developed for possible eventual application in CI Meter types of instruments. However, none of these oscillators worked satisfactorily with the Crystal Parameter Bridge.

Developments in power measurements included a Prototype Power Meter for use with the Crystal Parameter Bridge. This instrument was not suitable for use with the Crystal Measurements Standard.

From the above data it was decided that the initial efforts on the current project should be directed toward:

1. obtaining instruments having improved calibration and determining their accuracy in the Crystal Measurements Standard,

2. obtaining a receiver or other instrument having sufficient null detection sensitivity,

3. developing a means for measuring crystal drive level in the Crystal Measurements Standard, and

4. investigating other promising crystal measurement systems.

The study under Item 1. resulted in the purchase of a new General Radio Type 1602B Admittance Meter and accessory equipment. This purchase included special calibration of the instrument to better than normal accuracy.

The study under Item 2. resulted in the purchase of an Eddystone Model 770U UHF Communications Receiver. This item was evaluated for use as a sensitive null detector. The receiver performed satisfactorily in all respects except for r-f leakage. Extensive efforts were directed toward reducing this leakage.

The study under Item 3. resulted in the development of a power measuring system which provided sufficient accuracy for use with the Crystal Measurements Standard. The long- and short-term stability of the system was more than adequate; however, the system does not yet include facilities for self calibration. Such facilities do not appear to be necessary, after initial calibration, except for an occasional check.

The studies under Item 4. included various systems based upon, or related to, the methods which were proposed by Dr. Issac Koga for use at lower frequencies. One such system resulted in the moderately accurate determination of the Q of a quartz crystal at 175 mc/sec. Mathematical analysis of this system became so complicated, however, that it was felt that tests should be discontinued temporarily in favor of simpler systems. Another related measurement system, which has been called the Equivalent Circuit Crystal Measurement Method, was theoretically designed. A prototype of this system was constructed and put through initial tests. Evaluation of this system is not yet complete due to the lack of suitable test instruments. In addition, some doubt presently exists concerning the validity of the theoretical design because of uncertainty as to the configuration of the crystal equivalent circuit.

During the performance of the contract, the need for r-f isolation and amplification between the Admittance Meter and the signal generator became apparent. Considerable effort was directed toward the construction of such instruments. Meanwhile, such instruments became available commercially. Accordingly, two Instruments for Industry Model 530 wide-band chain amplifiers were purchased and evaluated. These amplifiers proved entirely satisfactory for use up to a frequency of 300 mc/sec.

A Hewlett-Packard Model 425A DC Micro Volt-Ammeter was also purchased during the contract period for application in both the Power Measurement

System and the Equivalent Circuit Measurement System. The noise and drift characteristics of this instrument were evaluated.

Complete holder and overtone data have been obtained on approximately 25 VHF quartz crystals during the contract period. In addition, some of the data have been repeated several times. Most of this work was completed during the fourth quarter and has not been reported previously. The principle purpose in obtaining these data was to determine more accurately the typical parameters of VHF quartz crystals. No definite conclusions are yet possible concerning the holder parameters; however, evidence indicated that the conventional crystal equivalent circuit is not satisfactory for complete analysis at higher frequencies.

B. Crystal Measurements Standard

1. Introduction

The Crystal Measurements Standard, as it existed at the inception of this project, is illustrated in Figure 1. Many modifications in the system have since been made. A block diagram of the system presently in use is shown in Figure 2.

Two chain amplifiers have been added to the system for the purpose of increasing the crystal drive level and providing isolation between the various instruments. With the connections illustrated in Figure 2, one of the amplifiers is used to provide additional crystal drive while at the same time isolating the signal generator from the Admittance Meter. The latter feature is necessary to prevent frequency pulling of the signal generator by the crystal under test. The other chain amplifier is used to provide additional drive for the frequency measuring equipment and to isolate this equipment from the Admittance Meter. Isolation is necessary here since the frequency measuring equipment generates a number of spurious frequencies at its input terminals. Although these spurious signals do not materially affect the crystal admittance measurement, they do

appreciably affect the accuracy of the Power Measurement System. Other arrangements of the amplifiers have been used at times.

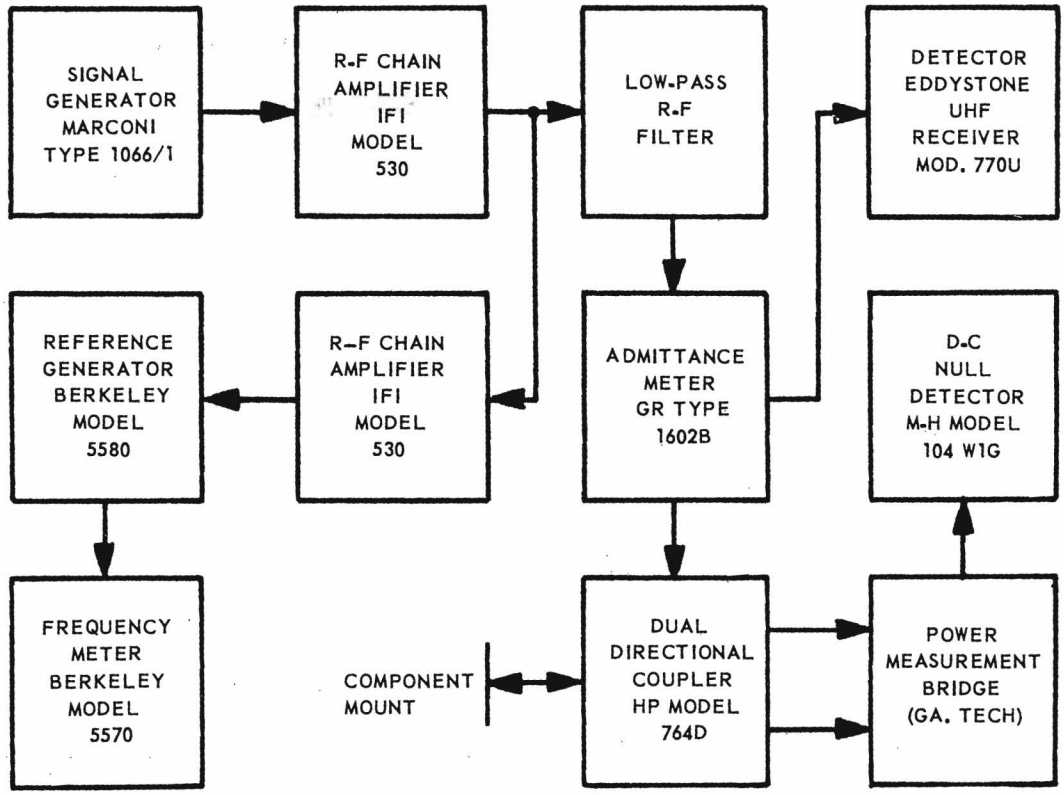

Figure 2. Block Diagram of the Present Crystal Measurements Standard.

A radio-frequency low-pass filter has been added between the first chain amplifier and the Admittance Meter. This unit is necessary at times because of harmonic frequencies occasionally generated by the chain amplifier. It is not generally necessary for routine measurements.

A commercial UHF receiver has been added as a null detector in place of the mixer-rectifier, local oscillator and i-f amplifier shown in Figure 1. This unit resulted in an appreciable increase in null detection sensitivity while at the same time reducing the number of spurious detector responses to a minimum.

A Power Measurement System consisting of a dual directional coupler, a d-c bridge, and a d-c null detector has been added to the system. This equipment permits the accurate measurement of crystal drive level simultaneously with crystal admittance measurements. The directional coupler, however, introduced additional errors into the admittance measurements. Thus, the Power Measurement System is used at present only when limited accuracy in crystal admittance measurements are acceptable.

The individual components of the block diagram of Figure 2 are discussed in detail in the following sections of this report.

2. Calibration of Instruments

Data from the previous project (Contract No. DA-36-039 SC-71191) indicated that the principal source of error in the Crystal Measurements System was the lack of precise calibration of the various instruments which were used. Justification for this conclusion was based upon the assumption that terminations used as impedance standards were precisely calibrated. The terminations used were the General Radio Type 874-W100 and 874-W200 which are claimed to have an impedance magnitude accuracy of one percent with a very small phase angle at frequencies below 300 mc/sec. No provisions were available locally for checking the calibration of these terminations. However, one sample of the GR-874-W100 termination was submitted to the National Bureau of Standards by USASRDL for calibration purposes. The resulting data are given in Table I.

In the calibration of the W100 termination, a General Radio Type 874-WN3 Short-Circuit Termination was used to establish the reference plane. A difference in length of approximately 0.8 cm between the W100 termination and the short-circuit termination was not taken into account by the National Bureau of Standards. These data were subsequently corrected by means of a digital computer at Georgia Tech. Both the original data and the corrected data are

included in Table I. If it is assumed that this sample of the W100 type termination is typical, then the validity of previous work based upon this type of termination is verified.

TABLE I

ELECTRONIC COMPUTER CORRECTIONS OF NATIONAL BUREAU OF STANDARDS DATA ON GENERAL RADIO TERMINATION TYPE 874-W100, SERIAL NO. 111

	NBS DATA		CORRECTED DATA	
Frequency (mc/sec)	Impedance Magnitude (ohms)	Impedance Angle (degrees)	Impedance Magnitude (ohms)	Impedance Angle (degrees)
50	99.9	-0.8	99.91	-0.096
60	99.8	-0.9	99.82	-0.057
70	99.8	-1.1	99.83	-0.116
80	99.8	-1.2	99.83	-0.076
90	99.7	-1.4	99.74	-0.137
100	99.7	-1.5	99.75	-0.097
110	99.7	-1.7	99.77	-0.156
120	99.6	-1.8	99.68	-0.118
130	99.6	-2.0	99.70	-0.178
140	99.6	-2.1	99.71	-0.138
150	99.5	-2.3	99.63	-0.201
160	99.5	-2.4	99.64	-0.160
170	99.4	-2.6	99.57	-0.224
180	99.4	-2.7	99.58	-0.184
190	99.3	-2.9	99.51	-0.248
200	99.3	-3.0	99.52	-0.208
210	99.3	-3.2	99.55	-0.268
220	99.2	-3.3	99.47	-0.233
230	99.2	-3.5	99.50	-0.293
240	99.1	-3.6	99.42	-0.258
250	99.0	-3.8	99.36	-0.324
260	99.0	-3.9	99.38	-0.284
270	98.9	-4.1	99.32	-0.350
280	98.9	-4.2	99.34	-0.311
290	98.8	-4.4	99.28	-0.377
300	98.8	-4.5	99.31	-0.337

Note: The nominal impedance of this termination is 100 ohms. The data are corrected for an effective difference in length of 0.783 cm between the termination and the reference short.

A consideration of many other possible sources of system errors indicated that the principal source of error was due to the bridge or basic impedance measuring instrument. The conclusion was the same whether the General Radio Type 1602B Admittance Meter or the Hewlett-Packard Model 803A VHF Bridge was used. It was thus necessary that a more accurate bridge be obtained before other sources of error could be accurately evaluated. Various inquiries were made concerning current commercial instruments, including the availability of special calibration. Upon this basis, a new General Radio Type 1602B Admittance Meter was ordered and received. The General Radio Company agreed to calibrate the instrument in their laboratory to within approximately one percent over the frequency range from 175 to 300 mc/sec. This accuracy was to apply at an admittance level of 20 millimhos and would be somewhat poorer at greatly different admittances.

The calibration charts which were supplied with the Admittance Meter are included here as Figures 3 and 4 to illustrate the types of corrections and the order of accuracy to be expected both with and without the application of corrections. It should be noted that these charts are valid only for the particular Admittance Meter with the serial number indicated. It should also be noted that this instrument is a standard production run instrument and was not modified in any way to obtain this accuracy.

Also ordered and received with the Admittance Meter were three resistive terminations and one component mount. The component mount together with its open and short terminations were specially adjusted in length by General Radio Company to equal the length of the standard resistive terminations (approximately 3.5 cm). Calibration data on the resistive terminations are shown in Figure 5. These terminations were purchased as an aid in calibrating the complete Crystal Measurements Standard.

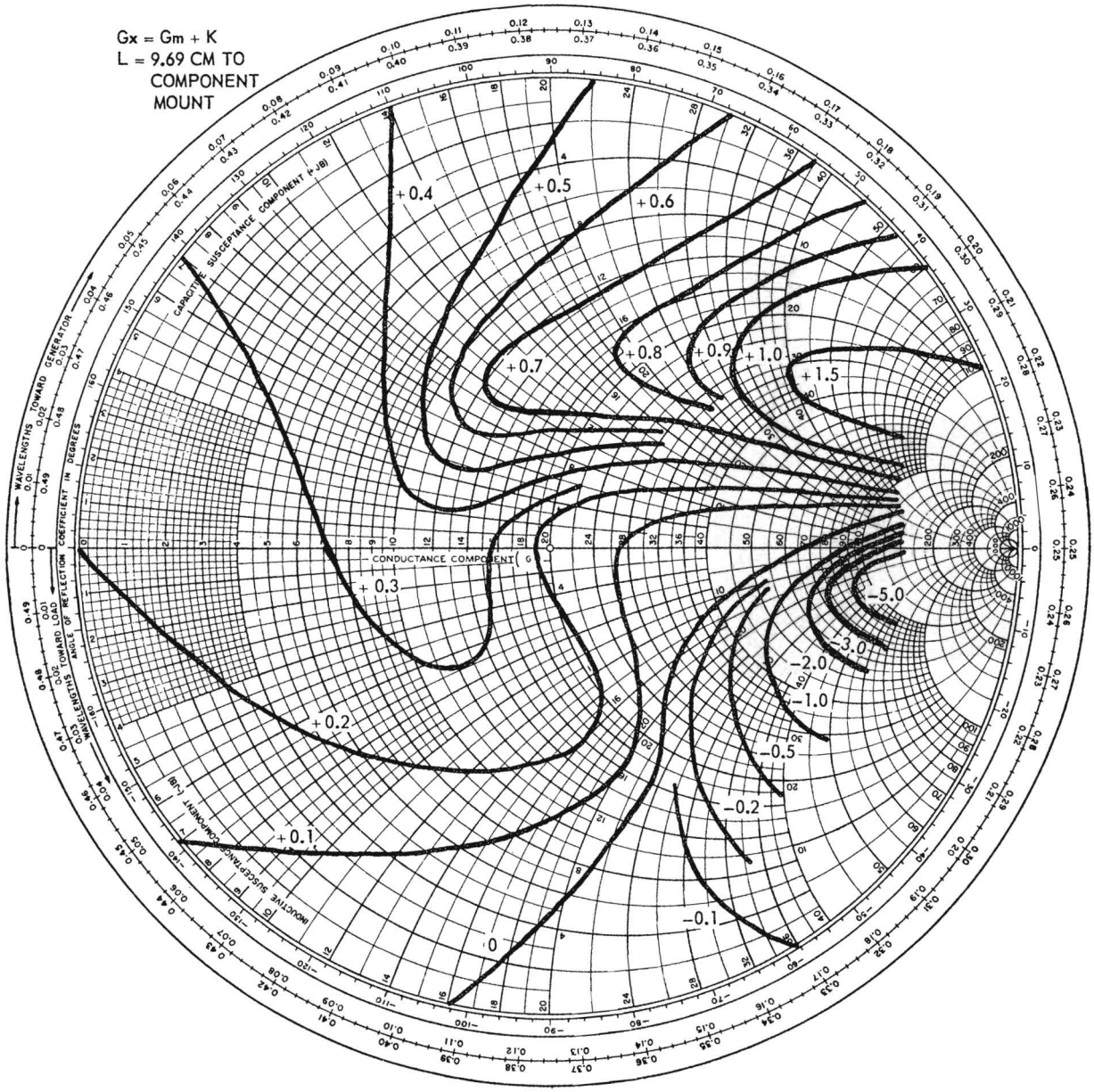

Figure 3. Conductance Corrections for GR Admittance Meter Serial No. 1401.

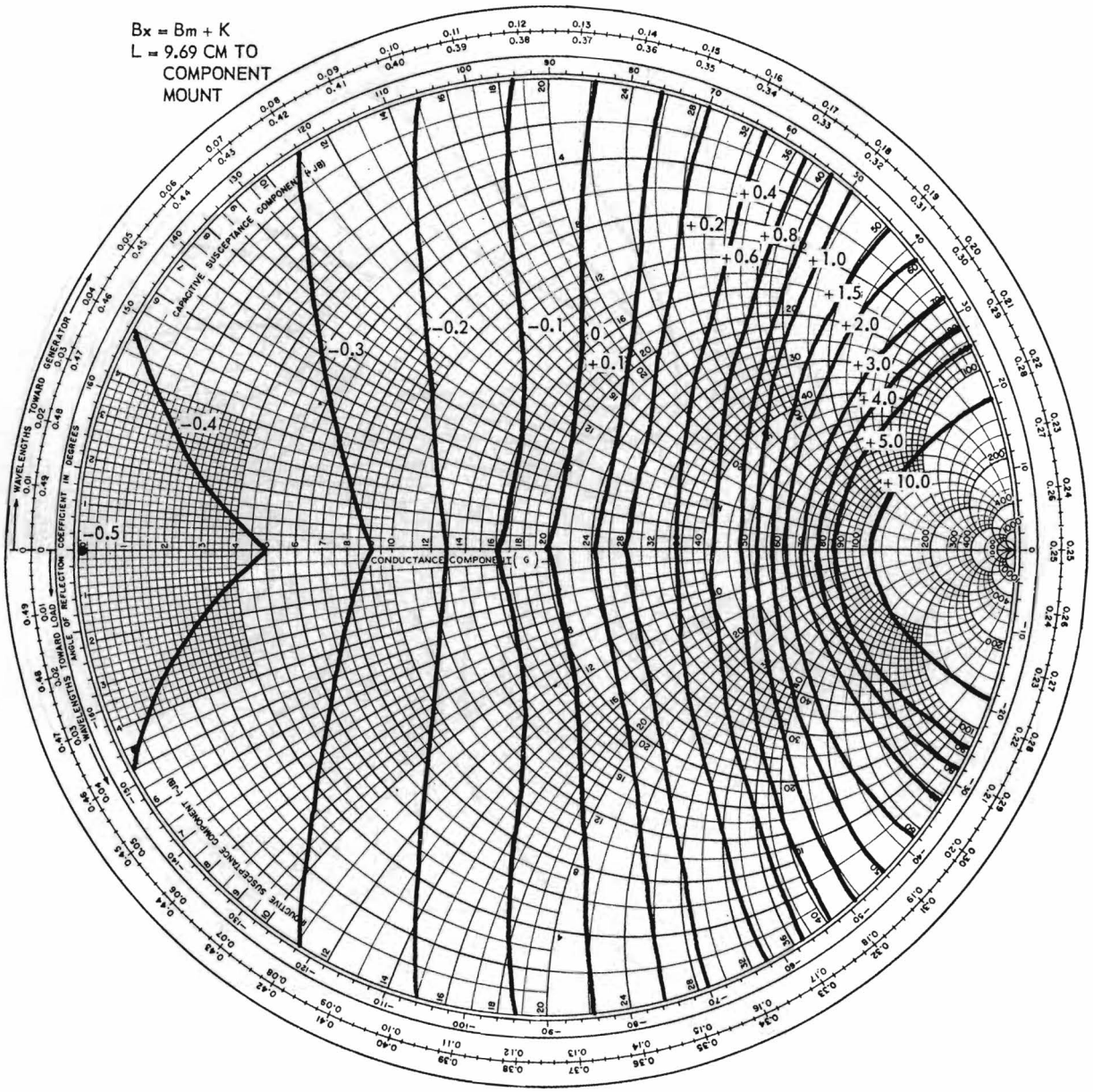

Figure 4. Susceptance Corrections for GR Admittance Meter Serial No. 1401.

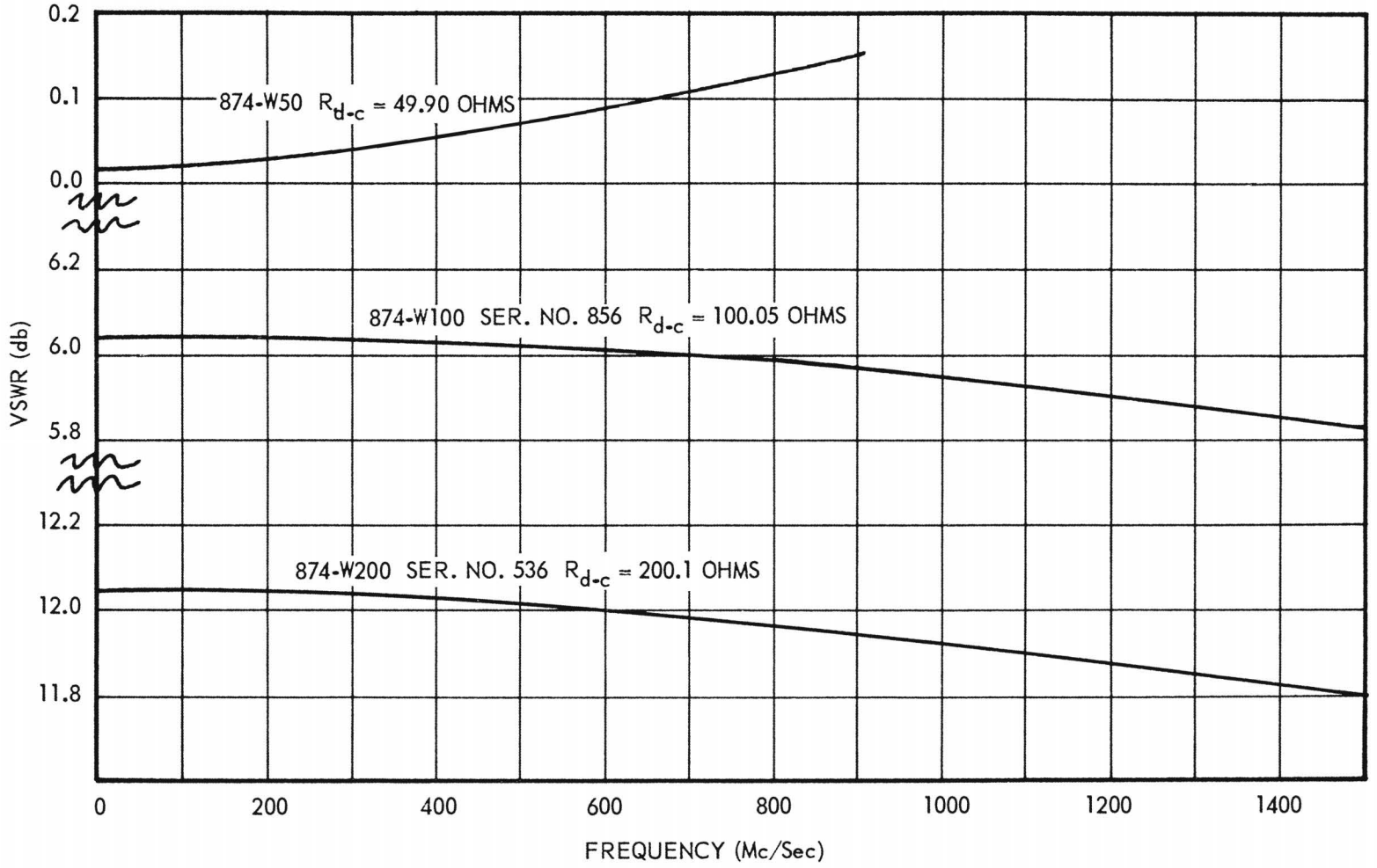

Figure 5. Calibration of GR Resistive Terminations with Serial Numbers as Shown.

Extensive efforts have been made to determine the accuracy of the new General Radio Admittance Meter Type 1602B. No definite conclusions can yet be made concerning the expected overall accuracy of the Crystal Measurements Standard using this instrument; however, some of the more important calibration data are presented here.

As indicated above, it was believed that accuracies of the order of one percent for impedance magnitude and one degree for phase angle could be obtained when measuring impedances near 50 ohms resistance. This was substantiated by the data shown in Figure 6 for three different terminations mounted directly on the Admittance Meter. It will be noted that the accuracy with the 50-ohm termination is well within one percent for magnitude and one degree for phase angle. The accuracy with the 100-ohm termination is slightly poorer than was obtained with the 50-ohm termination. For the 200-ohm termination the error exceeds one percent for magnitude but is almost within one degree for phase angle. This data run was repeated on two other occasions with approximately the same results.

A study of the Admittance Meter dials partially explains the errors shown in Figure 6. For example, the resolution at 5 millimhos on the dials (200 ohms) is only one percent if it is assumed that readings can be made to one-tenth of the smallest division. This precision in reading is generally not possible without optical aids.

The data shown in Figure 6 were obtained with the terminations mounted directly on the Admittance Meter. The calculated electrical separation between the termination terminals and the internal bridge terminals was 9.69 cm. The Admittance Meter readings were first corrected by using Figures 3 and 4. The 9.69 cm of 50-ohm transmission line were then subtracted by a digital computer using a specially prepared program. No line losses were considered since the correction charts included such effects.

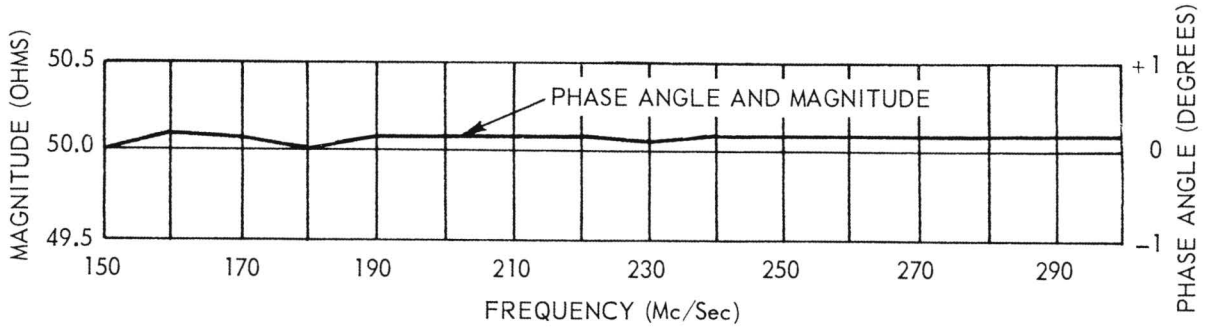

(a) 50-OHM TERMINATION

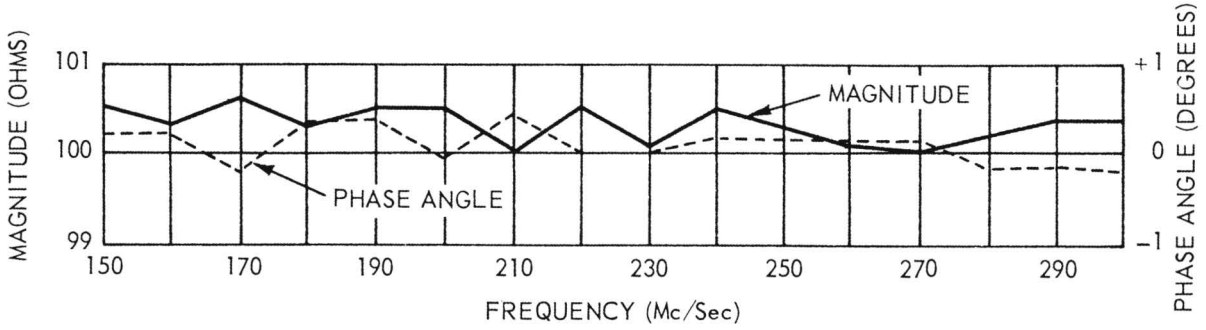

(b) 100-OHM TERMINATION

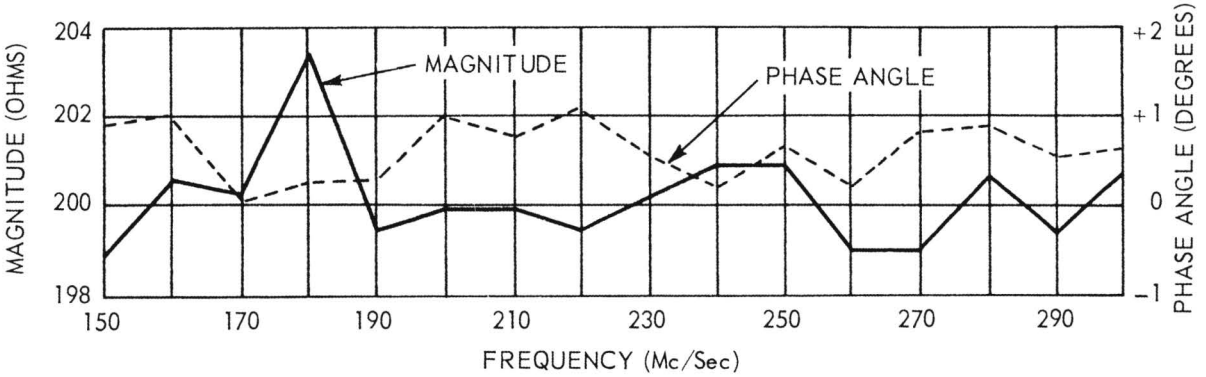

(c) 200-OHM TERMINATION

Figure 6. Admittance Meter Measurements on Resistive Terminations with Minimum Line Length.

The particular terminations, line lengths, and frequencies used in the above run are capable of checking the calibration of the Admittance Meter only over a very limited range of the Smith chart, as shown by the heavy lines in Figure 7. As a result, the data presented cannot lead to any general conclusions concerning the overall accuracy of the instrument.

Since the procedure for measuring the drive level of a crystal involves the insertion of a Hewlett-Packard Dual Directional Coupler Model 764D between the component mount and the Admittance Meter, additional data runs were made with the coupler in position but using the standard terminations to replace the component mount. The results are shown in Figure 8. The data for these curves were again obtained by applying the instrument corrections and then subtracting the electrical length of the complete transmission line. It was necessary to determine this electrical length by a series of open- and short-circuit measurements over the frequency range. As the calculated length showed wide variations under various conditions, an average value was calculated. The accuracy of the choice can be evaluated from the phase angle curves of Figure 8.

It was first assumed that the large errors indicated by Figure 8 were due to excessive losses in the directional coupler. The coupler was therefore replaced by an approximately equal (40-cm) length of air-dielectric transmission line. A repeat of the data run yielded the results shown in Figure 9. It will be observed that the errors are of approximately the same magnitude.

A series of evaluation tests were initiated to determine the sources of error when the directional coupler or additional transmission line was in use. First considered was the effect of the multiplying dial of the Admittance Meter. It is desirable, due to the construction of the instrument, that all measurements be made such that conductance and susceptance readings both

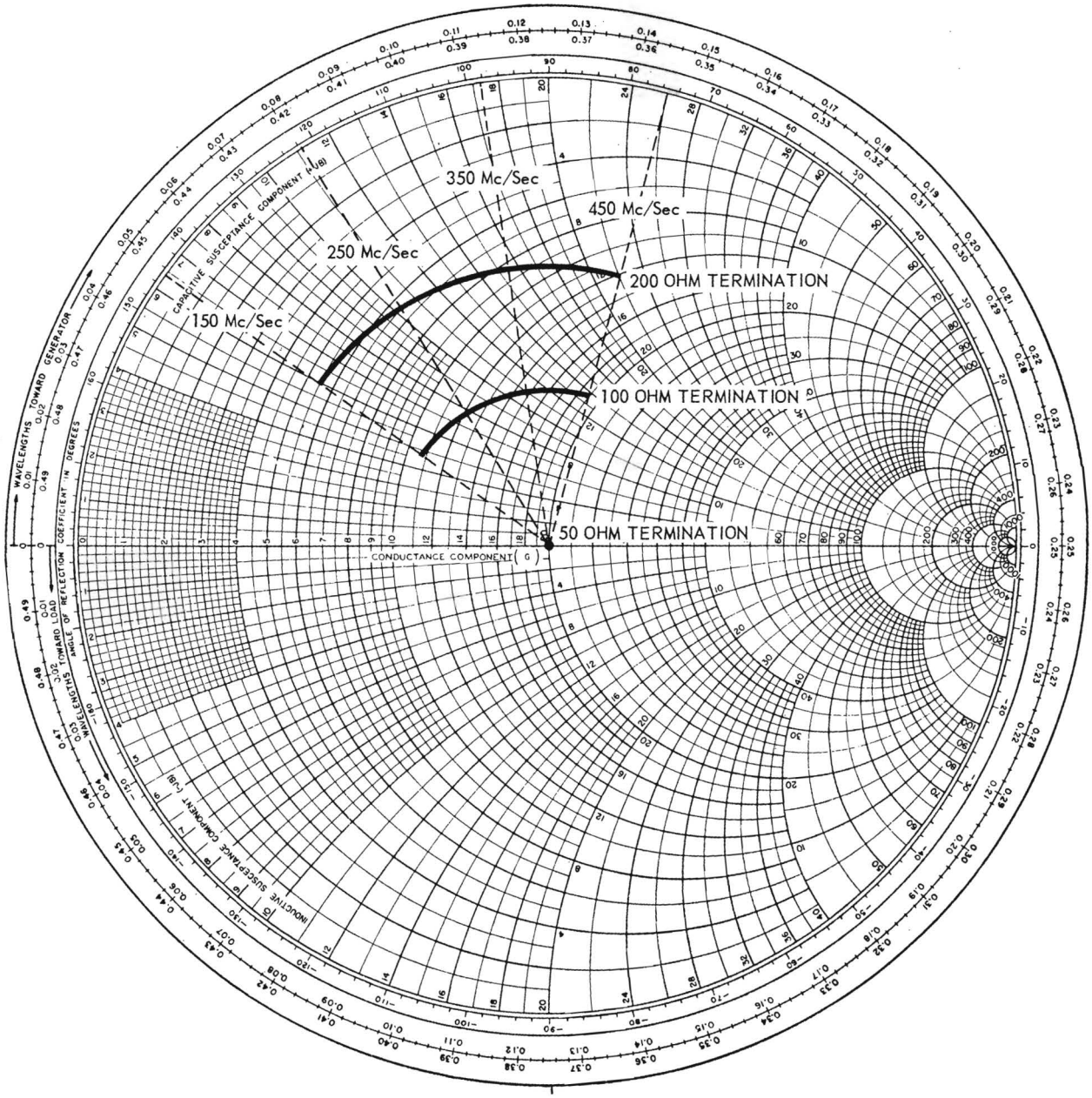

Figure 7. Loci of Points Which Can Be Calibrated with a 9.69 Cm Line Length.

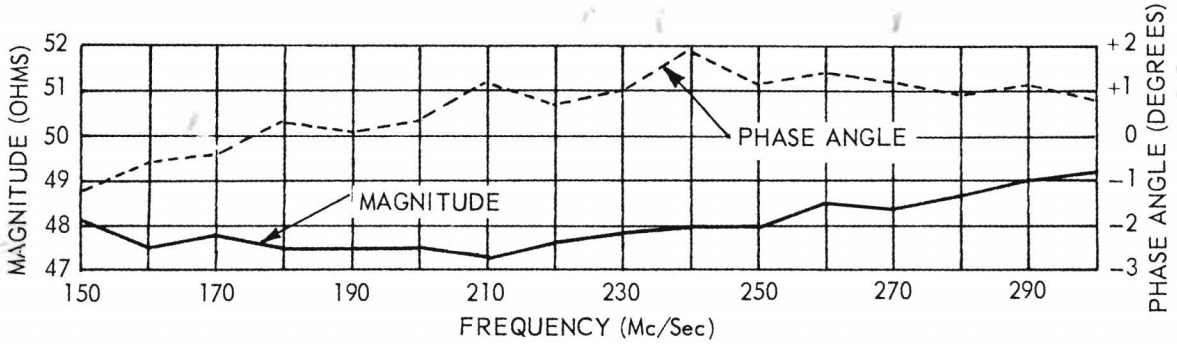

(a) 50-OHM TERMINATION

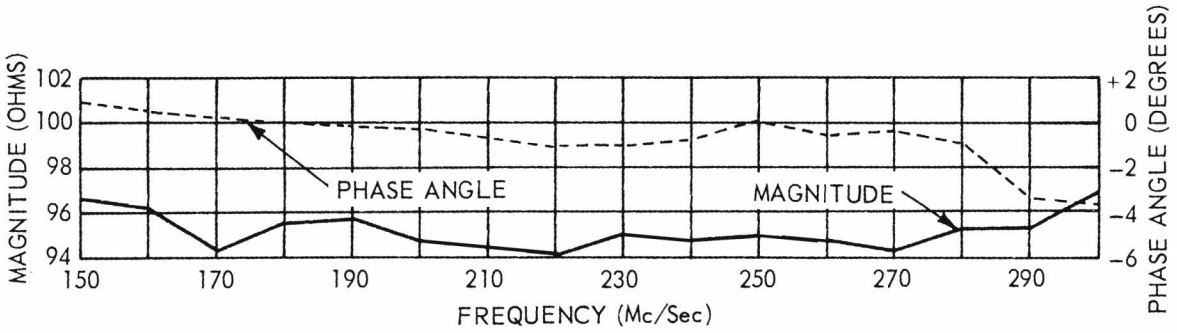

(b) 100-OHM TERMINATION

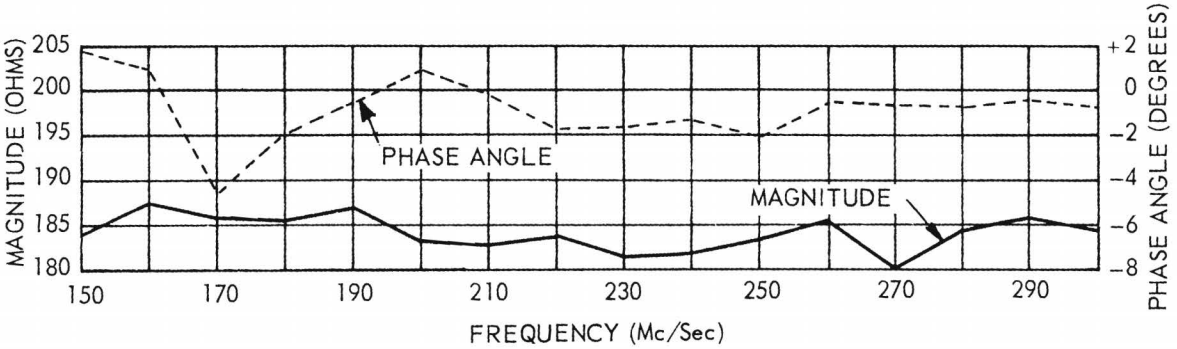

(c) 200-OHM TERMINATION

Figure 8. Admittance Meter Measurements on Resistive Terminations with a Dual Directional Coupler Inserted in the Coaxial Line.

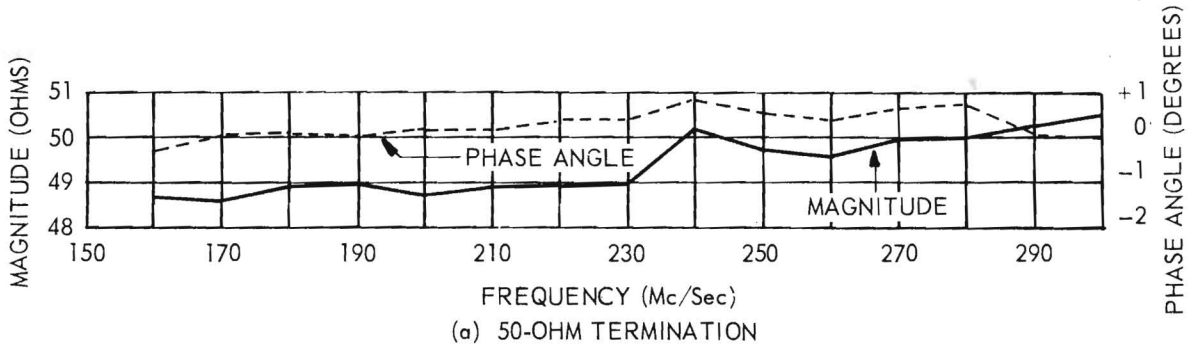

(a) 50-OHM TERMINATION

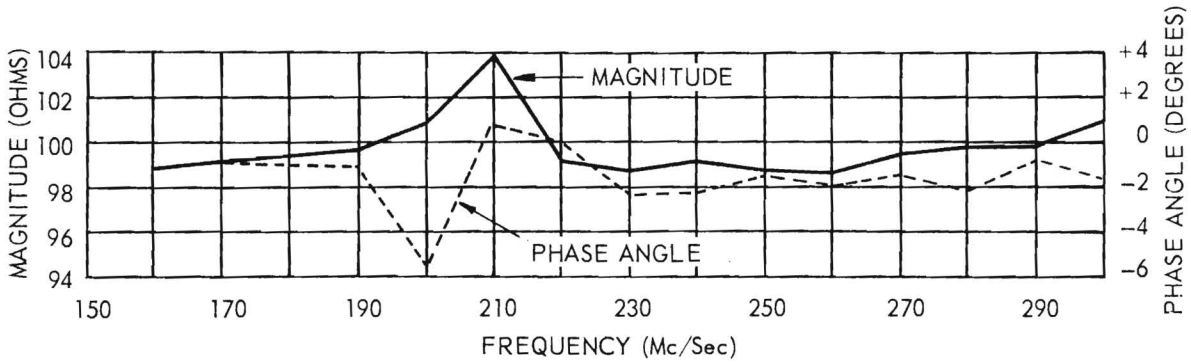

(b) 100-OHM TERMINATION

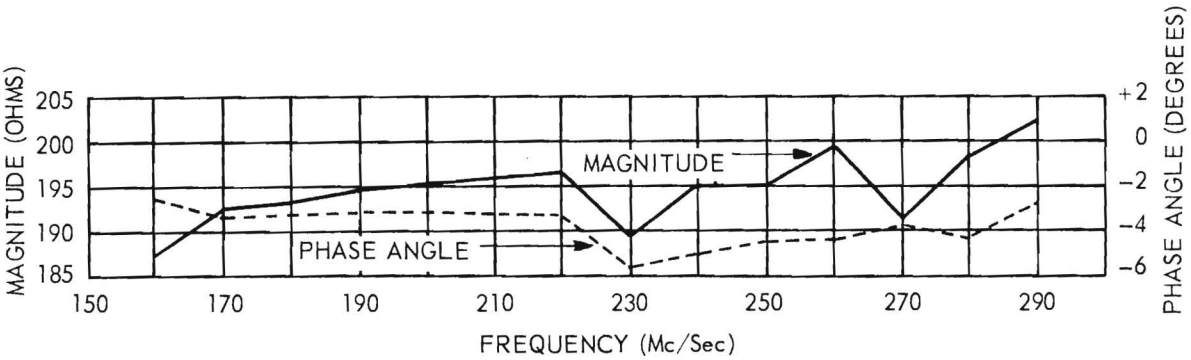

(c) 200-OHM TERMINATION

Figure 9. Admittance Meter Measurements on Resistive Terminations with a 40-Cm Line Length.

remain less than 20-millimhos or such that the multiplying factor is unity. This was possible with the choice of terminations and frequencies used with the 9.69 cm line length as shown in Figure 7. However, when the longer line lengths were used, multiplying factors as high as 5 were required. To determine the magnitude of errors introduced by the multiplier dial, a series of measurements were made by setting the multiplier to discrete values between one and two and recording the conductance and susceptance readings. It was found that the multiplier could account for errors greater than one percent. A recheck of the data of Figures 8 and 9, however, showed no general correlation between the multiplying factor and the observed errors. Although this source of error is important, it is not considered to be the major factor in this case.

Probably the most logical sources of error are transmission line deficiencies of various types. The following method was considered for correcting some of these deficiencies.

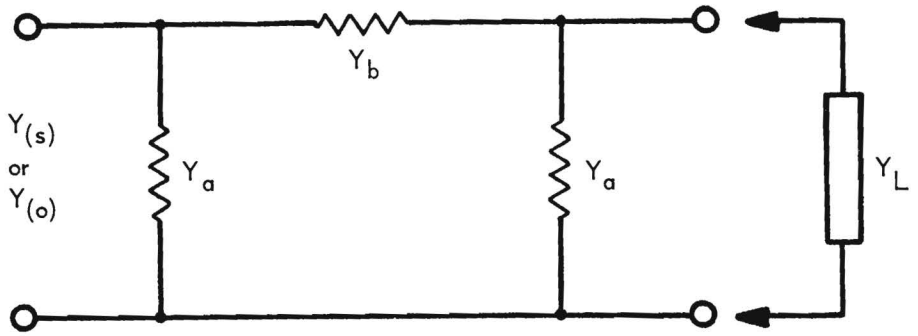

Figure 10. Network Approximation of a Transmission Line.

At any single frequency, a transmission line of arbitrary length may be represented as a two-terminal pair network as shown in Figure 10. Since the line is symmetrical, both shunt admittances may be labeled Y_a. Y_b is the

series admittance of the equivalent pi-circuit. Y_L represents an aribtrary load. If $Y_{(s)}$ and $Y_{(o)}$ are used to represent the sending-end admittance with the load terminals respectively shorted and opened, the conventional transmission line equation,

$$Z = Z_o \frac{Z_R + Z_o \tanh \gamma \ell}{Z_o + Z_R \tanh \gamma \ell} , \tag{1}$$

becomes

$$Y_{(s)} = \frac{1}{Z_o} \coth \gamma \ell \tag{2}$$

for the short-circuit condition and

$$Y_{(o)} = \frac{1}{Z_o} \tanh \gamma \ell \tag{3}$$

for the open-circuit condition, where Z_R represents the receiving end condition, γ is the propagation constant, ℓ is the line length, and Z_o is the characteristic impedance of the line.

But, from Figure 10,

$$Y_{(s)} = Y_a + Y_b \tag{4}$$

and

$$Y_{(o)} = Y_a + \frac{Y_a Y_b}{Y_a + Y_b} . \tag{5}$$

Substituting Y_a from Equation 4 into Equation 5 yields

$$Y_{(o)} = Y_{(s)} - Y_b + \frac{(Y_{(s)} - Y_b)Y_b}{Y_{(s)}} \tag{6}$$

or

$$Y_{(o)}Y_{(s)} = (Y_{(s)} - Y_b)(Y_{(s)} + Y_b) = Y_{(s)}^2 - Y_b^2 , \qquad (7)$$

from which

$$Y_b^2 = Y_{(s)}^2 - Y_{(o)}Y_{(s)} . \qquad (8)$$

Letting $Y_o = 1/Z_o$ in Equation 8 and substituting $Y_{(s)}$ and $Y_{(o)}$ from Equations 2 and 3 gives

$$Y_b^2 = Y_o^2 \coth^2 \gamma\ell - Y_o^2 \tanh \gamma\ell \coth \gamma\ell$$

$$= Y_o^2 (\coth^2 \gamma\ell - 1) = Y_o^2 \operatorname{csch}^2 \gamma\ell \qquad (9)$$

or

$$Y_b = \frac{Y_o}{\sinh \gamma\ell} . \qquad (10)$$

From Equation 4

$$Y_a = Y_{(s)} - Y_b = Y_o \coth \gamma\ell - \frac{Y_o}{\sinh \gamma\ell}$$

$$= Y_o \left(\frac{\cosh \gamma\ell - 1}{\sinh \gamma\ell}\right) . \qquad (11)$$

But,

$$\cosh X - 1 = 2 \sinh^2 \frac{X}{2} \qquad (12)$$

and

$$\sinh X = 2 \sinh \frac{X}{2} \cosh \frac{X}{2} \qquad (13)$$

or

$$\frac{\cosh X - 1}{\sinh X} = \frac{\sinh X/2}{\cosh X/2} = \tanh \frac{X}{2} . \qquad (14)$$

Therefore,

$$Y_a = Y_o \tanh \frac{\gamma\ell}{2} . \qquad (15)$$

When the load, Y_L, of Figure 10 is connected, the input admittance, Y, becomes

$$Y = Y_a + \frac{(Y_a + Y_L)\, Y_b}{Y_a + Y_b + Y_L}$$

$$= \frac{Y_a(Y_a + Y_b) + Y_L(Y_a + Y_b) + Y_a Y_b}{(Y_a + Y_b) + Y_L} . \qquad (16)$$

Equation 16 may be simplified by replacing $(Y_a + Y_b)$ by $Y_{(s)}$, as in Equation 4, to yield

$$Y = \frac{Y_{(s)}(Y_a + Y_L) + Y_a Y_b}{Y_{(s)} + Y_L}$$

$$= \frac{\frac{Y_a Y_b}{Y_{(s)}} + Y_a + Y_L}{Y_{(s)} + Y_L} \cdot Y_{(s)} \qquad (17)$$

Further simplification results from substituting Equation 5 into Equation 17 to obtain

$$Y = Y_{(s)} \frac{Y_{(o)} + Y_L}{Y_{(s)} + Y_L} \qquad (18)$$

or

$$Y_L = Y_{(s)} \frac{Y_{(o)} - Y}{Y - Y_{(s)}} . \qquad (19)$$

For a half-wavelength line, since $Y_{(s)}$ is very large,

$$Y_{\lambda/2} = Y_{(s)} \frac{Y_{(o)} + Y_L}{Y_{(s)} + Y_L} \Bigg|_{Y_{(s)} \to \infty} = Y_{(o)} + Y_L \qquad (20)$$

or

$$Y_L = Y_{\lambda/2} - Y_{(o)} \cdot \qquad (21)$$

Equation 19 was programmed on a digital computer and used to correct the original data of Figures 8 and 9. The results were approximately the same as obtained from line subtractions. Even greater errors were obtained in some cases near quarter- and half-wavelength points where either $Y_{(o)}$ or $Y_{(s)}$ became very large. This method of line length correction was cross-checked with the 9.69-cm data of Figure 6 and showed very good agreement. It is interesting to note that this method of line length subtraction does not require a knowledge of the actual line length or of the frequency. In addition, it should compensate for some, if not all, of the line deficiencies; however, on a practical basis, it did not accomplish this purpose.

In an attempt to reduce some of the errors encountered when using the directional coupler or a coaxial line section between the Admittance Meter and the termination, several sources of error were considered.

The first consideration concerned the admittance calculation procedure just described. As mentioned above, when the frequency is such that the line length is near a quarter- or half-wavelength, the admittance of either the short- or open-circuit termination is very large and, therefore, requires a large multiplying factor on the Admittance Meter dial. At such lengths, if the conductance with the open- or short-circuit termination were actually zero, as it would be for a perfect termination and perfect coaxial line, but were recorded as 0.1 millimho (one-fifth of the smallest division on the conductance scale), a multiplying factor of ten would make the conductance appear to be 1 millimho instead of zero. This becomes an appreciable conductance, when compared with the readings with the resistive terminations, and would introduce large errors in the calculations of the impedances of the terminations. In an attempt to eliminate this

occurrence, the line was assumed to be lossless and the conductive readings of either the open-circuit termination, the short-circuit termination, or both were assumed to be zero. The directional coupler and 40-cm line data were rerun on the computer with each of these three assumptions and the results replotted. The accuracies were improved near 150 and 300 mc/sec, but the overall accuracy was as poor or poorer than that of the line subtraction methods. This result would seem plausible since under the above assumptions, the admittance calculation method reduces to a line subtraction method and thus defeats its originally intended purpose.

One possible source of error in the measurement system is incorrect coaxial line impedances. Accordingly, the diameters of the center conductor of several samples of coaxial line were measured. It was found that the variations in diameters could produce variations in the impedance of the lines greater than one percent.

Assuming that the lines were lossless, but of the wrong impedance, three samples of the 40-cm line data, one for each of the resistive terminations, were selected for further study. By trial and error, a resistive impedance (Z_o = 51.39 ohms) was found which, when used in conjunction with the transmission line equation, resulted in impedance magnitudes of 50, 100, and 200 ohms respectively for the three terminations. The remaining 40-cm line data were then run in the computer using 51.39 ohms for Z_o instead of 50 ohms. The results are shown in Figure 11. It can be seen from the graph that this type of compensation is not adequate since the magnitude of the impedance of the terminations is increased too much at the lower frequencies while it is not increased enough at the higher frequencies. The data indicated that the errors in the 40-ohm line run and the directional coupler run were caused by line losses in addition to a possible impedance error.

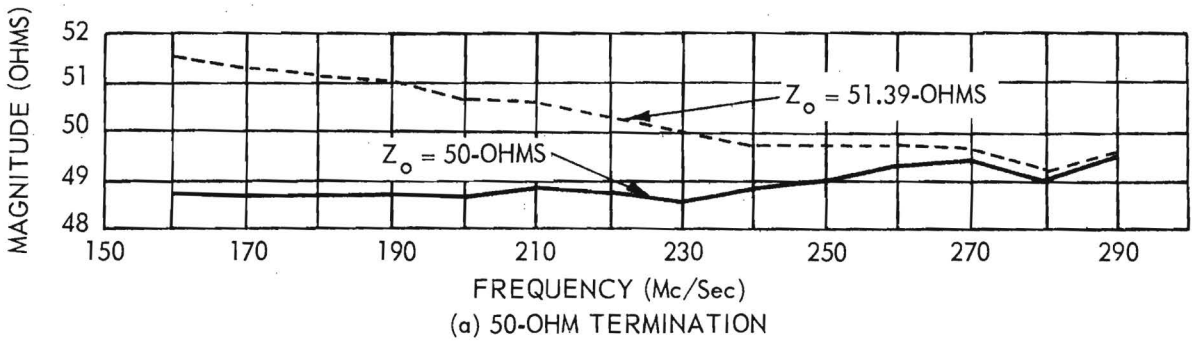

(a) 50-OHM TERMINATION

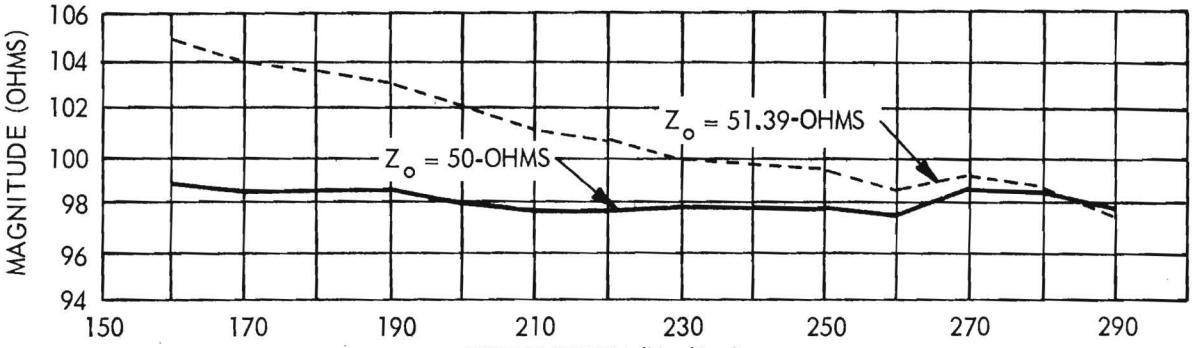

(b) 100-OHM TERMINATION

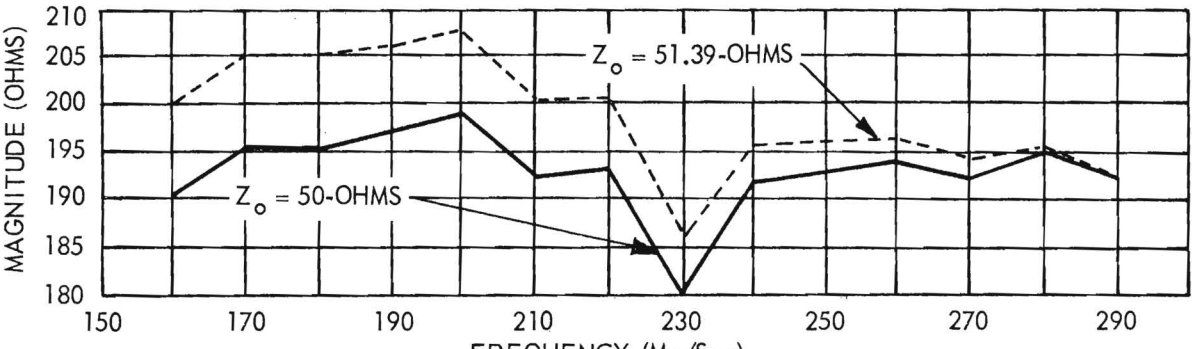

(c) 200-OHM TERMINATION

Figure 11. Impedance Level Compensation of 40-Cm Transmission Line Data.

The general transmission line equation which applies to any uniformly distributed parameter line is

$$Z = Z_o \frac{Z_r + Z_o \tanh \gamma \ell}{Z_o + Z_r \tanh \gamma \ell} \tag{22}$$

where

$$\gamma = \sqrt{(G + j\omega B)(R + j\omega L)} \tag{23}$$

and

$$Z_o = \sqrt{\frac{R + j\omega L}{G + j\omega B}} \quad . \tag{24}$$

It can be seen that both Z_o and γ are functions of frequency and that five unknowns (G, B, R, L and ℓ) exist for any given line. Solving for these five unknowns is a difficult task, due to the complexity of the equations involved, even if the input data are precise. The difficulty is further compounded by the limited resolution of the Admittance Meter and limited accuracy of the correction charts. Also, the above equation is valid only if the line is uniform, which, due to connectors and the physical qualities of the line, is not entirely true.

Because of the lack of personnel time, further efforts to correlate these factors were temporarily discontinued.

An alternate method of improving the measurement accuracy with the directional coupler is to place the coupler in a half-wavelength transmission line. This method has the advantage that the Admittance Meter directly reads the actual admittance of the crystal or termination after dial corrections have been made, thus eliminating the necessity of using the computer for line subtractions. Also, if the total line is lossless, the actual physical length and impedance of the line need not be known. The disadvantages of the half-wavelength method are threefold: (1) line loss compensations are inconvenient to make, (2) the method requires more personnel time for obtaining the same amount of data than

does the fixed line method due to the time required to set up the half-wavelength line for each frequency, and (3) Admittance Meter calibrations cannot be readily checked since only one point is represented on a Smith chart for each termination as frequency is varied.

The normal procedure used in setting up a half-wavelength line is to place an open-circuit termination on the end of the coaxial line and vary the length of the line until the Admittance Meter and detector system null at zero susceptance. When this setup procedure was used, phase angles of the order of 3 or 4 degrees were obtained for the terminations. However, an inspection of Figure 4 showed the susceptive correction for a reading of 0 + j0 to be -j0.5. The line was therefore not set at an exact half-wavelength. In a second run, the Admittance Meter was set to a reading of 0 + j0.5 and the line adjusted so that the detector indicated a null. After corrections then, the susceptance of the open-circuit termination was zero, indicating a half-wavelength line. The results for such a run with the three terminations using a coaxial air line are shown in Figure 12. The directional coupler was not used in the line for the run since it was desirable to determine the best possible accuracy.

The accuracies with the 50- and 100-ohm terminations are comparable to that for the 9.69-cm run, while the accuracy with the 200-ohm termination, although better than other coaxial line runs, was not as good as the 9.69-cm run.

Measurements were made using the directional coupler as a part of a half-wavelength line. The data were only slightly poorer than for the half-wavelength line without the directional coupler.

The following conclusions may be drawn from the preceding data: (1) Measurement errors of less than one percent for impedance magnitude and one degree for phase angle are possible when the terminations are placed directly

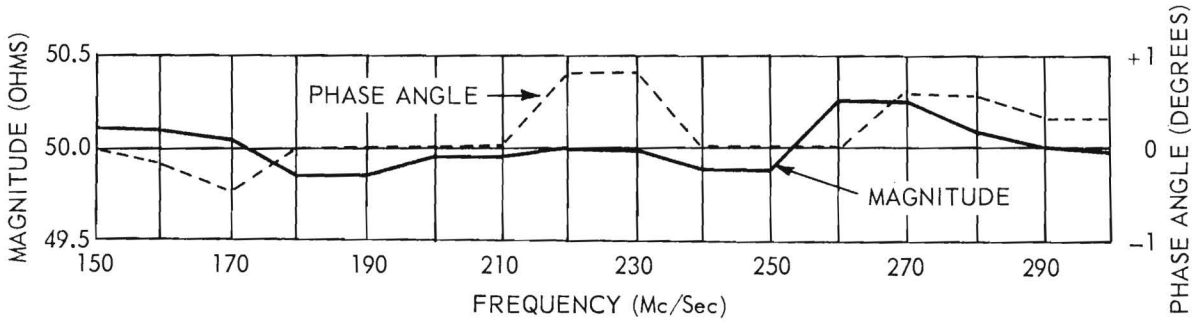

(a) 50-OHM TERMINATION

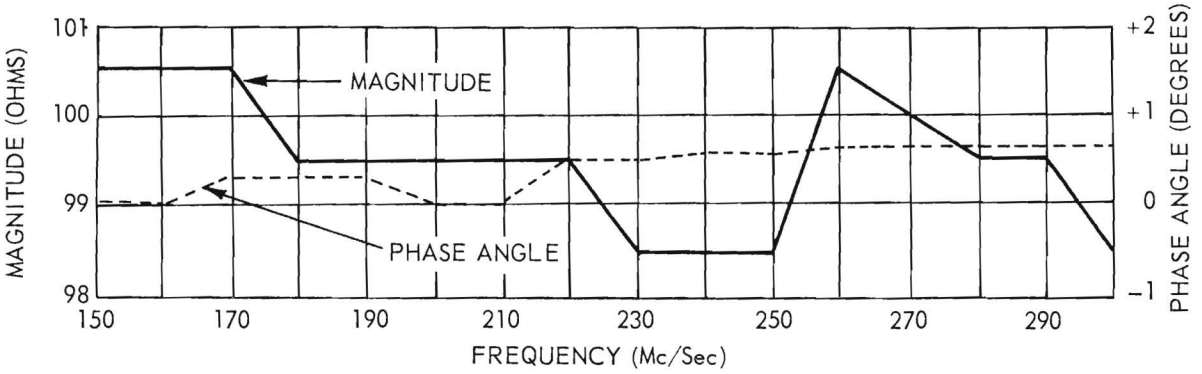

(b) 100-OHM TERMINATION

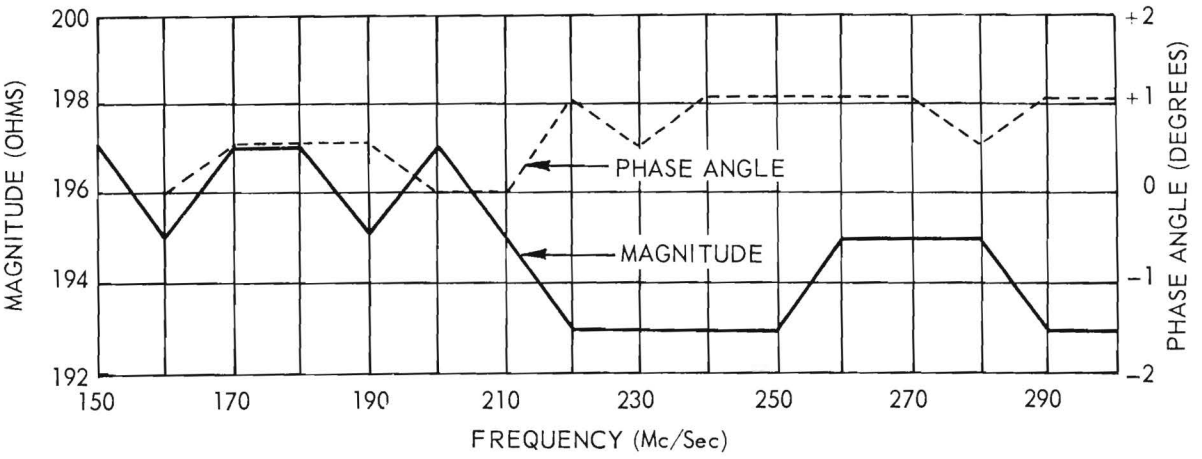

(c) 200-OHM TERMINATION

Figure 12. Admittance Meter Measurements on Resistive Terminations with Half-Wavelength Line.

on the Admittance Meter terminals (9.69 cm line length) and when the impedance magnitude is of the order of 50-ohms. (2) Both the directional coupler and arbitrary lengths of coaxial line introduce appreciable errors in measurements. (3) Half-wavelength lines introduce less errors, generally, than do random line lengths. (4) The directional coupler introduces only slightly greater errors than does an equal length of air-dielectric transmission line.

Neither mechanicalnor mathematical methods have yet been found to compensate for the additional errors introduced by the directional coupler and transmission line lengths. This is apparently due to the complicated way in which the losses occur. The fact that each line connector introduces a discontinuity also complicates the mathematical analysis of the system. It is presently believed that a complete and practical analysis will not be possible.

An alternate solution to the calibration problem is to calibrate the Admittance Meter with the directional coupler and component mount in position. This would be possible only if a sufficient number of accurately calibrated standards were available and if the standards were compatible with the component mount. Such standards are available at the National Bureau of Standards, Boulder, Colorado. It is also possible to modify the component mount slightly to permit direct connection of the standards. Such a calibration procedure would involve obtaining sufficient data to cover a Smith Chart with closely spaced correction contours which could then be used to correct the crystal admittance data.

3. Radio-Frequency Amplifiers

Initial tests of the Crystal Measurements Standard System indicated that the Marconi Signal Generator could not provide sufficient drive to test all crystals at the desired maximum drive level. Also, the stability of the generator was much poorer when it was operated without isolation from the Admittance

Meter. Thus several attempts were made to construct satisfactory r-f amplifiers to be inserted between the generator and the Admittance Meter. Before a successful model was developed, commercial amplifiers suitable for the purpose became available. Thus two Instruments for Industry Model 530 wide band chain amplifiers were purchased. Originally, only one amplifier was ordered, but the gain of one amplifier alone was not sufficient for some crystal measurement applications, particularly under mismatched conditions.

The manufacturer specifies that the bandpass of the amplifier is 10 kc to 300 mc/sec, having 18 db voltage gain into a matched load. The input and output impedances of the amplifier are 135 and 150 ohms respectively.

Since the Crystal Measurements Standard System uses 50-ohm coaxial components, the inputs and outputs of the amplifiers will be mismatched and the gain of each amplifier will be reduced. A matching network could be placed on each of the inputs and outputs to match the amplifiers; however, the loss due to the insertion of the networks is often greater than the loss due to mismatched conditions.

In initial tests of the amplifiers it was observed that the output was not constant for constant input conditions. It was assumed that the output variations were due to variation in grid bias. Thus the internal bias source was disconnected and replaced by a 6-volt dry cell. The output fluctuations continued, but were not as severe. The internal B^+ supply was then replaced by an external regulated supply. This reduced the fluctuations to a negligible amount.

A plot of the power gain for various load conditions is given for one of the amplifiers in Figure 13. Also included is a plot of the power gain for the other amplifier working into a 50-ohm load, and a plot of the two amplifiers in cascade working into the same load. The cable impedance in all cases was 50 ohms.

The apparent cycling of the gain as frequency was varied was due to the mismatch of the coaxial line at both input and output of the amplifier. Since

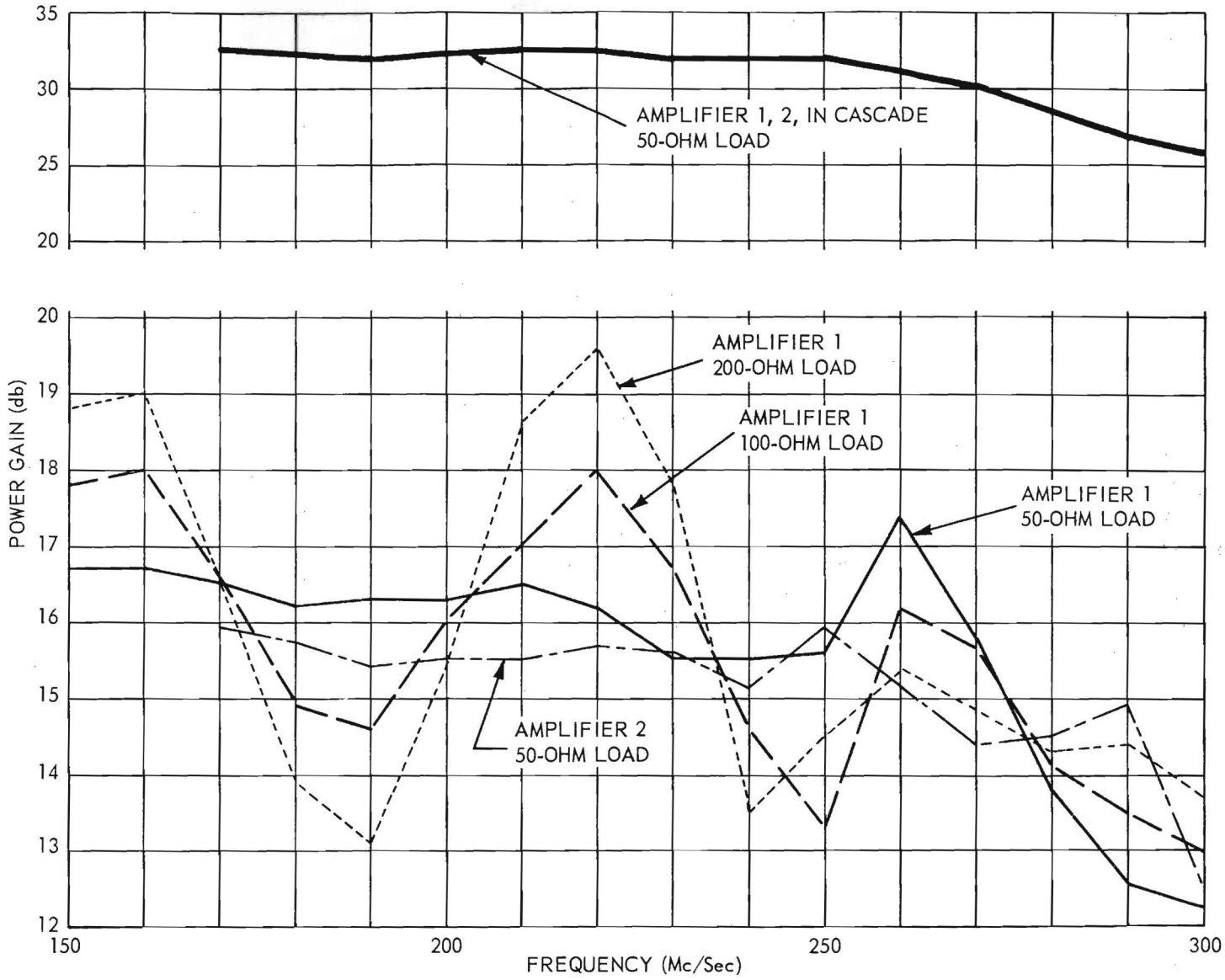

Figure 13. Power Gain Characteristics of IFI Chain Amplifier.

the minimum gain of the two amplifiers in cascade, as shown in Figure 13, is greater than the original requirement of 20 db, and since the power must be adjusted to predetermined values at each frequency and load as indicated by the power measurement system, it was not considered necessary that the gain of the amplifiers be constant over their frequency range.

A test run was made on one of the amplifiers to determine the magnitude of harmonic distortion that would be introduced into the system. The Marconi Signal Generator was adjusted to a frequency of 90 mc/sec and data were obtained as shown in Table II. The data are only approximate and depend on the dial calibration of an AN/APR-4 radar receiver which was used as an output indicator.

TABLE II

THE HARMONIC GENERATION OF A RADIO-FREQUENCY AMPLIFIER

Fundamental Frequency (Mc/Sec)	Amplifier Input Level (Mv)	Harmonic Frequency (Mc/Sec)	Harmonic Output (Db Below Fundamental)	
			Signal Gen. (Db)	Amplifier (Db)
90	2	180	44	44
90	2	270	36	36
90	100	180	48	27
90	100	270	40	40

With an input of 2 mv, the amplifier does not introduce appreciable harmonic distortion. However, it can be seen that more distortion is introduced with an input of 100 mv. To eliminate possible errors in crystal measurements due to harmonic excitation, two Microlab Corporation low-pass filters were purchased. The cutoff frequencies specified by the manufacturer are 300 mc/sec for the Model FL-301, and 400 mc/sec for the Model FL-401. Microlab specifies that the stop band limit of their filters is greater than six times the cutoff frequency. A 200 mc/sec low-pass filter (Model LP-200, Microphase Corporation)

was already in possession of the project. The characteristics of the three filters are shown in Figure 14. It can be noted that for any frequency in the range 175 to 300 mc/sec, use of the various filters will provide harmonic rejection of at least 40 db up to the sixth harmonic of the fundamental, assuming a stop band limit as specified.

It is anticipated that the filters will not normally be required for crystal measurements when using the Crystal Measurements Standard since the harmonic output from the amplifiers is relatively small and since the crystals are relatively linear. For accurate power measurements, however, the filters may be required since the Power Measurement System does not include provisions for frequency discrimination.

4. Detector Systems

A source of error in the Crystal Measurements Standard System was the lack of sufficient null detection sensitivity to permit accurate adjustment of the bridge. This difficulty arises from one of the requirements of the system, to maintain the crystal drive at very low levels (between 0.2 and 4 mw). Previous data indicated that none of the several null detection systems tested had sufficient sensitivity. The possibility of using commercial high-frequency communication receivers was considered. However, it was found that a very limited number of such receivers were manufactured. Of those available, only one, the Eddystone Model 770U, was found which was both reasonably priced and covered all of the desired frequency range. The distributor of this receiver provided data which indicated that it would offer appreciable improvement over previous detection systems. The receiver was ordered and was delivered in December 1957.

The null-detection sensitivity curve for the Eddystone receiver is presented in Figure 15.

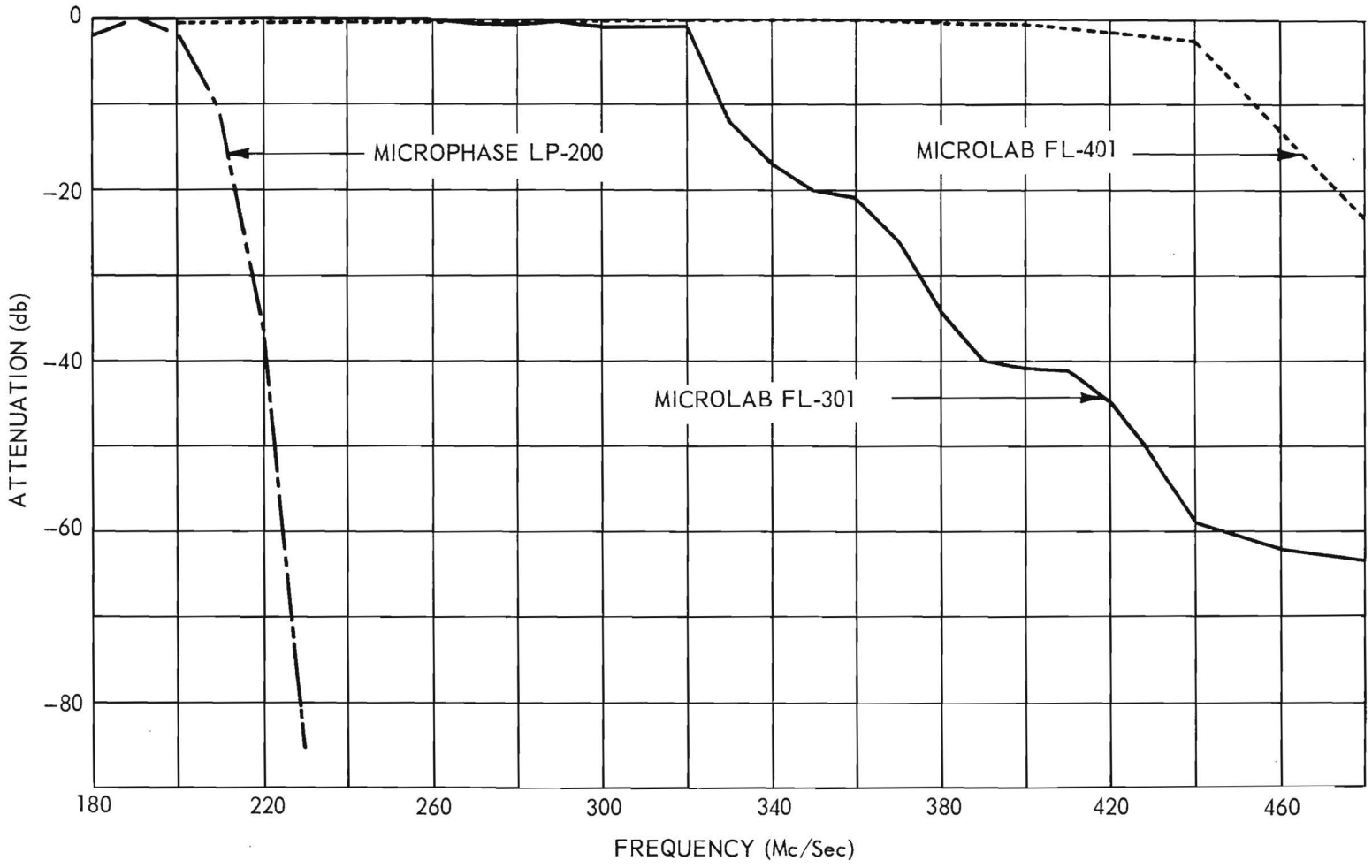

Figure 14. Frequency Characteristics of Low-Pass Radio-Frequency Filters.

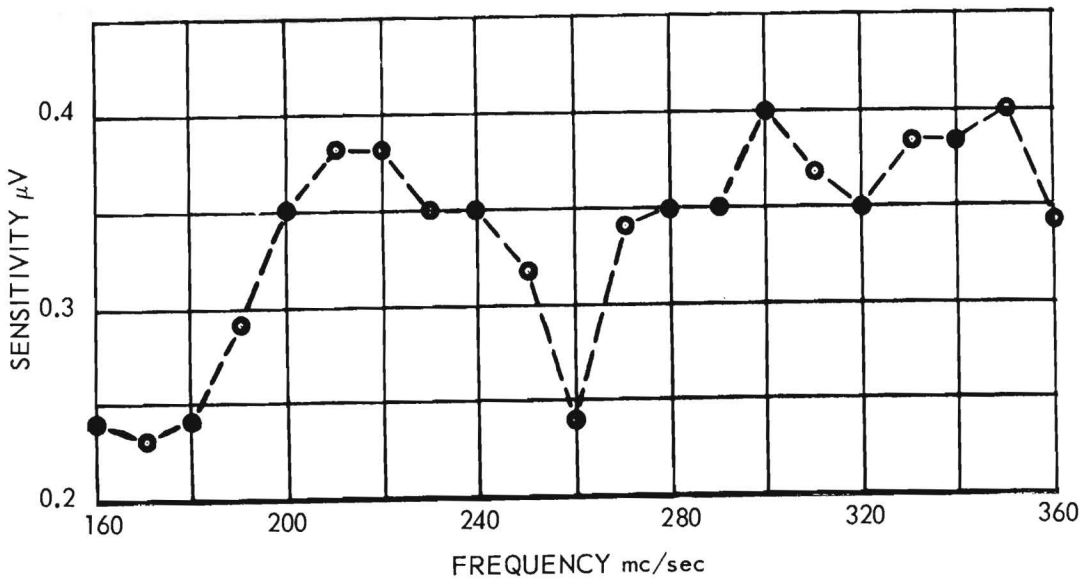

Figure 15. Null Detection Sensitivity of Eddystone Receiver Type 770U.

One difficulty encountered with the Eddystone receiver was that of r-f leakage from external sources. This was objectionable only at frequencies where television stations or other strong signals were present. However, it was felt that the source of leakage should be eliminated because of the possibility of direct coupling between the signal generator or other instruments and the receiver.

When the receiver was enclosed in a screened box, it was found that a principal source of leakage was the power cable. Thus a filter consisting of two feed-thru capacitors and an r-f choke was installed in each power connection at the receiver.

To use the receiver as a null detector it was desirable to replace the internal signal level meter with an external meter of greater sensitivity. The connection of these additional leads to the receiver became another source of r-f leakage. Thus, choke-capacitor filters were installed in these leads also.

Even with the filter installations indicated above, the r-f leakage was still appreciable. This was due to the relatively large openings in the case of the receiver. Because of the difficulty of installing copper screening in the receiver case, a small double shielded screen box was constructed to house the entire receiver. Additional filters were added at each of the external connections. The resulting total signal leakage was reduced by more than 40 db.

Further evaluation data indicated that the first filters installed between the outer shield box and the receiver did not provide sufficient isolation. To further improve the filtering, these components were replaced by four Tobe Filterettes as shown in Figure 16. The manufacturer's specifications state that this filter has a 45-db attenuation at 150 kc/sec and greater than 45-db attenuation from 150 kc/sec to 1000 mc/sec. It was also determined that the standard RG-58 BNC cable used between the receiver antenna terminal and the Admittance Meter was not sufficiently shielded to eliminate it as a source of stray signal pickup. Tests were made with other types of commercial cable, with the same results. A special cable was finally made up by inserting an RG-58 cable into a copper tube and soldering both ends to BNC connectors. This modified cable provided adequate shielding.

To determine the effectiveness of the various shieldings, several data runs were made. The first run was performed with all shieldings in use and with no external signal source. The receiver remained in the shield box with the cover closed. One end of the special copper-covered cable was placed on the antenna terminal and the other end was terminated with a short-circuit. A plot of the output current versus frequency is given in Figure 17(a). Except for two isolated responses, one at 225 mc/sec, and the other at 270 mc/sec, the signal-level-meter output current was less than 40 ua. These two isolated responses did not change in magnitude upon opening the door of the shield box, and it was therefore assumed that they were internal, spurious responses of the receiver.

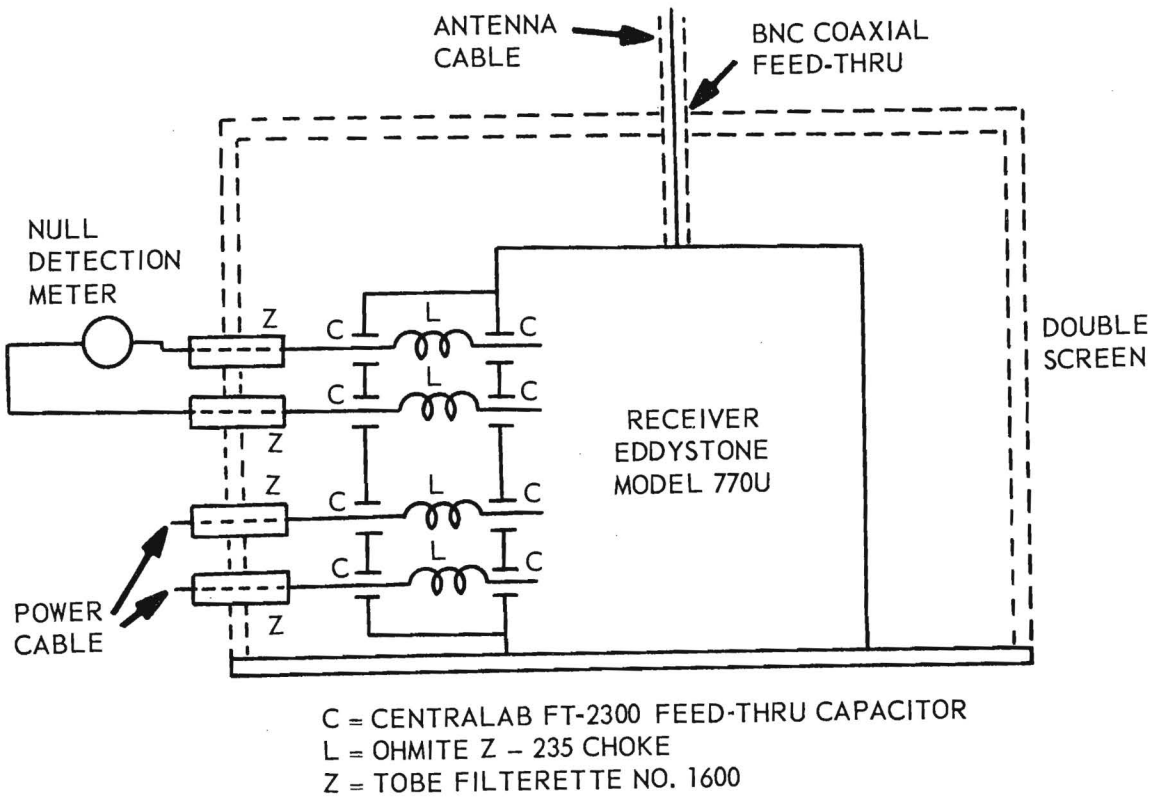

Figure 16. Stray Signal Shielding of The Eddystone UHF Receiver.

It was originally proposed to remove all the shieldings to show the increase in the various responses of the receiver. However, by merely opening the door of the shield box, the responses increased so greatly that it was not necessary to completely remove the shieldings to domonstrate this effect. A graph of these results is given in Figure 17(b).

In a third run the receiver remained in the shield box with the door closed, but the copper-covered cable was replaced by the standard RG-58/U cable. The increased responses, as shown in Figure 17(c), at 155, 198, and 204 mc/sec may be noted, with the latter two due to television Channel 11. Two interesting phenomena occurred during this run. The first was the reduction of the magnitude of the spurious responses at 225 and 270 mc/sec. It was first believed that the length of cable used on the antenna input caused the occurrence of these spurious responses. To eliminate such occurrences, a matching network

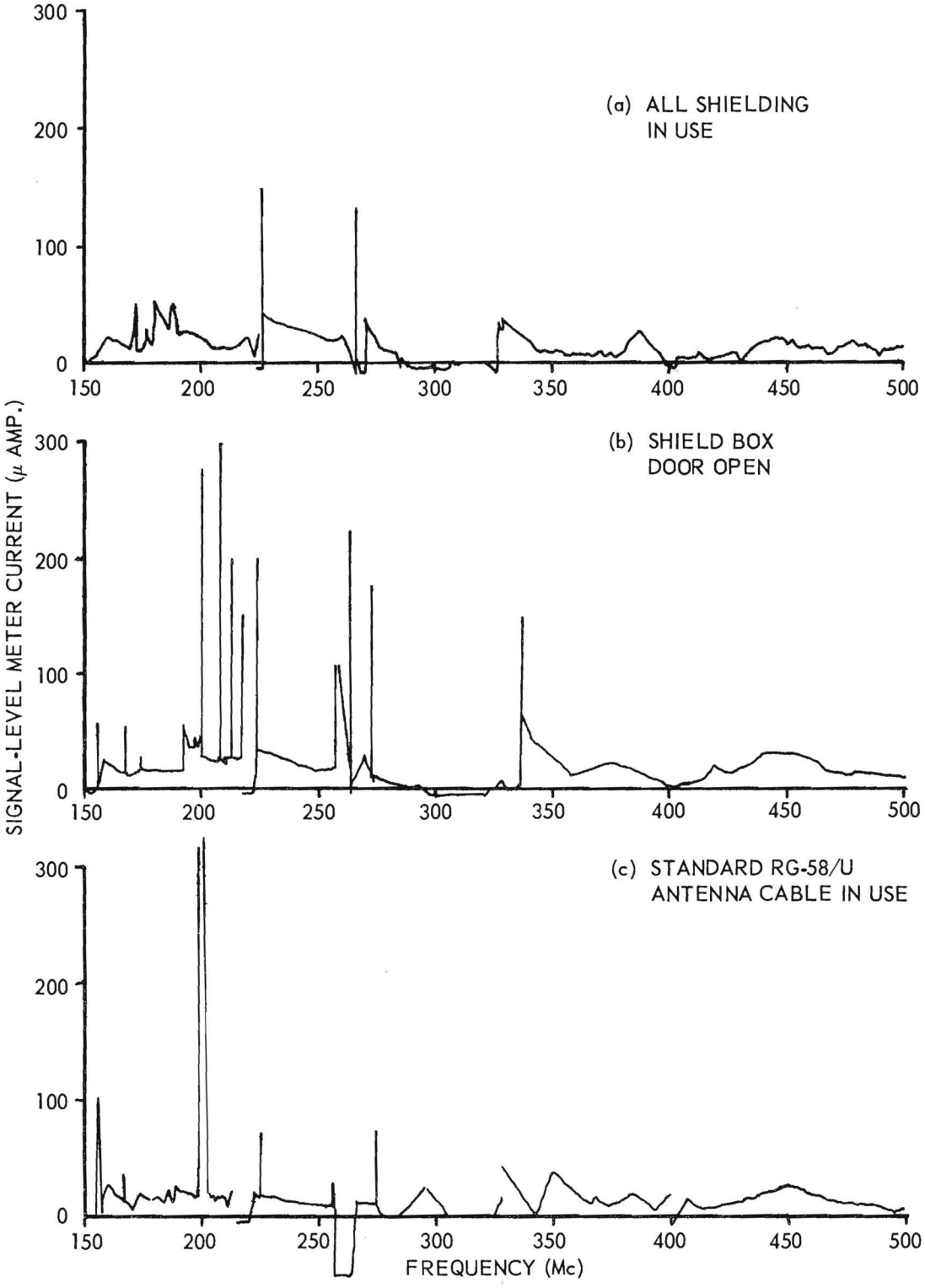

Figure 17. Results of Shielding the Eddystone UHF Receiver.

consisting of a 22-ohm series resistor and a 220-ohm shunt resistor was put in series with the antenna cable at the input of the receiver. The spurious responses still remained, however, with the same magnitude as before and were still a function of the type and length of cable used. Due to the decreased sensitivity of the system, the matching network was removed.

The second interesting phenomena was the extreme negative reading of the d-c ammeter in the frequency range from 262 to 267 mc/sec. This was caused by the r-f section of the receiver going into oscillation. This oscillation was directly attributed to the BNC cable used in the third run. At the frequency of oscillation, the length of the cable was such as to reflect an impedance into the antenna terminals which caused the receiver to oscillate. The oscillation and negative reading of the ammeter were eliminated by simply changing the length of cable used for the antenna. The special copper-covered cable was of such a length that oscillations did not occur at any frequency within the range of the receiver.

Two sensitivity runs, one with the AVC on and the other with the AVC off, as shown in Figure 18, were made at 250 mc/sec to determine the relation between the signal level meter reading and the r-f signal input voltage. It may be noted from the graph that the curve is much steeper with the AVC turned off than it is when the AVC is on; however, the dynamic range of the curve is much less. For initial measurements in locating a null, the AVC control should be left on, but as the exact null is reached, better resolution may be obtained with the control turned off. The occurrence of the negative reading of the ammeter due to excessive input signal may also be noted from this graph.

Figure 18 will aid in estimating the amplitudes of the responses shown in Figure 17. No efforts were made to determine the amplitudes of the various responses in microvolts since day-to-day changes produce variations by factors as great as five. Also, the sensitivity curve of Figure 18 is subject to some variation with ambient conditions and is valid only at the frequency specified.

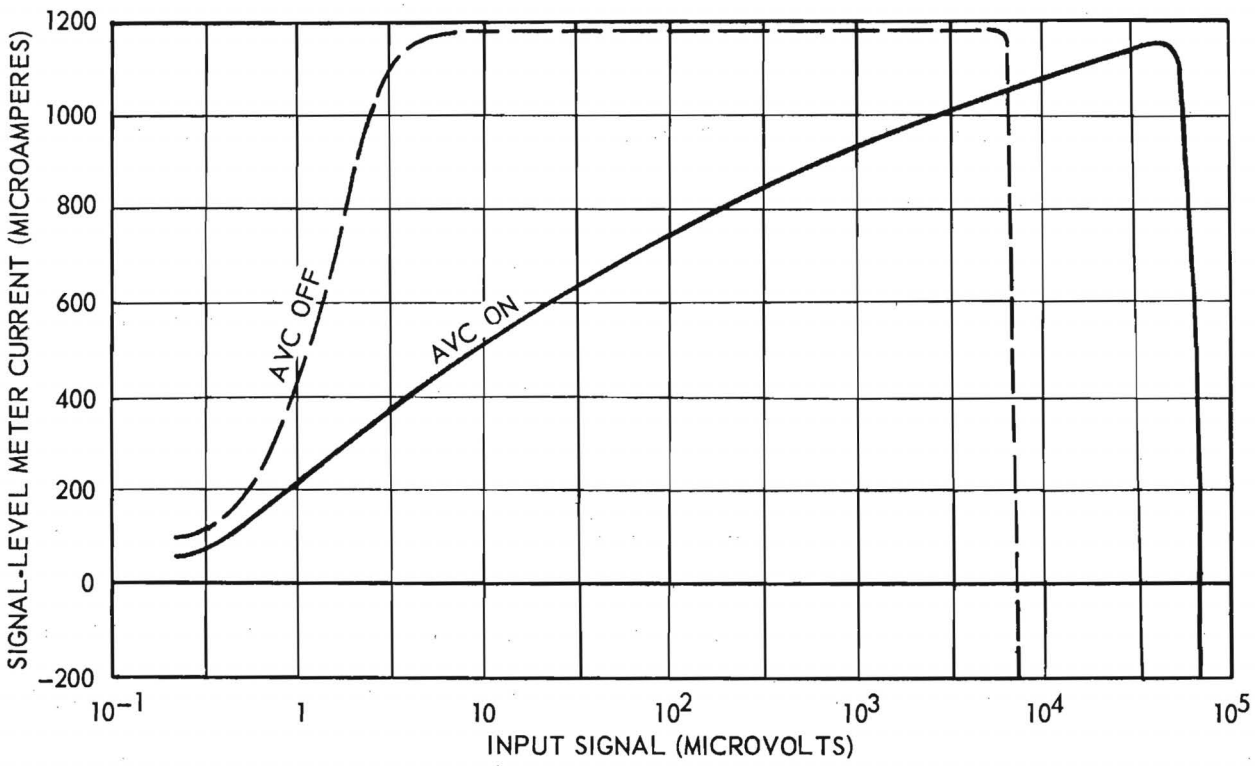

Figure 18. Eddystone Signal-Level Meter Sensitivity at 250 Mc/Sec.

Other tests indicated that the equivalent noise at the input of the receiver is less than 0.3 μv at all frequencies.

The two occurrences of negative signal-level-meter reading referenced above are due to excessively large signals in the i-f channel of the receiver. When very large signals are applied to the receiver, the AVC diode is overloaded and draws excessive current from the delay bias source. The delay bias is obtained from a voltage divider between the receiver's plate supply line and ground. The same divider is used in the signal level meter bridge circuit. Thus, when the AVC diode is overloaded, the negative reading of the signal level meter results.

5. Power Measurements

In the Crystal Measurements Standard System, it is desirable that some means be provided for continuously monitoring the crystal drive level. The power measurement system must satisfy three conditions:

1. it must be able to measure r-f power down to 0.2 mw with accuracies on the order of $\pm$ 20 percent,

2. it must not affect the crystal impedance measurements to any noticeable degree, and

3. it must be simple to operate, preferably direct reading.

From transmission line theory, the net forward power in any coaxial system is equal to the incident power less the reflected power, according to the relation:

$$P = \frac{(E^+)^2}{R_o} - \frac{(E^-)^2}{R_o} \qquad (25)$$

where R_o is the characteristic resistance of the line. Therefore, by independently monitoring the incident and reflected voltages, E^+ and E^-, on the coaxial line, it is possible to determine the net forward power. The Hewlett Packard 764D dual directional coupler provides a means for monitoring the incident and reflected voltage waves since the voltages at its two outputs are proportional to E^+ and E^-. Furthermore, previous data indicated that the insertion of the coupler into the coaxial line had negligible effects on the accuracy of the crystal impedance measurements.

To measure the r-f voltage out of the directional coupler, a square-law detector was used. This detector provided a d-c voltage proportional to $(E^+)^2$ or $(E^-)^2$ and thus proportional to incident or reflected power. The d-c voltages were measured by the bridge setup shown in Figure 19. A 5000 ohm Helipot potentiometer (P) was used as the balancing device for the bridge. The potentiometer linearity of $\pm$ 0.5 percent permitted the bridge to be calibrated by a known d-c voltage to establish a reference reading on the microammeter (A). The unknown voltage then could be read directly from the Helipot dial. A Minneapolis Honneywell Electronik Null Indicator was used to provide adequate sensitivity for balancing the bridge.

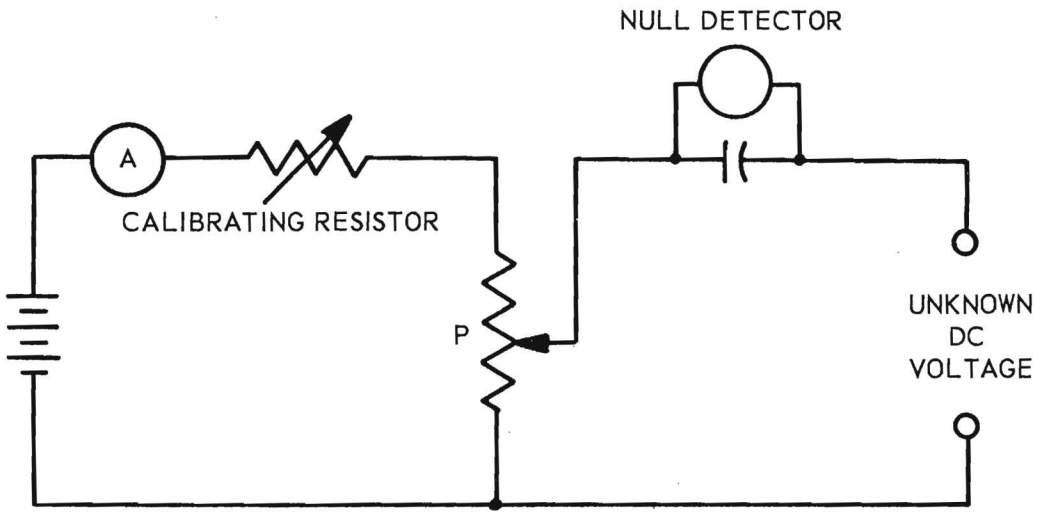

Figure 19. D-C Bridge for Power Measurement System.

Since power is proportional to the difference of the squared incident voltage and the squared reflected voltage, it is therefore proportional to the difference of the d-c voltages from the two detectors, one on each of the outputs of the directional coupler. This assumes that both detectors are precisely square-law and have matched gain factors. The output voltage, E, of a diode detector for an r-f input voltage, $\underline{e}$, is approximated by

$$E = Ae^{k} \tag{26}$$

where A and $\underline{k}$ are constants. The constant $\underline{k}$ must have a magnitude of 2 to provide square-law detection. Also, if two diodes are to provide the same output when supplied with the same input voltage, the constants, A, must be equal.

From a limited supply of diodes, two were selected that were fairly well matched and these were placed in the system shown in Figure 20. Resistances of 50 ohms were chosen for R_1 and R_2 to terminate the coaxial line from the directional coupler and thus provide the proper r-f voltage across the detectors. The values of the diode load resistors, R_3 and $(R_4 + R_5)$, were made sufficiently

small so that the sensitivity of the null indication would not be greatly reduced. As a first choice, a value of 22 K was selected for each resistor.

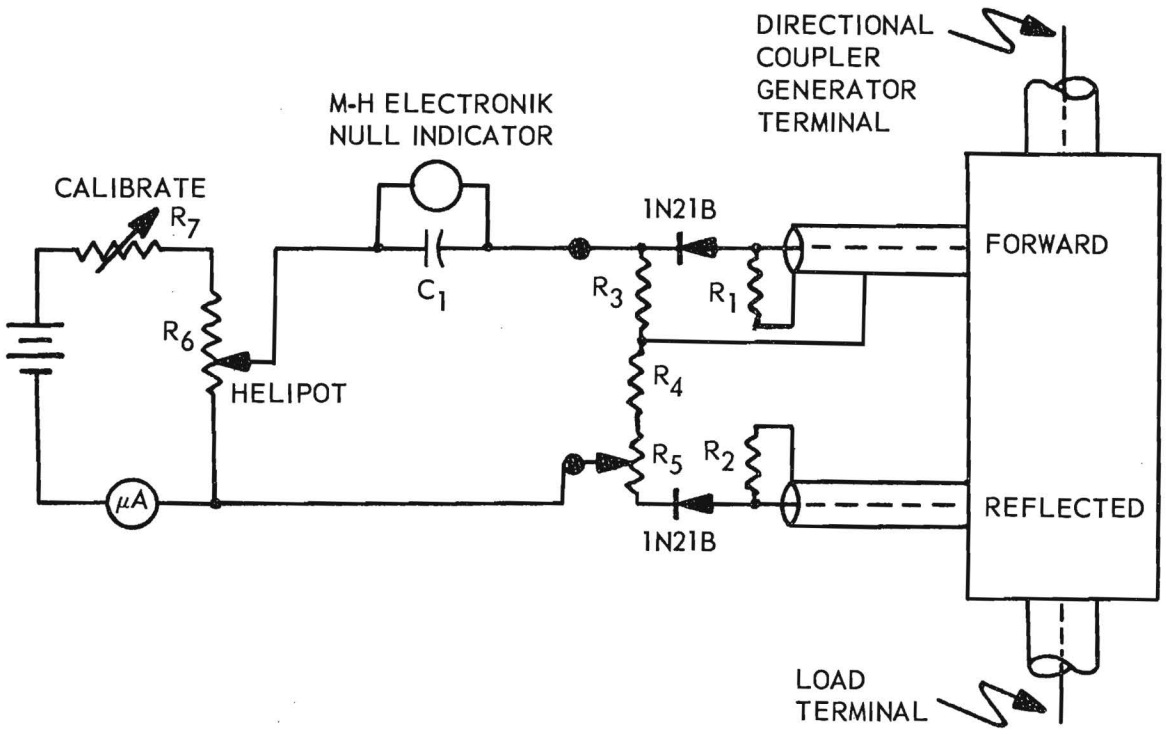

Figure 20. The Crystal Power Measurement System.

By using the Marconi Signal Generator and the variable attenuator at its output, r-f voltage versus d-c voltage curves were run on each of the diodes. After plotting on log-log paper, it was found that the output of both diodes had the form of Equation 26 but the exponent, k, was of the order of 1.8 instead of 2, which would introduce power measurement errors. After some study it was determined that the exponents, k, varied with the value of the load resistors. After considerable experimentation, it was found possible to correct the value of k from 1.8 to 2 for the two particular diodes by making the load resistors respectively 8 K and 12 K. It was necessary to correct the value of A in Equation 26 for one of the diodes used in the power measuring system in order to improve the overall accuracy. First attempts to match the diodes consisted of tapping

down on the output of the diode with the larger value of A by use of fixed resistors, keeping the total load resistance on the diode the same. This varied the value of A without affecting k. Because of the thermal sensitivity of the diode, when soldering test resistors into position or even touching the diode mount by hand, exact matching was difficult to obtain. To adjust the output of one of the diodes without handling the mount, a potentiometer, R_5, was included as shown in Figure 20. The potentiometer knob provided thermal isolation from the diode mount.

To adjust the potentiometer, the transmission line was terminated in an open circuit. This meant that E^+ and E^- were of equal magnitude, neglecting losses in the line. The potentiometer was then adjusted so that the resultant d-c voltage of the two diodes was zero.

To measure the accuracy of the system, the setup shown in Figure 21 was used. Since the output voltage amplitude of the Marconi Signal Generator was not sufficient, a Georgia Tech constructed cavity amplifier was used so that tests could be made up to a drive level of 9 mw. Originally the VSWR was determined by removing one of the rectifiers and reading forward and reverse power independently. However, this necessitated handling of the rectifier mounts which thereby introduced thermal errors. To eliminate these errors, a second directional coupler and a Millivac voltmeter were used. The Millivac does not read the exact r-f voltage at each output of the directional coupler due to inaccuracies in the meter itself, and due to mismatch and line length between the coupler probe and meter probe. The mismatch and line length errors cancel, however, since the mismatch and line lengths are identical at each directional coupler output and since only the voltage ratio is required to determine the VSWR. Inaccuracies in the meter only lead to small errors in the calculation of the VSWR.

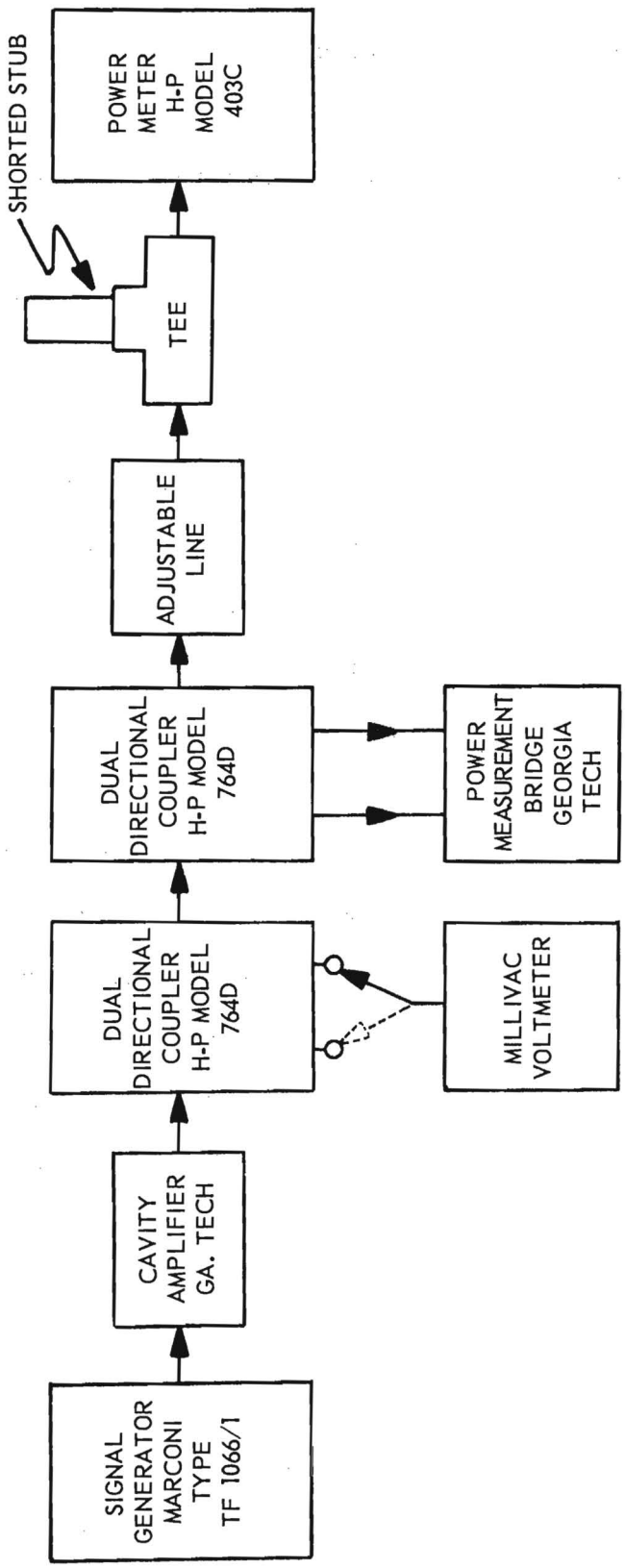

Figure 21. Setup for Determining the Accuracy of the Power Measurement System.

The system was first evaluated at 200 mc/sec, which is the frequency at which the diodes were originally matched and tested. The resulting data are given in Table III.

For a VSWR of unity and drive levels from 0.1 mw to 9 mw, the measurement system agreed with the Hewlett-Packard power meter to within +2.5 percent and -0 percent. As the VSWR was increased, the errors increased. Two sources can contribute to these increased errors: (1) errors internal to the measurement system, and (2) actual power losses in the reactive stub and adjustable line producing the high VSWR.

To confirm the second item as a source of error, it may be noted that the power measurement system always reads high with standing wave ratios greater than unity. Any loss in the reactive stub would be read by the power measurement system only, and not by the HP power meter. Differences between two readings with the same VSWR but different line lengths can be attributed to a failure in obtaining exactly the same VSWR, or a change in the position of E_{max} and E_{min} and therefore the magnitude of losses which might occur at certain discontinuities in the line. For the system at 200 mc/sec, the maximum error for VSWR of from 1 to 6.5 is approximately 5 percent for power levels greater than 0.2 mw.

The output of the directional coupler varies with frequency; however, both outputs vary in the same manner. If, at frequency f_1,

$$E_{01} = KE^{+} \quad , \tag{27}$$

then

$$E_{02} = KE^{-} \tag{28}$$

where E_{01} and E_{02} represent the outputs from the forward and reverse couplers respectively. The d-c voltage to the bridge will be

TABLE III

POWER MEASUREMENT SYSTEM ERRORS AT 200 MC/SEC

Power Measured By H-P 403C (Mw)	Power Measured By Power Measurement System: Short Line (Mw)	Power Measured By Power Measurement System: Long Line (Mw)	VSWR	Maximum Error (%)
.05	.06		1	20
.05	.06	.05	1.2	20
.05	.06		1.4	20
.05	.06	.05	2.3	20
.05	.06		3.0	20
.05	.06	.05	5.0	20
.05	.06		6.5	20
.10	.10		1.0	0
.10	.11	.10	1.2	10
.10	.11		1.4	10
.10	.11	.10	2.3	10
.10	.11		3.0	10
.10	.11		5.0	10
.10	.10	.09	6.5	10
.20	.20		1.0	0
.20	.20	.20	1.2	0
.20	.20		1.4	0
.20	.20	.20	2.3	0
.20	.20		3.0	0
.20	.20		5.0	0
.20	.19	.19	6.5	5
.40	.41		1.0	2.5
.40	.40	.41	1.2	2.5
.40	.40		1.4	0
.40	.40	.40	2.3	0
.40	.39		3.0	2.5
.40	.31		5.0	2.5
.40	.37	.37	6.5	7.5
.60	.61		1.0	1.7
.60	.61	.61	1.2	1.7
.60	.61		1.4	1.7
.60	.61	.60	2.3	1.7
.60	.60		3.0	0
.60	.58		5.0	3.4
.60	.57	.61	6.5	5.1
.80	.80		1.0	0
.80	.82	.82	1.2	2.5
.80	.82		1.4	2.5
.80	.82	.81	2.3	2.5

TABLE III (Continued)

POWER MEASUREMENT SYSTEM ERRORS AT 200 MC/SEC

Power Measured By H-P 403C (Mw)	Power Measured By Power Measurement System: Short Line (Mw)	Power Measured By Power Measurement System: Long Line (Mw)	VSWR	Maximum Error (%)
.80	.81		3.0	1.3
.80	.79		5.0	3.8
.80	.77	.77	6.5	3.8
1.0	1.02		1.0	2
1.0	1.01	1.00	1.2	1
1.0	1.02		1.4	2
1.0	1.02	1.00	2.3	2
1.0	1.02		3.0	2
1.0	1.00		5.0	0
1.0	1.03	0.96	6.5	3
2.0	2.01		1.0	0.5
2.0	2.00	2.04	1.2	2.0
2.0	2.00		1.4	1.5
2.0	2.03		2.3	1.5
2.0	2.03	2.02	4.0	1.5
2.0	2.01		5.0	0.5
2.0	2.00	2.00	6.5	0
3.0	3.04		1.0	1.3
3.0	3.04	3.10	1.2	1.3
3.0	3.06		1.4	2.0
3.0	3.06	3.08	2.3	2.7
3.0	3.06		5.0	2.0
3.0	3.06	3.12	6.5	2.0
4.0	4.02		1.0	0.5
4.0	4.06	4.14	1.2	1.5
4.0	4.13		1.4	3.3
4.0	4.11	4.11	2.3	2.9
4.0	4.10		3.0	2.5
4.0	4.10		5.0	2.5
4.0	4.13	4.10	6.5	3.3
5.0	5.06		1.0	1.2
5.0	5.09	5.16	1.2	3.2
5.0	5.12		1.4	2.4
5.0	5.14	5.14	2.3	2.8
5.0	5.14		3.0	2.8
5.0	5.18	5.14	5.0	3.6
5.0	5.23		6,5	4.6

TABLE III (Concluded)

POWER MEASUREMENT SYSTEM ERRORS AT 200 MC/SEC

Power Measured By H-P 403C (Mw)	Power Measured By Power Measurement System: Short Line (Mw)	Power Measured By Power Measurement System: Long Line (Mw)	VSWR	Maximum Error (%)
6.0	6.08		1.0	1.3
6.0	6.13	6.23	1.2	2.2
6.0	6.18		1.4	3.0
6.0	6.21	6.20	2.3	3.5
6.0	6.21		3.0	3.5
6.0	6.23	6.20	5.0	3.8
6.0	6.26		6.5	4.3
7.0	7.14		1.0	2.0
7.0	7.18	7.27	1.2	3.9
7.0	7.20		1.4	2.9
7.0	7.26	7.26	2.3	3.7
7.0	7.26		3.0	3.7
7.0	7.31	7.28	5.0	4.4
7.0	7.35		6.5	5.0
8.0	8.15		1.0	1.9
8.0	8.17	8.31	1.2	3.9
8.0	8.27		1.4	3.4
8.0	8.26	8.34	2.3	4.5
8.0	8.36		3.0	4.5
8.0	8.38	8.32	5.0	4.8
8.0	8.35		6.5	4.4
9.0	9.12		1.0	1.3
9.0	9.25	9.35	1.2	3.9
9.0	9.29		1.4	3.2
9.0	9.38	9.39	2.3	4.3
9.0	9.38		3.0	4.2
9.0	9.48	9.38	5.0	5.3
9.0	9.41		6.5	4.6

$$V_{d-c} = A(E_{01})^2 - A(E_{02})^2 = AK^2 [(E^+)^2 - (E^-)^2] = CP, \qquad (29)$$

where

$$P = \frac{1}{R_o} [(E^+)^2 - (E^-)^2] \qquad (30)$$

and

$$C = AK^2R_o \quad . \tag{31}$$

If, at frequency f_2,

$$E_{01} = K'KE^+ \tag{32}$$

then

$$E_{02} = K'KE^- \tag{33}$$

and

$$V_{d-c} = A(E_{01})^2 - A(E_{02})^2 = AK^2(K')^2\,[(E^+)^2 - (E^-)^2] \tag{34}$$

$$= (K')^2\,(CP)$$

where P and C are given by Equations 30 and 31.

Thus the effect of the directional coupler is to change the magnitude of the d-c voltage applied to the bridge by a multiplier, $(K')^2$, which is a function only of frequency and can therefore be compensated for by changing the value of the standard current in the bridge.

A plot of the required standard current versus frequency to make the Power Measurement System direct reading is given in Figure 22. By setting up the power measuring system from this graph it is possible to read power directly from the Helipot dial on the bridge at any given frequency.

If the transmission line is terminated in an open circuit, equal voltages are applied to both diodes. If any given value of voltage is applied to the line, and the potentiometer (R_5) is adjusted so that the resultant d-c output is zero, then if the diodes are perfectly matched, the resultant d-c output should remain zero as the input voltage is reduced to zero. For the power measuring system it has been determined that for any input voltage that produces a power, X, into a 50-ohm load, by setting the system up by the above procedure the output remains zero to within 0.01X. This is true regardless of the

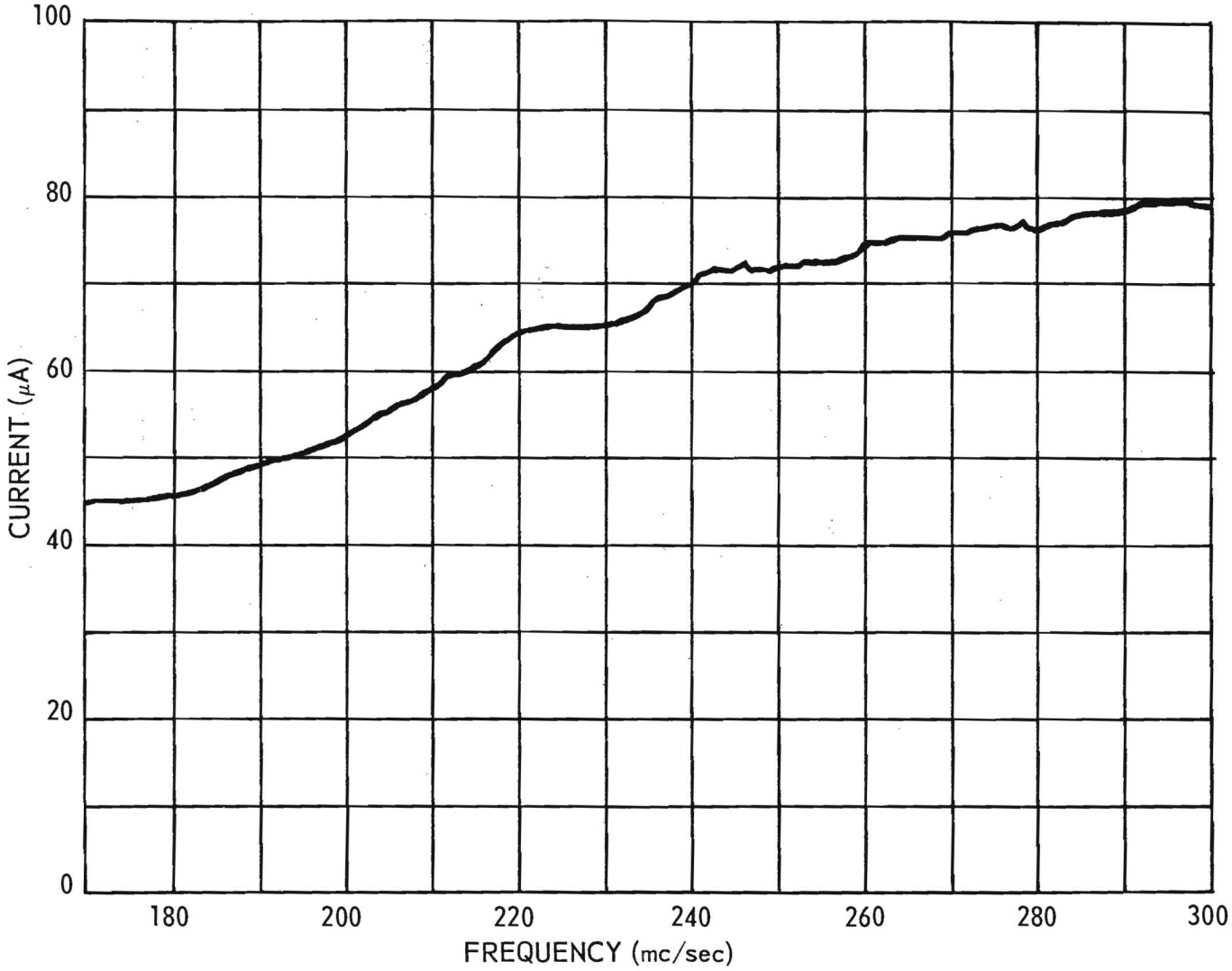

Figure 22. Calibration Currents for the Power Measurement System.

frequency; however, it has been found that the actual value of k for both diodes does vary somewhat with frequency and this will tend to increase the maximum system error slightly.

To determine the overall accuracy of the system, the setup shown in Figure 21 was again used. To initially calibrate the instrument the graph of Figure 22 was used to set up the standard current through the bridge at each frequency. To set the potentiometer (R_5), an open circuit was placed on the end of the transmission line and the potentiometer adjusted for zero output with maximum voltage input. After placement of the reactive stub in parallel with the open circuit, the power measuring system indicated a certain amount of power depending on the drive level and the position of the stub. By readjusting the potentiometer (R_5), it was possible to compensate for these losses with any given stub length, at all drive levels, with the same accuracy as defined above (i.e. -0.01X). However, this compensated for losses at a VSWR of infinity and, therefore, did not entirely compensate for losses at VSWR other than infinity. Also, as the stub length was changed, the magnitude of the losses changed and, therefore, the compensation was not effective at all stub lengths. A setting for (R_5) was chosen to give a minimum error over the range of stub lengths to be used. This compensating adjustment of R_5 therefore establishes a least upper bound on the error of the entire system.

Other measurement accuracy data were obtained over the frequency range from 175 to 300 mc/sec for a VSWR from 1 to 6.5. The VSWR at 300 mc/sec was limited to 5.3 due to the minimum length of the shorting stub used in the test. Graphs of the results are given in Figures 23 through 26. Since complete data had already been obtained for the system at 200 mc/sec, typical points were selected for the graph at 200 mc/sec from the data presented in Table III.

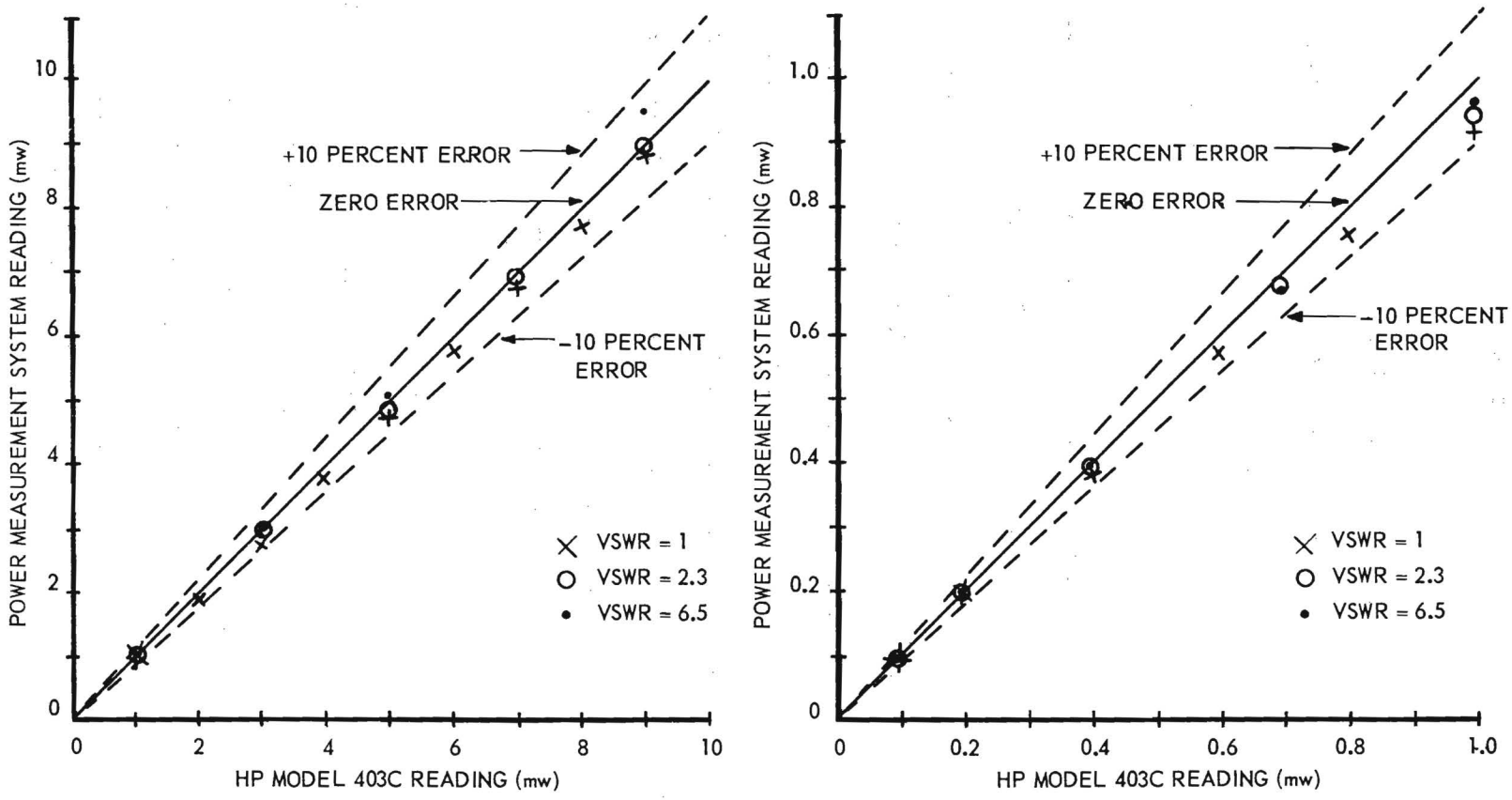

Figure 23. Power Measurement System Errors at 170 Mc/Sec.

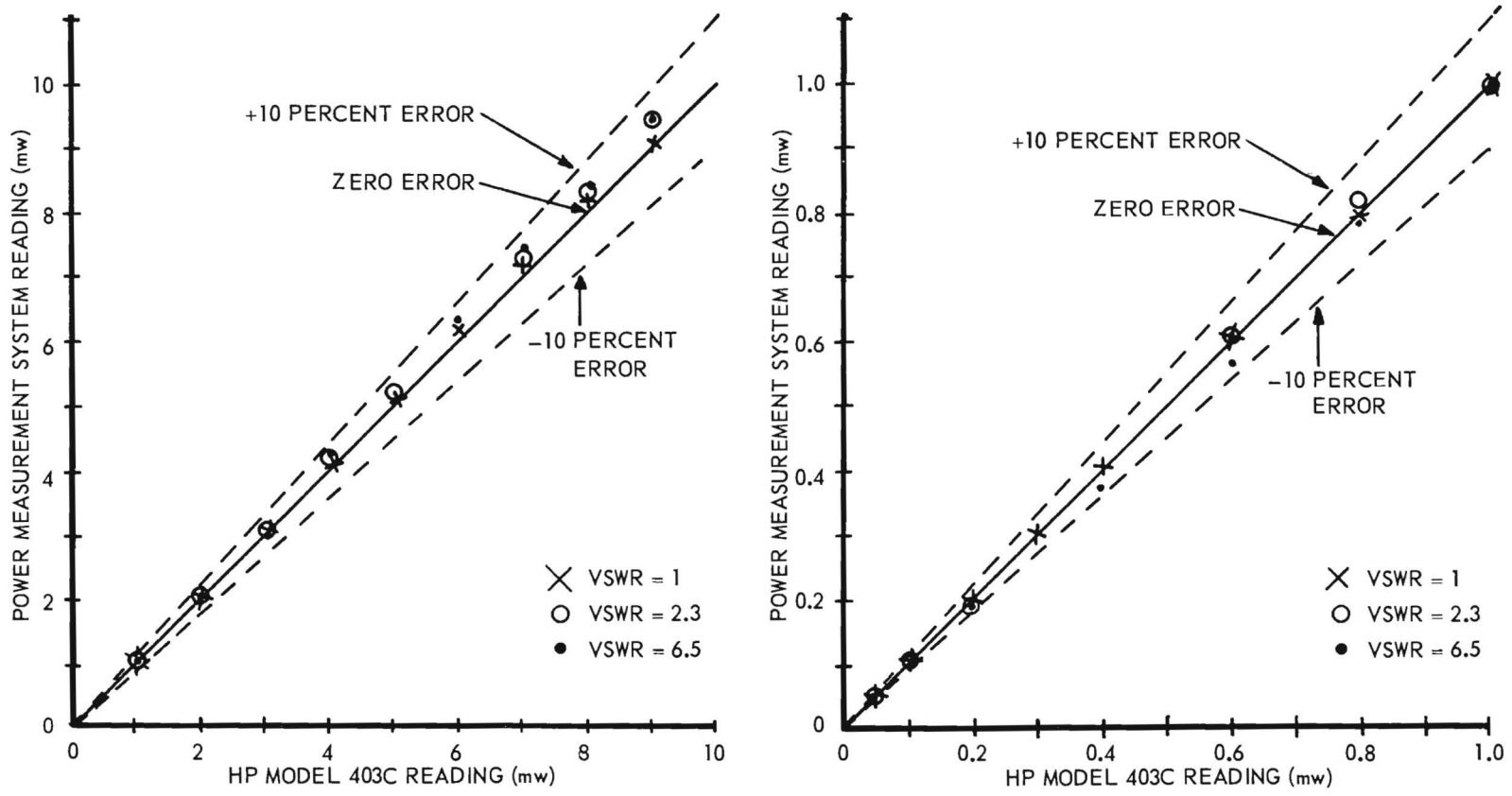

Figure 24. Power Measurement System Errors at 200 Mc/Sec.

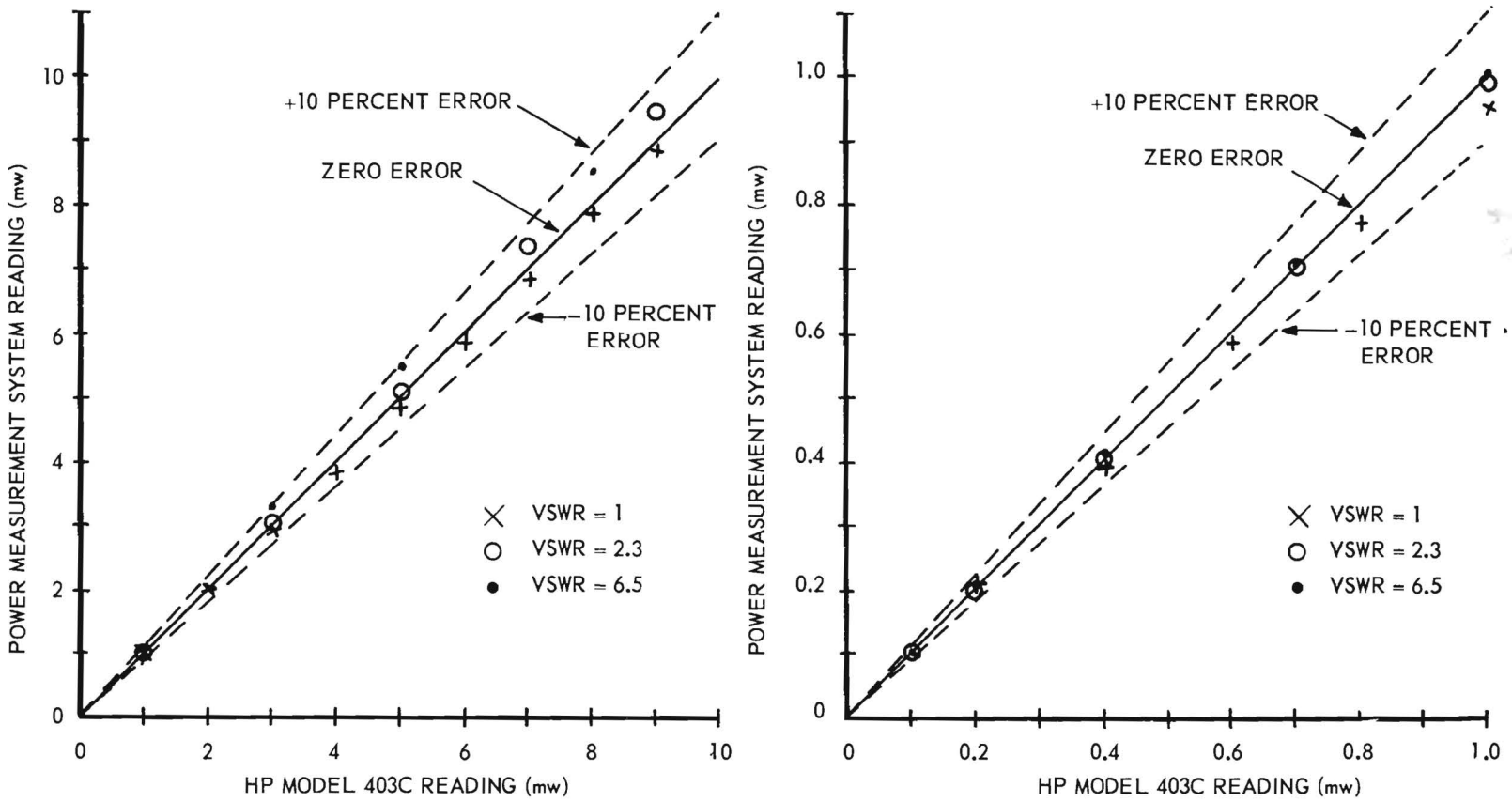

Figure 25. Power Measurement System Errors at 250 Mc/Sec.

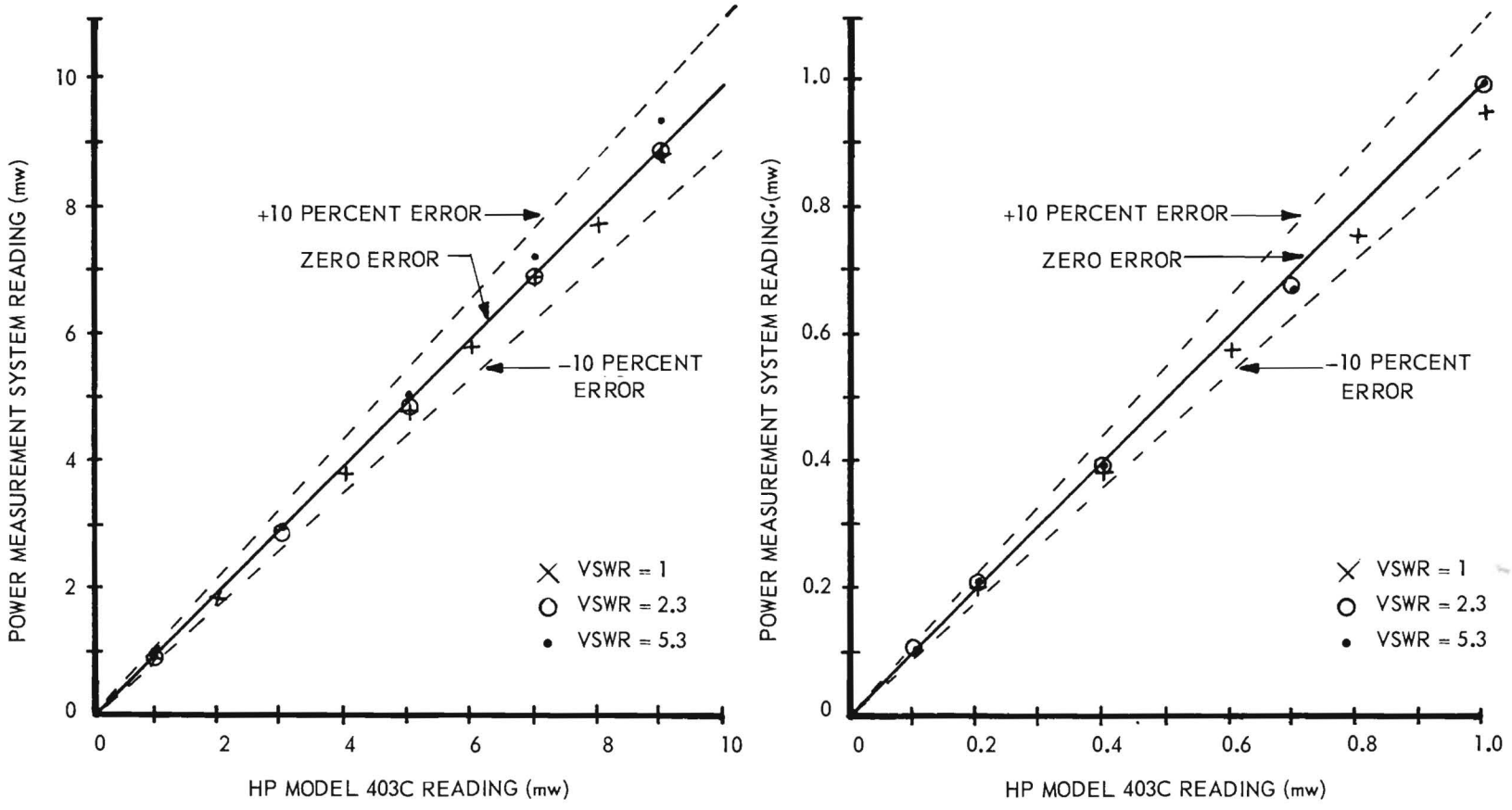

Figure 26. Power Measurement System Errors at 300 Mc/Sec.

The solid line on each graph represents the desired zero error reading of the power measurement system. The dotted lines enclose an area representing regions of error less than 10 percent. It can be seen that the Power Measurement System has an overall error of less than $\pm$ 10 percent for a VSWR from 1.0 to 6.5, power levels from 0.1 to 10.0 mw, and frequencies from 175 to 300 mc/sec.

It must be noted that the error of $\pm$ 10 percent is referred to the HP-403C which has a specified error of less than $\pm$ 5 percent. The linearity of the HP-403C was appreciably better than $\pm$ 5 percent. The small nonlinearity would tend to increase or decrease the Power Measurement System error only slightly. The error of $\pm$ 5 percent represents a reference calibration error, and can be eliminated by the procurement of a more accurate power standard.

The actual sources of error in the system come from three areas:

(1) the inaccuracy in setting up the initial standard current from Figure 22,

(2) variations in the value of the constant k of the diodes with frequency, and

(3) overcompensation of the line losses with the potentiometer (R_5).

The errors due to (1) are usually small and may be considered negligible. The errors due to (2) are the largest errors in the system and could be reduced appreciably by varying the d-c load on the diodes as the frequency is changed. Such a complication of the system is considered unjustified, however, since overall accuracy is already within the required limits. The error due to (3) is not actually an error in the power measuring system but rather a power loss caused by the method used in testing the system. That this is true is apparent since the total coaxial line length beyond the directional coupler should be considered a part of the load; however, the HP-403C Power Meter reads only the power in its resistive termination. Thus, losses occurring in the line stubs

used to produce the high VSWR are read by one system but not by the other. It has not yet been possible to prove this hypothesis since no method has been found to eliminate the unwanted losses. A possibility for making more precise calibrations would be to obtain tunable bolometers, having various resistance values other than 50 ohms and calibrated for use with the HP-403C Power Meter, which could be used for producing VSWR values other than unity. If this were done, it is believed that the accuracy of the system would be found to be much better than the $\pm$10 percent stated above. In other words, it is believed that the greater portion of the 10 percent error is due to actual power losses in the lines used to produce the high VSWR values.

Various methods have been considered for simplifying the power measurement procedure. The greatest improvement would be to eliminate the balancing procedure which requires the use of a Helipot and null detector. This can be accomplished by attaching a sufficiently sensitive d-c voltmeter directly to the series-connected diodes at the outputs of the directional coupler. Until recently, sufficiently sensitive and accurate instruments of this type were not available. During the second quarter of the contract period, four of the then available sensitive voltmeters were tested in the laboratory. Only two of the instruments had the necessary floating input and one of these instruments had too low an input impedance. The remaining instrument, the Hewlett-Packard Model 425A, was purchased.

This instrument, which has not yet been tested with the Power Measurement System, is capable of measuring voltages from 10 microvolts to 1 volt full scale in 11 voltage ranges, and measuring currents from 10 micro-microamperes to 3 milliamperes full scale in 18 current ranges. The manufacturer states accuracy of measurement to within $\pm$ 3%, on all ranges.

The input impedance of the instrument is 1 megohm on all ranges. By removing an input current shunting resistor, the input impedance on the voltage ranges exceeds 50 megohms. Elimination of the resistor prevents use of the nine lowest current scales of the instrument. Since the voltmeter was ordered for use in conjunction with the Power Measurement System, which has an output impedance of less than 10,000 ohms, the input impedance of 1 megohm is sufficiently high. The micro-voltmeter has the necessary floating input, as required by the Power Measurement System. It was determined that the impedance from either side of the input to ground was several hundreds of megohms.

The manufacturer specifies that, after fifteen minutes warmup, the drift of the instrument, referred to its input, is less than 2 microvolts per hour, and the noise is less than 0.2 microvolts rms. The external output terminals of the voltmeter were connected to an Esterline-Angus 1 milliampere recorder and the drift and noise characteristics were measured over a period of five days. Figure 27 shows the noise variation over this period of time. On the 100 μv range the noise was negligible. On the 10 and 30 μv ranges the noise remained less than 0.3 μv, except during a three hour period on each of three evenings. It will be noted that the noise appears to be a function of the time of day, indicating that the a-c line source was probably the cause of the noise.

The instrument was run continually throughout the five days. After 20 minutes initial warmup, on the 10 μv range, the drift rate was approximately 0.8 μv/hr and decreased to zero after 8 hours. The drift remained essentially zero on all ranges after the first 8 hours of operation. One exception was a sudden shift of 1.5 μv in the zero position which occurred at 1:00 a.m. each morning. The cause of this shift is unexplained.

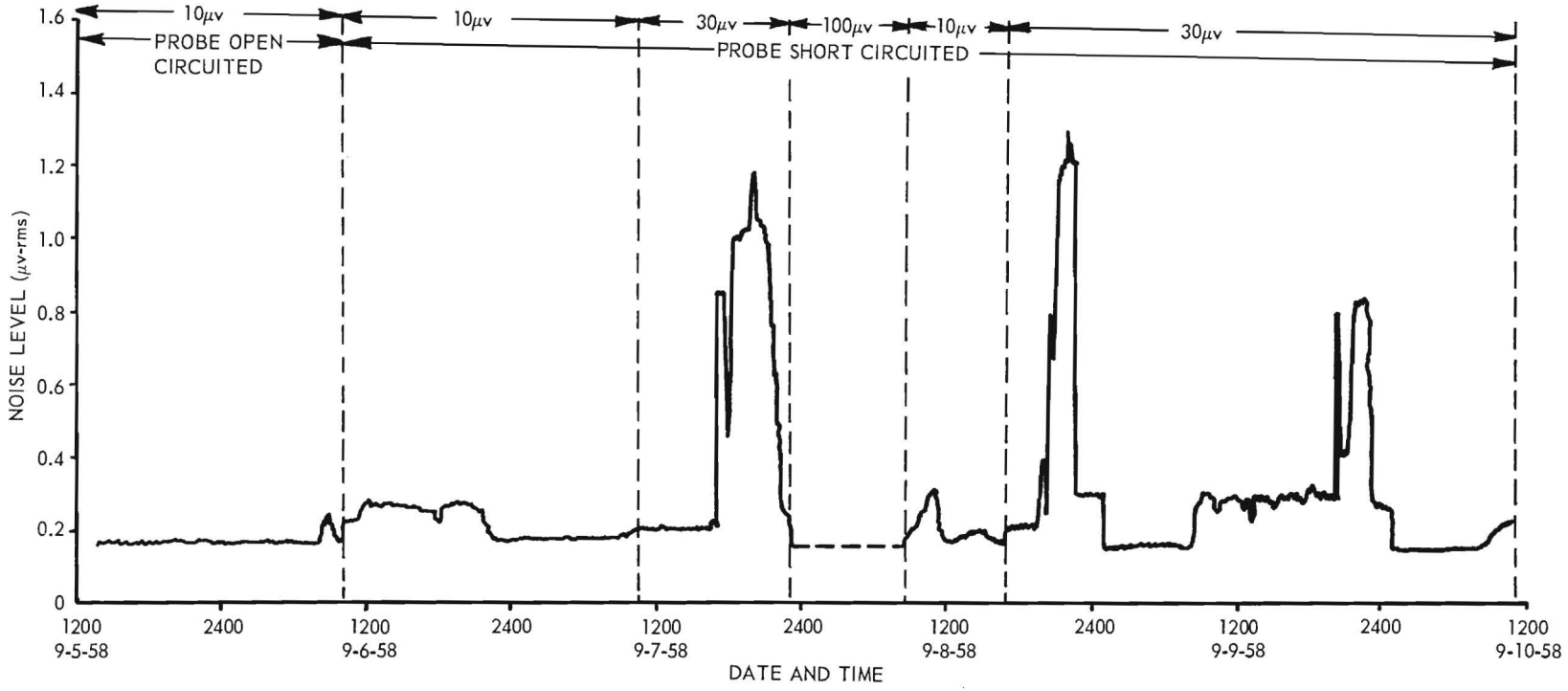

Figure 27. Noise Level of Hewlett-Packard Micro Volt-Ammeter.

6. Experimental Crystal Data

The Crystal Measurements Standard, as shown in Figure 2, was used to measure the parameters of approximately 25 crystals. The holder responses as well as all overtone responses from 150 to over 300 mc/sec were measured. Table IV shows a summary of responses measured on most of these crystals. In all cases, the responses were measured with the component mount attached directly on the Admittance Meter, without the Power Measurement System in use. Drive level was adjusted by measuring the voltage across a resistor which replaced the crystal in the component mount. The power level was adjusted to less than 2 mw at all frequencies below 300 mc/sec. At higher frequencies, where the chain amplifiers could not be used, lower drive levels were accepted.

TABLE IV

SUMMARY OF RESPONSES MEASURED BY THE CRYSTAL MEASUREMENT STANDARD

Crystal No.	Fundamental Frequency (mc/sec)	Overtone Responses Measured								Highest Overtone Freq. Measured (mc/sec)
		5	7	9	11	13	15	17	19	
5	16.67			X	X	X	X	X		284
6	16.67			X	X	X	X	X		284
12	19.96			X	X	X	X			300
13	19.97			X	X	X	X			300
FA-67	29.93	X	X	X	X					330
FA-106	32.93	X	X	X						297
FA-115	34.93	X	X	X	X					385
MA-23	16.17				X	X	X	X	X	308
MA-24	16.17				X	X	X	X	X	308
MA-25	16.18				X	X	X	X	X	308
MA-26	16.17				X	X	X	X	X	308
MA-35	16.17				X	X	X	X	X	308
MA-36	16.17				X	X	X	X	X	308
MA-37	16.17				X	X	X	X	X	308
MA-50	17.96			X	X	X	X	X		306
MA-51	17.96			X	X	X	X	X		306
MA-52	17.96			X	X	X	X	X		306
MA-58	14.97				X	X	X	X	X	285
MA-70	17.96			X	X	X	X	X		306
MA-71	17.96			X	X	X	X	X		306
MA-72	17.96			X	X	X	X	X		306
FA-116	35.00	X	X	X	X	X				455

The 9.69 cm length of transmission line separating the crystal and the internal Admittance Meter connections was subtracted from the crystal responses by a digital computer. The resulting data were plotted and filed for future analysis. The data for three typical crystals are shown in Figures 28, 29, and 30. The overtone responses for some of the other crystals were appreciably poorer for the same order of frequencies because of the higher overtone numbers required by the lower fundamental frequencies.

The computer program used to subtract the 9.69 cm of line length assumed that the transmission line was lossless. The computer time required was approximately 3.5 seconds per point of data. The output was available in either polar form or rectangular form and in terms of either impedances or admittances. Generally, the rectangular form of admittance (conductance and susceptance) was used.

For crystals with no previous data available, it was generally desirable to determine the approximate frequencies of the overtone responses by means other than the Crystal Measurements Standard because of the excessive time consumed when using the Standard. These frequencies were determined by means of the setup shown in Figure 31. This system is not frequency sensitive and thus does not require detector tuning. As the generator is swept through the range of frequencies, the presence of an overtone response is indicated by a dip in the null detector reading.

Very few difficulties were encountered while making the crystal measurements. More than adequate drive level and null detection sensitivity were available at all frequencies between 150 and 300 mc/sec. Frequency pulling was completely eliminated by the use of the chain amplifiers. The frequency stability of the signal generator proved adequate in all but a very few instances where low-frequency frequency-modulation caused a broadening of

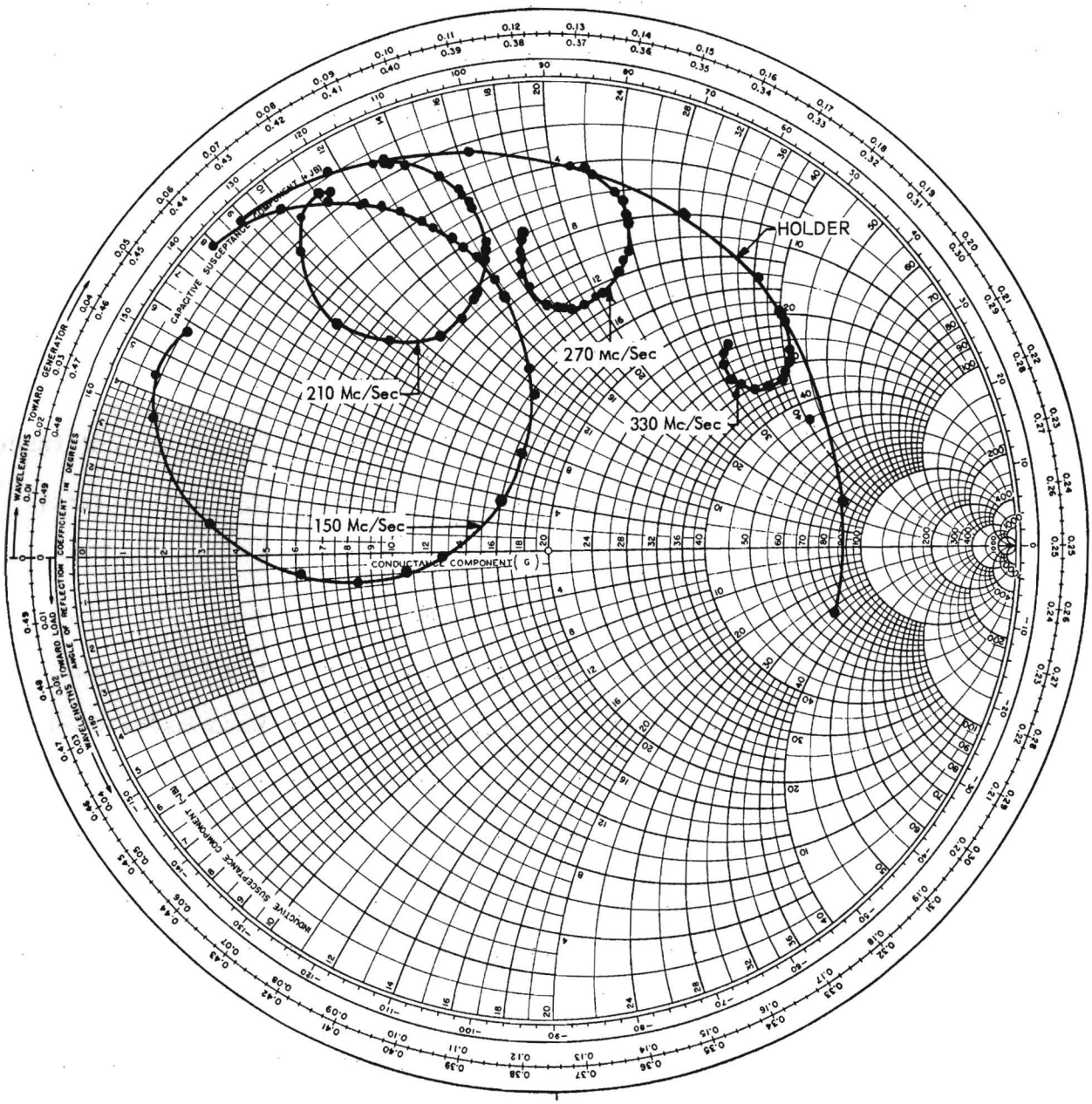

Figure 28. Admittance Characteristics of Test Crystal No. FA-67 with Transmission Line Subtracted.

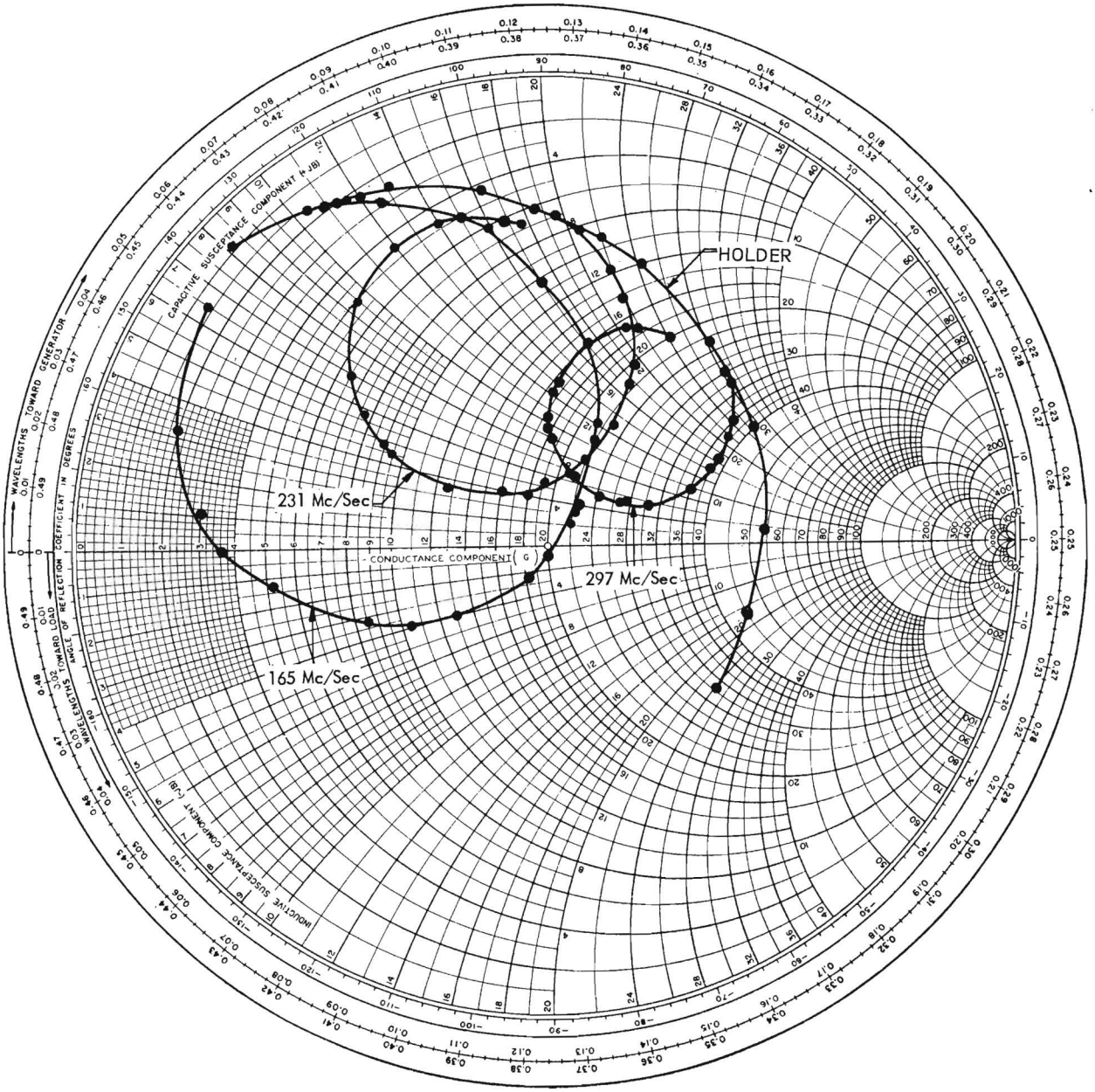

Figure 29. Admittance Characteristics of Test Crystal No. FA-106 with Transmission Line Subtracted.

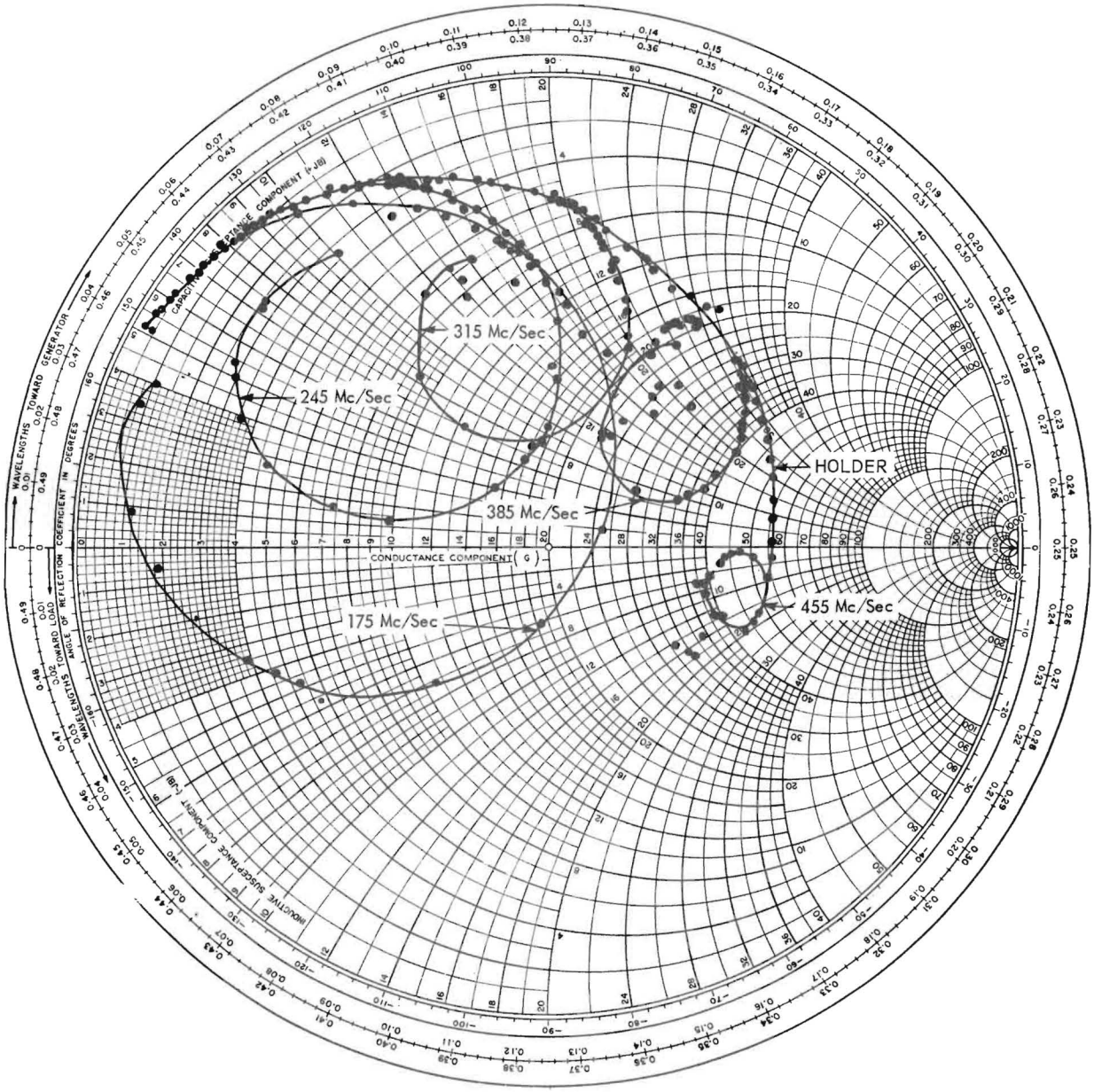

Figure 30. Admittance Characteristics of Test Crystal No. FA-116 with Transmission Line Subtracted.

the null indication. Warm-up drift of the equipment was slightly troublesome in some cases where attempts were made to make crystal measurements only a few minutes after the equipment was turned on. Appreciable difficulties were encountered, at times, with the frequency measuring equipment; however, this was due primarily to the age and deterioration of the equipment.

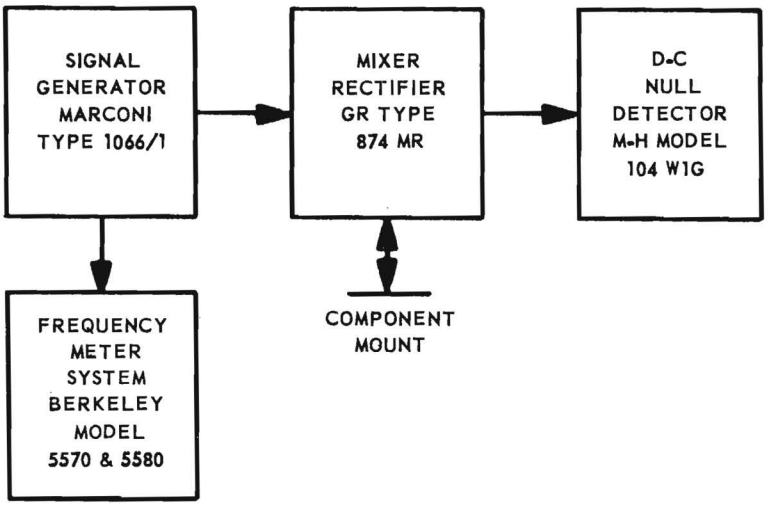

Figure 31. Setup for Locating Crystal Overtone Responses.

7. Crystal Data Analysis

Several methods exist for reducing crystal data, such as presented in the previous section, to crystal equivalent circuits. The methods differ both in theory and results; however, each of the common methods is based on its particular assumed equivalent circuit. The most commonly used equivalent circuit for VHF-UHF crystals is shown in Figure 32. The element, C_o', may or may not be required, depending upon the method of mounting the crystal holder while making the measurements.

The first step normally taken when making a crystal analysis is to reduce the original measurement data to perfect circle approximations. For Crystal No. FA-116, the perfect circle approximations of the data of Figure 30

are shown in Figure 33. It may be observed that points on the low frequency side of motional arm resonance are considered more significant, because of the distortion which occurs on the high frequency side due to spurious responses.

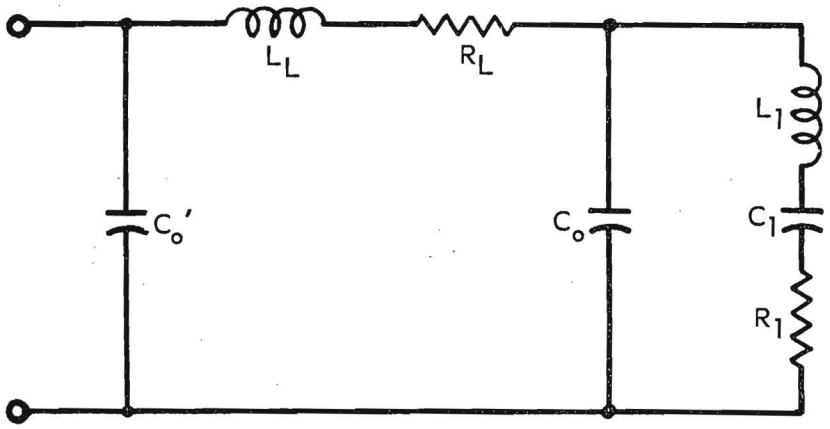

Figure 32. Common Equivalent Circuit for a VHF Quartz Crystal.

An examination of the holder response of Figure 33 will reveal that the holder circle is not perfectly centered about the zero susceptance axis. This can be caused by subtracting an incorrect line length, when transforming from the original Admittance Meter data, or it can be caused by the presence of a C_o' across the terminals of the holder. Since the length of the component mount is precisely calibrated, any error in length must be attributed to fringing effects at the junction of the crystal and the mount. Whether to attribute the holder circle displacement to a line length error or to a C_o' is determined by choosing the condition which best matches the original holder data. For example, if the line length for the data of Figure 33 is assumed to be correctly subtracted, a value of C_o' of 0.69 mmfd may be found which, when subtracted from the holder characteristics, will leave a circle which will be centered about the zero susceptance axis, as shown by the dotted circle of

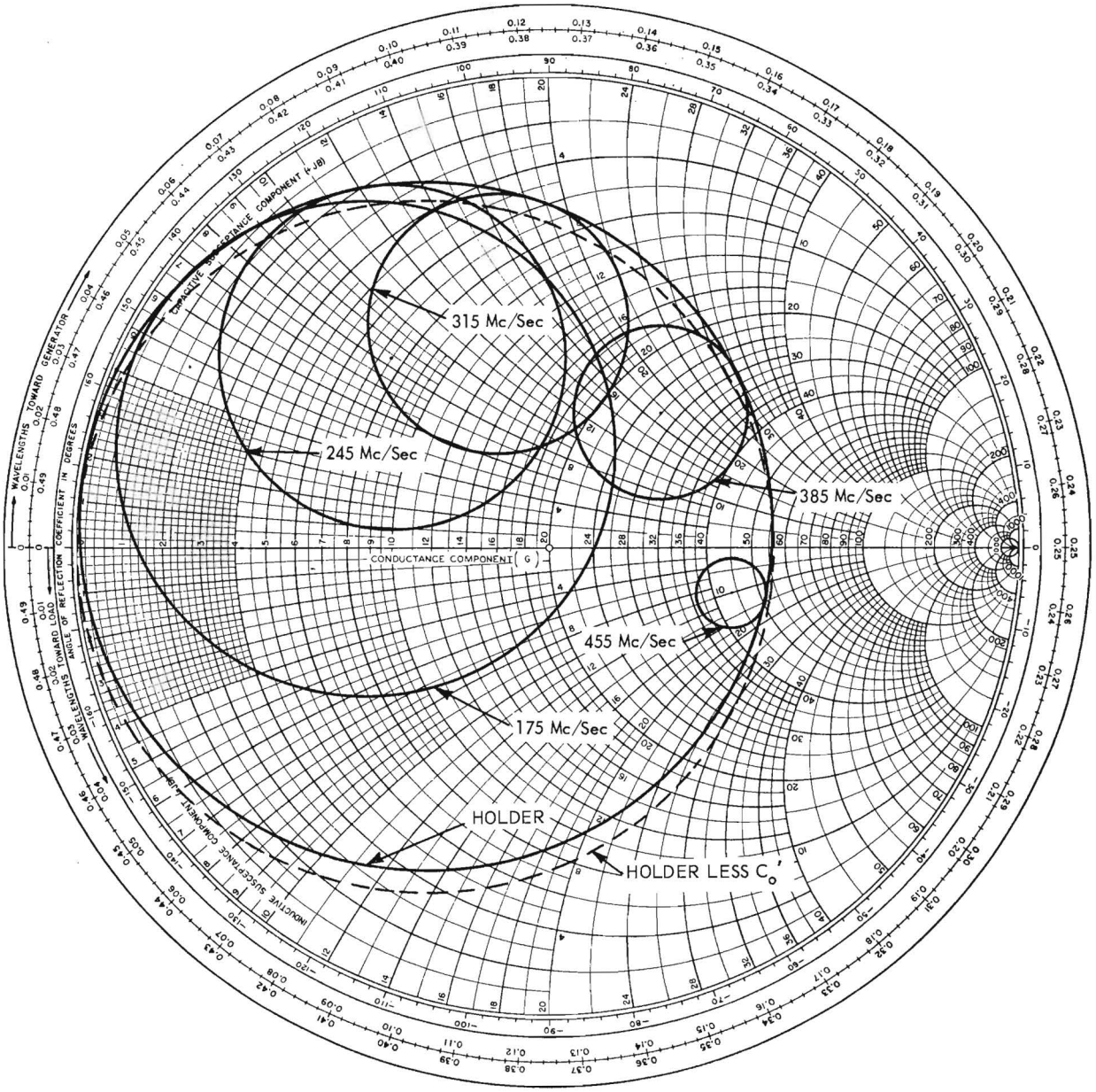

Figure 33. Perfect Circle Approximations of Test Crystal Characteristics.

Figure 33. The remaining holder element values may then be determined by analyzing the dotted circle as a series resonant circuit. For Figure 33, such an analysis yields values as follows: R_L = 17.5 ohms, L_L = 29.9 mμh, and C_o = 4.393 mmfd. If the holder parameters of such a circuit are subtracted from the original holder data of Figure 30, the maximum residue is found to be less than 0.13 millimhos for conductance and susceptance. The average residue was 0.07 millimhos for conductance and 0.02 millimhos for susceptance.

After all of the holder parameters are calculated, the holder may be subtracted from each of the crystal overtone responses by means of a specially prepared computer program. The admittance of the remaining function should represent a series resonant circuit.

When the above holder parameters are subtracted from the 175 mc/sec response of Figure 30, the resulting admittance function is as shown in Figure 34. Admittance magnitude and phase angle were used for these curves because of the greater convenience in comparing with universal resonance curves for series resonant circuits. Shown also in Figure 34 are the universal resonance curves calculated for best match with the crystal curves. The phase angle curve matches almost perfectly while the magnitude curve shows disagreement on both sides. The larger disagreement at frequencies above resonance can be attributed to the effects of spurious responses; however, the low frequency disagreement is unexplained. Any error in the holder equivalent circuit could, of course, account for the disagreements.

During the search for better methods of analyzing crystal data, it was decided to examine a method proposed by Dr. E. Hafner of USASRDL [1]. His

[1] Measurements of VHF Crystal Parameters--A Graphical Method of Data Reduction, Engineering Report No. E-1216, U. S. Army Signal Research and Development Laboratories, 25 September 1957.

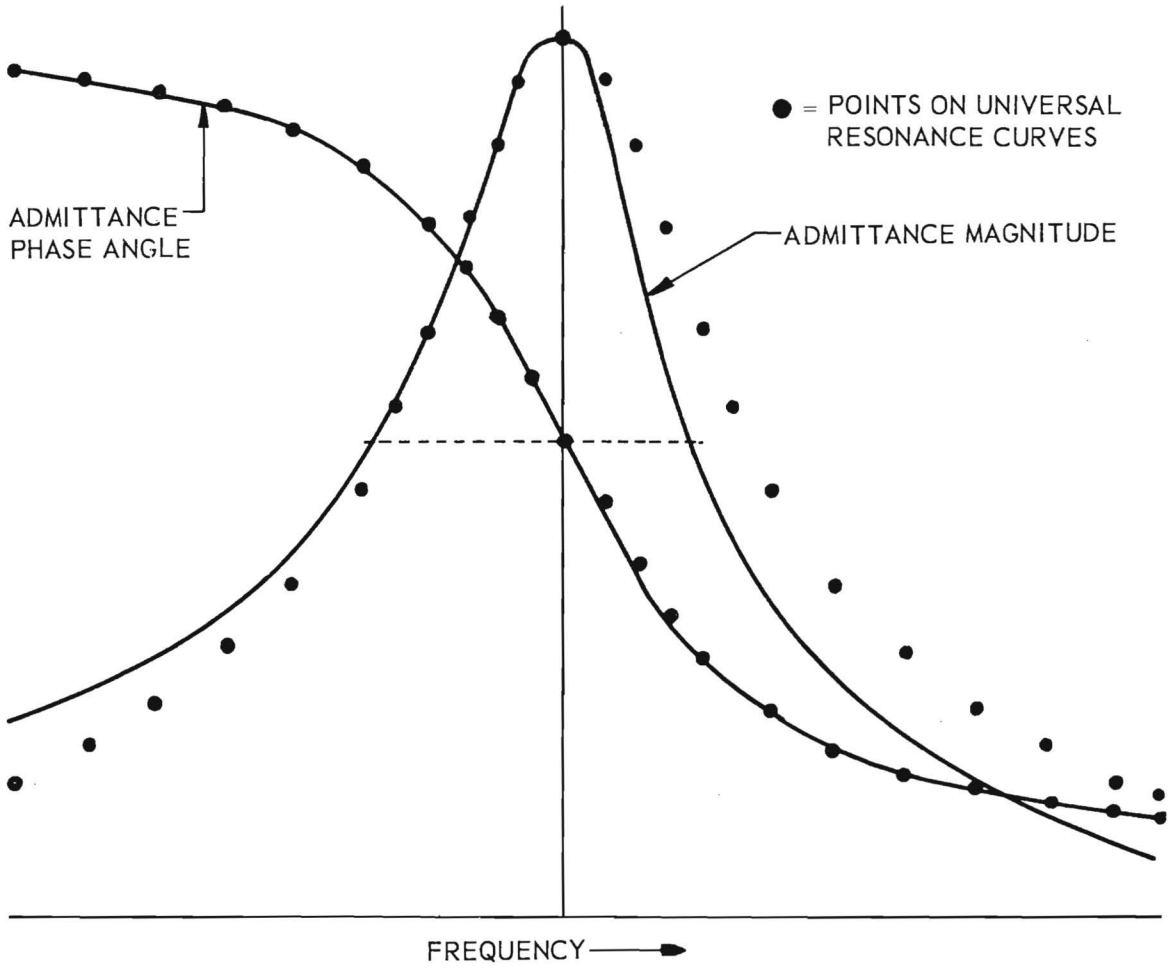

Figure 34. Admittance Characteristics of Crystal No. FA-116 with Conventional Holder Subtracted.

method divides the holder resistance as shown in Figure 35. Using the Hafner method, values for R_L and R_o of 0.7 and 16.8 ohms respectively were found. Other element values were the same as for the conventional holder. When this holder was subtracted from the 175 mc/sec response of Figure 30, the resulting admittance function of Figure 36 was obtained. Both the phase and magnitude curves are displaced slightly from the curves of Figure 34. Again, attempts were made to match the characteristics with universal resonance curves, as shown dotted in Figure 36. This attempt resulted, however, in a poorer match than was obtained for Figure 34. Therefore, it might be concluded that the Hafner procedure results in a poorer representation of the motional arm of this particular crystal than does the conventional holder.

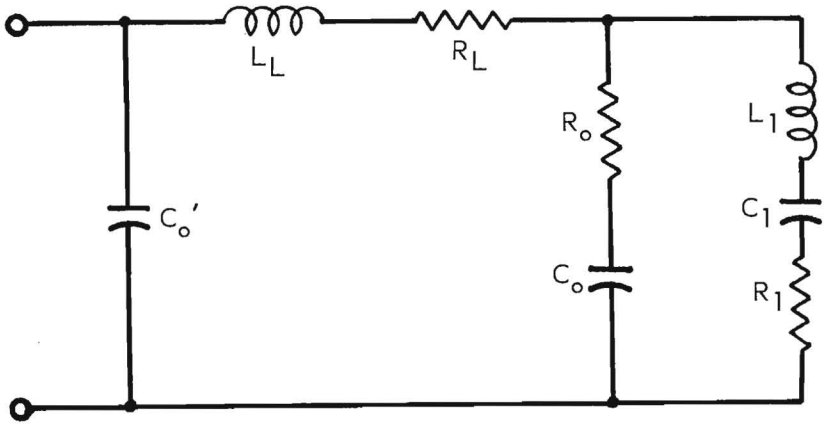

Figure 35. Hafner Equivalent Circuit for a VHF Quartz Crystal.

While applying the Hafner method, it was observed that several possible sources of inaccuracy exist because of limited Smith Chart resoltuion. It was therefore decided to apply the method to a theoretical crystal, the composite characteristics of which had been calculated on a digital computer.

Two sets of parameter values were chosen, differing only in the division of the total holder resistance. Element values which were the same for both

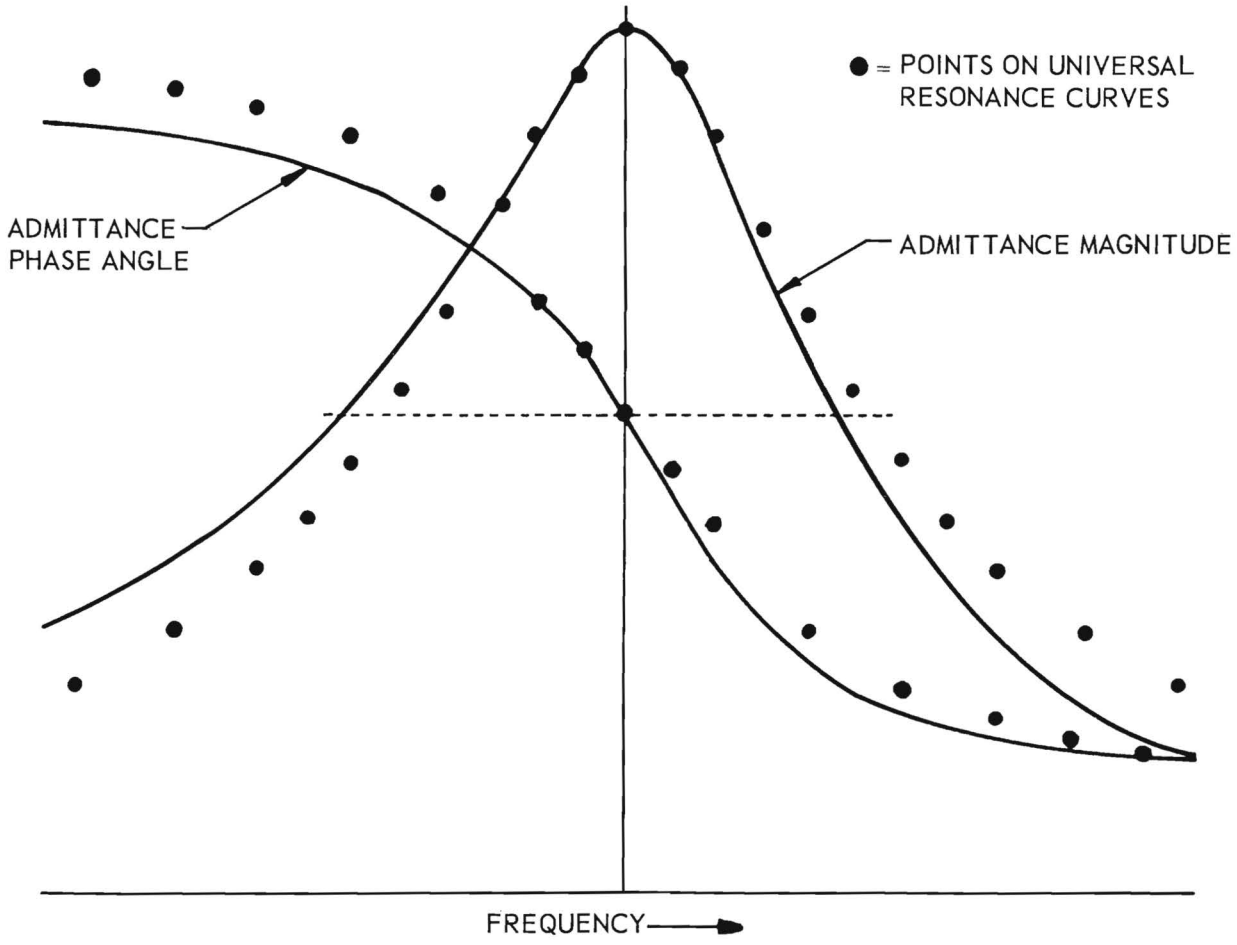

Figure 36. Admittance Characteristics of Crystal No. FA-116 with Hafner Holder Subtracted.

crystals were: C_o = 6.38 mmfd, L_L = 15 mμh, L_1 = 2.3 mh, C_1 = 2.7532993 X 10^{-16} farads and R_1 = 5.0 ohms. Values for R_L and R_o are shown in Table V. The admittance characteristic of this equivalent circuit was calculated by a digital computer over the frequency range including the motional arm resonance. The Hafner analysis was then performed with results as shown under Analysis A in Table V. The calculations were made by the same engineer who selected the theoretical values for the crystal, which may account for the very close agreement. The same data was then analyzed by two other individuals who had worked with the Hafner method but who had no knowledge of the nature of this particular data. The resulting element values are shown under Analyses B and C in Table V. A careful study of the construction sheets revealed that the errors indicated are due to misalignment and lack of symmetry of the Smith Charts. It was concluded that the Hafner method would generally give results with appreciable errors unless very large precision Smith Charts were employed. However, the errors were not sufficiently large to account for the results with Crystal No. FA-116 as noted above.

TABLE V

HAFNER HOLDER ANALYSIS OF THEORETICAL CRYSTALS

Condition	Theoretical Crystal No. 1		Theoretical Crystal No. 2	
	R_L (ohms)	R_o (ohms)	R_L (ohms)	R_o (ohms)
Original Value	1.5 ohms	6.7 ohms	8.2 ohms	0.0 ohms
Analysis A	1.5 ohms	6.6 ohms	8.1 ohms	0.0 ohms
Analysis B	1.5 ohms	6.4 ohms	8.75 ohms	0.0 ohms
Analysis C	2.0 ohms	5.95 ohms	9.5 ohms	-0.78 ohms

To further evaluate the characteristics of typical quartz crystal holders, the Crystal Measurements Standard data on a set of 21 crystals were extensively analyzed. Although the data analysis is not yet complete, certain conclusions

can already be stated.

The first step in the analysis was to examine the holder responses of the crystals to determine whether or not they could be represented with reasonable accuracy by a simple equivalent circuit. The data for crystals FA-67 and FA-106, as shown in Figures 29 and 30, were typical of most of the crystals. The circle approximations of the holders of these crystals are shown in Figure 37. It may again be observed that the centers of these circles do not fall on the zero susceptance axis. If the assumption is made that the displacement is due to a C_o' and the holder parameters are calculated for each holder, a theoretical circle may be obtained which agrees very closely with the original circle approximation. However, an examination of the frequency distribution around the circle shows a large disagreement, indicating that a sufficiently accurate equivalent circuit has not been found. This disagreement is illustrated by the small circles and crosses, which should fall at the same points on the holder circles of Figure 37. Since this result was typical of most of the crystals measured, the need for further studies of the holder characteristics was indicated.

One possible cause of the holder circuit disagreements was the subtraction of an incorrect line length. The electrical length between the crystal and Admittance Meter was known to be 9.69 cm; however, the effective length could be greater due to fringing at the crystal terminals. Thus, a series of 14 line lengths from 9.69 cm to 12.5 cm were subtracted from the original data for crystals FA-67 and FA-106. Equivalent holder circuit parameters including C_o' were then calculated at each line length. The theoretical circles were plotted against the measured circles with approximately the same frequency disagreements as shown in Figure 37.

Several other efforts were made to find a more precise equivalent circuit representation of the holder. All such efforts, however, gave the same order

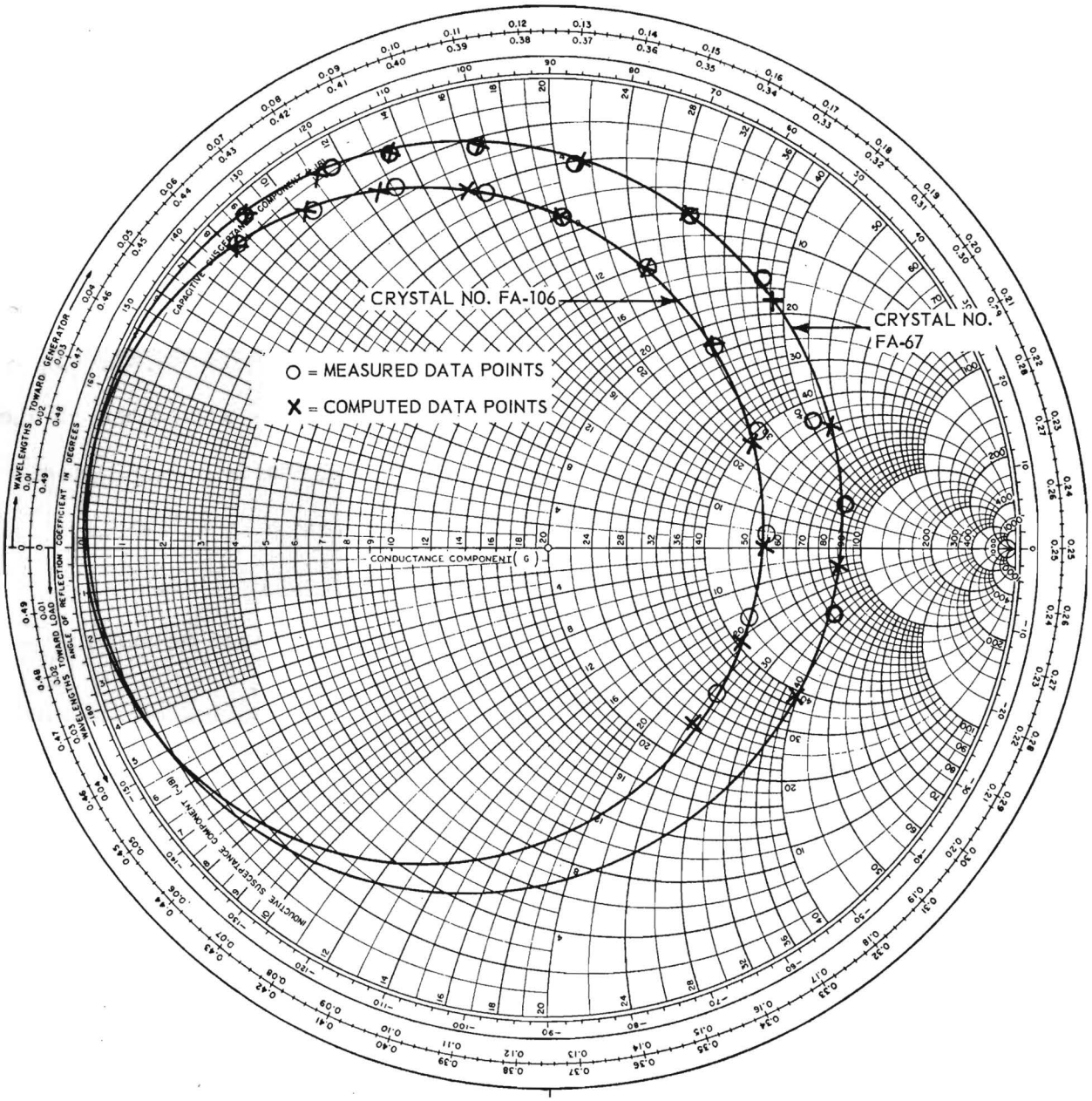

Figure 37. Circle Approximations of the Holders of Crystal Nos. FA-67 and FA-106.

of disagreements as has been illustrated. This either implies that no linear equivalent circuit exists (i.e., the element values are not constant) or that a suitable circuit must be considerably more complicated than has been supposed.

It should be noted that, when only the crystal holder response is of concern, the conventional holder and the Hafner holder become identical since $(R_o + R_L)$ for the Hafner holder should equal to R_L for the conventional holder. Thus the holder analysis discussed above is not dependent upon the type of analysis to be used on the crystal overtone response.

For the 21 crystals whose holders could not be accurately synthesized, it was decided to continue the conventional and Hafner analyses of crystal overtone responses, using the holder element values and line lengths which gave the least holder circle errors. Analyses were performed with results as indicated in Table VI and Table VII. Only two crystal responses, FA-67 at 150 mc/sec and FA-106 at 165 mc/sec, are represented in Table VI. Two line length subtractions were used for each of these crystals; (1) the standard length of 9.69 cm which required the use of a C_o' to correct the position of the holder circle and (2) a length which corrected the position of the holder with only a vernier adjustment using a C_o'. A line length could have been found which would require a zero value for C_o', however, this would have required an excessive amount of computer time with the particular programs which were used. It will be noted that the values of line length chosen require a negative value of C_o'. This, however, introduces very little error into the final results.

The conventional holder parameters were calculated as indicated under Run Nos. 5, 6, 12, and 13 in Table VI. The values of R_L under these runs should represent the total holder resistance as determined by the diameter of the holder circles. They should also represent the sums of R_o and R_L for the respective Hafner calculations if graphical errors can be completely avoided.

TABLE VI

SUMMARY OF CRYSTAL HOLDER CALCULATIONS BY VARIOUS METHODS

Run No.	C_o' (mmfd)	R_L (ohms)	L_L (mμhy)	C_o (mmfd)	R_o (ohms)	Line Length (cm)	Method
	CRYSTAL NO. FA-67				OVERTONE FREQUENCY 150 MC/SEC		
1	1.71	1.25	36.5	5.05	17.6	9.69	Hafner
2	----	10.0	23.2	7.00	-3.75	9.69	Hafner
3	----	10.5	27.2	5.55	1.0	12.1	Hafner
4	-0.06	5.75	32.6	5.01	8.25	12.1	Hafner
5	-0.06	11.5	32.6	5.01	0.0	12.1	Conventional
6	1.71	11.5	36.5	5.05	0.0	9.69	Conventional
	CRYSTAL NO. FA-106				OVERTONE FREQUENCY 165 MC/SEC		
7	0.97	16.25	33.1	6.31	0.47	9.69	Hafner
8	0.97	12.0	33.1	6.31	8.8	9.69	Hafner
9	----	13.25	26.4	7.3	3.15	9.69	Hafner
10	----	13.25	29.0	6.52	7.9	11.3	Hafner
11	-0.186	12.0	30.5	6.29	10.0	11.3	Hafner
12	-0.186	18.5	30.5	6.29	0.0	11.3	Conventional
13	0.97	18.5	33.08	6.31	0.0	9.69	Conventional

The remaining runs in Table VI were performed by the Hafner method. For Run Nos. 1, 4, 7, 8, and 11, the digital computer was used to calculate values of C_o and L_L. For Run Nos. 2, 3, 9, and 10, two points were chosen on the holder circle and holder parameters were chosen by the method described by Hafner, ignoring the possible presence of a C_o'. The division of R_o and R_L, as determined from the construction sheets, is tabulated for each run. It will be noted that the sum of R_o and R_L for each run generally disagrees appreciably with R_L for the respective conventional holder. In one case, a negative value of R_o was given by the Hafner calculations.

It was to be expected that the Hafner and conventional methods of analysis would yield appreciably different holder characteristics since the conventional method does not include the possible existance of an R_o, however, the Hafner method, under different conditions, failed to show reasonable agreement.

Table VII shows a summary of data obtained for several other crystal overtone responses, using the Hafner method of analysis.

TABLE VII

SUMMARY OF HAFNER HOLDER CALCULATIONS ON SEVERAL CRYSTAL RESPONSES

Crystal No.	Overtone Frequency mc/sec	Computer Calculated C_o' mmfd	C_o mmfd	L_L mμhy	R_T ohms	Hafner Calculations R_L ohms	R_o ohms
6	150	1.91	4.51	35.6	10.2	1.00	13.90
6	184	1.91	4.51	35.6	10.2	0.00	16.00
6	217	1.91	4.51	35.6	10.2	0.00	13.30
6	250	1.91	4.51	35.6	10.2	-8.75	21.85
MA-23	178	1.58	4.59	35.2	12.3	0.50	13.70
MA-23	210	1.58	4.59	35.2	12.3	**	**
MA-24	178	1.32	4.39	37.3	11.6	-26.50	37.90
MA-58	165	1.54	5.40	33.5	11.1	9.50	6.40
MA-71	198	1.54	5.51	31.6	11.6	2.08	11.93
MA-71	198	1.54	5.51	31.6	11.6	-13.75	35.10
FA-115	175	1.17	5.75	31.5	18.2	14.25	5.50
FA-115	175*	----	----	----	18.2	12.00	3.27
FA-115	245	1.17	5.75	31.5	18.2	11.25	7.00
FA-115	315	1.17	5.75	31.5	18.2	12.50	6.55

* C_o and L_L calculated by Hafner method using two points on holder circle.

** Crystal circle degenerated to a point at one stage in the analysis causing the method to fail completely.

The data of Tables VI and VII indicate that no reliable methods have yet been found for determining the holder parameters of high-frequency quartz crystals. Some of the disagreements in the tables can be attributed to graphical errors while others cannot. In an attempt to reduce the graphical errors, typical Smith Charts used by the project were carefully examined. It was found that the charts were appreciably distorted. Accordingly, new charts were prepared. The reproductive processes were carefully controlled to eliminate as much distortion as possible. It is probable that, if the above

data were rerun, closer agreement between holder parameters could be obtained.

The parameters of a crystal's motional arm are also of interest. As an example, the holder parameters described in Table VI were subtracted from the respective overtone responses for each run indicated. The resulting perfect circle approximations are shown in Figures 38 and 39. The numbers associated with the circles correspond to the Run Nos. of Table VI. The two sets of dots on the circles of the figures represent points of equal frequency for each set. Thus Figures 38 and 39 show the maximum variations in motional arm parameters that may be expected from different analyses procedures. For FA-67, the maximum variation in R_1 for the various methods was $\pm$ 10 percent. For FA-106, the maximum variation was $\pm$ 7.5 percent. Although the resonant frequency of the motional arm is dependent upon the method of analysis, the Q of the motional arm is affected very little, as indicated by the corresponding frequency points of the figures.

It may be observed that the two conventional holder substractions for each crystal resulted in essentially identical circles in Figures 38 and 39. Thus, the effects of a C_o' and a short line length error are almost indistinguishable.

From the above data, it may be concluded that, for determining the motional arm resistance and Q within $\pm$ 10 percent, the method of analysis and the division of holder resistance is relatively unimportant. For greater accuracy, neither the conventional nor the Hafner holder equivalent circuits are satisfactory for the particular crystals reported here.

C. Other Measurement Systems

1. Introduction

It was desirable that a practical crystal test instrument be developed such that the use of external auxiliary equipment would be minimized. Such

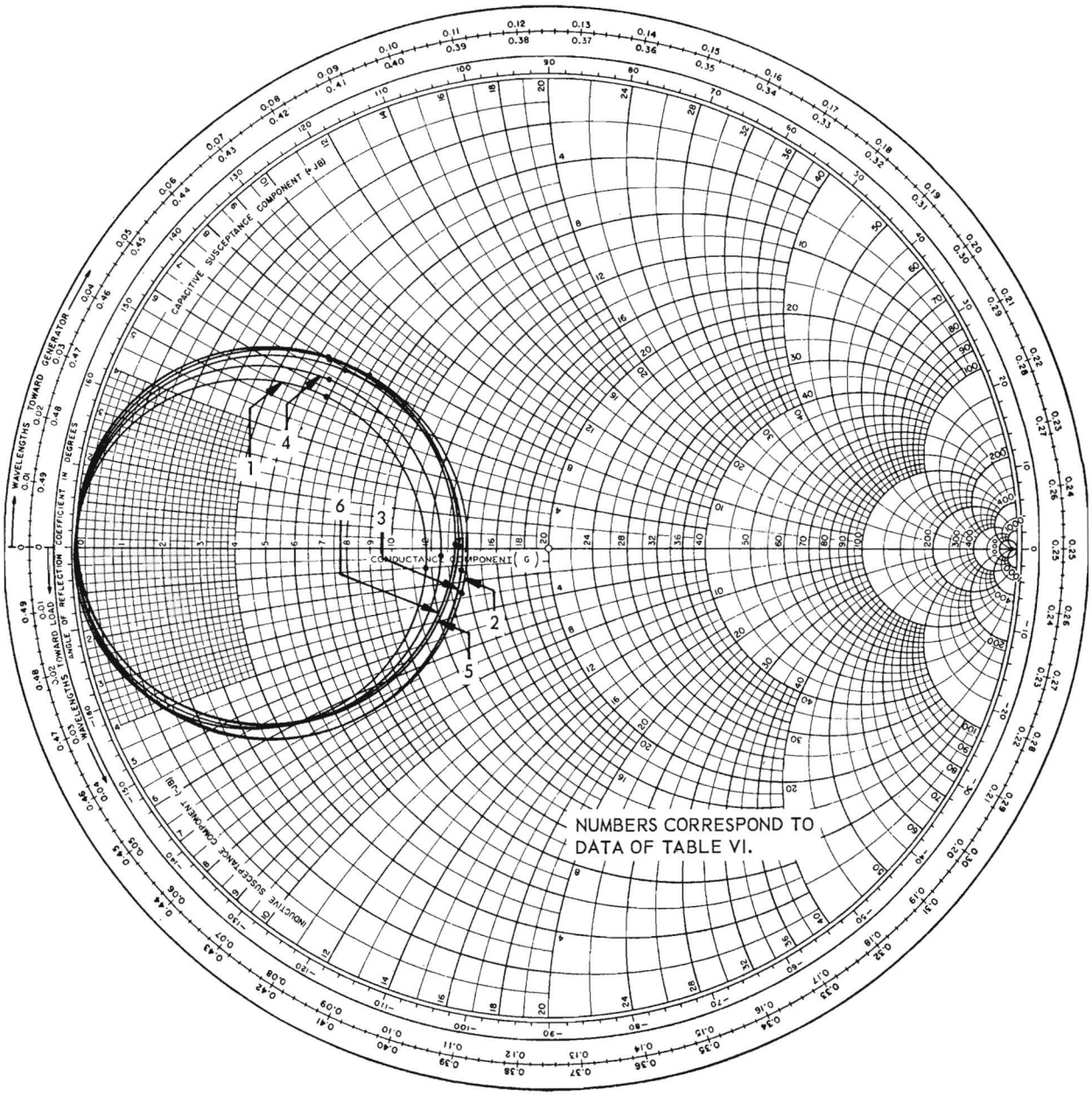

Figure 38. Motional Arm Circles for Crystal No. FA-67 As Obtained by Several Methods.

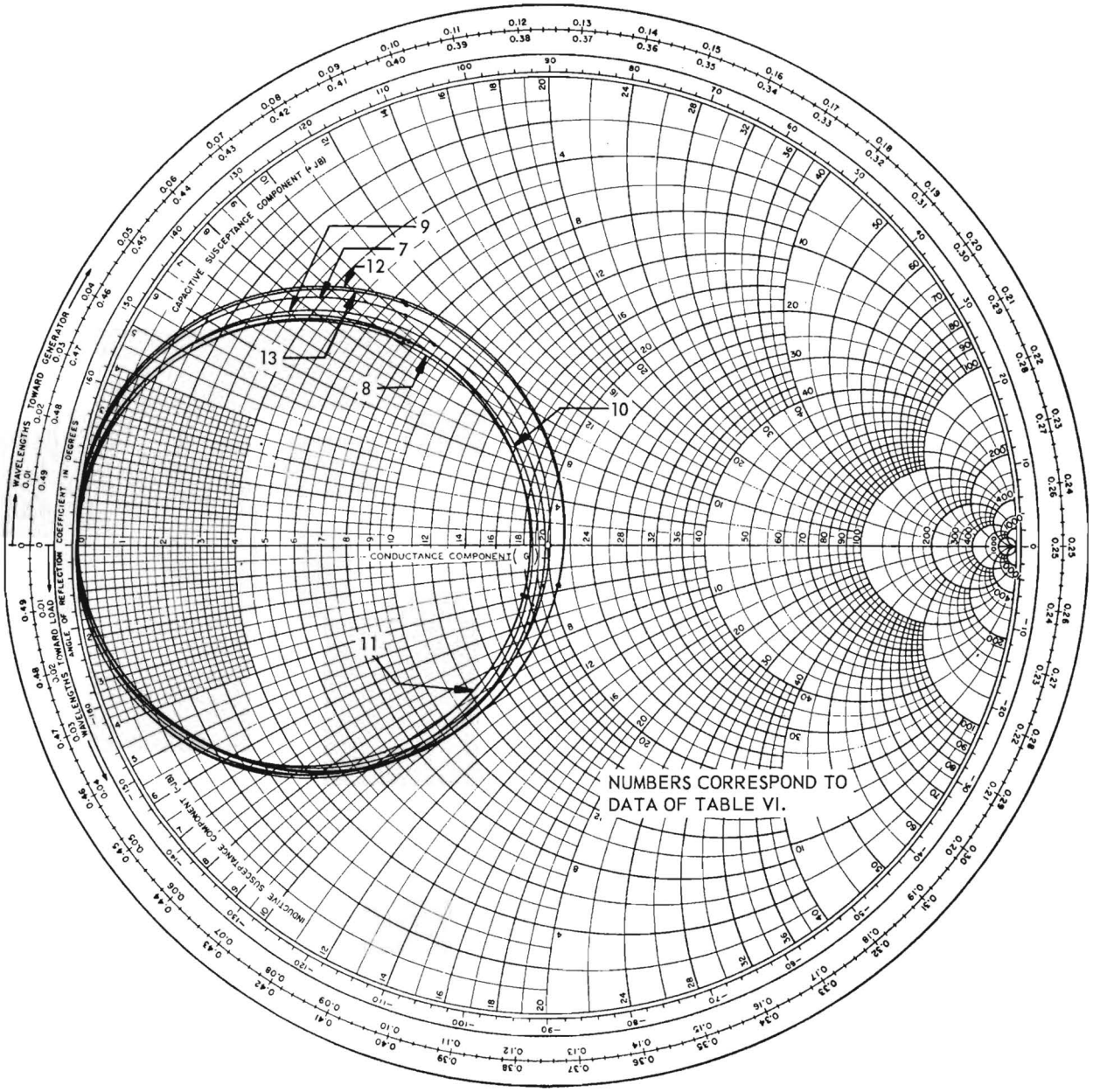

Figure 39. Motional Arm Circles for Crystal No. FA-106 As Obtained by Several Methods.

instruments as the various Crystal Impedance Meters satisfy this requirement at frequencies below about 175 mc/sec. It is evident that the Crystal Measurements Standard does not satisfy this requirement.

Other desirable properties of a practical crystal test instrument are that it (1) be easy to operate, (2) provide data in a form readily interpreted, (3) be readily portable, and (4) be self-calibrating or require only infrequent external calibrations.

The substitution method satisfies all of these requirements in theory. However, when attempts are made to apply substitution principles at frequencies above 200 mc/sec, many difficulties are encountered. In particular, practical circuit elements can no longer be represented as lumped elements. This effect produces additional sources of phase shift in oscillator circuits such that the phase stability of crystal controlled oscillators becomes very poor. Also, at higher frequencies most crystals do not display a zero-phase-shift resonance so that resistive substitution is meaningless.

The Crystal Parameter Bridge, which was developed on the preceeding contract (DA-36-039 SC-71191), is capable of providing reasonably accurate measurements at the higher frequencies provided it can be suitably excited. Two methods of excitation are possible: (1) excitation by a simple oscillator whose frequency is controlled by the bridge and crystal under test and (2) excitation by a highly stable, self-controlled oscillator. Several attempts have been made to design oscillators to be controlled by the crystal under test, but none have been successful because of the large degradation of crystal-Q by the bridge. The use of a highly stable, self-controlled oscillator violates the requirement of keeping the instrument simple. In addition, the adjustment procedure for the Crystal Parameter Bridge is not as convenient as might be desired.

For the above reasons, it appeared that a new and different approach to the crystal measurement problem was desirable. Such an approach was provided by Dr. Issac Koga in a series of lectures presented at the School of Electrical Engineering of the Georgia Institute of Technology during October and November 1957*.

2. The Koga Method

The method of quartz crystal measurements proposed by Dr. Koga is summarized as follows. In Figure 40, the series combination of C_A and C_S is made

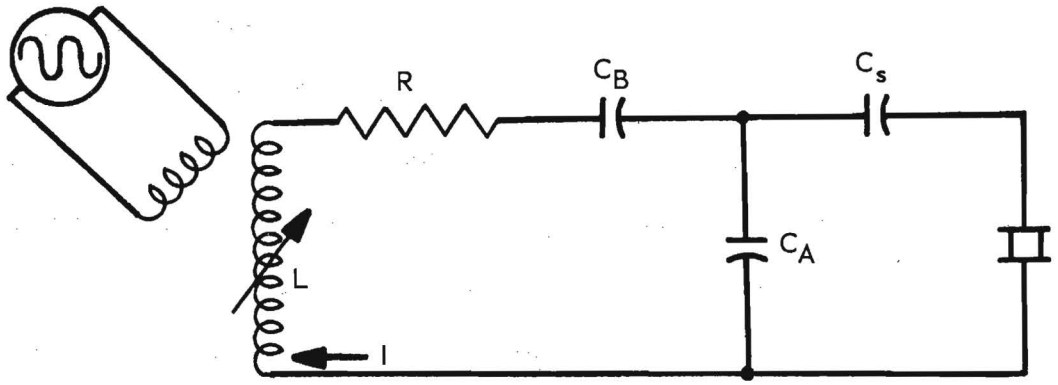

Figure 40. The Koga Method of Crystal Measurements.

equal to the desired load capacitance of the crystal. The capacitor C_B is made small compared to C_A. The circuit is excited by loosely coupling a variable frequency oscillator to the inductance as shown. The inductance, L, is tuned so that the electric circuit resonance occurs at the crystal resonant frequency. As the oscillator frequency is varied in the vicinity of crystal resonance, the current variation will be as indicated in Figure 41. Figure 42 shows an expanded scale portion of Figure 41. In Figure 42, the currents I_A and I_B are recorded.

---

*A limited number of copies of a paper entitled "Some Notes on Quartz Crystal Units" by Dr. Issac Koga are available by contacting Samuel N. Witt, Jr., Engineering Experiment Station, Georgia Institute of Technology, Atlanta, Ga.

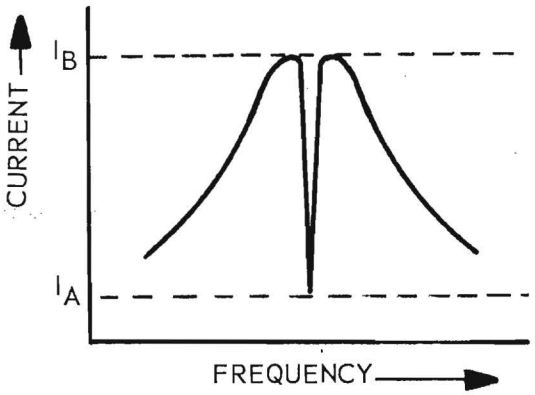

Figure 41. Current-vs-Frequency Response of Figure 40.

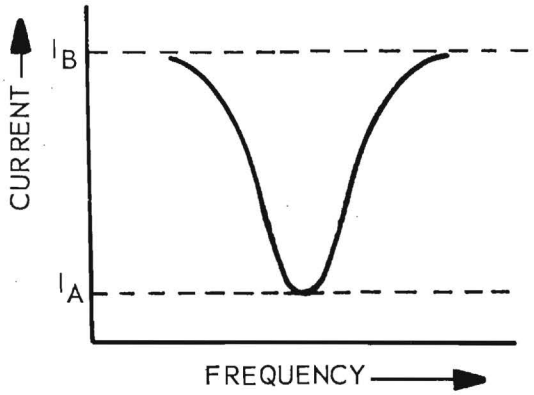

Figure 42. Scale Expansion of Figure 41.

The equivalent resistance, R_Q, of the crystal is then given approximately by

$$R_Q = K \frac{1}{I_B/I_A - 1} \tag{35}$$

where

$$K = \frac{1}{R} \left(\frac{1}{\omega C_A}\right)^2 . \tag{36}$$

It may be observed that only the ratio of I_B to I_A is required; however, absolute values of R and C_A are required. The frequency may, of course, be readily measured.

The necessity of measuring R and C_A may also be dispensed with by removing the crystal and C_S and substituting a resistor, W, which must be large enough so that $1/W^2$ can be neglected compared with $(\omega C_A)^2$. The phase angle of the resistor at the frequency of concern must be very nearly zero. If I_C is the maximum value of current with W connected and I_D is the maximum current with W

removed, then K of Equation (36) becomes

$$K = W\left(\frac{I_D}{I_C} - 1\right). \qquad (37)$$

Again, it is not necessary that the absolute values of current be measured since only the ratio appears in the equation.

The above procedure is applicable for practical crystal measurements only when the crystal can be accurately represented by the equivalent circuit of Figure 43.

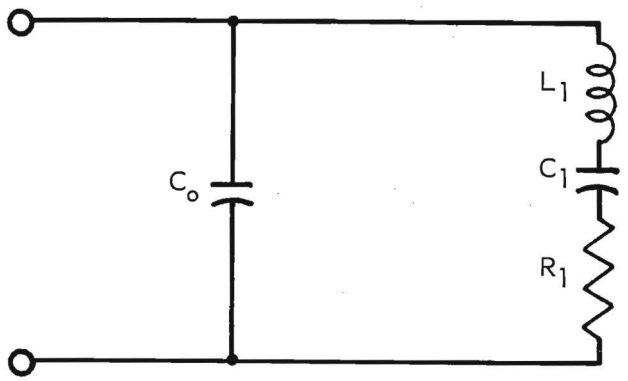

Figure 43. Low-Frequency Equivalent Circuit of a Quartz Crystal.

At high frequencies where holder inductance and resistance become appreciable, Equations (35), (36), and (37) must be appropriately modified. This, however, requires an exceedingly complicated mathematical procedure which has not yet been fully developed. It was concluded that sufficient personnel time was not available on the project to develop the necessary mathematics. However, the method was tested in the laboratory at a frequency of 175 mc/sec. The equivalent resistance of the crystal was not calculated because a suitable resistor, W, was not available. Alternate calculations of the Q of the crystal were made using mathematics provided by Dr. Koga. Values of Q ranging from

20,000 to 40,000 were obtained, compared to a value of 53,000 obtained from bridge measurements. The curve from which the Q was calculated is reproduced in Figure 44.

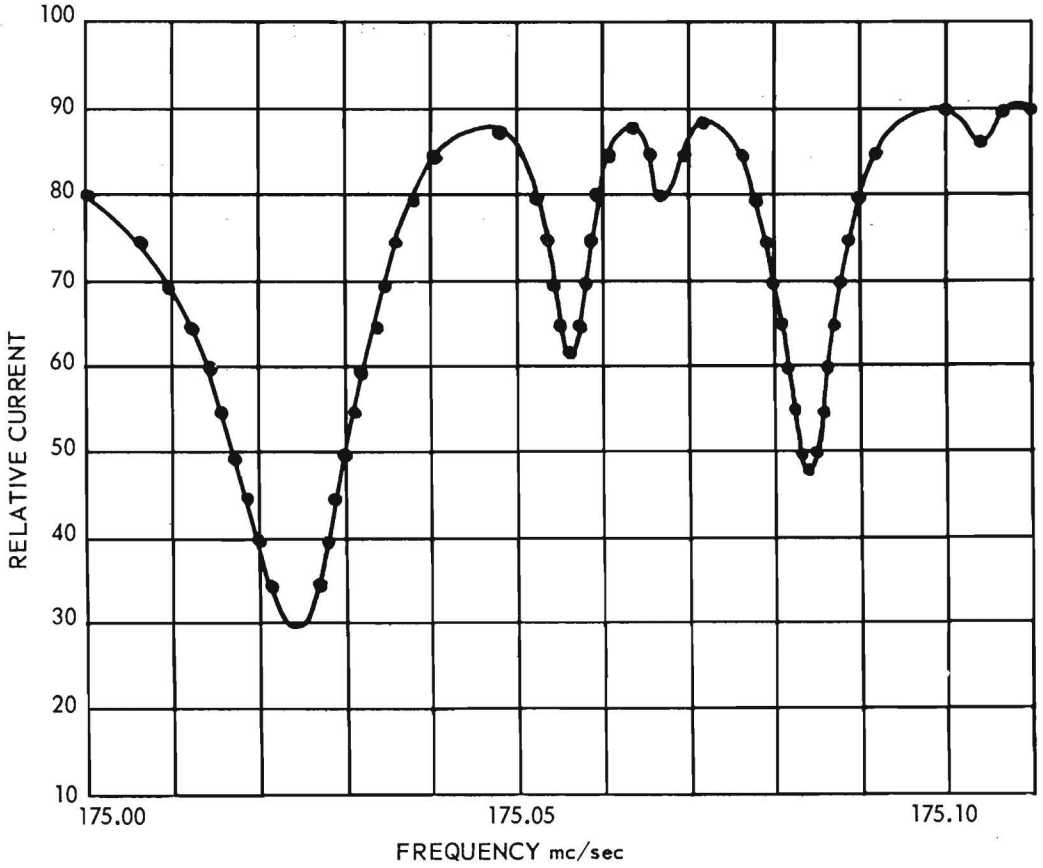

Figure 44. Current Variations for Crystal No. FA-116 in Circuit Similar to Figure 40.

Figure 44 reveals some interesting information concerning the crystal, for purposes other than parameter determination. For example, the frequencies and relative magnitudes of spurious responses are readily determined. It is also obvious that the spurious responses distort the main response in such a way that the Q is not constant. In particular, the value of Q changes rather suddenly at the point of minimum current. It is, of cource, necessary to take this into account when comparing the Q determination by this method with the determination from bridge measurements.

A mechanical-electric sweeping system was also constructed to vary the frequency of the source oscillator and provide a synchronized oscilloscope sweep voltage. An oscillogram obtained while using this system is shown in Figure 45. It should be noted that the ordinate in this figure is proportional to the square of the current, which accounts for differences in appearance between Figures 44 and 45. Additional differences occur due to excessive sweep speed (several cycles per second) used with the latter. This difficulty could be readily eliminated.

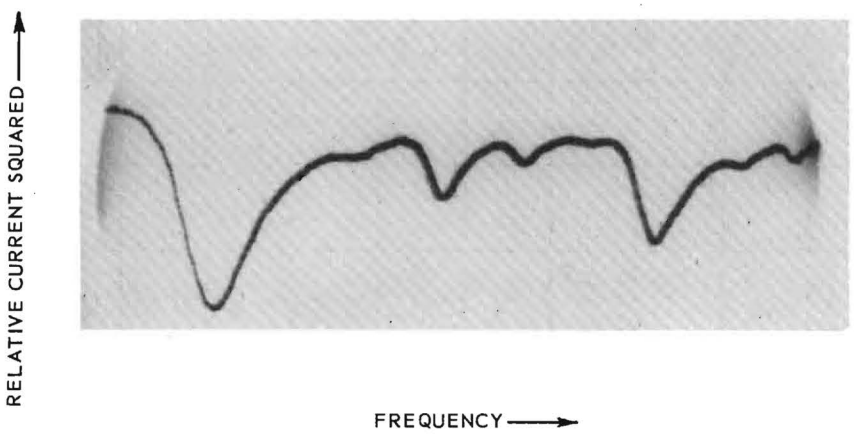

Figure 45. Photographic Record Corresponding to Figure 44.

3. The Equivalent Circuit Crystal Measurement Method

A crystal measurement system similar to the Koga method has been devised for use at higher frequencies. The mathematical derivation for this system is included in the appendix section of this report. A practical circuit arrangement for the application of this method is shown in Figure 46. The only instruments required are a reasonably stable signal generator and an instrument for measuring the r-f current. In the figure, the inductor, L_2, is used to resonate the circuit consisting of L_2, L_L, R_L, C_o and R_2 to the

crystal frequency. The resistor, R_2, is included in the circuit to facilitate the measurement of current by means of an r-f voltmeter. Resistor R_g is the unavoidable internal resistance of the signal generator; however, it serves the useful purpose of reducing the Q of the electric circuit resonance. The summarizing paragraphs of the appendix describe the method used to calculate the more important parameters of the crystal.

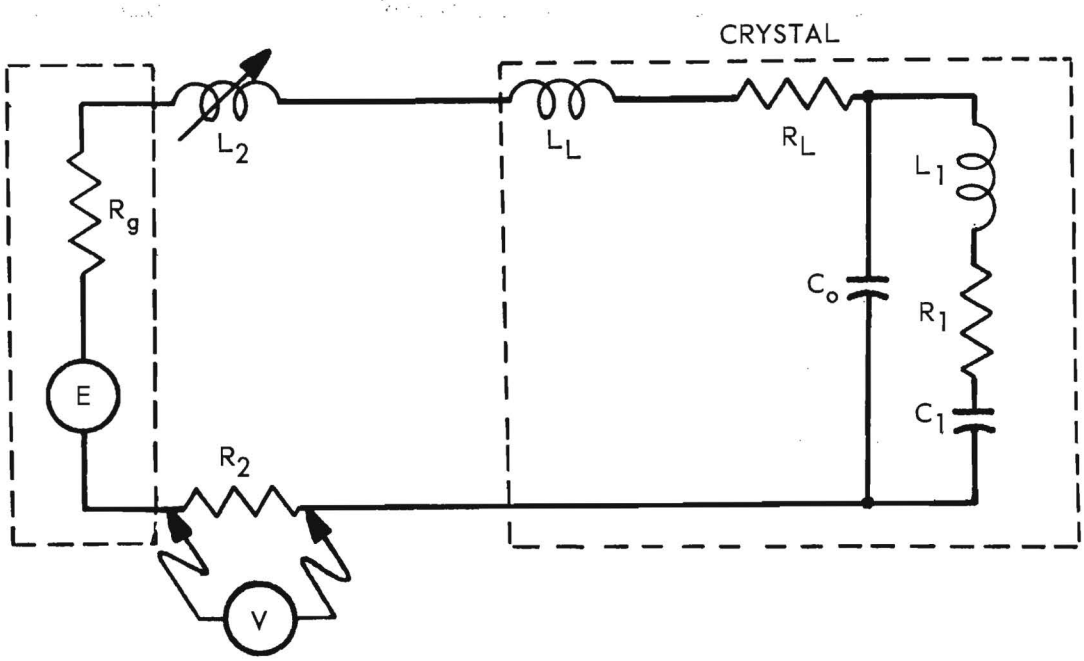

Figure 46. The Equivalent Circuit Crystal Measurement Method.

From laboratory considerations, a number of deficiencies of this method become apparent. These may be understood by considering the physical arrangement of the components of Figure 46, as shown in the sketch of Figure 47.

The sketch shows three crystal sockets and a type N coaxial connector with interconnections as indicated. The inductor, L_2, and resistor, R_2, are mounted on crystal bases which may be plugged into the sockets provided. The pins of the adjacent crystal sockets were directly soldered together in order

to eliminate as much lead length as possible. Three crystal mounts were used in the system, one for the actual crystal under test, one for the addition of a variable inductor or a variable capacitor, and one for the addition of a standard resistor. The electrical circuit was made to resonate at approximately the resonant frequency of the crystal by the adjustment of an added inductance or capacitance. The current flowing in the circuit was measured by placing a diode across the standard resistor and reading the d-c voltage output. The current was then a constant multiplier of the square root of the measured d-c voltage.

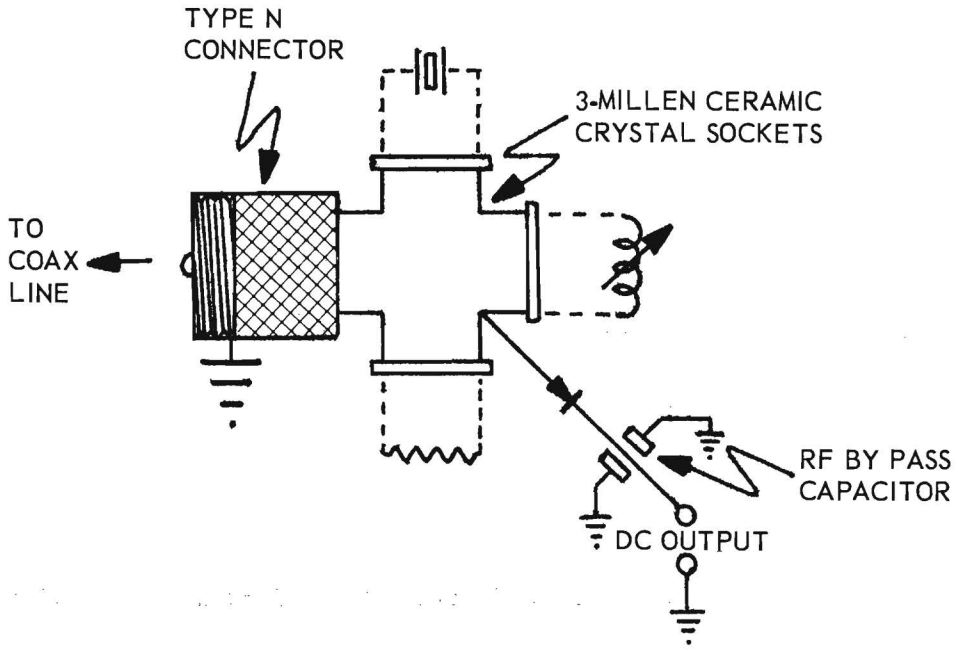

Figure 47. Component Mount for the Equivalent Circuit Crystal Measurement Method.

The use of a diode for voltage (and, therefore, current) measurement was selected to obtain sufficiently sensitive current measurements while at the same time not loading the circuit capacitively. This procedure, however, requires that the input-output characteristics of the diode be carefully determined. Accurate diode calibration has not yet been accomplished because

of the very low voltages and currents involved. Sample crystal curves have, however, been run, but satisfactory parameter calculations have not yet been possible because of the lack of current calibration. This deficiency of the system may be overcome by finding a calibrated means for measuring the current (or voltage) which does not upset the lumped parameter configuration of the circuit.

Crystal No. FA-116 was chosen for initial tests of the Equivalent Circuit Measurement Method since large amounts of previous data on this crystal were available for comparison of results. The first test was performed at 245 mc/sec. From the equations given in the APPENDIX, Q_o (Q_o is here defined as the Q of the crystal's motional arm) was calculated to be 36,000, R_1 to be 144 ohms, and f_o' to be 245.0442 mc/sec. From Progress Report No. 4 of Contract DA-36-039 SC-71191, pp 22-25, Q_o was given as 36,000, R_1 as 103 ohms, and f_o' as 245.0460 mc/sec for the same crystal. Similar tests were performed on this crystal at 175 mc/sec yielding Q_o = 34,000 and R_1 = 66 ohms. Calculations from Admittance Meter data at 175 mc/sec gave Q_o = 53,000 and R_1 = 33 ohms.

It can be seen from the above data that very close agreement was achieved at 245 mc/sec while very poor agreement was obtained at 175 mc/sec.

Errors in the Equivalent Circuit Measurement Method can arise from many sources. Three main sources of errors are:

(1) use of resistive elements having reactive components,

(2) presence of distributed parameters in the circuit, and

(3) failure to keep the source voltage constant.

The results at 245 mc/sec indicate that the equivalent circuit method can provide fairly close agreement with Admittance Meter measurements if the errors can be sufficiently reduced.

To further evaluate the source of the large errors at 175 mc/sec, the electrical resonance data were plotted over the frequency range from 120 to 240 mc/sec as shown in Figure 48 (original circuit). It can be seen that the graph given does not resemble a series resonant circuit response. The data indicated that a more nearly constant voltage source was needed, thus the circuit was modified as shown in Figure 49. The 47-ohm series resistor and the 5-ohm shunt resistor were used to terminate the coaxial line from the Marconi Signal Generator in approximately 50 ohms, over a wide range of frequencies. Then, by adjusting the carrier signal input to the coaxial line by use of the signal level meter on the signal generator, the signal applied to the actual crystal circuit was held constant. The crystal was again tested at 175 mc/sec and the electrical resonance data shown in Figure 48 (modified circuit) were obtained. The Q of the electrical circuit was calculated from the half-power points. The universal resonance curve for a series resonant circuit with the same Q is also plotted on Figure 48 (circles). The similarity in shape of the two curves indicated that the circuit was functioning as predicted by mathematics. The calculated Q of the crystal then agreed more closely with that calculated by other methods.

Recent measurements made by the Crystal Measurements Standard have indicated that the equivalent circuit of a VHF quartz crystal, shown in Figure 46, does not adequately represent the crystal admittance characteristics. It has not yet been possible to develop a more accurate equivalent circuit representation. It is thus probable that the equations for the Equivalent Circuit Crystal Measurement Method are not sufficiently accurate for describing the crystal characteristics. Further work with this method was therefore delayed until the recently begun investigations of the equivalent circuits are completed.

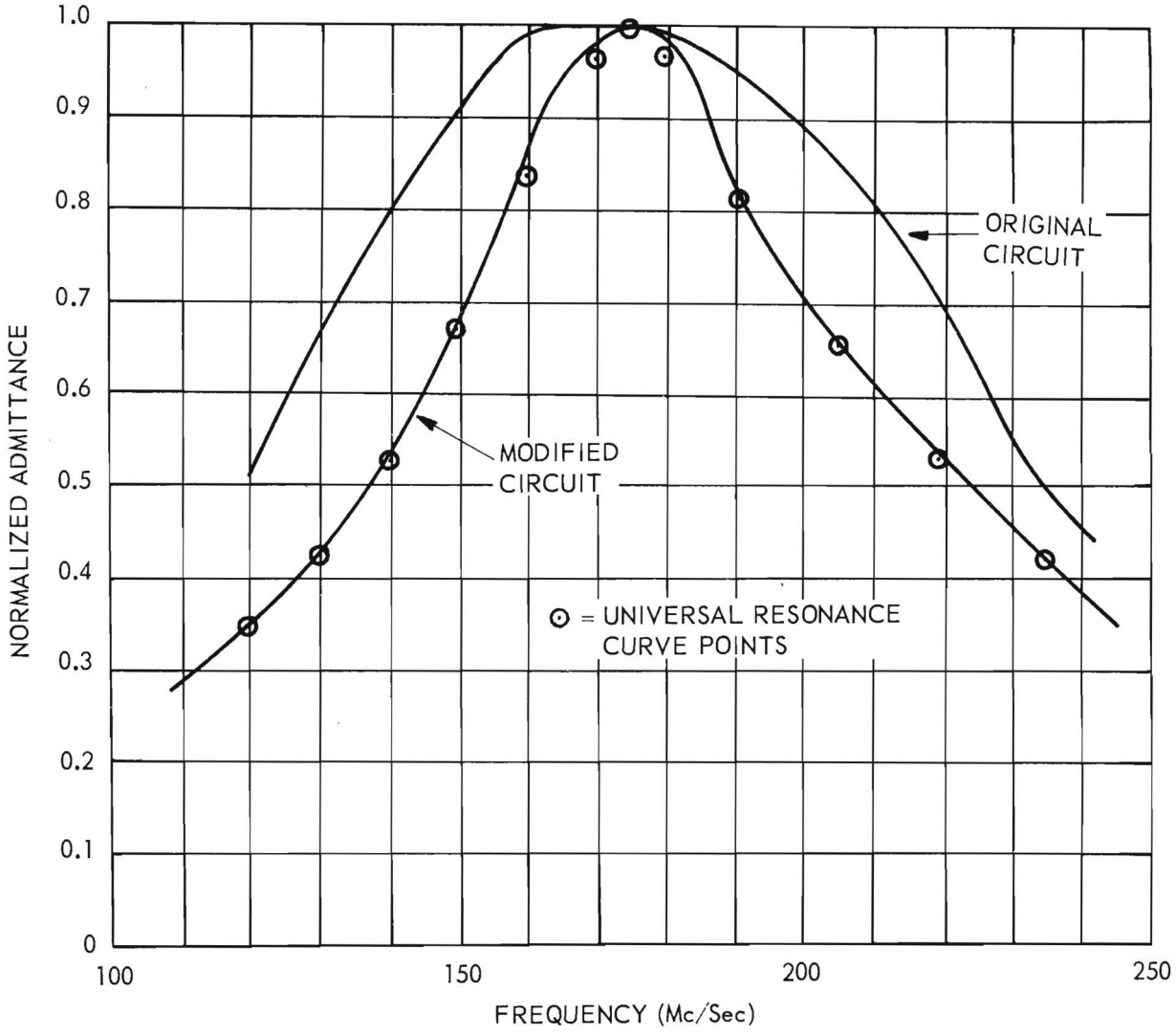

Figure 48. Electrical Resonance Characteristics of the Equivalent Circuit Crystal Measurement System.

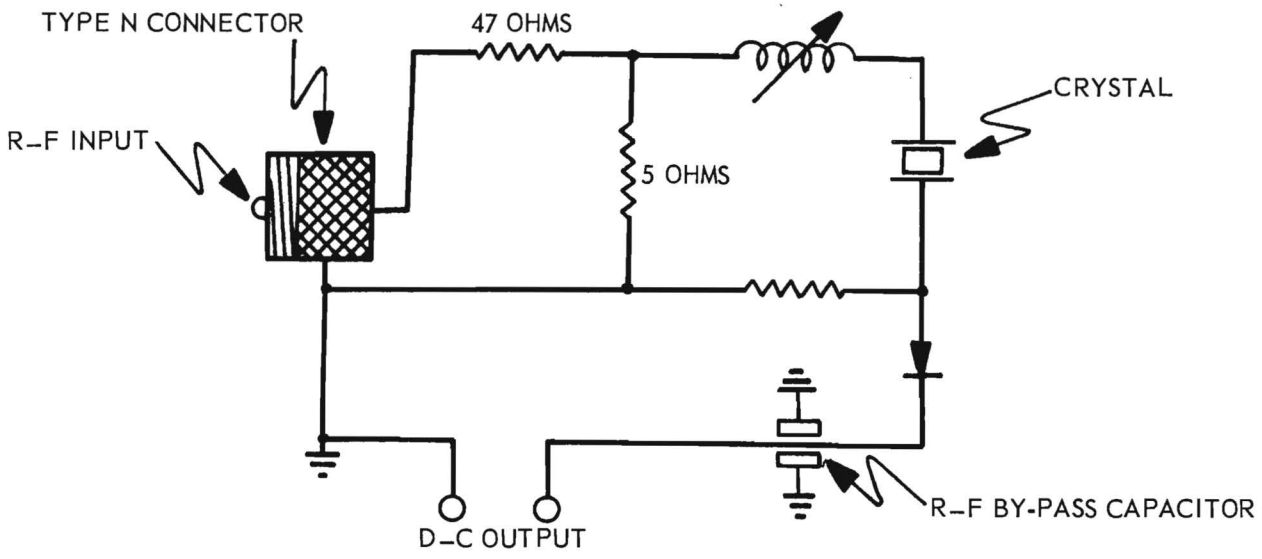

Figure 49. Modified Component Mount for the Equivalent Circuit Crystal Measurement Method.

V. CONCLUSIONS AND RECOMMENDATIONS

The development of the Crystal Measurements System has been essentially completed. The problems concerning signal stability, frequency measurement and null detection have been satisfactorily solved, for the frequency range from 150 to 450 mc/sec. In some instances, adequate drive level and isolation cannot be obtained at frequencies above 300 mc/sec. The calibration of the General Radio Admittance Meter has not been fully evaluated, independently of the factory claims. It is presently believed, however, that disagreements in attempting to verify the calibration have resulted primarily from losses in the transmission lines used.

A system for measuring crystal drive level has been developed and calibrated to provide the required accuracy; however, the system required the insertion of a dual directional coupler between the Admittance Meter and the crystal component mount. The directional coupler greatly reduces the accuracy of the admittance measurements. No method of analytically compensating for the errors has been found. It is possible, however, to calibrate the Admittance Meter with the directional coupler in use. Equipment to perform this calibration was not available to the project, but is available at the National Bureau of Standards Laboratories in Boulder, Colorado.

A representative number of VHF crystal measurement runs have been made using the Crystal Measurements Standard System. Analyses of the resulting data have indicated that the conventionally accepted equivalent circuit of a VHF quartz crystal does not describe the crystal admittance characteristics satisfactorily. The analyses are not yet complete and have not yet indicated a more satisfactory equivalent circuit.

Several other methods for determining the parameters of VHF quartz crystals have been investigated. One such method, the Equivalent Circuit Crystal Measurement Method, gave reasonably accurate parameter values in some cases while

failing to do so in other cases. Further evaluation of this method was discontinued when the disagreements concerning the conventional crystal equivalent circuit were found. The method still shows promise of providing accurate data if a satisfactory equivalent circuit for typical crystals can be developed.

Various phases of the investigative work of the project have indicated the need for an urgent decision as to which parameters of a VHF crystal are the most important from the standpoint of crystal applications. Such a decision is necessary before simplified Crystal Impedance Meter type of instruments can be developed.

A consideration of the accomplishments of the project has indicated the need for further investigative and developmental work in the following areas:

1. the investigation of the equivalent circuits of VHF quartz crystals should be continued,
2. a study of typical quartz crystal oscillators for use at frequencies above 150 mc/sec should be made to determine which parameters of the crystals are important to the designer,
3. an admittance calibration of the Crystal Measurements Standard, with the Power Measurement System attached, should be accomplished, and
4. further effort should be applied to the development of a Crystal Impedance Meter type of measurement instrument.

VIII. IDENTIFICATION OF KEY TECHNICAL PERSONNEL

The personnel who have contributed to this project are as follows:

James E. Lane	Technical Assistant	525 Hours
Samuel N. Witt, Jr.	Project Director Research Engineer	830 Hours
Vance K. Woodcox	Research Assistant	1720 Hours

The background and qualifications of these men are presented in the following paragraphs.

Mr. James E. Lane, Technical Assistant, was employed by this project for part-time work on 1 January 1958. Mr. Lane has previously been associated with the Station as a technician on various other projects including the forerunner of this project. He has had 4 years' experience in military electronic maintenance and was recently in the employment of Radiation, Inc., Melbourne, Florida for a period of 9 months. Mr. Lane received his Bachelor's Degree in Industrial Management at Georgia Tech and is currently pursuing studies toward the Bachelor's Degree in Physics at Georgia Tech.

Mr. Samuel N. Witt, Jr., Project Director and Research Engineer, was employed half-time by the project at its initiation. Mr. Witt, who holds the degree of Master of Science in Electrical Engineering from Georgia Tech, is currently pursuing studies toward a Doctor of Philosophy degree in that field. Mr. Witt has been with the station more than 7 years on various electronic research and developmental projects which have included work in the fields of transistors, oscillators, radar circuitry and communication circuitry. He was employed half-time on the forerunner of this project. He has also served one year as an electronics instructor in the U. S. Navy and one year as electrical engineering instructor at Tennessee Polytechnic Institute and is currently serving half-time as Lecturer in the School of Electrical Engineering at Georgia

Tech. He is a licensed Professional Engineer in the state of Georgia, a member of Eta Kappa Nu, Sigma Xi, Kappa Mu Epsilon and IRE.

Mr. Vance K. Woodcox, Research Assistant, was employed full-time by this project at its initiation. Mr. Woodcox completed work toward his Bachelor's Degree in Electrical Communications with highest honors at Georgia Tech and is currently pursuing studies toward a Master's Degree in the same field. He has had various experience in electronic parts and servicing. He is a member of Phi Eta Sigma, Eta Kappa Nu, Tau Beta Pi and Phi Kappa Phi.

Respectfully submitted:

Samuel N. Witt, Jr.
Project Director

Approved:

J. E. Boyd, Director
Engineering Experiment Station

VIII. APPENDIX

The equivalent electrical parameters of a quartz crystal can be represented to a fair approximation by the circuit of Figure 50. The elements L_1, C_1 and R_1 represent the motional arm. The holder is represented by L_L, R_L and C_o. Typical element values for a crystal at an overtone response of 250 mc/sec are:

$L_1 = 2.23 \cdot 10^{-3}$ hy $\qquad L_L = 3.0 \cdot 10^{-8}$ hy

$C_1 = 1.82 \cdot 10^{-16}$ fd $\qquad C_o = 5.0 \cdot 10^{-12}$ fd

$R_1 = 100$ ohms $\qquad R_L = 15$ ohms

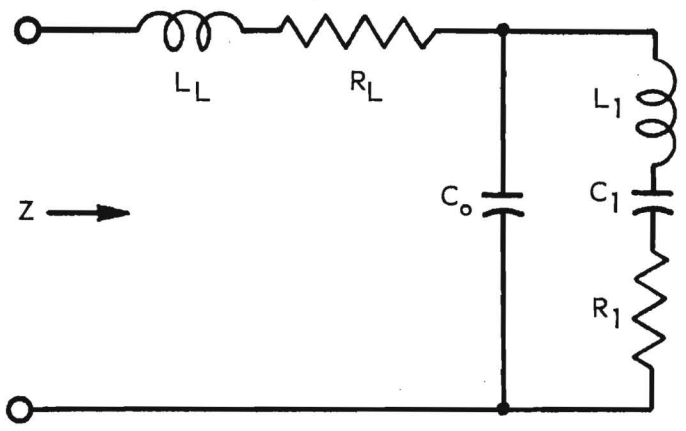

Figure 50. The Equivalent Circuit of a VHF Quartz Crystal.

The impedance, Z, of the crystal as a function of frequency, ω, can be written as

$$Z = j\omega L_L + R_L + \frac{1}{j\omega C_o} + \left(\frac{1}{\omega C_o}\right)^2 \left(\frac{1}{R_1 + j\omega L_1 + \frac{1}{j\omega C_1} + \frac{1}{j\omega C_o}}\right). \qquad (38)$$

Let ω_o be defined as a frequency for which

$$j\omega_o L_L + \frac{1}{j\omega_o C_o} = j\omega_o L_1 + \frac{1}{j\omega_o C_1} + \frac{1}{j\omega_o C_o} = 0. \qquad (39)$$

To satisfy this condition it is generally necessary that the value of L_L be increased by the addition of an external inductance.

For $\omega = \omega_o$, the impedance of the crystal becomes

$$Z = R_L + \left(\frac{1}{\omega_o C_o}\right)^2 \frac{1}{R_1} \tag{40}$$

and for ω near ω_o the impedance may be approximated as

$$Z \approx R_L + \left(\frac{1}{\omega_o C_o}\right)^2 \left(\frac{1}{R_1 + j\omega L_1 + \frac{1}{j\omega C_1} + \frac{1}{j\omega C_o}}\right) \tag{41}$$

where it is assumed that

$$\frac{\omega L_L}{R_L} \ll \frac{\omega L_1}{R_1} \quad .$$

Let $X = \omega L_1 - \frac{1}{\omega C_1}$ and $K_1 = \frac{1}{\omega_o C_o} \approx \frac{1}{\omega C_o}$ for $\omega \approx \omega_o$. Equation (41) becomes

$$Z \approx R_L + \left(\frac{1}{\omega_o C_o}\right)^2 \frac{R_1 - j(X - K_1)}{R_1^2 + (X - K_1)^2} \quad . \tag{42}$$

If K_2 is defined as $R_1 K_1^2 + R_L R_1^2$, Equation (42) becomes

$$Z \approx \frac{K_2 + R_L(X - K_1)^2 - jK_1^2(X - K_1)}{R_1^2 + (X - K_1)^2}$$

or

$$|Z|^2 \approx \frac{[K_2 + R_L(X - K_1)^2]^2 + K_1^4 (X - K_1)^2}{[R_1^2 + (X - K_1)^2]^2} \quad . \tag{43}$$

Current maximums and minimums occur when

$$\frac{d|Z|^2}{d\omega} = \left\{[K_2 + L_L(X - K_1)^2]^2 + K_1^4(X - K_1)^2\right\} (-2)[R_1^2 + (X - K_1)^2]^{-3}(2) \cdot$$

$$(X - K_1) + [R_1^2 + (X - K_1)^2]^{-2} \cdot \left\{2[K_2 + R_L(X - K_1)^2]\, R_L(2)(X - K_1)\right.$$

$$\left. + K_1^4(2)(X - K_1)\right\} = 0. \qquad (44)$$

One factor of this expression is $(X - K_1) = 0$ giving a solution $X = K_1$ as a maximum value of $|Z|^2$ and therefore of $|Z|$. However, this defines the frequency ω_o. Therefore, the impedance at this maximum becomes

$$Z = R_L + \left(\frac{1}{\omega_o C_o}\right)^2 \frac{1}{R_1} = R_L(\omega_o L_L)^2/R_1 \qquad (45)$$

without any approximations. Since $Z = |Z|$ at $\omega = \omega_o$, R_1 may be determined by determining a ratio of voltage to current magnitudes providing R_L, ω_o and L_L can be determined.

Figure 51 shows a sketch of the variations of $|I| = |E|/|Z|$ as a function of frequency. The frequency, ω_o, may be readily identified and determined as the point of minimum current.

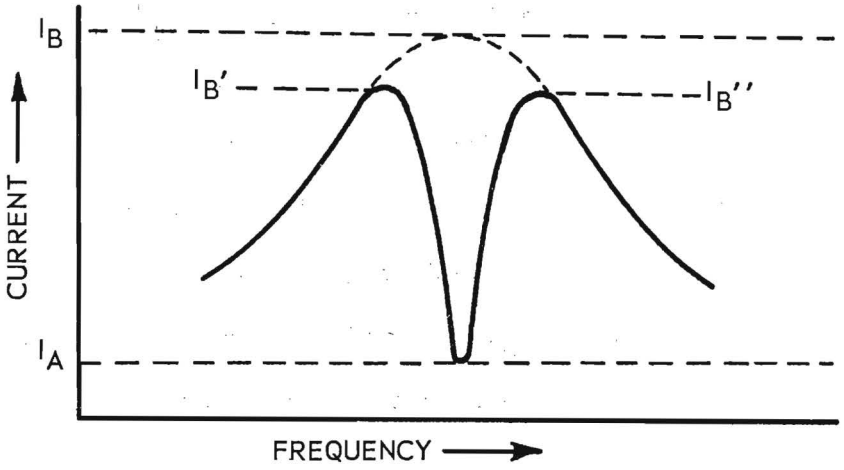

Figure 51. High-Frequency Crystal Current Variations.

If the motional arm, (R_1, L_1 and C_1), of the crystal could be removed, the impedance of the holder would be

$$Z_H = R_L + j\omega L_L + \frac{1}{j\omega C_o} \quad . \tag{46}$$

At $\omega = \omega_o$, the impedance would become

$$Z_H = |Z_H| = R_L = |E| / |I_B| \quad . \tag{47}$$

If $Z = |Z|$ of Equation (45) is replaced by E/I_A, where I_A is the minimum current as shown in Figure 51, and if the result is divided by Equation (47), then

$$\frac{I_B}{I_A} = 1 + \frac{1}{R_L} \left(\frac{1}{\omega_o C_o}\right)^2 \frac{1}{R_1} \quad . \tag{48}$$

If the motional arm can be de-energized, as supposed in arriving at Equation (46), and if R_L and C_o can be determined by some other means, it is then not even necessary to provide absolute voltage and current calibrations. For example, the voltage may be held constant for all measurements and only the relative current measured. Referring again to Figure 51, it may be seen that if I_B can be shown to be approximately equal to I_B' or I_B'' it is then not even necessary to remove the motional arm. (The difference between I_B, I_B', and I_B'' is exaggerated in the figure for convenience in defining the terms.)

The two current maximums may be found by obtaining the magnitude of Z in Equation (38), differentiating this with respect to ω, and setting the result equal to zero. The approximation of Equation (40) can no longer be used since ω is not now sufficiently close to ω_o. The mathematics involved in the proposed differentiation process become very difficult, thus other approximations will be required.

Consider the admittance plot of Figure 52, where $Y = \frac{1}{Z}$ of Equation (38) and the parameters are such that Equation (39) is satisfied. The insert is

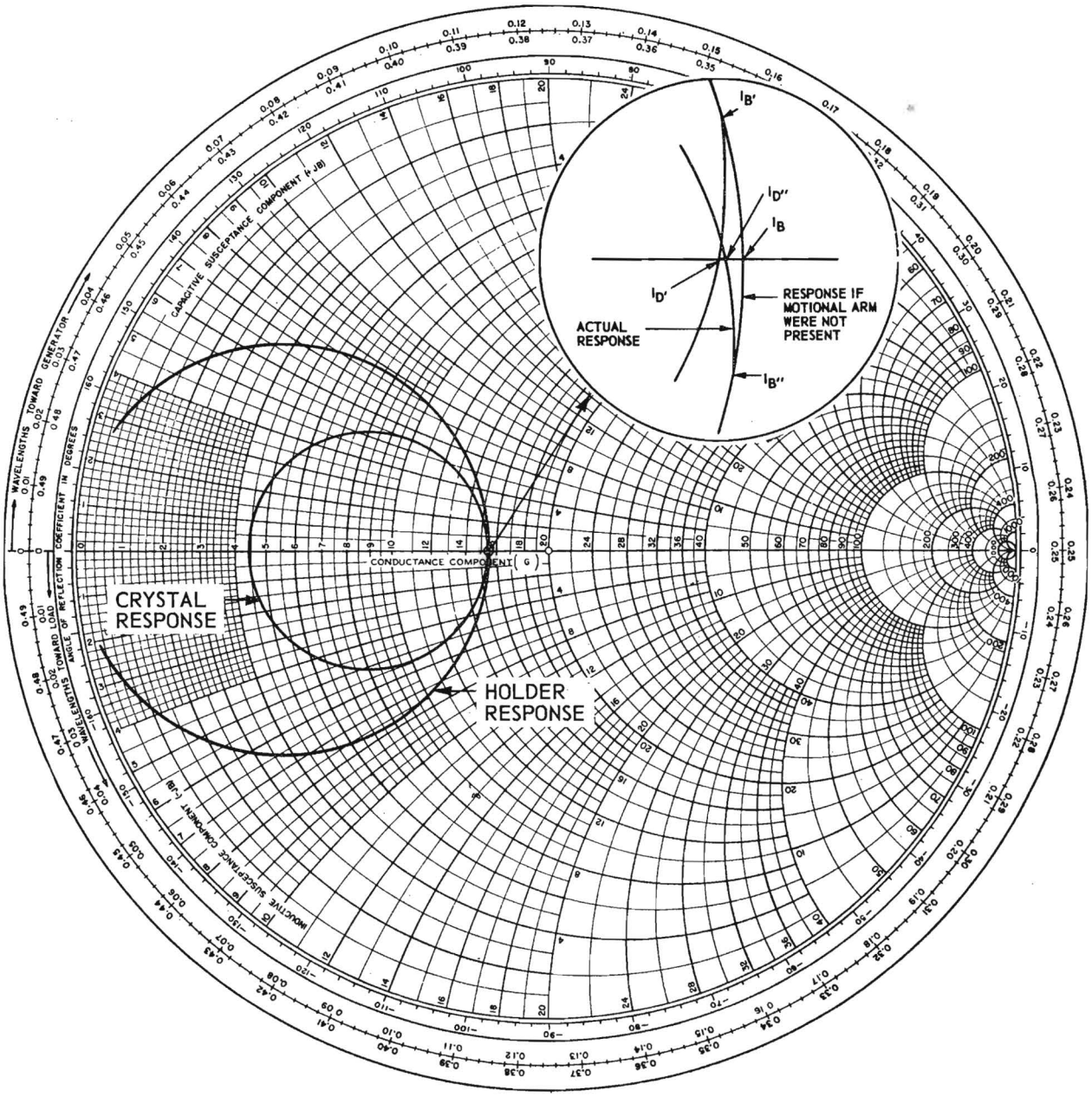

Figure 52. Admittance Diagram of a High-Frequency Crystal.

exaggerated so that the various points may be readily identified. It may be seen that $|Y_B'|$ and $|Y_B''|$ are always less than $|Y_B|$. Also, $|Y_D'|$ and $|Y_D''|$ are always less than $|Y_B'|$ and $|Y_B''|$. Thus if $|Y_D'|$ and $|Y_D''|$ can be shown to be sufficiently close to $|Y_B|$ then $|Y_B'|$ and $|Y_B''|$ will be sufficiently close for use as an approximation to $|Y_B|$. But $|Y_D'|$ and $|Y_D''|$ occur when the susceptance of the circuit is zero, which is the same as saying that the reactance of the circuit is zero. Thus, it is sufficient to set the imaginary part of Z equal to zero. Therefore,

$$\omega L_L - \frac{1}{\omega C_o} - \left(\frac{1}{\omega C_o}\right)^2 \frac{\omega L_1 - \frac{1}{\omega C_1} - \frac{1}{\omega C_o}}{R_1^2 + \left(\omega L_1 - \frac{1}{\omega C_1} - \frac{1}{\omega C_o}\right)^2} = 0. \tag{49}$$

Rearranging,

$$\omega^2 = \frac{1}{L_L C_o}\left(\frac{\omega L_1 - \frac{1}{\omega C_1}}{\omega L_1 - \frac{1}{\omega C_1} - \frac{1}{\omega C_o}}\right)$$

$$= \frac{1}{L_L C_o}\left[\frac{\omega^2 - (\omega_o')^2}{\omega^2 - \omega_o^2}\right] \tag{50}$$

where

$$(\omega_o')^2 = \frac{1}{L_1 C_1} \qquad \text{and} \qquad \omega_o^2 = \frac{1}{L_1}\left(\frac{1}{C_1} + \frac{1}{C_o}\right) = \frac{1}{L_L C_o}$$

and under the assumption that

$$R_1^2 \ll \left(\omega L_1 - \frac{1}{\omega C_1} - \frac{1}{\omega C_o}\right)^2 . \tag{51}$$

Factoring,

$$\omega^2 = \omega_o^2 \frac{(\omega - \omega_o')(\omega + \omega_o')}{(\omega - \omega_o)(\omega + \omega_o)} . \tag{52}$$

Since

$$\left.\begin{aligned} &\frac{\omega + \omega_o'}{\omega + \omega_o} \approx 1, \\ &\omega^2 = \omega_o^2 \frac{\omega - \omega_o'}{\omega - \omega_o} \end{aligned}\right\} \tag{53}$$

or

$$\omega = \omega_o \sqrt{\frac{\omega - \omega_o'}{\omega - \omega_o}} = \omega_o \sqrt{1 + \frac{\omega_o - \omega_o'}{\omega - \omega_o}} \quad .$$

Since $\omega_o - \omega_o' \ll \omega - \omega_o$, Equation (53) may be approximated as

$$\omega \approx \omega_o + 2\omega_o \left(\frac{\omega_o - \omega_o'}{\omega - \omega_o}\right) \quad . \tag{54}$$

Let $\omega = \omega_o + \Delta\omega$. Then Equation (54) becomes

$$\omega_o + \Delta\omega = \omega_o + 2\omega_o \left(\frac{\omega_o - \omega_o'}{\omega_o + \Delta\omega - \omega_o}\right)$$

or

$$\Delta\omega = 2\omega_o \left(\frac{\omega_o - \omega_o'}{\Delta\omega}\right) \tag{55}$$

giving

$$\Delta\omega^2 = 2\omega_o (\omega_o - \omega_o') \quad . \tag{56}$$

Therefore,

$$\Delta\omega = \pm\sqrt{2\omega_o(\omega_o - \omega_o')} \tag{57}$$

and

$$\omega \approx \omega_o \pm\sqrt{2\omega_o(\omega_o - \omega_o')} \quad . \tag{58}$$

It must now be shown that $Z \approx R_L$ at the frequency specified by Equation (58). This may be accomplished by considering separately the real and imaginary parts of Z.

The real part of Z becomes

$$\mathrm{Re}(Z) = R_L + \left(\frac{1}{\omega C_o}\right)^2 \frac{1}{R_1}\left[\frac{1}{1 + \frac{\left(\omega L_1 - \frac{1}{\omega C_1} - \frac{1}{\omega C_o}\right)^2}{R_1^2}}\right] . \qquad (59)$$

It is only necessary to show that the second term is negligible. In the braketed term, let

$$\omega L_1 - \frac{1}{\omega C_1} - \frac{1}{\omega C_o} = X_o = \frac{L_1}{\omega}(\omega^2 - \omega_o^2) \qquad (60)$$

and substitute

$$\omega^2 = (\omega_o + \Delta\omega)^2 \approx \omega_o^2 + 2\Delta\omega\omega_o$$

$$= \omega_o^2 \pm 2\omega_o\sqrt{2\omega_o(\omega_o - \omega_o')} \quad ,$$

which is obtained from Equation (57), into Equation (60), giving

$$X_o = \frac{2L_1\omega_o}{\omega}\sqrt{2\omega_o(\omega_o - \omega_o')} \quad . \qquad (61)$$

Therefore,

$$\frac{X_o^2}{R_1^2} = \left(\frac{\omega_o L_1}{R_1}\right)^2 \frac{8}{\omega^2}\left[\omega_o(\omega_o - \omega_o')\right] \qquad (62)$$

and Equation (59) may be written as

$$\mathrm{Re}(Z) = R_L + \left(\frac{1}{\omega C_o}\right)^2 \frac{1}{R_1}\left[\frac{1}{1 + X_o^2/R_1^2}\right] \quad . \tag{63}$$

For the purpose of showing that $X_o^2/R_1^2 \gg 1$, ω in Equation (62) may be replaced by ω_o giving

$$\frac{X_o^2}{R_1^2} = \frac{8Q_o^2}{\omega_o}(\omega_o - \omega_o') \tag{64}$$

where

$$Q_o = \frac{\omega_o L_1}{R_1} \quad .$$

Equation (64) may be further simplified since

$$\omega_o - \omega_o' = \sqrt{\frac{1}{L_1}\left(\frac{1}{C_1} + \frac{1}{C_o}\right)} - \sqrt{\frac{1}{L_1}\left(\frac{1}{C_1}\right)}$$

$$\approx \left[\sqrt{\frac{1}{L_1 C_1}} + \frac{1}{2}\,\frac{1/L_1 C_o}{\sqrt{\frac{1}{L_1 C_1}}}\right] - \sqrt{\frac{1}{L_1 C_1}}$$

$$= \frac{1}{2}\,\omega_o' \frac{C_1}{C_o} \approx \frac{1}{2}\,\omega_o \frac{C_1}{C_o} \tag{65}$$

where the first approximation is obtained by using only the first two terms of a binomial expansion.

Therefore,

$$\frac{X_o^2}{R_1^2} \approx \frac{8Q_o^2}{\omega_o}\left(\frac{1}{2}\right)\omega_o \frac{C_1}{C_o} = \frac{4Q_o^2 C_1}{C_o}$$

$$= \frac{4\omega_o L_1 C_1 Q_o}{R_1 C_o} = \frac{4Q_o}{\omega_o R_1 C_o} \quad . \tag{66}$$

For a crystal having the parameters

$$\begin{aligned} Q_o &= 10^4, \\ \omega_o &= 300 \cdot 2\pi \cdot 10^6 \text{ rad/sec}, \\ R_1 &= 200 \text{ ohms}, \\ \text{and } C_o &= 7 \cdot 10^{-12} \text{ fd}. \end{aligned} \tag{67}$$

Equation (66) becomes

$$\frac{X_o^2}{R_1^2} \approx 1.6 \cdot 10^4.$$

(It may be noted that this result validates the assumption of Equation (51) since the right side of Equation (51) is X_o^2.)

Equation (63) becomes

$$\text{Re}(Z) = R_L + 18 \cdot 10^{-4} \approx R_L$$

where R_L will generally be greater than 50 ohms in a practical measurement system.

The imaginary part of Z is zero within the accuracy of the approximations by the condition imposed by Equation (49). For the parameter values of Equations (67), Im(Z) is less than one percent of R_L for practical values of R_L. The error in calculating the magnitude of Z due to Im(Z) is therefore less than 0.01 percent.

It will be observed that the parameter values of Equation (67) were chosen for the most adverse conditions likely to be encountered.

The results of Equations (49) through (67) may now be applied to rewrite Equations (48) as

$$\frac{I_B}{I_A} \approx \frac{I_B'}{I_A} \approx \frac{I_B''}{I_A} \approx 1 + \frac{1}{R_L}\left(\frac{1}{\omega_o C_o}\right)^2 \frac{1}{R_1} \quad . \tag{68}$$

Before R_1 can be calculated it is still necessary, of course, to determine the values of R_L and C_o. C_o of the crystal can be measured at low frequency. R_L can be calculated from Equation (47) provided absolute voltage and current calibrations can be made, since I_B may be replaced by I_B' or I_B''. R_L may also be determined by combining with Equation (68) a second similar equation obtained by increasing R_L by some amount ΔR and again determining the current ratio. The two equations may then be solved simultaneously for R_L. R_1 may then be calculated from Equation (68).

Q_o may be determined from the following consideration. Let

$$\left.\begin{aligned} \Delta &= \frac{\omega}{\omega_o} - \frac{\omega_o}{\omega} \quad , \qquad & Q &= \frac{\omega_o L_L}{R_L} \\ \text{and} \qquad Q_o &= \frac{\omega_o L_1}{R_1} = \frac{1}{R_1 \omega_o C_1} \quad . \end{aligned}\right\} \tag{69}$$

The normalized current, U, is

$$U = \frac{I}{E} R_L \quad . \tag{70}$$

From Equations (38), (69) and (70)

$$\frac{1}{U} = 1 + jQ\Delta + K \frac{1}{1 + jQ_o\Delta} \tag{71}$$

where

$$K = \frac{1}{R_L R_1}\left(\frac{1}{\omega C_o}\right)^2 \quad . \tag{72}$$

The quantity K is essentially constant over the frequency range near ω_o. Therefore,

$$K \approx \frac{1}{R_L R_1} \left(\frac{1}{\omega_o C_o}\right)^2 \quad . \tag{73}$$

For $Q\Delta \ll 1$, which is true for ω very near to ω_o, Equation (71) becomes

$$(Q_o\Delta)^2 = \frac{(1 + K)^2 U^2 - 1}{1 - U^2} \quad . \tag{74}$$

If the current variations are as indicated in Figure 53 and since K is considered constant, K may be evaluated at $\Delta = 0$ from Equation (71) as

$$K + 1 = \frac{1}{U} = \frac{b}{a} \quad . \tag{75}$$

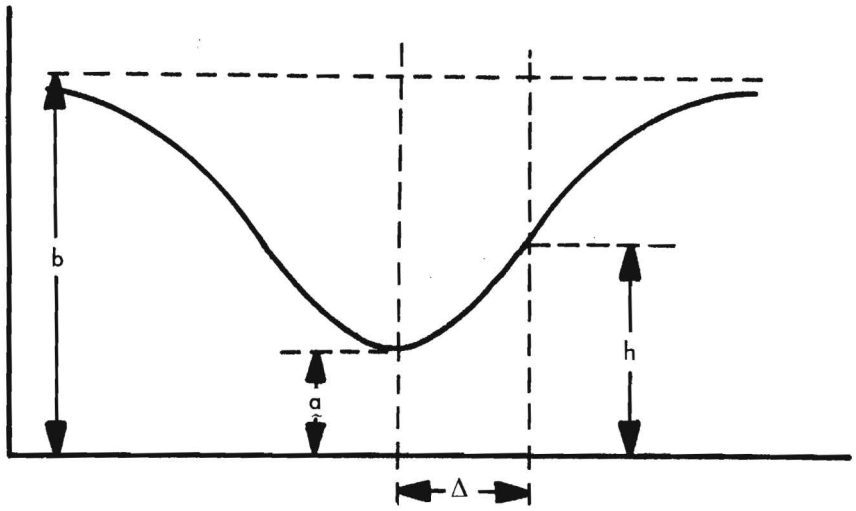

Figure 53. Crystal Current Variations.

With this result, Equation (74) becomes

$$(Q_o\Delta)^2 = \frac{\left(\frac{h}{a}\right)^2 - 1}{1 - \left(\frac{h}{b}\right)^2} = \frac{b^2}{a^2}\,\frac{h^2 - a^2}{b^2 - h^2} \quad . \tag{76}$$

Since Δ is readily measured, Q_o may be readily calculated from Equation (76).

To summarize, the crystal parameters may be obtained as follows:

1. Plot points on the current response curve as indicated by Figure 53, recording relative current amplitude and frequency at points a and b and some arbitrary point h.

2. Increase R_L by adding an external resistor and record the new currents a and b.

3. Substitute the two values of a and b into Equation (68) and solve for R_L (note that I_A and I_B are respectively equal to a and b).

4. Measure C_o at some low frequency and substitute C_o, R_L and ω_o together with a and b into Equation (68) and solve for R_1.

5. Substitute a, b and h into Equation (76) and solve for Q_o (Δ is the difference of two known frequencies).

6. Since Q_o, ω_o and R_1 are now known, L_1 and C_1 may be found from the last of Equations (69).

This procedure has been applied to a theoretical crystal by use of an electronic computer. Typical element values for the equivalent circuit of a crystal were selected and the corresponding current plotted for unity voltage. From this curve alone, the above steps were used to calculate the various crystal parameters. The calculated data agreed with the original data to an accuracy limited only by the resolution in reading the curve. This indicated that none of the approximations in arriving at the above steps contributed any appreciable errors.